Using the Thermal Power of Light to Affect Myalgic Encephalomyelitis/Chronic Fatigue Syndrome (ME/CFS)

Doctoral thesis for obtaining the

academic degree

Doctor of Natural Sciences (Dr. rer. nat.)

submitted by

Barbara Hochecker

at the

Faculty of Sciences

Department of Biology

Konstanz, 2025

Tag der mündlichen Prüfung: 25.09.2025

1. Referent: Prof. Dr. Alexander Bürkle

2. Referent: Prof. Dr. Jörg Bergemann

Table of contents

Summary

Myalgic encephalomyelitis/chronic fatigue syndrome (ME/CFS) is a mysterious disease. To date, the aetiology and pathophysiology of the disease have not been clarified. Moreover, the exact diagnosis of ME/CFS is also difficult because there are no biomarkers, which means that the disease has to be recognised on the basis of symptoms. The list of possible symptoms is long, but they can vary from one person to another and the severity can vary from each day. In addition to the main symptom of fatigue, cognitive impairments such as problems with memory or thinking also occur. Patients also suffer from muscle or joint pain, brain fog, non-restorative sleep and dizziness that worsens when moving from lying or sitting to standing. These are some, but not all, of the symptoms that can occur with ME/CFS. In addition, there is another characteristic feature of the disease - post-exertional malaise (PEM) - which is the worsening of symptoms after minor physical and/or mental exertion. This long list and type of symptoms reflects the multisystemic nature of the disease and the severe restriction of normal life. A severely affected person is bedridden and unable to lead a normal life. It is a highly disabling, severe condition that has been largely overlooked and even questioned as a disorder by medicine and research for decades, which explains, among other things, the lack of knowledge about this disease. Another consequence is that the lack of understanding of ME/CFS means that no causal therapy is possible. However, there are either treatment options to alleviate the symptoms with suitable medication or specific behavioural therapies. These therapies initially enable behavioural adaptation to the disease in order to increase the possible activity level again in the next step. The approach of this work to make a possible contribution to helping ME/CFS patients, is the cellular investigation of the influence of hyperthermia. Hyperthermia has been used successfully for many years and is defined as an abnormally elevated body temperature. In modern medicine, hyperthermia is primarily used in cancer therapy. Its effectiveness in shrinking tumours has been proven in numerous studies on various types of cancer. Heat treatment is not only useful in cancer therapy, however, but also has an antidepressant effect with lasting therapeutic benefits in severe depression or leads to a significant reduction in blood pressure in arterial hypertension. Nevertheless, the cellular and molecular mechanisms underlying these positive effects have not yet been sufficiently researched and understood.

As mentioned above, the content of this thesis is the investigation of hyperthermia as a potential treatment option for ME/CFS and is divided into three sections. The first section compares the functionality of the central cellular processes autophagy and mitochondrial function in PBMCs from healthy donors and ME/CFS patients. The second section describes the hyperthermia (39 °C, 1 h) of isolated PBMCs from healthy donors and from ME/CFS patients. In addition, human fibroblasts

from a healthy donor were analysed for their response to hyperthermia. In this so-called ex vivo study, autophagy and mitochondrial function as well as mRNA expression of the corresponding genes were also measured. In the last section, the in vivo study, nine ME/CFS patients were subjected to a whole-body hyperthermia session (one-hour whole-body hyperthermia-therapy with body-core temperature (Tc) max = 39 °C). The same parameters were measured as in the ex vivo study. In both studies, water-filtered infrared-A radiation, which is already successfully used for whole-body hyperthermia, was used as a special heat source.

The comparison of the cellular parameters of healthy donors and ME/CFS patients shows increased autophagy and an increase in the analysed mitochondrial parameters in ME/CFS patients. While the ex vivo study shows an increasing effect on autophagy and a slightly decreasing effect on mitochondrial function due to hyperthermia, the in vivo study shows a decreasing effect on autophagy and an increasing effect on mitochondrial function due to hyperthermia. Since the overall goal is to treat ME/CFS patients and not just their cells, the results of the in vivo study are better suited to evaluate hyperthermia as a potential treatment option for ME/CFS. As previously mentioned, autophagy is increased in ME/CFS compared to healthy donors, but a session of whole-body hyperthermia decreases autophagy back to healthy levels. In addition, mitochondria are activated by hyperthermia. The different results between ex vivo and in vivo hyperthermia provided the necessary evidence to develop a hypothesis for a possible explanation of the clinical picture of ME/CFS, which is described in the discussion. To summarise, the results of this work support hyperthermia as a possible treatment option for ME/CFS.

Zusammenfassung

Myalgische Enzephalomyelitis/Chronisches Fatigue-Syndrom (ME/CFS) ist eine rätselhafte Erkrankung. Bis heute sind die Ätiologie und Pathophysiologie der Krankheit nicht geklärt. Darüber hinaus ist die genaue Diagnose von ME/CFS auch deshalb schwierig, weil es keine Biomarker gibt, was bedeutet, dass die Krankheit anhand der Symptome erkannt werden muss. Die Liste der möglichen Symptome ist lang, aber sie können von einer Person zur anderen variieren und der Schweregrad kann von Tag zu Tag unterschiedlich sein. Neben dem Hauptsymptom der Müdigkeit treten auch kognitive Beeinträchtigungen wie Gedächtnisprobleme oder Schwierigkeiten beim Denken auf. Die Patienten leiden auch unter Muskel- oder Gelenkschmerzen, nicht erholsamem Schlaf und Schwindel, der sich verschlimmert, wenn sie sich vom Liegen oder Sitzen zum Stehen aufrichten. Dies sind einige, aber nicht alle, der Symptome, die bei ME/CFS auftreten können. Darüber hinaus gibt es ein weiteres charakteristisches Merkmal der Krankheit - das postexertionelle Unwohlsein (PEM) - das heißt die Verschlimmerung der Symptome nach geringer körperlicher und/oder geistiger Anstrengung. Diese lange Liste und Art von Symptomen spiegelt den multisystemischen Charakter der Krankheit und die starke Einschränkung des normalen Lebens wider. Ein schwer betroffener Mensch ist bettlägerig und nicht in der Lage, ein normales Leben zu führen. Es handelt sich um eine stark behindernde, schwerwiegende Erkrankung, die von der Medizin und der Forschung jahrzehntelang weitgehend übersehen und sogar als Krankheit in Frage gestellt wurde. Dieser Umstand erklärt, unter anderem, das mangelnde Wissen über die Erkrankung. Eine weitere Folge ist, dass das mangelnde Verständnis von ME/CFS bedeutet, dass keine kausale Therapie möglich ist. Dafür gibt es jedoch entweder Behandlungsmöglichkeiten, um die Symptome mit geeigneten Medikamenten zu lindern, oder spezifische Verhaltenstherapien. Diese Therapien ermöglichen zunächst eine Verhaltensanpassung an die Krankheit, um im nächsten Schritt das mögliche Aktivitätsniveau wieder zu erhöhen. Der Ansatz dieser Arbeit, einen möglichen Beitrag zur Hilfe für ME/CFS-Patienten zu leisten, ist die zelluläre Untersuchung des Einflusses von Hyperthermie. Hyperthermie wird seit vielen Jahren erfolgreich eingesetzt und ist definiert als eine abnorm erhöhte Körpertemperatur. In der modernen Medizin wird die Hyperthermie vor allem in der Krebstherapie eingesetzt. Ihre Wirksamkeit bei der Tumorverkleinerung wurde in zahlreichen Studien zu verschiedenen Krebsarten nachgewiesen. Die Wärmebehandlung ist aber nicht nur in der Krebstherapie nützlich, sondern hat auch eine antidepressive Wirkung mit dauerhaftem therapeutischen Nutzen bei schweren Depressionen oder führt zu einer deutlichen Senkung des Blutdrucks bei arterieller Hypertonie. Die zellulären und molekularen Mechanismen, die diesen positiven Wirkungen zugrunde liegen, sind jedoch noch nicht ausreichend erforscht und verstanden.

Wie bereits erwähnt, ist der Inhalt dieser Arbeit die Untersuchung der Hyperthermie als mögliche Behandlungsoption für ME/CFS. Die Arbeit ist in drei Abschnitte unterteilt. Der erste Abschnitt

vergleicht die Funktionalität der zentralen zellulären Prozesse Autophagie und Mitochondriale Funktion in PBMCs von gesunden Spendern und ME/CFS-Patienten. Der zweite Abschnitt beschreibt die Hyperthermie (39 °C, 1 h) von isolierten PBMCs von gesunden Spendern und von ME/CFS-Patienten. Darüber hinaus wurden menschliche Fibroblasten eines gesunden Spenders auf ihre Reaktion auf Hyperthermie untersucht. In dieser sogenannten ex vivo-Studie wurden auch die Autophagie und die mitochondriale Funktion sowie die mRNA-Expression verwandter Gene gemessen. Im letzten Abschnitt, der in-vivo-Studie, wurden neun ME/CFS-Patienten einer Ganzkörper-Hyperthermie-Sitzung unterzogen (einstündige Ganzkörper-Hyperthermie-Therapie mit Körperkerntemperatur (Tc) max = 39 °C). Es wurden die gleichen Parameter gemessen wie in der ex-vivo-Studie. In beiden Studien wurde als spezielle Wärmequelle wassergefilterte Infrarot-A-Strahlung verwendet, die bereits erfolgreich für die Ganzkörperhyperthermie eingesetzt wird. Der Vergleich der zellulären Parameter von gesunden Spendern und ME/CFS-Patienten zeigt eine erhöhte Autophagie und eine Zunahme der analysierten mitochondrialen Parameter bei ME/CFS-Patienten. Während die ex-vivo-Studie einen zunehmenden Effekt auf die Autophagie und einen leicht abnehmenden Effekt auf die Mitochondriale Funktion durch die Hyperthermie zeigt, zeigt die in-vivo-Studie einen abnehmenden Effekt auf die Autophagie und einen zunehmenden Effekt auf die Mitochondriale Funktion durch die Hyperthermie. Da das Gesamtziel darin besteht, ME/CFS-Patienten zu behandeln und nicht nur ihre Zellen, sind die Ergebnisse der in-vivo-Studie besser geeignet, um die Hyperthermie als mögliche Behandlungsoption für ME/CFS zu bewerten. Wie bereits erwähnt, ist die Autophagie bei ME/CFS im Vergleich zu gesunden Spendern erhöht, aber eine Sitzung mit einer Ganzkörper-Hyperthermie senkt die Autophagie wieder auf ein gesundes Niveau. Darüber hinaus werden die Mitochondrien durch Hyperthermie aktiviert. Die unterschiedlichen Ergebnisse zwischen der ex-vivo- und der in-vivo-Hyperthermie lieferten die notwendigen Beweise, um eine Hypothese für eine mögliche Erklärung des Krankheitsbildes von ME/CFS zu entwickeln, die in der Diskussion beschrieben wird. Zusammenfassend lässt sich sagen, dass die Ergebnisse dieser Arbeit die Hyperthermie als eine mögliche Behandlungsoption für ME/CFS unterstützen.

Abbreviations

°C	degree centigrade
µg	microgram
µL	microliter
β2AdR	β_2-adrenergic receptors
A	
AMP	adenosine monophosphate
AMPK	AMP-activated protein kinase
AMPK1α	protein kinase AMP-activated catalytic subunit alpha 1
ANOVA	analysis of variance
AO/PI	Acridine Orange/Propidium Iodide
APT	Adaptive Pacing Therapy
ATG2A	autophagy-related gene 2A
ATG3	autophagy-related gene 3
ATG4	autophagy-related gene 4
ATG5	autophagy-related gene 5
ATG7	autophagy-related gene 7
ATG9A	autophagy-related gene 9A
ATG10	autophagy-related gene 10
ATG12	autophagy-related gene 12
ATG13	autophagy-related gene 13
ATG14L	autophagy-related gene 14L
ATG16L	autophagy-related gene 16L
ATG101	autophagy-related gene 101
ATP	adenosine triphosphate
B	
Bcl-2	B cell lymphoma-2
BECN1	Beclin 1
BNIP3	BCL2/adenovirus E1B 19 kDa protein-interacting protein 3
BH3	Bcl-2 homology 3 domain
C	
CCC	Canadian Consensus Criteria
CCD	Central coiled-coil domain
CMA	chaperone-mediated autophagy
COPD	chronic obstructive pulmonary disease
CoQ	coenzyme Q
CQ	chloroquine
CSF	cerebral spinal fluid
D	
DAPI	4′,6-Diamidin-2-phenylindol
DMEM	Dulbecco's Modified Eagle's Medium
DMSO	Dimethyl sulphoxide
E	
ECD	evolutionarily conserved domain
EDTA	Ethylenediaminetetraacetic acid
ER	endoplasmic reticulum

F

FACS	fluorescence-activated cell sorting
FBS	Fetal Bovine Serum
FCCP	carbonyl cyanide-4-(trifluoromethoxy)-phenylhydrazone
FDR	first-degree relative
FIP200	focal adhesion kinase family-interacting protein of 200 kDa
FITC	fluorescein isothiocyanate
FOXO3	forkhead box O3

G

GFP	Green Fluorescent Protein
GTP	guanosine triphosphate
GWAS	genome-wide association study

H

H_2O_2	hydrogen peroxide
HeLa	Henrietta Lacks
HLA	human leukocyte antigen
Hsc70	heat Shock Cognate Protein 70
Hsp70	heat shock protein 70
HSPA5	heat shock protein family A (Hsp70) member 5

I

IL-10	Interleukin 10
IOM	Institute of Medicine
IR-A	infrared-A radiation

L

LAMP-2A	lysosomal membrane protein 2A
LC3	light chain 3 system of microtubule-associated protein 1
LC3-I	cytosolic LC3
LC3-II	membrane-associated LC3-PE
LIRs	LC3-interacting regions

M

MAP1LC3B	microtubule associated protein 1 light chain 3 beta
ME/CFS	Myalgic encephalomyelitis/Chronic fatigue syndrome
MFI	Median fluorescence intensity
MHC	major histocompatibility complex
min	minutes
mL	millilitre
MRI	magnetic resonance imaging
mTORC1	Mechanistic Target of Rapamycin Complex 1

N

NAD^+	Nicotinamide adenine dinucleotide
NAM	National Academy of Medicine
NDUFS1	NADH: ubiquinone oxidoreductase core subunit S1
ns	not significant

O

$O_2^{\bullet-}$	superoxide radical anion
OCR	oxygen consumption rate

P

PAS	phagophore assembly site
PBS	Phosphate buffered saline
PDL	poly-D-lysine
PEM	post-exertional malaise
Pi	inorganic phosphate
PI3K	Class III PI3K complex I
PI3P	phosphatidylinositol-3-phosphate
ProLC3	LC3 precursor

Q

qPCR	quantitative polymerase chain reaction

R

RAB	RAS-related GTP-binding protein
RAS	Rat sarcoma virus
ROS	reactive oxygen species
RPLP0	ribosomal protein lateral stalk subunit P0

S

SEM	standard error of the mean
SIRT1	Sirtuin 1
SIRT3	Sirtuin 3
SNARE	soluble-N-ethylmaleimide-sensitive factor attachment protein receptors
SOD2	Superoxide dismutase 2

T

Tc	body-core temperature
TFAM	transcription factor A, mitochondrial

U

UBDs	ubiquitin-binding domains
ULK1	unc-51 like autophagy activating kinase 1
UVRAG	UV radiation resistance-associated gene protein

V

VPS15	vacuolar protein sorting 15
VPS34	vacuolar protein sorting 34

W

WBH	whole-body hyperthermia
WHO	World Health Organisation
WIPI	WD-repeat protein interacting with phosphoinositides
wIRA	water-filtered infrared-A

Figures

Tables

1 Introduction

"CFS patients feel effectively the same every day as an AIDS patient feels two months before death; the only difference is that the symptoms can go on for never-ending decades."

~ Prof. Mark Loveless, Head of the AIDS and ME/CFS Clinic at Oregon Health Sciences University

Can you imagine living a life like this?

In Europe alone, between 750,000 and 16,400,000 people have no choice [1]. They have myalgic encephalomyelitis/chronic fatigue syndrome (ME/CFS).

ME/CFS is a complex, multisystemic and often long-lasting disease characterised by pathological fatigue and malaise that worsens after exertion, sleep disturbances, cognitive dysfunction, neuroendocrine and immunological symptoms. Another key feature of this multisystemic disorder is post-exertional malaise (PEM), which is a worsening of symptoms after trivial physical or cognitive exertion, often with delayed onset and abnormally delayed recovery. The disease can severely affect patients' ability to lead their normal lives. [2,3] Outcomes are worsened by the fact that the condition goes undiagnosed for years due to inadequate medical education on the subject, provider bias and confusion about the diagnosis and treatment of the disease [4]. This confusion continues with the aetiology of ME/CFS. There is controversy about single or multiple causes. Moreover, there are many theories about the involvement of infections, the immune system, environmental factors including trauma and genetics, among others - which may or may not be a possible clue. [5] Due to the multisystemic nature of the disease, a dysfunction or dysregulation of fundamental cellular processes such as autophagy and mitochondrial function could also be considered.

Without comprehensive knowledge of the origin and mechanisms of the disease, it is difficult to find an effective and targeted treatment. Current treatment methods are mainly pharmaceutical therapies to alleviate symptoms, e.g. painkillers, or adaptive methods. One adaptive method to prevent PEM is Adaptive Pacing Therapy (APT). In this method, the patient's limits are first defined and then minimised. [6] The main aim is therefore to counteract the limitations imposed by the disease or, in the best case, to resolve them in order to return to the original state of health. This goal leads us to the explanation of the title of this work 'Using the thermal power of light to affect myalgic encephalomyelitis/chronic fatigue syndrome (ME/CFS)', i.e. the investigation of the influence of hyperthermia by water-filtered infrared-A (wIRA) irradiation on the central cellular

mechanisms autophagy and mitochondrial function in PBMCs of ME/CFS patients. Hyperthermia is defined as an abnormally high body temperature and can be caused by an infection or by external heat application such as electro-hyperthermia [7,8]. In this work, the heat effect is generated by light, more precisely by infrared-A radiation (IR-A). Due to the high penetration depth into human tissue, without thermal overload of the outer skin layers, the use of wIRA is an established form to perform hyperthermic applications [9]. In this context, it has already been shown in volunteers that increased temperature is associated with increased oxygen partial pressure and improved blood flow, among others [10]. Hyperthermia as therapy has a long history, particularly in the field of cancer therapy [11] and is still used in this field in modern medicine [12–15]. In addition, a significant reduction in blood pressure in arterial hypertension [16] or an antidepressant effect in severe depressive disorders has been demonstrated [17]. However, the cellular and molecular mechanisms underlying these positive effects have not yet been sufficiently researched and understood.

Since heat is a cellular stressor, activation of autophagy by hyperthermia would not be surprising. The best known activator of autophagy is the stress factor nutrient deprivation and the subsequent regulation by the energy sensor AMPK and its inhibition of the autophagy inhibitor mTOR, which leads to the activation of autophagy [18]. To counteract the nutrient deficiency, autophagy recycles cellular components by lysosomal degradation to generate new biological building blocks. In other cases, harmful or damaged structures are specifically degraded by autophagy [19]. The overarching function of autophagy is therefore to maintain cellular homeostasis and the energy balance of the cell [18]. A disruption of the autophagy process is suspected in numerous human diseases and pathophysiological conditions, including neurodegenerative, infectious, autoimmune, cardiovascular, rheumatic, metabolic, pulmonary and malignant diseases as well as ageing [20]. Due to the central function of autophagy in the cells and the multisystemic nature of ME/CFS, there could be a link between dysregulation of autophagy and the disease. Another hypothesis is the connection between impaired mitochondrial function and the main symptom of fatigue in ME/CFS. This assumption is based on the main function of mitochondria, which is to produce energy in the form of adenosine triphosphate (ATP) through oxidative phosphorylation [21]. In addition, the mitochondrial electron transport chain is the main source of reactive oxygen species (ROS), which contribute to a number of pathological processes [22].

Overall, it is clear that there is a need for research in the field of ME/CFS. To contribute to this problem, this thesis deals with the investigation of autophagy and mitochondrial function as well as the associated mRNA expression in PBMCs from ME/CFS patients compared to healthy donors. In addition, the effect of hyperthermia by wIRA treatment is investigated. The overall aim of this work is to contribute to a better understanding of the disease and its treatment and thus help people to alleviate their severe symptoms or improve their state of health.

1.1 The mystery of Myalgic encephalomyelitis/Chronic fatigue syndrome

In 2015, the Institute of Medicine (IOM) found that less than a third of medical school curricula and less than half of medical textbooks contain information about ME/CFS. Concerningly, many healthcare providers are sceptical about the seriousness of ME/CFS, confusing it with a mental illness or believing it to be a figment of the patient's imagination. This misinterpretation of the disease or lack of knowledge delays diagnosis and leads to inappropriate management of patients' symptoms. [4] A more recent study from 2021 confirms that medical education in the UK in relation to ME/CFS is inadequate and does not appear to have developed over the last two decades [23]. However, it is not easy to interpret a disease correctly when it is difficult to define the disease itself. Between 1986 and 2015, 25 case definitions and terminologies for ME/CFS were developed. In 2015 alone, there were three different publications on this topic, each with its own definition. Common symptoms in the summarised classification for ME/CFS case definitions are fatigue, cognitive impairment, sleep disturbance and orthostatic intolerance. [5] Of the 25 existing case definitions, four are frequently used in diagnostics and research. These four are the Fukuda Criteria, the Canadian Consensus Criteria, the International Consensus Criteria and the US Institute of Medicine (IOM), now National Academy of Medicine (NAM) criteria. Since the Fukuda criteria and the Canadian Consensus Criteria were used for the diagnosis in this work, these two diagnostic criteria are described in more detail below.

Fukuda Criteria

The Fukuda criteria were developed in 1994 by the International Chronic Fatigue Syndrome Study Group. To be diagnosed with CFS, a person must have clinically assessed, unexplained, persistent or intermittent chronic fatigue that is new or definite (not lifelong), is not the result of sustained exertion, is not substantially relieved by rest, and results in significant limitation of previous occupational, educational, social or personal activities. Additional symptoms include significant impairment of short-term memory or concentration, sore throat, sore lymph nodes, muscle aches, pain in multiple joints without swelling or redness, headache of new type, pattern or severity, unrestful sleep and post-exertional malaise lasting longer than 24 hours. [24]

Canadian Consensus Criteria

The first version of the Canadian Consensus Criteria (CCC) was published in 2003. Seven years later, in 2010, the CCC were revised to allow clinicians and researchers to better apply the criteria and improve diagnostic reliability, although the core categories remained unchanged. [25,26]. To receive a diagnosis of ME/CFS, the conditions listed in **Table 1** must be present and have persisted for at least six months. A thorough history, physical examination and tests are required to rule out other diseases.

Table 1: Canadian Consensus Criteria for ME/CFS

All of the following must be present		
▪ **Fatigue** – Significant physical and mental fatigue that is new onset, unexplained, persistent or recurrent, and substantially reduces activity level; ▪ **Post-exertional malaise and/or post-exertional fatigue** – General feeling of discomfort, weakness and/or fatigue, and potentially worsening associated symptoms, following physical or mental exertion; slow recovery which is usually longer than 24 hours; ▪ **Sleep dysfunction** – Unrefreshing sleep or disturbances in sleep quantity or rhythm; ▪ **Pain** – Significant degree of muscle and/or joint pain, and/or significant headaches of new type, pattern or severity.		
Two or more of the following neurological/cognitive manifestations must be present		
▪ Impairment of concentration and short-term memory consolidation; ▪ Perceptual and sensory disturbances; e.g. spatial instability and disorientation, and inability to focus vision; ▪ Difficulty with information processing, categorising and word retrieval; ▪ Confusion; ▪ Disorientation; ▪ Motor disturbances: ataxia, muscle weakness and fasciculations, loss of balance and clumsiness occur commonly; ▪ Overload phenomena: cognitive, sensory (e.g. hypersensitivity to noise and light), emotional overload which may lead to crash (temporary immobilising physical and/or mental fatigue) and/or anxiety.		
At least 1 symptom from 2 of the following categories must be present:		
Autonomic manifestations ▪ Orthostatic intolerance, postural orthostatic intolerance, delayed postural hypotension; ▪ Palpitations (with or without cardiac arrythmias); ▪ Light-headedness; ▪ Extreme pallor; ▪ Shortness of breath on exercise; ▪ Nausea and irritable bowel syndrome; ▪ Urinary frequency and bladder dysfunction.	**Neuroendocrine manifestations** ▪ Loss of thermostatic stability (temperature does not remain stable); ▪ Intolerances of extremes of heat and cold; ▪ Recurrent feelings of feverishness and cold extremities; ▪ Marked weight change (anorexia or abnormal appetite); ▪ Loss of adaptability and worsening symptoms with stress.	**Immune manifestations** ▪ Tender lymph nodes; ▪ Recurrent sore throat; ▪ Recurrent flu-like symptoms; ▪ General malaise (flu-like feelings of being ill and feverish); New sensitivities to food, medications and/or chemicals.

To summarise, all diagnostic criteria are based on clinical symptoms and the exclusion of other fatigue diseases - there is no biomarker.

Another factor that complicates the diagnosis of ME/CFS patients is the varying severity of the disease in different patients. In this work, the Bell Scale (**Table 2**) was used as an indicator of the severity of the disease. The scale is based on David S. Bell, M.D., a well-known expert and pioneer in the diagnosis and treatment of ME/CFS, and defines the degree of disability caused by chronic fatigue syndrome using criteria with increasing impairment from 100 to 0 points. At 100 points, there are no symptoms; at 0 points, the patient is unable to get out of bed independently. David S. Bell published the scale in 1995 in his book 'The Doctor's Guide to Chronic Fatigue Syndrome'. [27]

Table 2: Bell Scale

Points	Degree of disability
100	No symptoms at rest; no symptoms with exercise; normal overall activity level; able to work full-time without difficulty.
90	No symptoms at rest; mild symptoms with activity; normal overall activity level; able to work full-time without difficulty.
80	Mild symptoms at rest; symptoms worsened by exertion; minimal activity restriction noted for activities requiring exertion only; able to work full-time with difficulty in jobs requiring exertion.
70	Mild symptoms at rest; some daily activity limitation clearly noted. Overall functioning close to 90% of expected except for activities requiring exertion. Able to work full-time with difficulty.
60	Mild to moderate symptoms at rest; daily activity limitation clearly noted. Overall functioning 70%-90%. Unable to work full-time in jobs requiring physical labor, but able to work full-time in light activity if hours flexible.
50	Moderate symptoms at rest. Moderate to severe symptoms with exercise or activity; overall activity level reduced to 70% of expected. Unable to perform strenuous duties, but able to perform light duty or desk work 4-5 hours a day, but requires rest periods.
40	Moderate symptoms at rest. Moderate to severe symptoms with exercise or activity; overall activity level reduced to 50%-70% of expected. Not confined to house. Unable to perform strenuous duties; able to perform light duty or desk work 3-4 hours a day, but requires rest periods.
30	Moderate to severe symptoms at rest. Severe symptoms with any exercise; overall activity level reduced to 50% of expected. Usually confined to house. Unable to perform any strenuous tasks. Able to perform desk work 2-3 hours a day, but requires rest periods.
20	Moderate to severe symptoms at rest. Unable to perform strenuous activity; overall activity 30%-50% of expected. Unable to leave house except rarely; confined to bed most of day; unable to concentrate for more than 1 hour a day.
10	Severe symptoms at rest; bedridden the majority of the time. No travel outside of the house. Marked cognitive symptoms preventing concentration.
0	Severe symptoms on a continuous basis; bedridden constantly; unable to care for self.

1.1.1 Aetiology

Facts such as the nature of the diagnosis, the lack of a biomarker or that patients often do not look ill although they are severely affected by the disease, are factors that have been put forward in favour of a psychosomatic hypothesis [28,29]. The idea that ME/CFS is a psychosomatic illness originates from a publication by two psychiatrists, McEvedy and Beard. This publication refers to an unknown illness that broke out in 1955, which affected more than 300 members of the medical, nursing and ancillary staff of the Royal Free Group of Hospitals in London. The symptoms of this disease included memory and concentration problems, post-exertional malaise, unrefreshing sleep, myalgia, headaches of a new type or greater severity and tender lymph nodes. The disease was initially referred to as Royal Free disease, but the following year the name benign myalgic encephalomyelitis was coined to describe this and several similar outbreaks. The term chronic fatigue syndrome (CFS) was introduced in 1988 to describe a similar illness in Nevada, USA. Fifteen years later, McEvedy and Beard hypothesised that there was little evidence of an organic disease of the central nervous system and that epidemic hysteria was a much more likely explanation. [30] To date, the aetiology of ME/CFS has not been clarified and it is still disputed whether it is primarily an organic disease or a mental disorder, although the World Health Organisation (WHO) classifies the disease as a neurological disorder. There are many theories about the involvement of infections, the immune system and genetics in this complex interplay.

A study of 269 people with ME/CFS published in 2019 supports the infection theory. A history of frequent colds (odds ratio 8.286) and infections before the onset of the disease (odds ratio 25.5) were the strongest factors associated with a higher risk of ME/CFS compared to healthy controls. [31] Another study from 2023, involving 169 ME/CFS patients, confirmed these findings. An infectious diseases was associated with a singular or part of multiple events in 72.9% and 80.6%, respectively. Before the onset of the disease, one third of patients reported respiratory infections, followed by gastrointestinal infections (15.4%) and tick-borne diseases (16.2%). Viral infections were reported by 77.8% of respondents, with the Epstein-Barr virus being the most common. Interestingly, 90% of all patients recalled a triggering event and the time of occurrence. As already mentioned, a large proportion of these 90% were infectious diseases, but other events such as stress, emotional or physical trauma and surgery were also mentioned. [32] Chu *et al.* also reported that the top three triggering factors were an infectious disease (64%), stress or a significant life event (39%, e.g. job pressure, illness in the family, divorce) and exposure to an environmental/chemical toxin (20%). However, stressful events were rarely chosen as the sole trigger, with only 8% of respondents citing this, and they usually occurred in conjunction with infection or other triggers. [33] As drug treatment is a logical consequence of most infections, there is also evidence that the side effects of certain drugs could lead to ME/CFS. For example, the antibiotic class of gyrase inhibitors such as

fluoroquinolones could be suspected of triggering ME/CFS. [34] Also in the study of Chu *et al.*, 13% of respondents reported that at least one first-degree relative (FDR, e.g., blood-related father, mother, sibling, child) was affected by ME/CFS, and 21% responded that at least one FDR had chronic fatigue without a specific diagnosis. [33] It has been shown that ME/CFS also occurs in second- and third-degree relatives in a dose-response relationship, i.e. the greater the genetic distance between the ME/CFS patient and a relative, the lower the risk. [35,36] These analyses provide strong evidence for a heritable contribution to predisposition to chronic fatigue syndrome. However, ME/CFS diagnoses do not follow a predictable Mendelian pattern, indicating that there is not a single genetic variant that increases the risk of ME/CFS. Instead, ME/CFS is likely to be a complex, multifactorial disorder with many different genetic factors contributing to it. A genome-wide association study (GWAS) is ideal for discovering genetic causes of disease and new biology, especially when the aetiology of the disease is unknown, as is the case with ME/CFS. This is not only because it is comprehensive, but also because its results are not influenced by pre-existing biological assumptions or hypotheses. Unfortunately, a sufficiently meaningful GWAS study requires at least 10^4 participants and an equal or greater number of controls. However, recruiting thousands of people with ME/CFS - particularly severely affected individuals who are house or bed bound - is a difficult task. Existing evidence that genetic factors alter the risk of ME/CFS is not confirmed by studies of the larger CFS cohort (500,000 people) within the UK Biobank. [37] However, a 2020 study involving 426 ME/CFS patients shows that two independent human leukocyte antigen (HLA) types, characterised by HLA-C*07:04 or HLA-DQB1*03:03, are significantly associated with ME/CFS status. These alleles are each carried by approximately 10% of ME/CFS patients and change the risk by ~1.5-2.0-fold. [38] If these results can be replicated independently, they suggest that genetic differences in the human immune system alter the risk of ME/CFS. HLA proteins, also known as the major histocompatibility complex (MHC), enable the immune system to differentiate its own cells from foreign cells, such as foreign pathogens. Their genes exhibit extreme population polymorphism, and certain HLA types are genetically predisposed to certain autoimmune diseases. [39] However, this is not the only thing that ME/CFS has in common with autoimmune diseases. For example, ME/CFS is more frequent in women [40], runs in families, can be triggered by infections, can be alleviated by immunosuppressants and is associated with autoantibodies [41,42]. All these observations could lead to the conclusion that ME/CFS could have the character of an autoimmune disease.

1.1.2 Pathophysiology

The World Health Organisation classifies ME/CFS as a disease of the nervous system. And undeniably, many of the main symptoms such as cognitive impairment, mental fatigue, autonomic dysfunction, altered pain and sensory perception and sleep disturbances underline this categorisation. Indeed, neuroimaging in ME/CFS patients has revealed anatomical, neurochemical and functional changes in the brain. For example, magnetic resonance imaging (MRI) of the brain has revealed global changes in grey and white matter volume as well as differences in cortical and subcortical regional volume in ME/CFS patients. However, the underlying mechanism leading to these findings is unclear. Furthermore, the results were not consistent across studies and further research is needed to understand the neurological involvement in the pathology of ME/CFS. [43] However, the classification of ME/CFS as a disease of the nervous system does not take into account the immunological symptoms such as persistent sore throat, tender and enlarged lymph nodes and fever. These symptoms indicate chronic immune activation and reveal immune dysfunction as a key feature of ME/CFS. At the cellular level, these symptoms are reflected in a deterioration in the function and number of B- and T-lymphocytes and natural killer cells [44]. Another proposed underlying mechanism - the neuroinflammation theory - links the nervous and immune systems. A comprehensive systematic review and meta-analysis focused on neuroimaging features in patients diagnosed with ME/CFS. This review, comprising 65 studies with 3244 participants, suggests the presence of brain regional and neuroinflammatory abnormalities within the cortical-limbic network regions in individuals with ME/CFS. However, the authors noted that neuroinflammation is a common feature observed in various neurological diseases and not a unique pathophysiological feature unique to ME/CFS. This leads to the conclusion that this theory has the potential to improve the understanding of ME/CFS, but requires further research [45]. The discovery of elevated autoantibodies against ß$_2$-adrenergic receptors (ß2AdR) and M3-acetylcholine receptors in ME/CFS patients [41] led German researchers to a hypothesis about endothelial dysfunction and muscle and cerebral hypoperfusion in ME/CFS. As both ß2AdR and M3 acetylcholine receptors are important vasodilators, their dysfunction is expected to lead to vasoconstriction and hypoxaemia. [46,47]. However, the finding of reduced cerebral blood flow is not new. As early as 1995, Costa *et al.* showed reduced blood flow in the brainstem in ME/CFS patients compared to healthy donors. [48] A larger study of 400 ME/CFS patients showed that cerebral blood flow in the upright position compared to the supine position decreases on average more than threefold in ME/CFS patients compared to healthy controls and that the decrease in cerebral blood flow correlates with the symptom of orthostatic intolerance. [49] A finding shown in 2011 by Newton *et al.* for ME/CFS is also an impaired dilation of blood vessels, or endothelial dysfunction. [50]. A correlation between the severity of endothelial dysfunction and the severity of ME/CFS disease was demonstrated by

Scherbakov *et al.* in 2020 [51]. It is assumed that impaired blood circulation could reduce the oxygen supply to the tissue in ME/CFS. Oxygen is required in the body for aerobic energy production. If there is a lack of oxygen, body cells switch to anaerobic energy production, which is much less efficient and produces lactate. An increased lactate level in the cerebrospinal fluid has been documented in numerous studies in ME/CFS. Matthew *et al.* (2008), for example, found ventricular lactate levels in ME/CFS patients to be 3.5 times higher than in healthy controls [52]. But not only could a reduced blood flow lead to higher lactate concentrations, a dysfunction of the mitochondria could also be a possible explanation [52,53]. As the main function of the mitochondria is to generate energy in the form of adenosine triphosphate (ATP) through oxidative phosphorylation [21], disruption of this process would force the cells to switch to anaerobic energy production, which would also lead to the formation of lactate. At the cellular level, moderate to severe fatigue - which is a major symptom of ME/CFS - is associated with a loss of mitochondrial function [54]. Due to the close correlation between fatigue and mitochondrial dysfunction, a logical explanation could be a link between the disease and a disruption of mitochondrial function. The process of autophagy is worth mentioning in this context. The task of this biochemical process is to protect the cell from potentially harmful components, such as the aforementioned dysfunctional mitochondria [18]. Disruption of the autophagy process is implicated in numerous human diseases and pathophysiological conditions, including neurodegenerative, infectious, autoimmune, cardiovascular, rheumatic, metabolic, pulmonary and malignant diseases as well as ageing [20]. Due to the multisystemic nature of the ME/CFS, a dysfunction or dysregulation of a basic cellular process, such as autophagy, could be suspected.

1.1.3 Treatment

The main problem that arises from these knowledge gaps about the disease is that it is very difficult to fight something that is not understood. For this reason, the treatment of ME/CFS focuses on alleviating the symptoms or making the best of the situation by adapting lifestyle to the disease. Pharmacological drugs such as ibuprofen and naproxen are used to combat the symptoms of muscle pain and immunological abnormalities. They sometimes relieve frequent or severe joint and muscle pain, headaches and fever. [55] Other prescription drugs include anticonvulsants, also known as anti-seizure medications, like gabapentin and pregabalin are sometimes prescribed for pain and sleep problems. They seem to work best when used for nerve pain. Antidepressants are also prescribed to relieve depression and anxiety, increase concentration and improve sleep quality. [56] As gastrointestinal disturbances in ME/CFS are well documented [57], faecal microbiota transplantation, the infusion of liquid filtrate of a healthy donor's faeces into the gut of a recipient, is being considered as a potential treatment option. A study in which ME/CFS patients received faecal microbiota transplant therapy found that 41% achieved sustained symptom relief over a

period of 11-28 months [58]. ME/CFS patients tend to use more alternative medical treatments than people without ME/CFS. [59] This arises from the perception that their condition is unjustifiably attributed to psychological causes: they are given the message that "it's all a matter of the psyche". One aspect of alternative medicine is the intake of nutrients or mitoceuticals, such as essential fatty acids, magnesium, antioxidants and coenzymes. Dietary supplements can help ME/CFS patients with specific nutrient deficiencies, as has been observed in some studies [60,61]. However, a biochemical test for deficiencies should be performed prior to treatment to facilitate the choice of treatment. Counselling, behavioural and rehabilitation measures are another way of dealing with the disease. One of these interventions is cognitive behavioural therapy, a form of psychotherapy. However, ME/CFS is a physical and not a mental illness, and therefore psychological therapy cannot cure the disease, but it can help to manage it better. Graded exercise therapy, a form of physical activity that starts very slowly and gradually increases in intensity over time, is also a well-known measure. However, this form of therapy should be carefully modulated by an individualised pacing strategy with strict case definitions to avoid the push-crash cycle. Adaptive pacing therapy is a strategy that focuses on the patient's behaviour. However, unlike cognitive behavioural therapy, pacing therapy takes into account the characteristic fluctuations in symptom severity and delayed recovery from stress [62]. Patients receiving adaptive pacing therapy are instructed to set reasonable goals for their daily activities and exercise and to avoid possible overexertion (and worsening of symptoms) by establishing a balance between activity and rest. APT patients who are functioning within their individual limits then gradually increase their activity and exercise levels. The overall aim is therefore to increase performance levels, to raise the threshold before exhaustion sets in, or even to take a step back to ‘normal/healthy’ energy levels. One possible treatment option that could contribute to this goal is a form of therapy that has been used successfully for many years - heat treatment or hyperthermia. This form of treatment is presented in the following chapter.

1.2 Treatment with water-filtered infrared-A (wIRA)-hyperthermia

The power of heat and its healing effect on the human body is a subject that has fascinated various physicians and scientists since about 3000 years before Christ. Especially in the field of cancer therapy, hyperthermia has such a long history. Even Hippocrates, who is considered the 'father of medicine`, used heat to treat breast tumours and claimed that the disease must be incurable if it could not be cured by heat. [11] But also in modern medicine, hyperthermia has shown a tumour-reducing effect in numerous clinical studies and various types of cancer such as bladder [12], head and neck [13], skin [15], breast [63] and cervix [14,64]. Due to the microvasculature of tumours, they are more sensitive to heat and cannot tolerate elevated temperatures (temperatures between 40 and 44 °C) over longer periods of time as well as normal tissue [7]. Further studies have shown that hyperthermia also has positive effects on other diseases, for example in arterial hypertension, it leads to a significant reduction in blood pressure [16]. Another publication shows an antidepressant modality with a prolonged therapeutic benefit in major depressive disorder [17]. Incessant attempts to generate a high body temperature led to the development of various methods of systemic hyperthermia. It all began with the first paper on hyperthermia, published in 1866 by the German surgeon Carl D. W. Busch. He described the case of a woman with an advanced sarcoma on her face. After the tumour had been removed, the patient developed erysipelas. The disease caused a high temperature, which led to the regression of the tumour. Busch's discovery was of fundamental importance as it was the first case to show that high temperatures can selectively kill cancer cells while leaving healthy cells unaffected. [65] In addition to Busch's research, the connection between infection and cancer regression was also investigated by William B. Coley. In his studies, he injected various types of bacterial pyrogens into tumours and observed their behaviour. In 1891, he developed a toxin that triggered the typical erysipelas with its typical fever. The so-called Coley'a toxin was used for almost a century to treat various types of cancer. The results of Coley'a research showed that the five-year survival rate in patients with inoperable cancer increased from 28% to 64% depending on the temperature of the concomitant fever. Survival was longer at higher temperatures. However, the treatment of an infectious fever had a fundamental flaw - it was unpredictable. Every patient reacted differently to the toxin! [66] Nowadays, there are more controllable and therefore more predictable methods for generating clearly defined whole-body hyperthermia (WBH). The techniques used for therapeutic WBH include extracorporeal blood heating, water immersion, 27 MHz short waves, long-wave IR irradiation in a chamber with almost 100% humidity, IR A/B (‘near IR’) and wIRA irradiation. [67,68]

The wIRA irradiation is of particular importance in the context of this work, as this heat source was used for these investigations. The whole-body hyperthermia treatment of ME/CFS patients was carried out with the IRATHERM®1000M from the Von Ardenne Institute for Applied Medical Research GmbH. This institute also provided the so-called IRAcubator for the wIRA treatment of isolated PBMCs. The IRATHERM®1000M was specially developed to promote an increase in body temperature by inducing an 'artificial fever'. The device offers three levels of whole-body hyperthermia: mild, moderate and extreme. Depending on the therapeutic core body temperature and the duration of use, the possible medical applications of the WBH are extremely wide-ranging (**Table 2**).

Table 3: The three different temperature levels of whole-body hyperthermia

Mild WBH: < 38.5 °C	Moderate WBH: 38.5 °C - 40.5 °C	Extreme WBT: > 40.5 °C
Relaxation/wellness with short treatment durations during a mild WBH	Applications in rheumatology, dermatology, psychiatry, immunology and environmental medicine in the context of a moderate WBH up to max. 3 h treatment time	Treatment of chronic infections or oncological applications with extreme WBH

The treatment conditions in this study were a duration of 1 h at a maximum core body temperature of 39 °C, i.e. the moderate form of whole-body hyperthermia. Known effects of moderate WBH are increased blood flow to organs and tissues, intensification of supply and disposal, acceleration of metabolism [69,70], stimulation of the endocrine system [71], stimulation of the immune system, reduction of muscle tone and acceleration of nerve conduction [72,73]. Moderate WBH is used for the following conditions: arterial hypertension [74], chronic back pain [75], fibromyalgia syndrome [76], psoriatic arthritis [77], ankylosing spondylitis [78], systemic scleroderma [79], major depressive disorder [17] and cancer (as a complementary measure to standard therapies and immunomodulation) [80]. As mentioned above, this warming of the body's core temperature is achieved using water-filtered infrared-A radiation. Infrared-A radiation is short-wave IR radiation in the wavelength range from 780 to 1400 nm and is generated by a bulb emitter. The special feature of wIRA radiation is that this emitter is encased in a layer of water, among other things. This layer of water serves as a filter and the filtered radiation obtained is very similar to the earthly solar spectrum in the IR range. [81] As shown in **Figure 1**, the spectral transmission of the skin begins with long-wave visual light of around 600 nm wavelength and passes through the entire infrared-A up to its upper long-wave limit of around 1,400 nm wavelength. In contrast, the skin is almost impenetrable to heat radiation from the spectral ranges of infrared-B and infrared-C. This is why infrared-A heat radiation is referred to as 'deep heat', while infrared-B and infrared-C radiation is only referred to as 'surface heat'. [82]

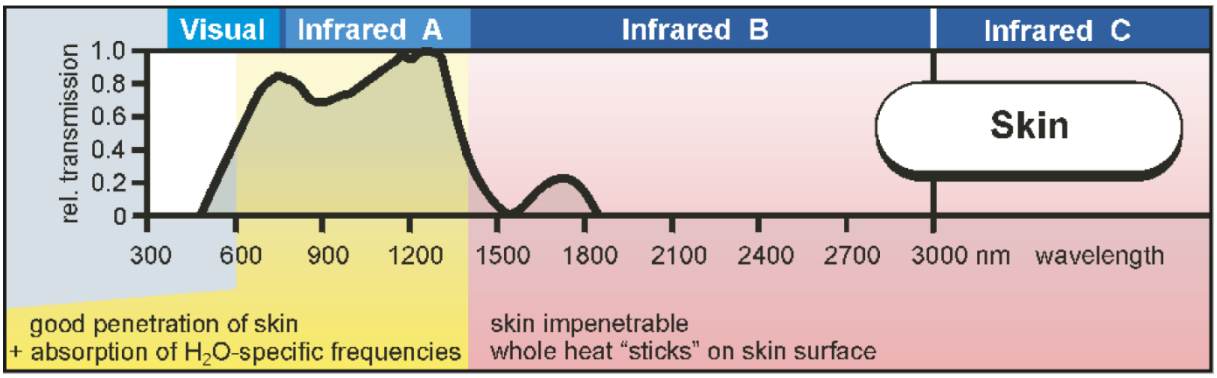

Figure 1: Spectral transmission of the skin. Infrared-A heat radiation is referred to as 'deep heat' because of the skin's permeability to infrared-A. Infrared-B and infrared-C are referred to as 'surface heat' because the skin is impenetrable to heat radiation from this spectral range. [82]

Red light emitters or halogen lamps are well-known and powerful radiant heaters. The latter usually operate at a higher output. The following illustration of the spectral distribution of a halogen lamp shows that its heat radiation contains 40% of the undesirable infrared-B and infrared-C radiation which are harmful to the skin (**Figure 2**).

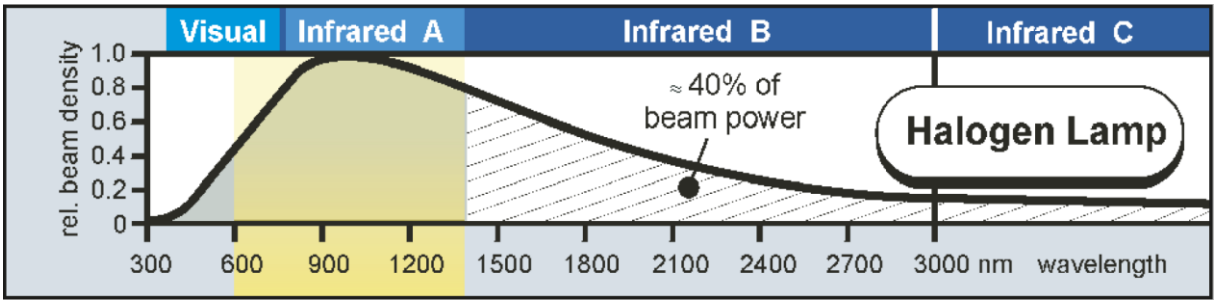

Figure 2: Spectral distribution of a halogen lamp. A halogen lamp contains 40% of the undesirable infrared-B and infrared-C radiation, which are harmful to the skin. [82]

Water is the most suitable filter for eliminating infrared-B and C radiation, as water, like skin, has a selective permeability to infrared radiation. This property results from the fact that 75% of an adult's skin consists of water. Just like the skin, water is a good transmitter of infrared-A radiation. While infrared-B and infrared-C are almost completely absorbed, there are only small absorption bands in the spectral range of infrared-A (at 950 nm and 1,150 nm) (**Figure 3**).

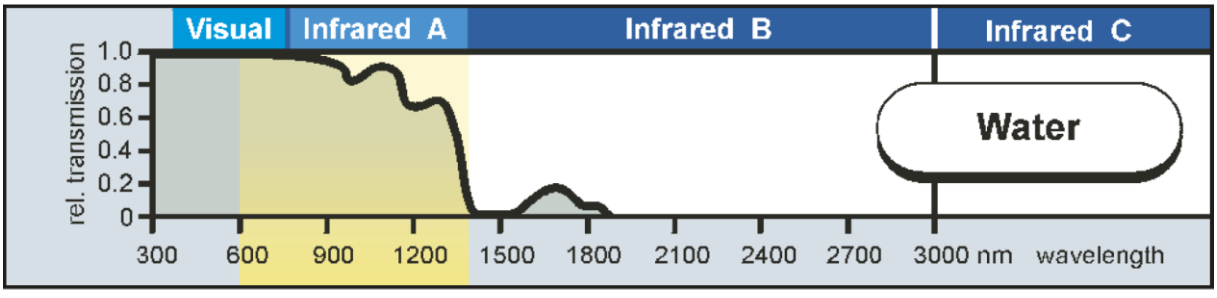

Figure 3: Spectral transmission of water. As 75% of an adult's skin consists of water, water is the most suitable filter for eliminating infrared-B and C radiation. Just like the skin, water is a good transmitter of infrared-A radiation, while infrared-B and infrared-C are almost completely absorbed. [82]

If a water filter is placed in front of a halogen lamp, heat radiation is generated with a spectral distribution that almost corresponds to the spectral transmission of the skin (**Figure 4**).

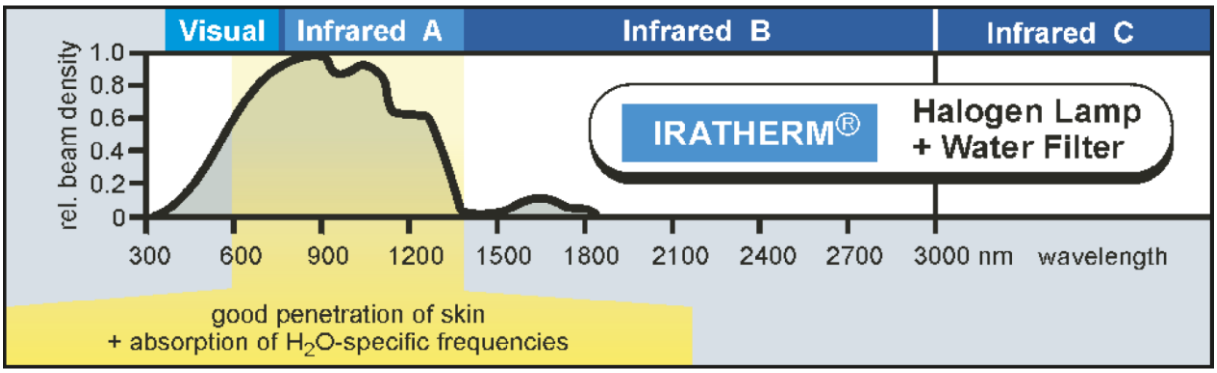

Figure 4: Spectral distribution of a halogen lamp with water filter. The unwanted infrared-B and infrared-C radiation, which are harmful to the skin, are filtered out by water. [82]

Water-filtered radiation is therefore an established form for carrying out hyperthermal applications. [9] In this context, it has already been shown in volunteers that increased temperature is associated with increased oxygen partial pressure and improved blood flow [10]. Clinical effects of wIRA in the form of whole-body hyperthermia have been demonstrated in the treatment of muscular pain [83], stimulation of the metabolism [84], and stimulation of the hormone and immune systems [85], among others. [82]

1.3 Autophagy

Impaired autophagy is associated with various diseases or pathophysiological conditions, including neurodegenerative, infectious, autoimmune, cardiovascular, rheumatic, metabolic, pulmonary and malignant diseases as well as ageing [20]. The link between autophagy and pathological processes is based on the fact that it is significantly involved in cellular homeostasis and the energy balance of the cell. The role of autophagy is the lysosomal degradation of parts of the cytoplasm and organelles, either because they are harmful, such as damaged organelles, or because the resulting degradation products are necessary to support metabolism. [18]

To date, four main pathways for the transport of autophagic substrates to the lysosomes have been distinguished: microautophagy, chaperone-mediated autophagy (CMA), crinophagy and macroautophagy (**Figure 5**). Microautophagy involves the direct uptake of cytoplasmic components through the lysosomal membrane [86]. Proteins that are degraded by CMA are identified in the cytosol by a chaperone complex (cognate heat shock protein of 70 KDa) that brings the substrate protein to the surface of the lysosomes after binding to the desired pentapeptide motif (KFERQ-like motif). Binding of the substrate to the cytosolic tail of the receptor protein lysosomal membrane protein 2A (LAMP-2A) promotes multimerisation of LAMP-2A to form a translocation complex. After unfolding, the substrate proteins cross the lysosomal membrane and reach the lysosomal

matrix where they are completely degraded. [87] During crinophagy, secretory granules that are no longer required or obsolete fuse directly with late lysosomes to eliminate unused secretions from the cytoplasm [88].

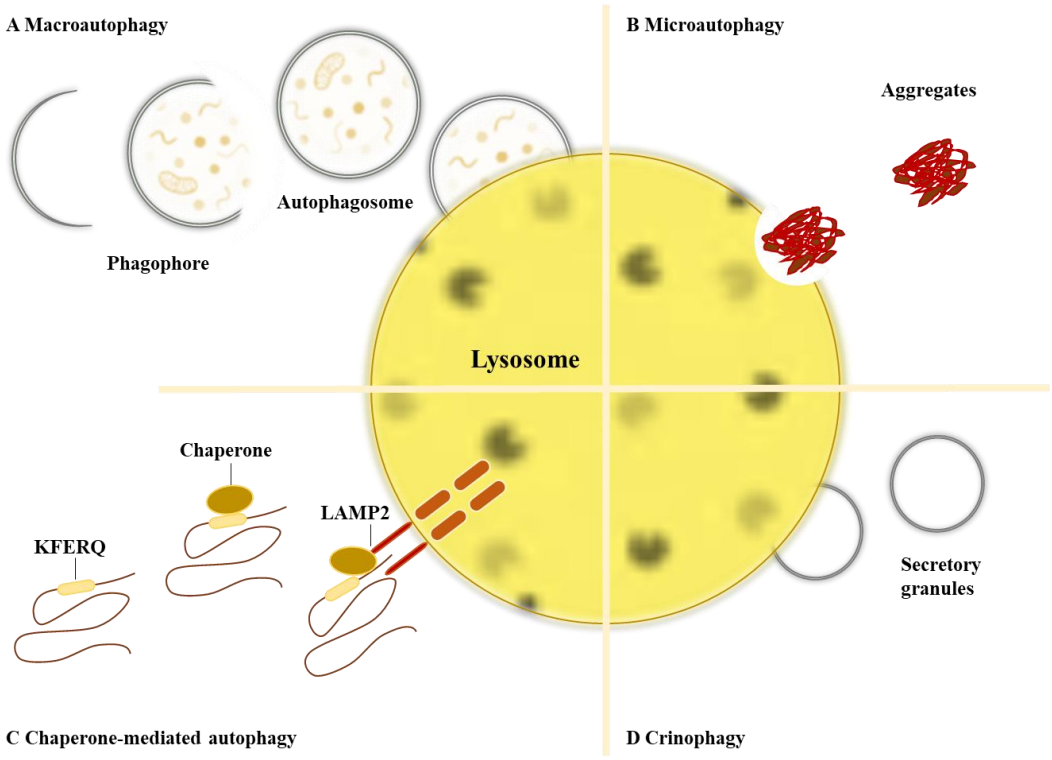

Figure 5: Four types of autophagy: macroautophagy, microautophagy, chaperone-mediated autophagy and crinophagy. A Macroautophagy involves the different phases of phagophore, autophagosome and autolysosome assembly for cargo degradation. **B** In microautophagy, the cytosolic components enter the lysosome directly by fusing with the lysosomal membrane. **C** Proteins to be degraded by chaperone-mediated autophagy contain the unique motif KFERQ, which is recognised by the chaperone complex Heat Shock Cognate Protein 70 (Hsc70). On the lysosomal surface there is a protein called Lysosomal Membrane Protein 2A (LAMP-2A), which acts as a receptor for the substrate Hsc70 complex. **D** Crinophagy describes the direct fusion of secretory vesicles with lysosomes (Figure adapted from [89]).

Macroautophagy is by far the best characterised form of autophagy. For this reason, the term autophagy is used hereafter for macroautophagy. The autophagy process can be divided into six phases: initiation, nucleation, elongation, maturation, fusion and degradation (**Figure 6**). The initiation of macroautophagy can be triggered by stress factors such as nutrient deficiency, growth factor deprivation, oxidative stress and protein aggregation and includes the activation of unc-51 like autophagy activating kinase 1 (ULK1). Nutrient deficiency inhibits the Mechanistic Target of Rapamycin Complex 1 (mTORC1), a highly conserved negative regulator of autophagy. When nutrients are sufficient, mTORC1 phosphorylates ULK1 to inhibit autophagy. Upon starvation, mTORC1 sites on ULK1 are dephosphorylated and ULK1 dissociates from mTORC1, activating ULK1 kinase activity. The energy sensor AMP-activated protein kinase (AMPK) can also trigger autophagy by activating ULK1 through phosphorylation at low energy levels/glucose, i.e. when the

AMP/ATP ratio is elevated. [90] ULK 1 is part of the ULK1 initiation complex, which also contains the subunits autophagy related 13 (ATG13), focal adhesion kinase family-interacting protein of 200 kDa (FIP200) and ATG101. ATG101 binds and stabilises ATG13 and FIP200 acts as a scaffold protein. After activation, the ULK1 complex is recruited to the phagophore assembly site (PAS) and anchored by ATG13. Class III PI3K complex I (PI3K) is required for nucleation. This complex is specific for autophagy and contains Beclin1, vacuolar protein sorting 34 (VPS34), VPS15 and ATG14L. ATG14L interacts and binds to ATG13 of the ULK1 complex and thus to the PAS. The major component of the PI3K complex, VPS34, is the catalytic subunit and produces phosphatidylinositol-3-phosphate (PI3P) at initiation sites. VPS15 is a scaffold and protein kinase and binds to PIK3C3 to form the catalytic arm of PI3KC3-CI. Beclin1 is a central regulator that interacts with a variety of proteins and has three functional domains. These include the N-terminal B cell lymphoma-2 (Bcl-2) homology 3 domain (BH3), which interacts with the Bcl-2 family protein Bcl-XL. The second functional domain is the central coiled-coil domain (CCD). This domain mediates the interaction of Beclin1 with ATG14L and the UV radiation resistance-associated gene protein (UVRAG).The third domain is a C-terminal evolutionarily conserved domain (ECD), which mediates the interaction of Beclin1 with VPS34 and thus the activation of the kinase activity of VPS34 to regulate the size and number of autophagosomes. In addition to recruiting the PI3K complex, the ULK1 complex can also recruit the ATG9A traffic system, which contains ATG9A, WD-repeat protein interacting with phosphoinositides (WIPI)1/2 and ATG2A. ATG9A, the only transmembrane protein among the ATG core proteins, shuttles back and forth between the PAS and other membrane components in the form of ATG9A vesicles. Therefore, ATG9A vesicles are considered as carriers of membranes to promote expansion. ATG9A is required for the recruitment of the light chain 3 system of microtubule-associated protein 1 (LC3) and WIPI1/2 to the site of autophagosome formation and for phagophore expansion and elongation. The WIPI1/2-ATG2 complex is involved in the formation of the ATG9A-WIPI1/2-ATG2 trafficking system, mediates and regulates the ATG9A cycle and promotes the formation of LC3-positive autophagosomes during autophagy. The WIPI1/2-ATG2 complex localises to the expanding edge of the isolation membrane and plays a key role in the elongation and/or closure of the isolation membrane. During the expansion process, two ubiquitin-like conjugation systems are essential: the ATG12 and the LC3 system. ATG12 is sequentially activated by the ubiquitin-activating enzyme ATG7, and the ubiquitin-conjugating enzyme ATG10. After activation, it is conjugated to ATG5 to form an ATG12-ATG5-ATG16L1 complex at the autophagosomal membrane, which is important for the formation of the LC3 conjugation system. The LC3 conjugation system is downstream of the ATG12 system in the context of ATG protein organisation. Prior to conjugation, the LC3 precursor (ProLC3) must be cleaved by the cysteine protease ATG4 to expose the C-terminal glycine. The product, cytosolic LC3-I, is then activated by the enzyme ATG7 and the enzyme ATG3 and finally

conjugated to phosphatidylethanolamine (PE) to form the membrane-associated LC3-PE (LC3-II). In contrast to ATG12 conjugation, the final step of ATG3 conjugation requires an ubiquitin ligase enzyme, the ATG12-ATG5-ATG16L1 complex. Mediated by the two ubiquitin-like ATG conjugation pathways, the isolation membrane finally forms a closed bilayered membrane structure, the mature autophagosome with an inner and an outer membrane. The final step of autophagy is the fusion between the double-membrane autophagosome and lysosome, which leads to degradation of the autophagic cargo by the lysosomal hydrolases. The precise mechanism of autophagosome–lysosome fusion is still elusive. Three intracellular membrane-trafficking-associated protein families, RAS-related GTP-binding protein (RAB) GTPases, membrane-tethering complexes, and soluble-N-ethylmaleimide-sensitive factor attachment protein receptors (SNARE) proteins, are known to be involved in this process. [91–93]

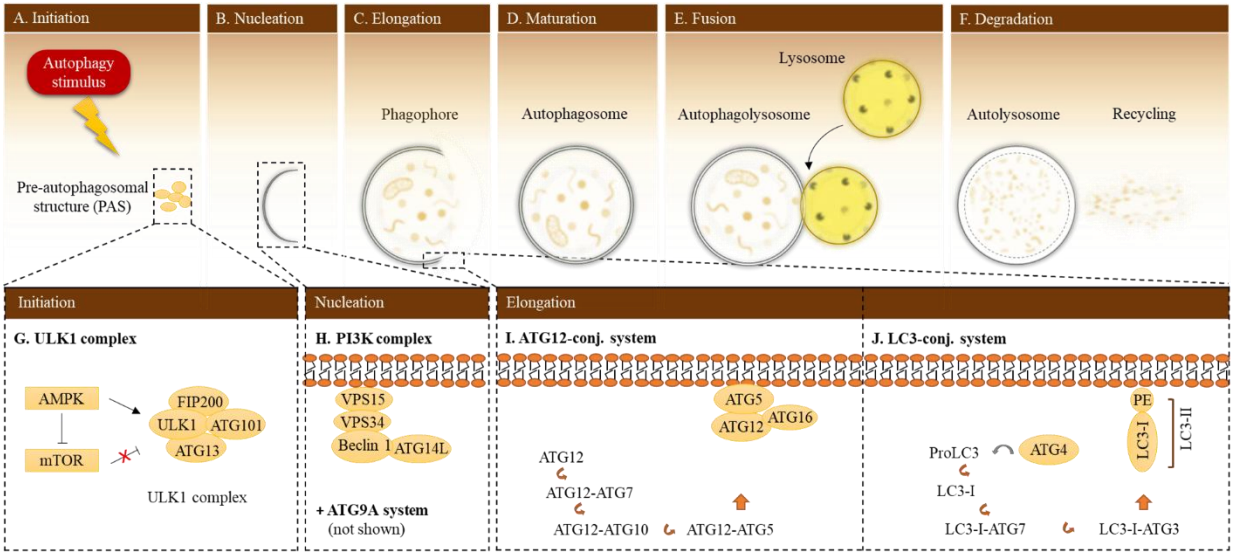

Figure 6: Schematic overview of autophagy. A Initiation of the process by the targeting of PAS by the ULK1 complex (**G**) after an autophagy stimulus. **B** Nucleation, ATG proteins forming the PI3K complex (**H**) and lipids are recruited to assemble the phagophore. **C** Elongation, cytoplasm and organelles are enveloped and engulfed by the conjugation systems ATG12 (**I**) and LC3 (**J**), the isolation membrane forms a closed bilayered membrane structure, the mature autophagosome (**D**). Docking and fusion (**E**) between autophagosome and lysosome with subsequent degradation (**F**) of the cargos in the autolysosome (Figure adapted from [93]).

This form of autophagy merely describes the mass degradation for the recycling of building blocks to compensate for nutrient deficiency and is presumably rather non-selective with regard to its substrates, the so-called cargoes. However, there is also another form of autophagy, the selective form, which is controlled by specific receptor proteins. This form of autophagy contributes to intracellular homeostasis in non-starved cells by selectively degrading cargo such as aggregated proteins, damaged mitochondria, excess peroxisomes and invading pathogens. Examples of forms of selective autophagy include mitophagy, pexophagy, ER phagy, ribophagy and lipophagy. One of these forms, namely mitophagy, is discussed in more detail in one of the following chapters (1.7). [19]

1.4 Measurement of Autophagy

A central method in the discovery and investigation of the autophagic process was electron microscopy. Using this method, irregularly shaped double membrane structures containing mitochondria, ER and ribosomes without hydrolytic enzymes were found and labelled as autophagosomes. This structure is later observed as a single membrane structure, the so called autolysosome, which exhibits different stages of organelle degradation by lysosomal enzymes. Based on these discoveries, de Duve defined this type of transfer of cytoplasmic material to the lysosomes for degradation as 'autophagy' in 1963. However, apart from the enormous importance of electron microscopy for these discoveries, this method is more suitable for studies on the morphology and location of autophagosomes than for quantification. In addition, the interpretation of the results achieved by this method requires a high level of expertise on the part of the user, combined with many years of experience. Further investigations of the autophagy process revealed specific proteins that are central to the function of the process and can therefore be used as markers for autophagy. [94] The most commonly used autophagosome marker at present is LC3, more precisely the membrane-bound form LC3-II. One method for determining LC3-I and LC3-II is the immunoblotting test. However, this method requires a large amount of sample material, is very time-consuming and the antibodies usually have a higher affinity for LC3-II, so that the signal ratio of LC3-I and LC3-II does not reflect the quantity ratio of cytosolic and membrane-bound LC3. [95] Other methods such as the LC3-HiBiT reporter assay or other reporter systems are not suitable for measuring the immediate cellular response, as transfection is required [96]. In this study, two cellular assay systems were established for the measurement of autophagy, one for fibroblasts and, as this assay was not suitable for human PBMCs, another assay was established. The CYTO-ID® Autophagy Detection Kit was used to quantify autophagosomes per nucleus in human fibroblasts. The fibroblasts used were obtained from skin biopsies and provide a powerful tool for studying skin behaviour under different conditions. Dermal fibroblasts are the most important cell type in the connective tissue of the skin, more precisely in the dermis. They also play an essential role in skin wound healing and skin bioengineering. [97] For autophagosome detection the CYTO-ID® assay uses a specific green dye that has been optimised by identifying titratable functional components that allow minimal staining of lysosomes while showing bright fluorescence when incorporated into pre-autophagosomes, autophagosomes and autolysosomes. In addition, staining the nucleus with Hoechst enables the detection of autophagosomes per nucleus (**Figure 7**).

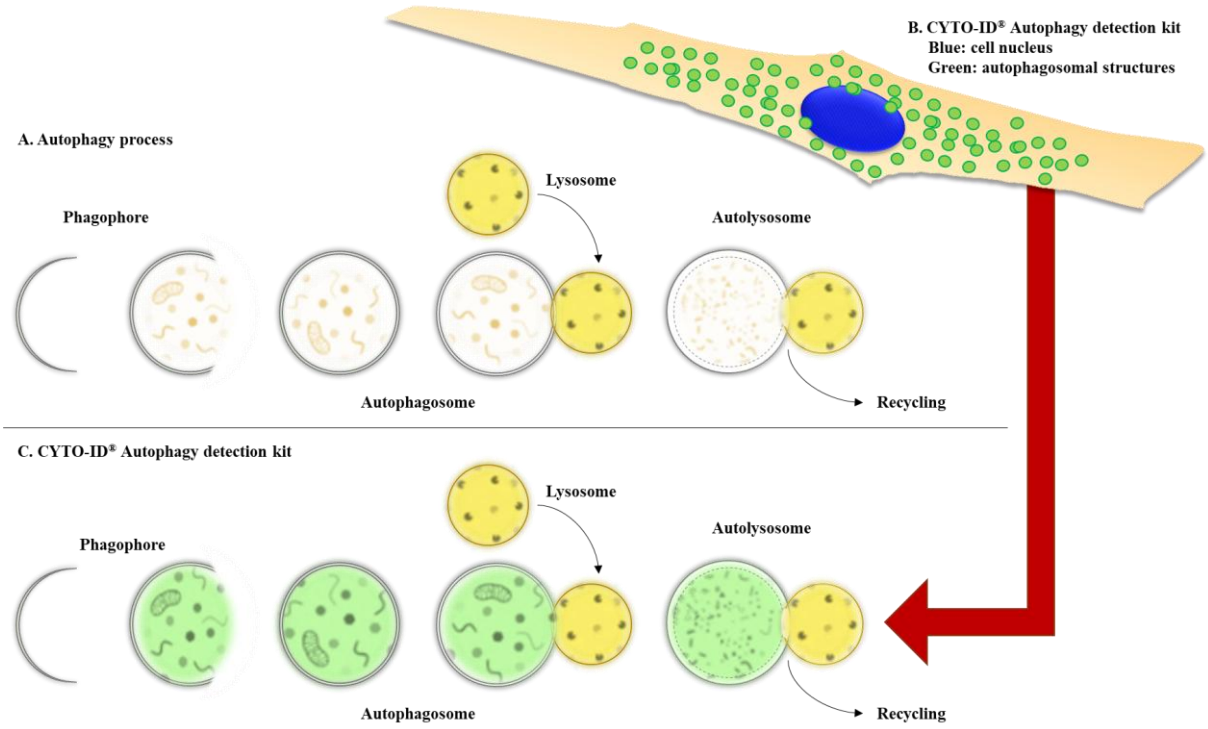

Figure 7: Schematic test principle of the CYTO-ID® Autophagy Detection Kit. A Overview of the autophagy process. **B** Human fibroblasts after CYTO-ID® performance with stained nucleus (blue) and autophagosomal structures (green). **C** Stained autophagosomal structures after the CYTO-ID® assay.

The subsequent imaging of the stained cell is carried out using a cell imager and analysed by a special software. The software first prepares the images in several image processing steps for the subsequent analyses. The cell nuclei are then counted and a defined mask is placed around each nucleus. All autophagosomes per mask are counted and assigned to the corresponding cell nucleus. (**Figure 8**)

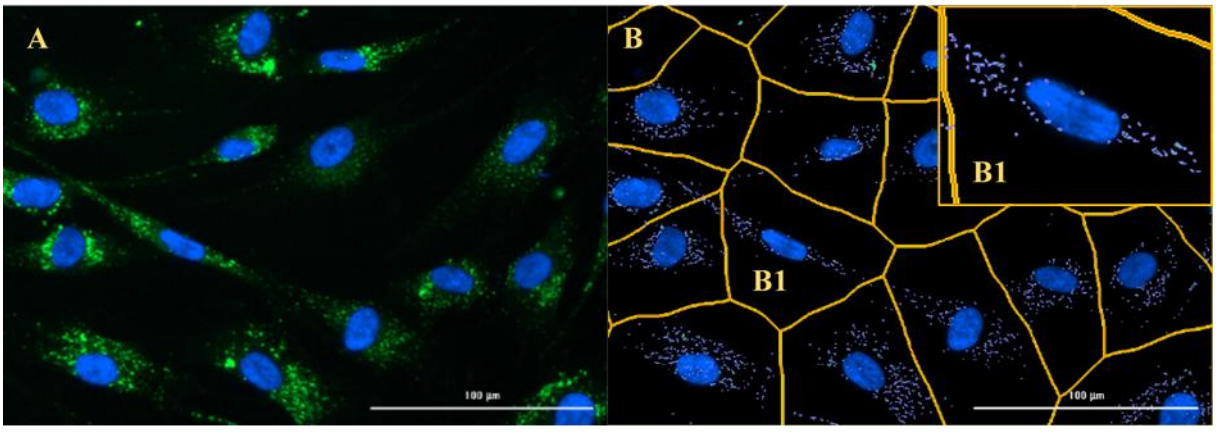

Figure 8: Image processing and subsequent analyses. **A** Image processing in several steps. **B** Software analyses of the cell images. **B1** Predefined masks are placed around the cell nuclei. All autophagosomes in this area are counted and assigned to the respective cell nucleus.

The CYTO-ID® method is not suitable for human PBMCs due to their morphology. PBMCs are very small and non-planar, which makes it difficult for the imager to find the focus and for the software to distinguish individual autophagosomes. For this reason, a different method was established to analyse PBMCs. The Guava® Autophagy LC3 Antibody-based Assay Kit was used to analyse this type of cells. As the name suggests, the principle of this assay is the labelling of LC3 by an anti-LC3 mouse monoclonal antibody conjugated to FITC (**Figure 9**). The antibodies are specific for LC3 and allow quantification of the protein by measuring FITC intensity using fluorescence-activated cell sorting (FACS).

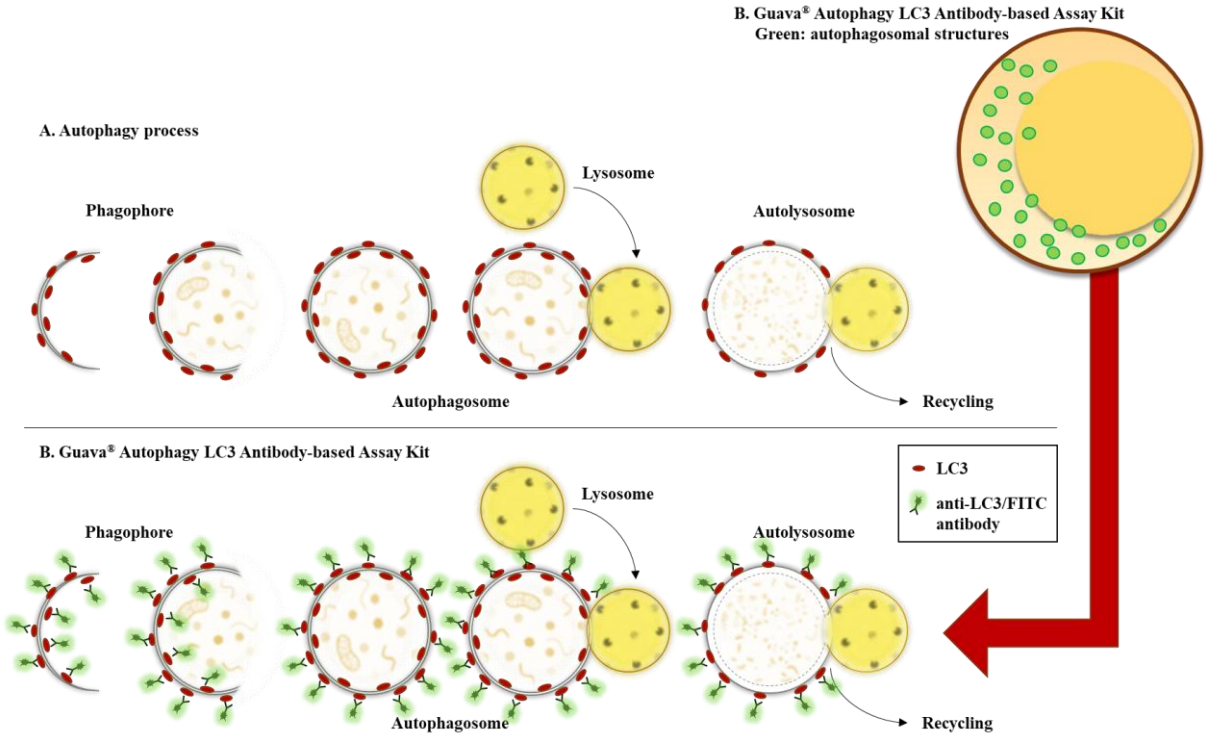

Figure 9: Schematic test principle of the Guava® Autophagy LC3 Antibody-based Assay Kit. **A** Overview of the autophagy process. **B** Human PBMC after Guava® performance with labelled LC3 by anti-LC3B antibody conjugated to FITC. **C** Labelled autophagosomal structures after the Guava® assay.

However, there are two problems that need to be eliminated. Firstly, the antibody is too large to penetrate the plasma membrane of the cells and secondly, the antibody cannot distinguish between the different forms of LC3 (LC3-I and LC3-II), whereby only LC3-II can be used as a membrane-bound form for statements about autophagosomal structures. As a solution to both limitations, the kit provides a reagent that permeabilises the cell membrane. This permeabilisation allows the antibody to reach its target and allows to distinguish the membrane-bound form (LC3-II) from the cytosolic form (LC3-I), as the cytosolic form leaves the cell through the holes in the membrane during the washing steps (**Figure 10**). The remaining membrane-bound LC3-II can now be quantified by FACS analysis.

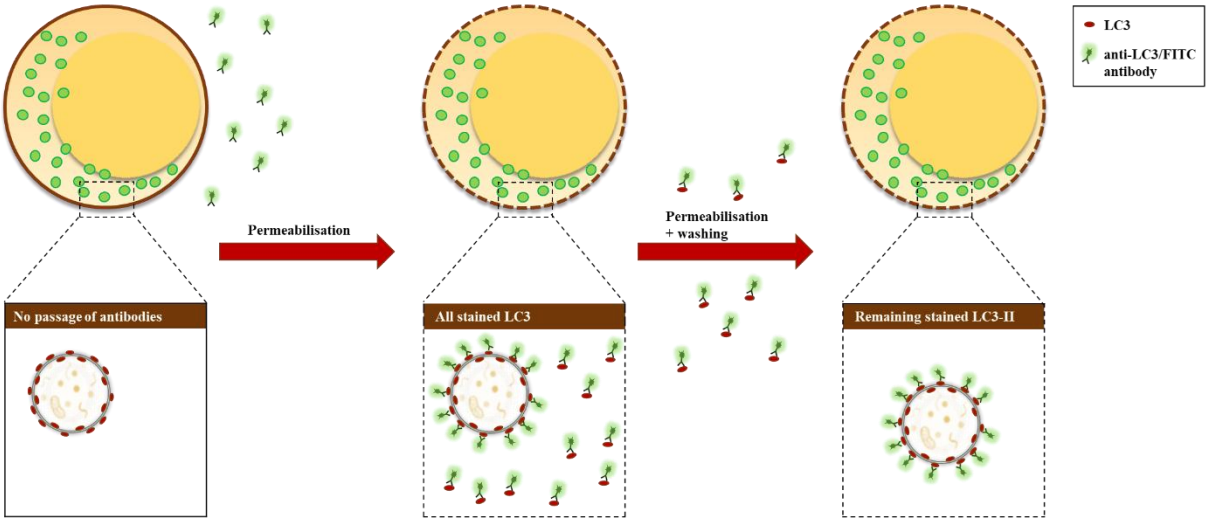

Figure 10: Permeabilisation of the cell membrane of PBMCs for LC3-II measurement. Since the anti-LC3/FITC antibody cannot penetrate the cell membrane and distinguish between the cytosolic and the membrane-bound form of LC3, the cell membrane is permeabilised and the cytosolic LC3 is washed out.

1.5 Mitochondrial function

As mentioned earlier, organelles are degraded by autophagy to maintain cellular homeostasis or to protect the cell from potentially harmful cellular organelles, like dysfunctional mitochondria. Mitochondrial dysfunction is associated with many common diseases. These include tumour diseases, inflammatory responses and neurodegenerative processes [98], such as Parkinson's, Alzheimer's and Huntington's disease [99]. This link between mitochondrial dysfunction and disease is based on the fact that mitochondria are involved in almost every cellular function and reflects the importance of healthy mitochondrial function. Mitochondria are involved in the regulation of apoptosis and ageing [100] as well as in the processes of autophagy (see chapter 1.7), stem cell differentiation and immune defence [101]. The mitochondrial function of regulating reactive oxygen species levels and calcium signalling is also important [102]. They are also involved in the synthesis of iron-sulphur clusters, the β-oxidation of fatty acids or the biosynthesis of haem, various phospholipids and other metabolites [103]. Mitochondrial dynamics, i.e. the fission and fusion of mitochondria, is an important component of cellular quality control. Defects have a detrimental effect on the bioenergetic supply and contribute to the development of neurodegenerative diseases. [104] For a long time, it was assumed that mitochondrial DNA only coded for 13 proteins that remain in the mitochondria. However, over twenty years ago, humanin was discovered, the first of its kind, a peptide that is encoded by mitochondrial DNA but is biologically active outside the mitochondrion. Since then, humanin has been found to inhibit apoptosis by interacting with pro-apoptosis proteins or with receptor proteins on the cell surface that are involved in metabolism and inflammatory signalling, among other things. In the meantime, eight more peptides of this type have been found and defined as mitochondrial-derived peptides (MDPs). [105] However, the main mission of mitochondria is the production of energy in the form of ATP. Without mitochondria, the entire ATP production would depend on glycolysis, which produces 15 times less ATP than oxidative phosphorylation in the mitochondria. The very mobile and plastic organelle has a radius of about 0.5 - 1 µm and takes up a considerable part of the cytoplasm. Each mitochondrion is enveloped by two specialised membranes that have very different functions. This forms two separate compartments of the mitochondria, the mitochondrial matrix and the intermembrane space. The inner mitochondrial membrane is usually convoluted and forms a series of folds, the cristae, which protrude into the matrix. Mitochondria can utilise pyruvate, which is derived from glucose, or fatty acids, which are derived from lipids, as raw material for energy production. The molecules are transported into the matrix of the mitochondria and converted by enzymes into the intermediate product acetyl-CoA, which is then fed into the citric acid cycle. The citric acid cycle oxidises the acetyl groups, generating high-energy electrons and transferring them to the NAD^+ and FAD molecules. The now formed high-energy molecules NADH and $FADH_2$ in turn transfer their high-

energy electrons to the inner membrane of the mitochondria, where they enter the electron transport chain. [106] Electrons from NADH enter the electron transport chain in complex I. These electrons are first transferred from NADH to flavin mononucleotide and then to coenzyme Q (CoQ). Coenzyme Q or ubiquinone is a small, lipid-soluble molecule that carries electrons from complex I through the membrane to complex III. In complex III, the electrons are transferred from cytochrome b to cytochrome c. Cytochrome c, a peripheral membrane protein bound to the outside of the inner membrane, then carries the electrons to complex IV, where they are finally transferred to O_2. Electrons from the citric acid cycle intermediate succinate enter the electron transport chain via $FADH_2$ in complex II. They are then transferred to coenzyme Q and transported through the rest of the electron transport chain as described above. The transfer of electrons from $FADH_2$ to coenzyme Q is not associated with a significant reduction in free energy, so that no protons are pumped through the membrane of complex II. [107] In contrast, complexes I, III and IV each pump protons into the intermembrane space. This process is called chemiosmosis because of the difference in H^+ ion concentration between the intermembrane space and the mitochondrial matrix and is utilised by the last complex of the respiratory chain, complex V or ATP synthase. ATP synthase consists of numerous protein subunits, including F0 and F1. The F0 part is hydrophobic, rooted in the phospholipid bilayer and contains a channel through which H^+ ions can pass to the F1 part. The hydrophilic F1 part is the most important catalytic site. H^+ ions migrate from the F0 part to the F1 part and force the F1 part to rotate, which catalyses the binding of ADP and inorganic phosphate (Pi) to produce ATP (**Figure 11**). [106–108])

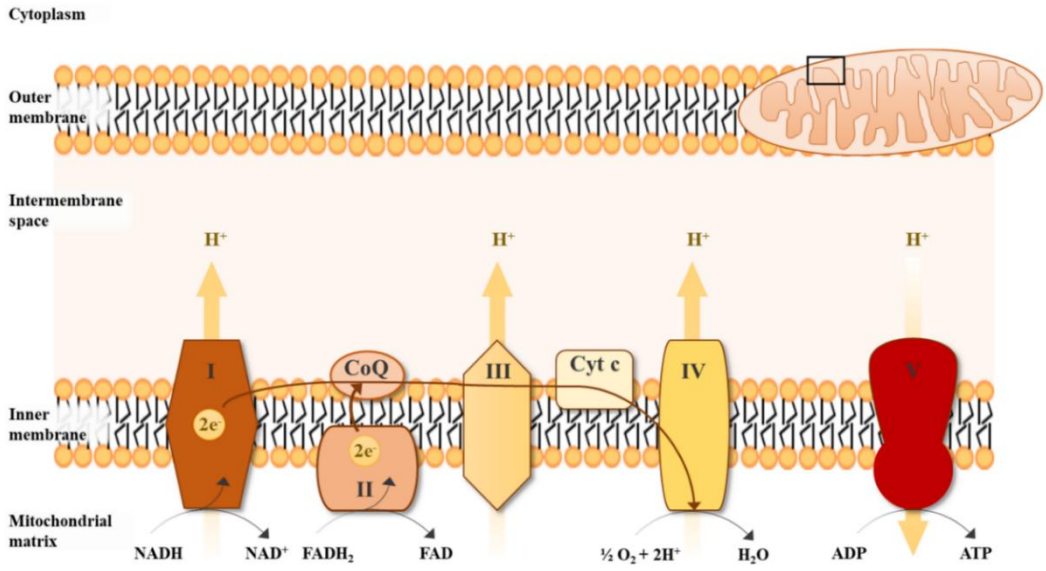

Figure 11: Schematic overview of oxidative phosphorylation in mitochondria. The electrons from NADH enter the electron transport chain in complex I and the electrons from $FADH_2$ enter in complex II. All electrons are first transferred to coenzyme Q and then to complex III. The electrons are further transported to cytochrome c and finally to complex IV, where they are transferred to O_2. Due to the considerable reduction in free energy in complexes I, III and IV, protons are pumped into the intermembrane space. These protons are used to drive complex V, which catalyses the binding of ADP and inorganic phosphate (P_i) to produce ATP.(Figure adapted from [109])

1.6 Measurement of Mitochondrial function

For the analysis of mitochondrial function the Agilent Seahorse XF Cell Mito Stress Test was used. This test enables the measurement of key parameters of mitochondrial function by directly measuring the oxygen consumption rate (OCR) of cells on the Seahorse XFe analyzers. The assay uses the built-in injection ports on XF sensor cartridges to add modulators of respiration into each well of the cell culture plate during the assay to reveal six different parameters of mitochondrial function. Firstly, the basal oxygen consumption, i.e. the basic level, is determined without the addition of a substance. This is followed by the addition of oligomycin, which inhibits the complex V. Respiration decreases by the amount of oxygen previously consumed for ATP synthesis. In the next step, carbonyl cyanide-4-(trifluoromethoxy)-phenylhydrazone (FCCP) is injected, which makes the inner mitochondrial membrane permeable to protons and thus decouples the electron transport chain from ATP synthase. As a result, the mitochondria work at maximum capacity, which allows their maximum respiration to be determined. Finally, antimycin A and rotenone are added, blocking complexes III and I of the mitochondrial respiratory chain, which then comes to a complete standstill. The remaining oxygen consumption can now be allocated to the entirety of the non-mitochondrial respiratory processes. Finally, a further parameter, the so-called proton leak, can be calculated. This refers to protons that diffuse through the inner mitochondrial membrane back into the matrix. As this process occurs independently of the ATP Synthase, no ATP is generated (**Figure 12**). [110]

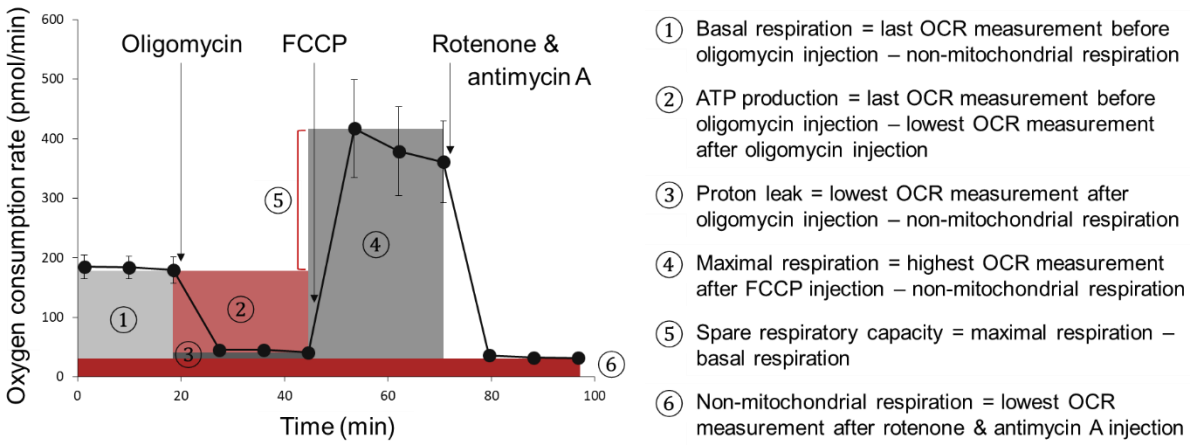

Figure 12: Schematic illustration of oxygen consumption over time during a Mito Stress Test. ① Basal respiration is defined as the last measurement point before oligomycin injection minus non-mitochondrial respiration. ② ATP production is defined as the last measured value before oligomycin injection subtracted by the lowest measured value after oligomycin injection. ③ Proton leak is the difference between the lowest OCR measurement after oligomycin injection and non-mitochondrial respiration. ④ Maximum respiration is defined as the highest measurement after FCCP injection minus non-mitochondrial respiration. ⑤ The spare respiratory capacity is the maximum respiration without basal respiration. ⑥ Non-mitochondrial respiration is the lowest OCR measurement after the last injection. [111]

1.7 Autophagy – Mitochondria crosstalk

The individual mechanisms and processes of our cells must be coordinated and work together in order to function as an overall cellular system. It is therefore important to consider the processes of autophagy and the function of mitochondria not only as individual, independent processes, but also to investigate their interactions with each other. Autophagy affects the health and number of mitochondria through the selective degradation of mitochondria in a process known as mitophagy. Severe damage can permeabilise mitochondrial membranes, leading to a loss of mitochondrial membrane potential. The loss of membrane potential is the starting point for mitophagy, as the voltage-sensitive kinase PINK1 is stabilised at the outer mitochondrial membrane. While PINK1 is continuously degraded in the mitochondria under normal circumstances, the rapid accumulation of PINK1 due to the loss of membrane potential activates the recruitment of Parkin. Parkin causes ubiquitin to be phosphorylated, leading to the formation of an ubiquitin chain on the surface of the mitochondria. Through the ubiquitin chain, more Parkin is recruited to the mitochondria. Subsequently, autophagy receptor proteins, including p62, contain both ubiquitin-binding domains (UBDs) that recognize phosphorylated ubiquitin chains, and LC3-interacting regions (LIRs) that facilitate interaction with LC3 family proteins, thereby initiating the autophagosome biogenesis machinery and degradation of the mitochondria (**Figure 13**). [112–114]

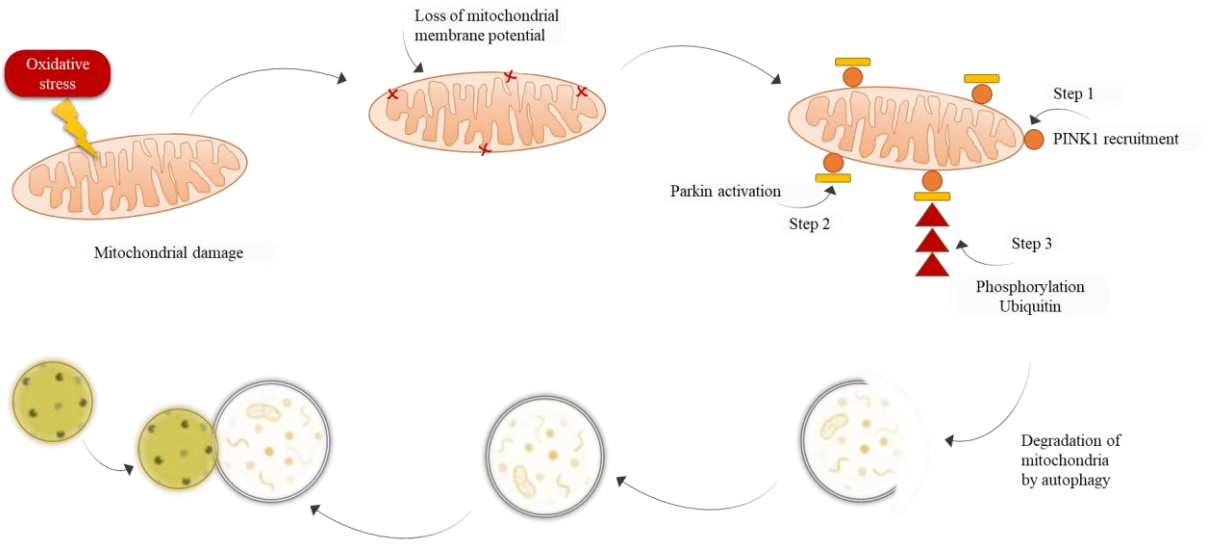

Figure 13: The pathway of mitophagy. The loss of mitochondrial membrane potential due to mitochondrial damage leads to the accumulation of Pink1. Pink1 activates the recruitment of Parkin, which causes the phosphorylation of ubiquitin and the formation of a ubiquitin chain. This chain is recognised by the autophagy mechanism and leads to the degradation of the labelled mitochondria. (Figure adapted from [112])

However, mitochondria are not only a substrate of autophagy, but there are several indications that mitochondria have an influence on the autophagic process. For example, the origin of the lipids of autophagosomal membranes is still controversial. In addition to possible origins such as the ER, the Golgi and the plasma membrane, there are also studies that point to mitochondria as a possible origin. [113,115] Another link between mitochondria and autophagy is the AMPK/mTOR regulation of autophagy. As already mentioned, an increased AMP/ATP ratio leads to the inhibition of mTOR by AMPK and activation of autophagy through the ULK1 complex. Since the mitochondria are the main source of ATP, the organelles can strongly influence the AMP/ATP ratio in the cell and thus the activation of autophagy. [116] There is also a complex interplay between oxidative stress and autophagy. It is known that ROS and changes in the cellular redox state can both trigger and regulate autophagy. For example, the autophagy protein ATG4 has been identified as the basis for the redox sensitivity of autophagy. In addition to the function of cleaving pro-LC3B to LC3B-I, ATG4 also has the function of removing LC3B-II from the autophagosome membrane by cleaving PE to recycle LC3B-I. [117] Oxidation of ATG4 inhibits the cleavage activity of ATG4 and enables LC3B-mediated autophagosome expansion. [118] On the other hand, autophagy may act as a cellular mechanism that regulates redox metabolism and can remove oxidatively damaged molecules under stress conditions. Autophagy removes damaged organelles such as mitochondria, which are an important source of mitochondrial ROS. Therefore, the removal of damaged mitochondria by mitophagy plays a protective role in maintaining normal cellular metabolism by reducing the generation of ROS and thus preventing the harmful effects of ROS. [119]

1.8 Associated Genes

In the previous chapters, the focus was on describing the cellular mechanisms of the investigated processes. However, the aim of this chapter is to look at these processes from a different perspective, namely by observing the mRNA expression of specific genes. All proteins required for the investigated processes have their origin in their specific gene. For this reason, the genes encoding the key proteins were selected to investigate the underlying molecular mechanisms of the selected cellular mechanisms. In the following, the selected genes of each investigated process are described individually.

Autophagy – associated genes

In order to obtain a good overview of the entire autophagic process, genes of proteins were selected that provide a picture of the regulation of autophagy on the one hand and the different stages during the autophagy process on the other. The genes of the proteins sirtuin 1 (SIRT1), forkhead box O3 (FOXO3) and AMPK were selected for the regulation of autophagy (**Figure 14**). To find out more about the molecular mechanisms during autophagy, the genes of the proteins ULK1, Beclin1, ATG7 and LC3B were analysed.

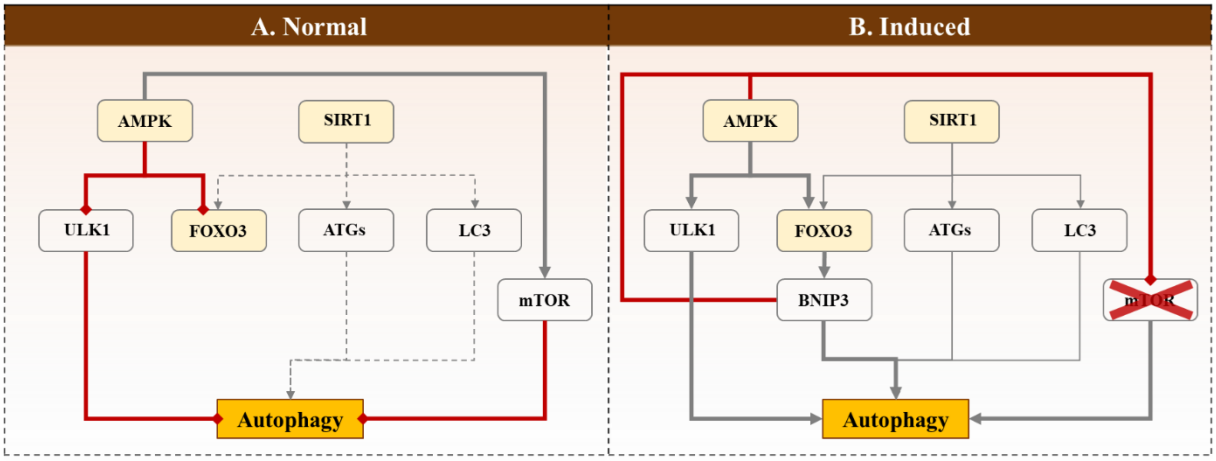

Figure 14: Schematic overview of the regulation of autophagy by AMPK, SIRT1 and FOXO3. A In the absence of an inductive energy stress inducer, autophagy occurs constitutively in the ground state (SIRT1). The energy sensor AMPK is not activated and therefore inhibits proteins such as FOXO3 and ULK1. mTOR inhibits autophagy by not being inhibited by AMPK. **B** Under energetic stress, AMPK activates autophagy directly through ULK1 phosphorylation. In addition, AMPK inhibits mTOR and activates FOXO3, both of which lead to the activation of autophagy. SIRT1 also activates autophagy through the activation of FOXO3. In addition, SIRT1 interacts directly with ATGs and LC3. FOXO3 activates autophagy via the BNIP3 signalling pathway

SIRT1 is a highly conserved nicotinamide adenine dinucleotide (NAD^+)-dependent histone deacetylase. The sirtuin family comprises seven members, sirtuin 1 to sirtuin 7, which are distributed differently in the cells, with sirtuin 1 being found in the nucleus and in the cytoplasm. [120] SIRT1 is regulated by cellular stress states, such as cellular starvation, heat and glucose deprivation, and

various protein factors. SIRT1 targets various factors regulating cell proliferation, differentiation, gene transcription, DNA damage repair, and autophagy in the cytoplasm and nucleus. [121] The protein regulates autophagy by influencing autophagy-related proteins (ATGs), forkhead box proteins (FOXOs) and the microtubule-associated protein light chain 3 (LC3). Under starvation conditions, SIRT1 directly deacetylates ATG5, ATG7, and ATG12, which in turn activates the formation of the ATG5-ATG12-ATG16 complex and contributes to the elongation of autophagic vesicles. [122] SIRT1 can also directly interact with FOXO3 to induce its deacetylation [123]. FOXOs are transcription factors that play a crucial role in DNA repair, oxidative stress, cell proliferation and apoptosis. [124] Deacetylated FOXO3 promotes BCL2/adenovirus E1B 19 kDa protein-interacting protein 3 (BNIP3) expression by binding to the BNIP3 promoter. [125] BNIP can regulate autophagy in three different ways. Either by direct binding and inhibition of mTOR, release of Beclin1 from an inhibitory complex with Bcl-2 or by induced permeabilisation of the mitochondrial membrane. [126] AMPK is a serine/threonine kinase that plays a fundamental role in the regulation of cellular energy balance. It is controlled by the AMP/ATP ratio. An increase in AMP and a decrease in ATP activates AMPK and triggers a series of subsequent physiological processes to rebalance the system. One physiological process targeted by the protein is the process of autophagy. AMPK activates this process directly by phosphorylating at least four sites on ULK1. In addition, autophagy is activated by the previously described process of inhibition of mTOR by AMPK. [127] Furthermore, FOXO3 is phosphorylated by AMPK, which in turn activates autophagy [128].

As already described, the process of autophagy can be divided into individual steps, namely initiation, nucleation, elongation, maturation, fusion and degradation. The selected genes are coding for proteins that are involved in initiation, nucleation and elongation. The investigated proteins ULK1, Beclin1, ATG7 and LC3 are highlighted in red in the following figure (**Figure 15**). The specific functions of these proteins are described in chapter 1.3.

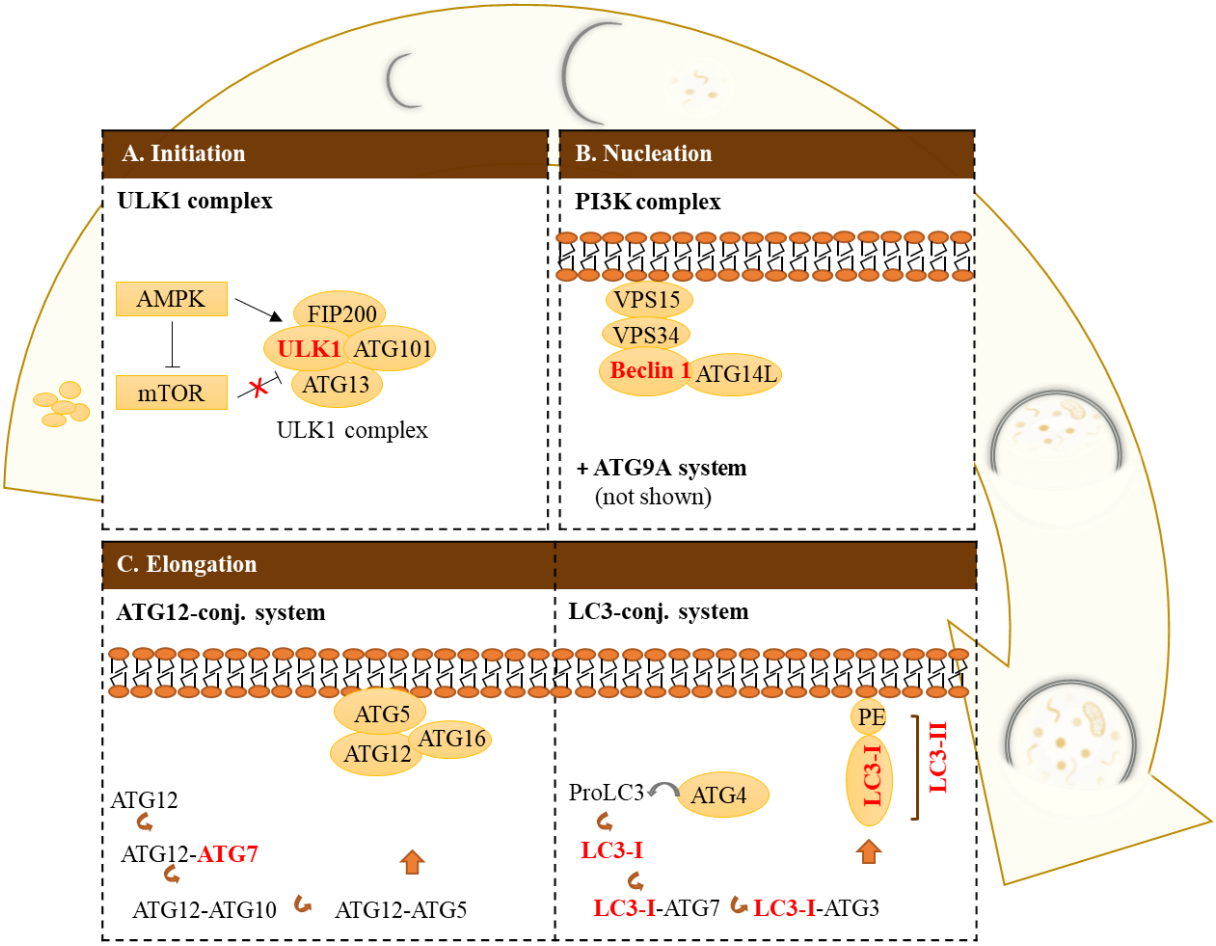

Figure 15: Quantification of mRNA expression of genes coding for the proteins ULK1, Beclin1, ATG7 and LC3. Proteins from three different steps of autophagy were selected. ULK1 is a key regulator in the initiation of autophagy. Beclin1 plays an important role in nucleation, and ATG7 and LC3 are required for the two conjugation systems during autophagosome elongation. (Figure adapted from [93])

Mitochondrial function - associated genes

In addition to autophagy, the integrity of mitochondrial function is also analysed. This examination includes a cellular assay that measures the oxygen consumption of the cells and thus allows conclusions to be drawn about various mitochondrial parameters (see chapter 1.6). On the other hand, the expression of certain genes associated with mitochondrial function is also analysed. These selected genes are coding for the proteins of sirtuin 3 (SIRT3), NADH: ubiquinone oxidoreductase nuclear subunit S1 (NDUFS1), transcription factor A, mitochondrial (TFAM) and superoxide dismutase 2 (SOD2). As SIRT3 is one of the most prominent deacetylases that can regulate acetylation levels in mitochondria, it was selected for this study. Like SIRT1, SIRT3 belongs to the sirtuin family and is mainly found in mitochondria. SIRT3 activates a number of substrates through deacetylation to promote mitochondrial function, increase ATP production and maintain mitochondrial metabolic homeostasis. [129] As already described in another chapter 1.7 of this thesis, there is a crosstalk between mitochondria and autophagy. The protein SIRT3 is another example of this interaction, as SIRT3 regulates mitophagy through multiple pathways, for example via the PINK11/Parkin signalling pathway. [130] In addition, SIRT3 is an important regulator of oxidative stress through the activation of SOD2, which is also examined in this work. [131] The mitochondrial SOD2 was chosen for investigation, because it is a major component of the metabolic machinery that handles ROS in the mitochondrial matrix. Specifically, SOD2 determines how much superoxide radical anion ($O_2^{\bullet-}$) is converted to hydrogen peroxide (H_2O_2). Its deletion, inhibition, or suppression causes significant oxidative damage to a variety of proteins. [132] This could lead to serious diseases such as neurodegenerative diseases like amyotrophic lateral sclerosis, Huntington's disease, Parkinson's disease and Alzheimer's disease [133]. Another protein whose dysfunction is associated with neurodegenerative diseases is TFAM. As the name suggests, TFAM is a mitochondrial transcription factor and is encoded in the nucleus. It plays an essential role in mtDNA metabolism and thus in mitochondrial biogenesis. Mitochondrial biogenesis is of crucial importance for the response to different physiological and environmental conditions, as the cellular metabolic functions require different amounts of energy. Most of that energy is provided by the oxidative metabolism of the mitochondria. [134,135] A dysregulation in the gene expression of TFAM could explain the lack of energy in ME/CFS patients by a lack of mitochondrial biogenesis, which is necessary to adapt to different energetic states. The last investigated mitochondrial-associated gene is NDUFS1, which codes for a protein in the mitochondrial respiratory chain. More precisely, NDUFS1 is the largest nuclear subunit of complex I. It is encoded by a nuclear gene and is responsible for the oxidation of NADH. [136] A study has shown that silencing of NDUFS1 in neurons impairs oxygen consumption and increases mitochondrial ROS formation, while upregulated NDUFS1 expression reduces ROS formation in astrocytes [137]. In skin fibroblasts

from patients with the NDUFS1 mutation, a high level of oxidative stress was observed, accompanied by a decrease in complex I activity, impaired oxygen consumption and increased glycolysis [138].

Additional genes

In addition to the genes just described that are associated with the cellular mechanisms of autophagy and mitochondrial function two additional genes were selected. These are the heat shock protein family A (Hsp70) member 5 (HSPA5) and interleukin-10 (IL-10), which are associated with the treatment method under investigation, namely hyperthermia. The ubiquitous and conserved heat shock proteins (HSPs) belong to a large family of proteins that are responsible for proteostasis. As their name suggests, HSPs react to heat, but also to other stress factors such as hypoxia, ischaemia, ROS or endotoxins and buffer these stress factors. Based on their molecular weight, HSPs are categorised into the families of large HSPs, HSP90, HSP70, HSP60, HSP40 and small HSPs, whose functions are involved in the entire metabolic process of proteins. They function as holdase, foldase, sequestrase, aggregase or disaggregase and work as a network to maintain proteostasis in the cells and as an efficient first line of defence in response to stress. HSPA5 is located in the endoplasmic reticulum (ER). [139] When the ER is stressed, HSPA5 is translocated to the cell surface, mitochondria and nucleus, where it forms a complex with other proteins to carry out its functions. As a master chaperone protein, HSPA5 in the ER reacts to the accumulation of misfolded or unfolded proteins and is involved in the degradation of misfolded proteins or in their correct folding. [140] Interleukin 10 (IL-10) is a cytokine that belongs to the class 2 cytokines. In humans, interleukin 10 is encoded by the IL-10 gene. [141] Cytokines are small secreted proteins that are released by different cell types and have specific effects on cellular signalling and communication by binding to their receptors on the cell surface. IL-10 is known to be a pleiotropic and potent anti-inflammatory and immunosuppressive cytokine produced by both innate and adaptive immunity. Dysregulation of IL-10 plays a role in the development of numerous inflammatory diseases such as neuropathic pain, Parkinson's disease and Alzheimer's disease. [142]

1.9 Investigation of human PBMC in the context with ME/CFS

As already described in chapter 1.1, the diagnosis of ME/CFS is mainly based on symptoms such as PEM, severe fatigue and flu-like symptoms. As symptom descriptions are often subjective, the biological characterisation of various biofluids such as saliva, cerebral spinal fluid (CSF), stool and urine can provide an objective systemic and local insight into the molecular disturbances underlying the disease pathology and symptoms. Another very important test material is whole blood and its fractions: serum/plasma and PBMCs. Blood serves as an important transporter of oxygen,

circulating nutrients, hormones and metabolites and reflects the systemic metabolic processes that contribute to the maintenance of homeostasis. A major advantage is that blood sampling is relatively simple and painless and that the isolation of PBMCs is also quick and easy. Different fractions of blood have different roles - plasma for transport and PBMCs for immune function. [143] As the name suggests, PBMCs are mononuclear cells of the blood, which mainly include lymphocytes, but also other cell types such as monocytes and dendritic cells. The frequency of these populations varies from person to person, but typically the populations are within a certain range, which is shown in **Table** 4.

Table 4: Frequency of the individual cell types in PBMCs. [144]

Human PBMCs	Frequency
Lymphocytes	70 – 90%
Total T cells (CD3+)	45 – 70%
CD4+ T cells	25-60% of total CD3
CD8 T cells	5 -30% of total CD3
Total B cells	5 – 15%
NK cells	5 – 10%
Monocytes	10 – 30%
Dendritic cells	1 – 2%
Stem cells	0.1 – 0.2%

Human PBMCs are not only used for molecular characterisation in medical examinations, but also in disease research. This includes, for example, the investigation of immunometabolic changes in PBMCs by RNA sequencing and gene expression [145] or proteomic profiling [146]. Furthermore, there are several research projects on PBMCs from ME/CFS patients for mitochondrial function, including studies on complex activity, cristae and ATP [147–149]. In the connection with this work, research in the field of autophagy in PBMCs of ME/CFS patients would also be of interest. In this regard, however, there is only one study on serum from ME/CFS patients [150]. Nevertheless, this does not rule out the possibility of investigating autophagy in PBMCs, as this has already been applied in many ways for other diseases or other applications [151–153].

1.10 Aims of this work

The multisystemic disease ME/CFS severely impairs the daily lives of those affected, and in severe cases patients are even bedridden. One of the main symptoms is fatigue, but difficulties sleeping, tender lymph nodes and pain are also common symptoms. In addition, all existing symptoms worsen after cognitive or physical exertion, known as PEM. To date, little is known about the disease, which leads to a lack of understanding and therefore too few treatment options to help those affected. Common treatment options include medications that target the symptoms, such as painkillers for pain or sleeping pills for sleep problems. Other methods include adapting lifestyle to the disease to avoid PEM and defining the patient's limitations to then minimise them. So the overall goal is to better understand ME/CFS and find possible treatments to improve the patient's quality of life.

This objective is pursued in this thesis and divided into three sub-questions:

1. **Do key cellular mechanisms differ in ME/CFS patients compared to healthy donors and if so, how?**
To answer these questions, PBMCs from healthy donors and ME/CFS patients were analysed and compared for autophagy and mitochondrial function.

2. **Does heat treatment have an effect on the central cellular mechanisms of isolated human cells?**
The effect of wIRA irradiation (39 °C, 1 hour) on autophagy, mitochondrial function and mRNA expression of related genes was investigated in isolated PBMCs from healthy donors and ME/CFS patients as well as in human fibroblasts from a healthy donor.

3. **Does whole-body hyperthermia in ME/CFS patients have an effect on central cellular parameters?**
The effect of a one-hour whole-body hyperthermia session with a maximum core body temperature (T_c) of 39 °C in ME/CFS patients on autophagy, mitochondrial function and mRNA expression of corresponding genes was investigated.

2 Materials and Methods

2.1 Materials

Table 5: Chemicals and Reagents

Chemical / Reagent	Manufacturer
Acridine Orange/Propidium Iodide (AO/PI) Stain	Logos Biosystems Inc., Anyang-si, South Korea
Antimycin A from *Streptomyces sp.*	Sigma-Aldrich / Merck KGaA, Darmstadt, Germany
Carbonyl cyanide 4-(trifluoromethoxy)phenylhydrazone (FCCP) ≥98%	Sigma-Aldrich / Merck KGaA, Darmstadt, Germany
Chloroquine diphosphate	Tocris BioscienceTM / Fisher Scientific GmbH, Schwerte, Germany
Dimethyl sulphoxide (DMSO) ≥99,5%, BioScience-Grade, for molecular biology	Carl Roth GmbH & Co. KG, Karlsruhe, Germany
di-Sodium hydrogen phosphate dihydrate (Na_2HPO_4 - 2 H_2O) ≥99.5%, p.a.	Carl Roth GmbH & Co. KG, Karlsruhe, Germany
Dulbecco's Modified Eagle's Medium (DMEM) - high glucose	Gibco™ / Fisher Scientific GmbH, Schwerte, Germany
Ethanol, ROTIPURAN®≥99.8%, p.a.	Carl Roth GmbH & Co. KG, Karlsruhe, Germany
Fetal Bovine Serum (FBS), Qualified	Gibco™ / Fisher Scientific GmbH, Schwerte, Germany
Ficoll-PaqueTM PLUS	Cytiva Europe GmbH, Freiburg i. B., Germany
Gentamycin 10 mg/mL	Gibco™ / Fisher Scientific GmbH, Schwerte, Germany
Hoechst 33342 ≥97.0%	Sigma-Aldrich / Merck KGaA, Darmstadt, Germany
HyCloneTM HyPureTM Molecular Biology Grade Water	GE Healthcare Life Sciences, Logan, USA
Isopropanol 70%, Molecular Biology Grade	Fisher BioReagents / Thermo Fisher Scientific Inc., Waltham USA
Oligomycin from *Streptomyces diastatochromogenes* ≥90% total oligomycins basis	Sigma-Aldrich / Merck KGaA, Darmstadt, Germany
PCR-grade H_2O	Roche Diagnostics / F. Hoffmann-La Roche AG, Basel, Schweiz
Poly-D-Lysine solution, 1.0 mg/ml	Sigma-Aldrich / Merck KGaA, Darmstadt, Germany
Potassium chloride (KCl) ≥99.5%, p.a., ACS, ISO	Carl Roth GmbH & Co. KG, Karlsruhe, Germany
Potassium dihydrogen phosphate (KH_2PO_4) ≥99%, p.a., ACS	Carl Roth GmbH & Co. KG, Karlsruhe, Germany
Rotenone ≥ 95%	Sigma-Aldrich / Merck KGaA, Darmstadt, Germany
RPMI 1640 without phenol red	Gibco™ / Fisher Scientific GmbH, Schwerte, Germany
Seahorse XF 1.0 M glucose solution	Agilent Technologies Inc., Santa Clara, USA

Seahorse XF 100 mM pyruvate solution	Agilent Technologies Inc., Santa Clara, USA
Seahorse XF 200 mM glutamine solution	Agilent Technologies Inc., Santa Clara, USA
Seahorse XF Calibrant solution	Agilent Technologies Inc., Santa Clara, USA
Seahorse XF DMEM medium, pH 7.4	Agilent Technologies Inc., Santa Clara, USA
Sodium chloride (NaCl) ≥ 99.5%, p.a., ACS, ISO	Carl Roth GmbH & Co. KG, Karlsruhe, Germany
Trypan blue solution, 0,4%	Gibco™ / Sigma-Aldrich / Merck KGaA, Darmstadt, Germany
Trypsin/EDTA (0.5%), 10x	Gibco™ / Fisher Scientific GmbH, Schwerte, Germany

Table 6: Buffer and Media

Buffer / Medium	**Composition**
Fibroblast cryo medium	90% FBS 10% DMSO
Fibroblast medium	DMEM, high glucose 10% FBS 50 µg/mL Gentamycin
PBMC cryo medium	RPMI 1640 without phenol red 20% FBS 10% DMSO
PBMC medium	RPMI 1640 without phenol red 20% FBS
Phosphate buffered saline (PBS), 10x, pH 7.4 500 mL	40 g NaCl 1 g KCl 13.4 g Na_2PO_4 – 7 H_20 1.2 g KH_2PO_4 in ultrapure water
Phosphate buffered saline (PBS), 1x, pH 7.4 500 mL	50 mL 10x PBS *ad* 500 mL ultrapure water
Physiological saline solution	0.9% NaCl in ultrapure water sterile-filter solution before usage (0.2 µm filter)
Seahorse XF assay medium	Seahorse XF DMEM medium, pH 7.4 25 mM Glucose (Seahorse XF 1.0 M glucose) 4 mM Glutamine (Seahorse XF 200 mM glutamine) 1.25 mM Pyruvate (Seahorse XF 100 mM pyruvate)
Stopping solution	90% 1x PBS 10% FBS

Table 7: Laboratory equipment

Device	Manufacturer
-86 °C freezer HERAfreeze™ HFU 600	Fisher Scientific GmbH, Schwerte, Germany
BD FACSVerse™ Flow Cytometry System	Becton, Dickinson and Company, Franklin Lakes, USA
Centrifuges Centrifuge 5804 R Centrifuge 5810 R Centrifuge 5424 Centrifuge 5417 R	Eppendorf AG, Hamburg, Germany
CO_2 Incubator Hera cell 150	Kendro Laboratory Products GmbH, Langenselbold, Germany
Cryogenic storage vessel, Arpege 170	Air Liquide, Paris, France
Freezing Container, Mr. Frosty™	Thermo Scientific / Thermo Fisher Scientific Inc., WalthamUSA
Imaging reader, Cytation 1	Biotek Instruments GmbH, Bad Friedrichshall, Germany
IRAcubator	Von Ardenne Institut für Angewandte Medizinische Forschung GmbH, Dresden, Germany
Laminar flow clean bench BDK-SK 1800	BDK Luft- und Reinraumtechnik GmbH, Sonnenbühl, Germany
LightCycler® 480 qPCR platform	Roche Diagnostics GmbH, Mannheim, Germany
Luna-FL™ automated cell counter	Logos Biosystems, Inc., purchased via Biozym Scientific
Microscope Primovert	Carl Zeiss Microscopy GmbH, Jena, Germany
Mini centrifuge Rotilabo®	Carl Roth GmbH & Co. KG, Karlsruhe, Germany
NanoDrop™ One Microvolume UV-Vis Spectrophotometer	Thermo Scientific / Thermo Fisher Scientific Inc., Waltham USA
Neubauer counting chamber improved	Carl Roth GmbH & Co.KG, Karlsruhe, Germany
Pipette aids Pipetboy acu 2	INTEGRA Biosciences GmbH, Biebertal, Germany
Pipettes, Eppendorf Research® Plus	Eppendorf AG, Hamburg, Germany
Seahorse XFe96 Analyzer	Agilent Technologies Inc., Santa Clara, USA
Thermal cycler Biometra TRIO	Analytik Jena AG, Jena, Germany
Ultrapure water unit Pureflex 3	ELGA LabWater, High Wycombe, UK
Vortex mixer Vortex-Genie® 2	Scientific Industries, Inc., Bohemia, NY, USA
Water bath	GFL Gesellschaft für Labortechnik mbH, Burgwedel, Germany

Table 8: Consumables

Consumable	Manufacturer
Cell culture dishes, sterile Cell culture dish 100 mm Cell culture dish 100 mm, Cell+	SARSTEDT AG & Co. KG, Nuembrecht, Germany
Cell culture flask, sterile T175, Cell+	SARSTEDT AG & Co. KG, Nuembrecht, Germany
Centrifuge tubes 15 mL and 50 mL	SARSTEDT AG & Co. KG, Nuembrecht, Germany
Leucosep™, with porous barrier, 50 mL	Greiner Bio-One GmbH, Frickenhausen, Germany
LightCycler® 480 Multiwell Plates 96, white	Roche Diagnostics Deutschland GmbH, Mannheim, Germany
LightCycler®480 Sealing Foil	Roche Diagnostic Deutschland GmbH, Mannheim, Germany
Multiply®-Pro cup 0.2 mL, polypropylene	SARSTEDT AG & Co. KG, Nuembrecht, Germany
Multiwell Plates 96, µClear®, polystyrene, black	Greiner Bio-One GmbH, Frickenhausen, Germany
Multiwell Plates 96, V-bottom, clear, polystyrene	Corning®, Merck KGaA, Darmstadt, Deutschland
Pipette tips 10 µL, 20 µL, 200 µL, 1,000 µL	SARSTEDT AG & Co. KG, Nuembrecht, Germany
Pipette tips with filter 10 µL, 20 µL, 200 µL, 1,000 µL	SARSTEDT AG & Co. KG, Nuembrecht, Germany
SafeSeal tube 1.5 mL and 2 mL	SARSTEDT AG & Co. KG, Nuembrecht, Germany
Safety-Multifly®-needle 21G with multi adapter	SARSTEDT AG & Co. KG, Nuembrecht, Germany
Serological pipettes 5 mL, 10 mL, 25 mL	SARSTEDT AG & Co. KG, Nuembrecht, Germany
S-Monovette® K3 EDTA 9 mL	SARSTEDT AG & Co. KG, Nuembrecht, Germany
Sterile filter Filtropur S 0.2 µm	SARSTEDT AG & Co. KG, Nuembrecht, Germany
Syringe Norm Ject® 10 mL and 20 mL	Henke-Sass, Wolf GmbH, Tuttlingen, Germany
XFe Cell Culture Microplates	Agilent Technologies Inc., Santa Clara, USA
XFe Sensor Cartridges	Agilent Technologies Inc., Santa Clara, USA

Table 9: Kits

Kit	Manufacturer
CYTO-ID® Autophagy Detection Kit	Enzo Life Sciences GmbH, Lörrach, Germany
GoTaq® qPCR Master Mix	Promega GmbH, Walldorf, Germany
Guava® Autophagy LC3 Antibody-based Assay Kit	Luminex Corporation, Austin, TX, USA
High Pure RNA Isolation Kit	Roche Diagnostics GmbH, Mannheim, Germany
LunaScript™ RT SuperMix Kit	New England Biolabs, Ipswich, MA, USA

Table 10: Primers for gene expression analysis

Gene	Sequence forward primer 5`- 3`	Sequence reverse primer 5`- 3`
AMPK1α	ttc aag tga ttc tcc cgc ct	gaa gct gag gtg gtg gat ca
ATG7	acc cag aag aag ctg aac ga	ggt ggg agc act cat gtc aa
BECN1	ggc tga gag act gga tca gg	ctg tcc act gtg cca gat gt
FOXO3	gca agc aca gag ttg gat ga	cag gtc gtc cat gag gtt tt
HSPA5	ggt gaa aga ccc ctg aca aa	gtc agg cga ttc tgg tca tt
IL-10	gag aac agc tgc acc cac tt	gca tca cct cct cca ggt aa
MAP1LC3B	ggt gag aag cag ctt cct gt	aga ttg gtg tgg aga cgc tg
NDUFS1	agg cag ttc tgc act cca aa	tcc atc tgc tcc cag gag aa
RPLP0	ccc gag aag acc tcc ttt tt	aga agg ggg aga tgt tga gc
SIRT1	gca gat tag tag gcg gct tg	tct ggc atg tcc cac tat ca
SIRT3	cat gag ctg cag tga ctg gt	gag ctt gcc gtt caa cta gg
SOD2	cac cag cac tag cag cat gt	ggt gac gtt cag gtt gtt ca
TFAM	ggg aag gtc tgg agc aga g	acg ctg ggc aat tct tct aa
ULK1	ggt cac acg cca cat aac ag	gcc cca caa ggt gag aat aa
β-Actin	gga ctt cga gca aga gat gg	agc act gtg ttg gcg tac ag

Table 11: Software

Software	Publisher
BD FACSuite™ software, version 1.0.6	Becton, Dickinson and Company, Franklin Lakes, USA
Citavi 6	Swiss Academic Software GmbH, Waedenswil, Switzerland
Gen5™, version 3.09.07	Biotek Instruments Inc. / Agilent Technologies Inc., Santa Clara, USA
GraphPad Prism, version 10.3.1	GraphPad Software, San Diego, USA
LightCycler® 480 Software, version 1.5.0 SP4	Idaho Technology Inc., Salt Lake City, USA
Microsoft Office Professional Plus 2016	Microsoft Corporation, Redmond (Washington), USA
Seahorse Analytics, version 1.0.0-749	Agilent Technologies Inc., Santa Clara, USA
Seahorse Wave Desktop Software, version 2.6.3	Agilent Technologies Inc., Santa Clara, USA

2.2 Methods

In order to investigate the effects of hyperthermia on autophagy and mitochondrial function in human PBMCs and human fibroblasts, preliminary work in the form of the establishment of autophagy assays was required. The first autophagy assay was established for human fibroblasts. Due to the different size and morphology of PMBCs, this assay was not suitable for blood cells, so a new assay was developed for PBMCs. Their establishment is described in the following chapter. Assays for measuring mitochondrial function and mRNA expression have already been established and are also described below. **Table 12** provides an overview of all assays, the topics covered and where the methods are described. It contains the wIRA treatment of human fibroblasts with subsequent measurement of autophagy as well as the study of autophagy, mitochondrial function and mRNA expression in human PBMCs. In human PBMCs, ex vivo treatment with wIRA was tested in cells from healthy donors and ME/CFS. In addition, an in vivo study was conducted by testing PBMCs from ME/CFS patients undergoing whole-body hyperthermia treatment.

Table 12: Overview of all methods described

2.2.1 Establishment of autophagy assays	**2.2.2 Description of already established assays** Human PBMCs	**2.2.3 Ex vivo Hyperthermia**	**2.2.4 In vivo Hyperthermia**
a) Human Fibroblasts CYTO-ID® Autophagy Detection Kit	**a) Mitochondrial function** Seahorse XF Mito Stress Test	**a) Ex vivo wIRA Treatment** human Fibroblasts (healthy)	**In vivo Hyperthermia** whole-body hyperthermia of ME/CFS patients
b) Human PBMCs Guava® Autophagy LC3 Antibody-based Assay Kit	**b) mRNA expression** RNA extraction, cDNA synthesis, qPCR analyses	**b) Ex vivo wIRA Treatment** human PBMCs (healthy, ME/CFS)	

2.2.1 Establishment of autophagy assays

a) Human Fibroblasts - CYTO-ID® Autophagy Detection Kit

The basis for measuring autophagosomes in human fibroblasts using the CYTO-ID® kit (Enzo Life Sciences GmbH, Lörrach, Germany)was the application note by Beckman *et al.* [154], published by biotek. This paper describes the treatment, the assay performance and readout of autophagosomes in HeLa cells using the Lionheart™ FX imaging reader. Cells were treated with 10 µM chloroquine (CQ), with starvation or with different concentrations of rapamycin. HeLa cells were seeded at 20,000 cells per well in black sided clear bottom 96-well microplates. For cell staining, cells were washed 2x with 200 µL 1x assay buffer containing 5% FBS. The assay buffer was replaced with 100 µL dual color detection solution containing 1 mL assay buffer, 1 µL Hoechst and

2 µL CYTO-ID® Green Detection Reagent and incubated for 30 min at 37 °C in the dark. Finally, cells were washed 2x with 200 µL assay buffer and imaged directly in 100 µL assay buffer. Images were acquired with a 20x objective on the Lionheart™ FX configured with DAPI and GFP light cubes. The DAPI light cube is configured with a 377/50 nm excitation filter and a 447/60 nm emission filter. The GFP light cube uses a 469/35 nm excitation filter and a 525/39 nm emission filter. All used reader and software settings are shown in **Table 13**.

Table 13: Reader and imager software settings

Imaging preprocessing		**Cellular analysis**	
Image set	DAPI	**Detection Channel:**	Tsf [DAPI 377,447]
		Primary mask and count	
Background	Dark	**Threshold**	7,000
Rolling bar diameter	Auto	**Secondary mask**	Tsf [GFP 469,525]
Image smoothing strength	5	**Measure within a secondary mask**	Checked
Image set	GFP	**Expand Primary mask**	30 µm
Background	Dark	**Threshold**	Unchecked
Rolling bar diameter	0.5 µm	**Count Spots**	Checked
Priority	Fine results	**Size**	0.5 to 3 µm
Image smoothing strength	0	**Advanced options**	Count spots options
		Rolling ball size	Default
		Threshold	1,200

To establish the autophagy CYTO-ID® assay in human fibroblasts, cells from donor Ast72 were first expanded to achieve an adequate cell number. For this purpose, 5,000,000 cells were thawed and cultured in five T175 flasks containing 20 mL fibroblast medium. After four days, cells were detached by adding 3 mL of 1x trypsin/EDTA and collected by adding 17 mL of stopping solution. After centrifugation, cells were resuspended in fibroblast cryo medium and transferred in cryo vials at a cell density of 500,000 cells/mL and stored at -80 °C. These cells were used for the assay establishment and for wIRA treatment.

The protocol just described by Beckmann *et al.* served as the basis for the establishment of the autophagy assay for fibroblasts. The adaptations of the protocol to fibroblasts led to the following protocol. Three days before cell treatment, 500,000 cells were thawed and seeded in a T175 cell culture flask containing 20 mL fibroblast medium and cultured for two days. For cell treatment 10,000 cells per well were seeded in 96 well plates (Multiwell Plates 96, µClear®, polystyrene, black, Greiner Bio-One GmbH, Frickenhausen, Germany), and incubated according to the appropriate treatment conditions. Each investigated condition were tested in six replicates. After treatment, the CYTO-ID® assay was performed. For this purpose, supernatant were discarded and cells were washed with 1x assay buffer. To stain the autophagosomes, 100 µL staining solution, consisting of 1.4 mL assay buffer, 1.4 µL Hoechst and 2.8 µL of CYTO-ID® Green Detection Reagent 2, was

added to all wells and incubated in a humidified incubator at 37 °C and 5% CO_2 for 30 min. To stop the staining, the supernatant was removed and the cells were washed twice with 200 µL of 1x assay buffer, 100 µL of 1x assay buffer was added for measurement. Autophagosome detection was performed with the Cytation 1 (Biotek Instruments GmBH, Bad Friedrichshall, Germany) imaging reader with a 20x objective configured with DAPI and GFP light cubes. The DAPI light cube is configured with a 377/50 nm excitation filter and a 447/60 nm emission filter. The GFP light cube uses a 469/35 nm excitation filter and a 525/39 nm emission filter. The parameter settings for image processing and image analysis are listed in **Table 14**

Table 14: Parameter settings for image processing and image analysis

Imaging preprocessing		**Image deconvolution**	
Image set	DAPI	**Image set**	Tsf [GFP 469,525] Tsf [DAPI 377,447]
Background	Dark	**Point spread function**	Auto, based on objective
Rolling bar diameter	66 µm	**Iterations**	5
Image smoothing strength	0	**Data out prefix**	Deconvolved
Image set	GFP		
Background	Dark		
Rolling bar diameter	1.5 µm		
Priority	Fine results		
Image smoothing strength	0		
Cellular analysis			
Primary mask and count	Deconvolved [Tsf [DAPI 377,447]] Deconvolved [Tsf [GFP 469,525]]	**Secondary Mask**	Deconvolved [Tsf [GFP 469,525]]
Threshold	Auto	**Background**	Dark
Background	Dark	**Measure within a primary mask**	Checked Use Primary Mask
Object selection		**Measure within a**	
Min. object size	5 µm	**secondary mask**	Checked
Max. object size	40 µm		
		Expand primary mask	50 µm
		Threshold	Unchecked
		Count spots	Checked
		Size	0.5–5 µm
		Advanced options	Count spots options
		Rolling ball size	Default
		Threshold	1200
Curve Analysis: Autophagosomes per nucleus			

In addition, a chloroquine (CQ) (Fisher Scientific GmbH, Schwerte, Germany) control was added for each condition studied. Chloroquine inhibits the fusion of lysosomes with autophagosomes and therefore leads to an accumulation of autophagosomes. In this context, the number of autophagosomes in the CQ control must be higher than in the corresponding condition without CQ.

This control can be used to assess the functionality of the assay. To prevent saturation of the system, a suitable CQ concentration had to be titrated first. For this reason, concentrations of 0.5, 1.0, 2.0, 2.5, 5.0 and 10 µM CQ were tested. The CQ solutions were added to the 96-well plates during cell seeding and incubated for 24 hours in a humidified incubator at 37 °C and 5% CO_2. After incubation, the read-out was performed as described above.

b) Human PBMCs - Guava® Autophagy LC3 Antibody-based Assay Kit

The establishment of the autophagy assay for PBMCs was the subject of Melanie Scherer's master's thesis and resulted in the following protocol [155]. PBMCs were seeded at a density of 500,000 cells/well in 200 µL RPMI 1640 (Gibco™/Fisher Scientific GmbH, Schwerte, Germany) without phenol red as triplicates in two 96-well V-bottom plates (Merck KGaA, Darmstadt, Germany), one for treatment and one as control. For each condition tested, a 40 µM CQ control was added in triplicate to evaluate the functionality of the assay. After treatment, the Guava® Autophagy LC3 Antibody-Based Detection Kit (Luminex Corporation, Austin, TX, USA) was used to stain the autophagy marker LC3 by antibody labelling. For this purpose, the plates were centrifuged at 300 x g for 5 min at RT. After centrifugation, the supernatant was discarded and the cells were washed by resuspending in 100 µL 1x assay buffer. After a further centrifugation step (5 min, 300 x g, RT), 100 µL of autophagy reagent B was added to the cells and centrifuged immediately (5 min, 300 x g, RT) without resuspending. After discarding the supernatant, the cells were resuspended in 100 µL antibody solution containing 95 µL 1x assay buffer and 5 µL 20x anti-LC3 FITC, clone 4E12. Incubation was carried out at room temperature for 30 min in the dark. After incubation, the plates were centrifuged (5 min, 300 x g, RT) and washed with 100 µL assay buffer. After a final centrifugation step (5 min, 300 x g, RT), the cells were resuspended in 100 µL 1x assay buffer. The plates remained in the dark for 10 min before the cells were analysed by flow cytometry using the BD FACSVerse™ Flow Cytometry System (Becton, Dickinson and Company, Franklin Lakes, USA). By using a selective permeabilisation solution, cytosolic LC3 is distinguished from autophagic LC3 by extracting the soluble cytosolic proteins, while LC3 sequestered in the autophagosome is protected.

2.2.2 Description of already established assays – human PBMCs

a) Mitochondrial function - Seahorse XF Cell Mito Stress Test

The six mitochondrial parameters basal respiration, ATP production, maximal respiration, spare respiratory capacity, non-mitochondrial respiration and the proton leak were measured using the Seahorse Bioscience XFe96 Extracellular Flux Analyzer (Agilent Technologies Inc., Santa Clara, CA, United States). To prepare for sensor calibration, 200 µL of XF calibrant was added to each

well of the XF sensor cartridge and incubated overnight at 37 °C without CO_2. Coating of the XF96 cell culture microplate was performed with 10 µL of a 50 µg/mL poly-D-lysine (PDL) solution (Merck KGaA, Darmstadt, Germany) per well. At least three wells were measured for each condition. 225,000 PBMCs per well were seeded in 50 µL XF medium and subsequently centrifuged for 1 min, 250 x g without brake at RT. All wells containing cells or background wells were filled with XF medium to a total volume of 180 µl. For brightfield cell counting, the cell plate was placed in the Cell Imager Cytation 1 (Biotek Instruments GmBH, Bad Friedrichshall, Germany) and kept there at 37 °C for 60 min. In the meantime, the sensor cartridge was loaded with the four cellular stressors oligomycin (20 µL), carbonyl cyanide-4 (trifluoromethoxy)phenylhydrazone (FCCP, 22 µL) and a combination of rotenone, antimycin A and the cell nuclei staining reagent Hoechst (25 µL) (all Merck KGaA, Darmstadt, Germany). After injection, the final concentration of oligomycin was 1.25 µM, of FCCP 1.0 µM, of rotenone and of antimycin A 1.67 µM each and of Hoechst 8.0 µM. To calibrate the sensors, the 96-well sensor cartridge was inserted into the XFe96 Extracellular Flux Analyzer. After calibration, the utility plate was replaced with the cell plate to start the measurement of mitochondrial respiration in PBMCs. The addition of Hoechst by the last injection enables the subsequent cell counting by the cell imager. Based on this cell count, the OCR can be normalized to 1,000 cells per well. A more detailed description of this method can be found in the methodological paper `Ex vivo Assessment of Mitochondrial Function in Human Peripheral Blood Mononuclear Cells Using XF Analyzer` by Alica Schöller-Mann [156].

b) mRNA Expression

Some 10^6 PBMCs were used for RNA isolation, which was performed with the High Pure RNA Isolation Kit (Roche Diagnostics GmbH, Mannheim, Germany). The LunaScript® Super Mix Kit (New England Biolabs, Ipswich, MA, USA) was used for cDNA synthesis. Both kits were used as described in the manufacturer's instructions. The LightCycler® 480 (Roche Diagnostics GmbH, Mannheim, Germany) in combination with the GoTaq® qPCR Master Mix (Promega GmbH, Walldorf, Germany) was used for quantitative polymerase chain reaction (qPCR) of multiple genes. Each qPCR consisted of 1 µl (0.5 pmol/µl) of each primer (biomers.net GmbH, Ulm, Germany), 10 µl GoTaq® qPCR Master and 8 µl cDNA. The qPCR analyses were performed in triplicate for each sample. The qPCR protocol used included the following steps: 5 min pre-incubation (95 °C), followed by 95 °C 10 s, 62 °C 10 s and 72 °C 10 s with fluorescence measurements at the end of the elongation phase. Melting curve analysis was performed after 45 cycles. Ribosomal protein lateral peduncle subunit P0 (RPLP0) and ß-actin were used as housekeeping genes to normalise the target genes. All measured genes are shown in **Table 10**. Calculation of n-fold mRNA expression was conducted using the $2^{-\Delta\Delta Ct}$ method [157].

2.2.3 Ex vivo Hyperthermia

a) Ex vivo wIRA Treatment – human Fibroblasts (healthy)

The effect of wIRA irradiation on human fibroblasts from a healthy donor was investigated. Information on the fibroblast donor is shown in **Table 15**

Table 15: Information on human fibroblasts studied

Cell type	Designation	Gender	Age	Passage
Fibroblast	hF130522/Ast72	male	8 years	8 - 10

The cell expansion and the test procedure have already been described in chapter 2.2.1 a). For the wiRA treatment, a 96-well plate with cells was placed in the preheated IRAcubator (Von Ardenne Institute of Applied Medical Research GmbH, Dresden, Germany) at 39 °C for one hour (**Figure 16**). At the same time, another prepared 96-well plate remained in the incubator at 37 °C and 5% CO_2 for one hour. After treatment, the autophagy assay was performed and the cells were analysed using the Cytation 1 imager. A more detailed description of this method can be found in the methodological paper 'Quantification of Autophagosomes in Human Fibroblasts Using Cyto-ID® Staining and Cytation Imaging' [158].

Figure 16: Placement of the treatment plate in the IRAcubator heat treatment device

b) **Ex vivo wIRA Treatment** - human PBMCs (healthy, ME/CFS)

A total of 33 people took part in the ex vivo study, including nine healthy donors and 24 ME/CFS patients, whereby participant number 15 had to be excluded due to an insufficient number of cells and an implausible test evaluation in mitochondrial function. Information about the participants is listed in **Table 16**.

Table 16: Participants of the ex vivo study

	Test person	Sex	Age	Autophagy	Mitochondrial function	mRNA expression
Healthy Donors	01	f	29	x	x	x
	02	f	39	x	x	x
	03	f	30	x	x	x
	04	m	45	x	x	x
	05	m	37	x	x	x
	06	m	61	x		x
	07	f	44	x		x
	08	m	62	x		x
	09	f	24		x	

	Test person	Sex	Age	Bell	Autophagy	Mitochondrial function	mRNA expression
ME/CFS Patients	01	f	40	30	x	x	x
	02	f	57	20	x	x	x
	03	f	29	30	x	x	x
	04	f	54	40	x	x	x
	05	f	30	50	x	x	x
	06	f	26	40-60	x	x	x
	07	f	30	20	x	x	x
	08	m	40	30	x	x	x
	09	f	28	60	x		
	10	m	55	50-60	x		x
	11	f	52	40	x		x
	12	f	31	60-70	x		x
	13	f	18	40	x	x	x
	14	f	64	40	x	x	
	15	f	56	80-90		(x) not applicable	
	16	f	59	20	x	x	x
	17	f	54	50	x	x	x
	18	f	32	40	x	x	x
	19	f	60	40	x	x	x
	20	f	65	40-50	x	x	x
	21	m	36	50	x	x	x
	22	f	49	50-60	x	x	x
	23	f	30	40	x	x	x
	24	f	57	40	x	x	

With and without wIRA treatment, Without wIRA treatment

The blood samples were taken either at the Albstadt-Sigmaringen University of Applied Sciences or at Dr. Pieper's practice (Constance, Germany) by trained personnel using S-Monovette® K3 EDTA (SARSTEDT AG & Co. KG, Nuembrecht, Germany). After transporting the samples, the PBMCs were isolated from the whole blood for subsequent analyses. Treatment with wIRA hyperthermia (39 °C, 1 hour) and subsequent measurements of mitochondrial respiration (2.2.2 a)) were performed with freshly isolated PBMCs. For autophagy assay and mRNA expression analysis (2.2.2 b)), the remaining cells were seeded in RPMI 1640 medium without phenol red containing 20% FBS and incubated overnight at 37 °C and 5% CO_2. A control was also measured for each assay, whereby these cells remained at 37 °C and 5% CO_2 for the hour of treatment (**Figure 17**).

Figure 17: Study design of the ex vivo study. After blood collection and PBMC isolation, some of the cells were treated directly in the IRAcubator (1 h at 39 °C) and mitochondrial function was determined. The remaining cells were incubated overnight at 37 °C in a CO_2 incubator. The next day, RNA isolation and autophagy were analysed, both also after IRAcubator treatment.

Isolation of PBMCs

Human PBMCs were isolated from 36 mL of human blood using Leucosep tubes (Greiner Bio-One GmbH, Frickenhausen, Germany) according to the manufacturer's instructions. PBMCs were resuspended in phosphate-buffered saline (1x PBS) and cell counts were determined using a Luna-FL™ automated cell counter (Logos Biosystems, Inc., Inc., Anyang-si, South Korea).

2.2.4 In vivo Hyperthermia

A total of nine ME/CFS patients participated in this study (**Table 17**). The ME/CFS patients were medically diagnosed using the diagnostic criteria of the Canadian consensus criteria [26] and the Furkuda criteria [24]. In addition, the severity of the disease was assessed using the Bell scale [159]. Hyperthermia treatment was performed on medical recommendation and not for this study. The patients agreed to donate blood for research purposes before and after the therapy. Since no healthy donors underwent whole-body hyperthermia, the data can only be compared with those of healthy donors without therapy. For mitochondrial function, the data from this ex vivo study were used. In the case of autophagy, the data from this study were not comparable as the test was performed one day after blood collection (appendix **Figure A60**). [160,161]

Table 17: Participants of the in vivo study

	ME/CFS Patients				**Healthy Donors**			
	Autophagy – Mitochondrial - mRNA expression				Autophagy		Mitochondrial	
Participant	Sex	Age	Bell -Scale	Symbol	Sex	Age	Sex	Age
01	f	31	20	●	f	61	f	30
02	f	53	40	■	m	57	f	39
03	m	41	30	▲	f	61	f	29
04	m	50	50	▼	f	39	m	37
05	f	35	30-40	◆	m	42	m	44
06	f	32	30-40	◑	m	41	f	24
07	f	47	20	◨	f	34	-	-
08	f	32	40 -60	◭	m	45	-	-
09	f	25	20 - 30	▽	f	53	-	-

Two consecutive days were required to investigate the influence of a session of whole-body hyperthermia on central cellular mechanisms in ME/CFS patients. On the first day, the basal values of the patients were determined. For this purpose, blood was taken in the morning in Constance by Dr. Stefan Pieper and transported to our laboratory. PBMCs were then isolated for the two cell tests to measure autophagy and mitochondrial function. In addition, RNA was isolated for subsequent qPCR. On the second day, the participants received whole-body hyperthermia. This heat therapy was carried out with the whole-body hyperthermia system 'IRATHERM®1000' (Von Ardenne Institute of Applied Medical Research GmbH, Dresden, Germany). The system enables a rapid increase in core body temperature (to 39 °C in approx. 45 min) through uniform irradiance over the entire patient using six water-filtered infrared-A (wIRA) radiant heaters. The treatment session lasted one hour with a maximum core body temperature of 39 °C. During the session, the temperature was monitored via three temperature sensors (rectal, axillary and dermal) as well as

the ear pulse and oxygen saturation. This treatment took place in the medical practice of Dr. Achim Schneider in Überlingen. After each session, blood was again taken from the participants and transported to our laboratory. Here too, autophagy (2.2.1 b)) and mitochondrial function (2.2.2 a)) were measured directly after PBMC isolation, as well as RNA isolation was conducted for the subsequent qPCR (2.2.2 b)). The entire procedure was performed three times with 3 participants each. The study design is shown in the following **Figure 18**.

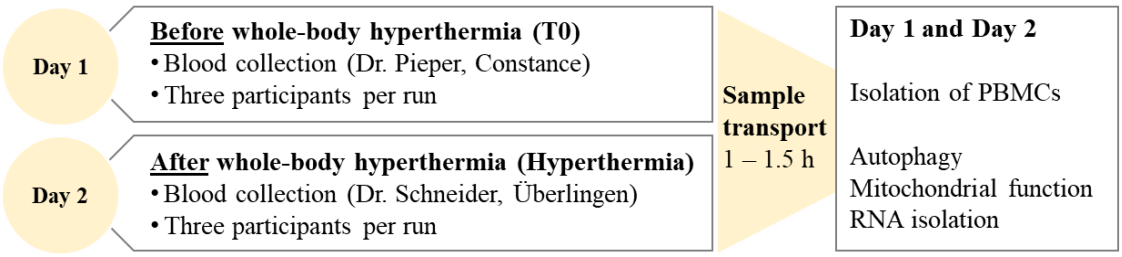

Figure 18: Study design of the in vivo study. The study was conducted on two consecutive days. On the first day, blood was drawn to measure basal levels of autophagy, mitochondrial function and mRNA expression. Whole-body hyperthermia was performed on the second day. After the treatment, blood was taken again and transported to our laboratory to determine the same cellular mechanisms as on day 1.

2.2.5 Data analyses

Graph-Pad Prism 10.3.1 for Windows (GraphPad Software Inc, San Diego, CA, United States) was used for statistical analyses and the creation of graphs. The results are presented as individual values, as grouped values with the mean ± SEM and the points of the individual values, as box-and-whiskers plots with minimum to maximum and line at the median and the individual point values, and as scatter plots with mean ± SEM. Individual values are only shown descriptively, as the amount of data is too small for statistical analysis. All grouped data were tested for normal distribution using the Shapiro-Wilk test. The parametric t-test was used for normally distributed data and the non-parametric Wilcoxon test or Mann-Whitney test for non-normally distributed data. Statistical significance was defined as ns $p > 0.05$, *$p \leq 0.05$, **$p \leq 0.01$, ***$p \leq 0.001$, ****$p \leq 0.0001$.

2.2.6 Ethical standards

The study was conducted in accordance with the guidelines of the Ethics Committee of the Baden-Württemberg Medical Association and in compliance with the principles of the Declaration of Helsinki. All participants who voluntarily provided a skin sample for the isolation of fibroblasts or voluntarily provided blood for the experiments were informed in advance and gave their written consent to the use of the skin sample or the collection and use of the blood samples. All information on the study participants was pseudonymised. The whole-body hyperthermia sessions were carried out on the recommendation of a doctor and not as part of this study.

3 Results

One main topic of this thesis is the investigation of central cellular mechanisms in PBMCs from ME/CFS patients compared to healthy donors. In addition, hyperthermia is being investigated as a potential treatment option. The results of these studies are divided into subsections, which are presented in **Table 18**. The study began with the establishment of autophagy assays for two different cell types, human fibroblasts and human PBMCs. The first chapter of the results deals with the evaluation of the functionality and reproducibility of these established assays. The second chapter focuses on the baseline values of autophagy and mitochondrial function in healthy donors and ME/CFS patients. The subsequent investigation of hyperthermia is divided into two separate studies, the ex vivo study and the in vivo study. In the ex vivo study, isolated cells were treated with the IRAcubator. PBMCs from ME/CFS patients and healthy donors were subjected to this treatment and analysed for autophagy, mitochondrial function and mRNA expression. In addition, fibroblasts from a healthy donor were treated and analysed for autophagy activity. The second study, the in vivo study, investigated the same cellular parameters, with the difference that not the isolated cells were treated, but the ME/CFS patients had one session of whole-body hyperthermia. The last chapter compares the ex vivo and in vivo study.

Table 18: Overview of the individual chapters presented in the results

3.1 **Establishment of autophagy assays** Fibroblasts, PBMCs	**3.2** **Heathy vs. ME/CFS** PBMCs	**3.3** **Ex vivo Hyperthermia** Fibroblasts, PBMCs	**3.4** **In vivo Hyperthermia** PBMCs	**3.5** **Ex vivo vs. In vivo Hyperthermia** PBMCs
3.1.1 Fibroblasts CYTO-ID® Autophagy detection	**3.2.1 Autophagy** PBMCs (healthy, ME/CFS)	**3.3.1 Autophagy** healthy Fibroblasts	**3.4.1 Autophagy** PBMCs (ME/CFS)	**3.5.1 Autophagy** PBMCs (ME/CFS)
3.1.2 PBMCs Guava® Autophagy LC3 Antibody-based Assay	**3.2.2 Mitochondrial function** PBMCs (healthy, ME/CFS)	**3.3.2 Autophagy** PBMCs (healthy, ME/CFS)	**3.4.2 Mitochondrial function** PBMCs (ME/CFS)	**3.5.2 Mitochondrial function** PBMCs (ME/CFS)
		3.3.3 Mitochondrial function PBMCs (healthy, ME/CFS)	**3.4.3 mRNA expression** PBMCs (ME/CFS)	**3.5.3 mRNA expression** PBMCs (ME/CFS)
		3.3.4 mRNA expression PBMCs (healthy, ME/CFS)		

3.1 Establishment of autophagy assays

3.1.1 Fibroblasts – CYTO-ID® Autophagy Detection Kit

In order to investigate the effect of hyperthermia on autophagy in human fibroblasts, a suitable test system first had to be developed. For human fibroblasts, an image-based method was chosen in which the cell nuclei and autophagosomes are visualised by specific staining with the CYTO-ID® Autophagy Detection Kit and read out and analysed with the Cytation 1 imager and Gen 5 software. The final protocol for the CYTO-ID® Autophagy Detection assay was published in the peer-reviewed journal Bio-protocol [158]. The basis for establishing the method was the protocol by Beckman *et al.* [154], which describes the analysis of HeLa cells. The adaptations of the protocol for the analysis of human fibroblasts are described in the methods (2.2.1 a)). To evaluate the reproducibility of the established assay, the assay was repeated five times under the same conditions. The results of these five experiments (E01-E05) are shown in **Figure 19**. The figure shows the mean value of at least three technical replicates per experiment and the standard error of the mean (SEM). Between the five experiments there are no visible major differences. This is confirmed by the statistical analysis using an ordinary one-way ANOVA with Tukey's multiple comparison test, which shows no significant (ns p = 0.8687) differences between the repeated experiments.

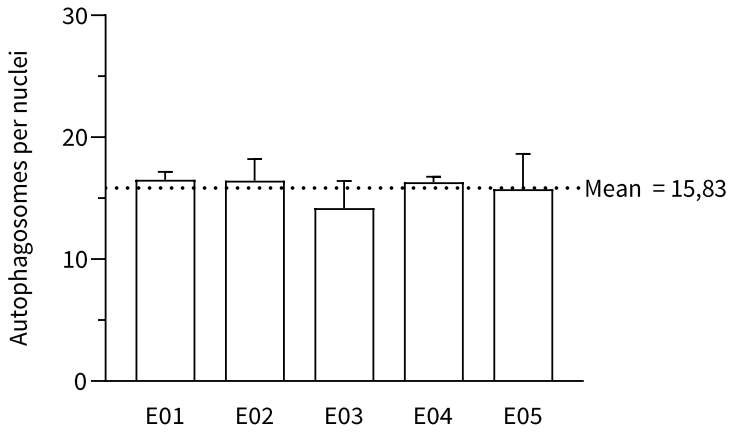

Figure 19: Evaluation of reproducibility of the CYTO-ID® assay for human fibroblasts. The repeated measurement of the established assay shows no major differences between the five experiments performed. The data for the individual experiments show at least three technical replicates with the standard error of the mean (SEM). Statistical verification also shows no significant differences (ordinary one-way ANOVA with Tukey's multiple comparison test shows no significant differences (ns p = 0.8687)).

The following table shows the numerical values of the mean and SEM of the repeated experiments (**Table 19**). The mean value of all five experiments is 15.83 autophagosomes per nucleus. The highest mean difference between the individual experiments and the mean of all five experiments is 1.65 autophagosomes per nucleus.

Table 19: Numerical values of the reproducibility assessment of the CYTO-ID® test for human fibroblasts

Experiment	Mean [Autophagosomes per nuclei]	SEM [Autophagosomes per nuclei]	Mean (E01 – E05) [Autophagosomes per nuclei]	Mean difference [Autophagosomes per nuclei]
E01	16.50	0.66		0.67
E02	16.43	1.77		0.60
E03	14.18	2.23	15.83	1.65
E04	16.30	0.46		0.47
E05	15.73	2.90		0.10

The addition of chloroquine leads to an accumulation of autophagosomes by inhibiting the fusion of autophagosomes and lysosomes. An additional CQ control in all conditions tested enables the functionality of the assay to be evaluated, as the CQ control must have a higher quantity of autophagosomes. The following figure shows the result of the titration of a sensible CQ concentration (**Figure 20**). The tested concentrations are 0.5, 1.0, 2.0, 2.5, 5.0 and 10 µM CQ compared to a control without CQ. The experiments were repeated three times (n=3) and the mean and SEM of these replicates are shown in the figure. The respective CQ concentrations were statistically compared with the control group using an unpaired t-test. At a concentration of 0.5 µM, the number of autophagosomes per cell nucleus increases by 40.70% (***p = 0.0006), at 1.0 µM by 56.57% (**p = 0.0024), at 2.0 µM by 60.79% (***p = 0.0005), at 2.5 µM by 70.80% (***p = 0.0004), at 5.0 µM by 70.03% (**p = 0.0037) and at 10 µM by 70.27% (**p ≤ 0.0016).

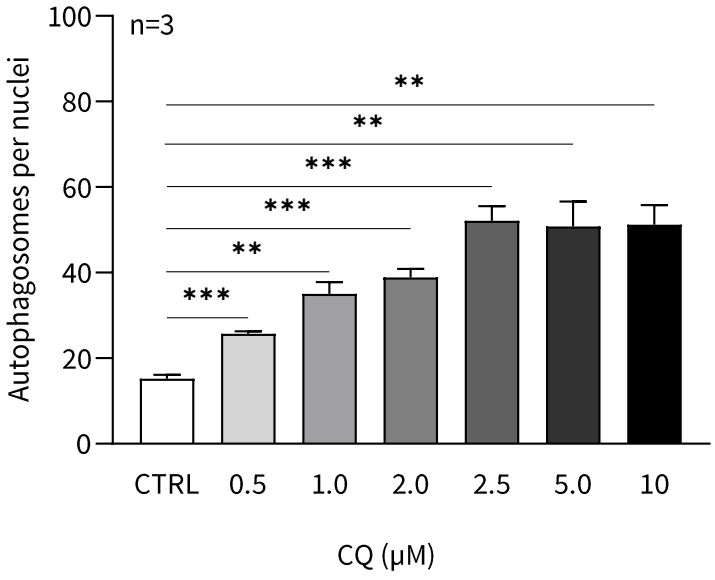

Figure 20: Titration of a sensitive CQ concentration. The statistical analysis of three independent experiments with different CQ concentrations shows a significant increase for all tested concentrations compare to an untreated control (0.5 µM: 40.70%, ***p = 0.0006; 1.0 µM: 56.57%, **p = 0.0024; 2.0 µM: 60.79%, ***p = 0.0005; 2.5 µM: 70.80%, ***p = 0.0004; 5.0 µM: 70.03%, **p = 0.0037; 10 µM: 70.27%, ** = 0.0016, unpaired t-test).

Originally, the test was to be transferred to PBMCs following its successful establishment in human fibroblasts. However, this was not successful due to the different cell morphology of PBMCs. PBMCs are small, round cells with a large nucleus and little cytoplasmic area. This causes the imager to have difficulty finding the correct focus in the round and non-planar objects, as well as the overlapping of autophagosomes, which is also due to the round cell morphology and limited space in the small cells. As a result, the software is not able to distinguish the individual autophagosomes (**Figure 21**). For this reason, a different assay has to be established for human PBMCs – the Guava® Autophagy LC3 Antibody-based Assay.

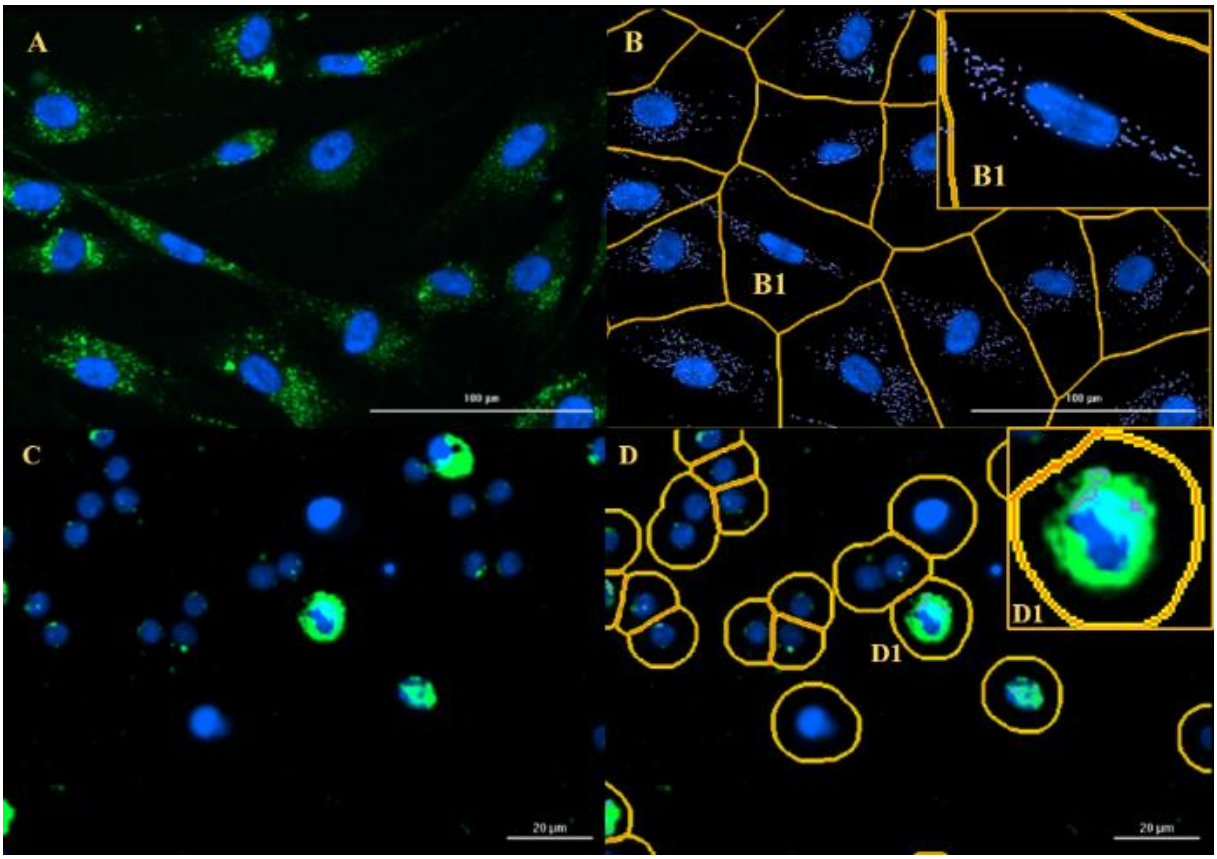

Figure 21: Comparison of the CYTO-ID test in human fibroblasts and human PBMCs. A-B1 The size and morphology of human fibroblasts allows the imager to find the right focus to obtain clear images and the software to recognise individual autophagosomes (green) and relate them to the nuclei (blue). **C-D**1 Due to the small size and non-planar morphology of human PBMCs, the imager has difficulty finding the correct focus, resulting in the software being unable to distinguish individual autophagosomes.

3.1.2 PBMCs – Guava® Autophagy LC3 Antibody – based Assay

The establishment of a suitable autophagy assay for PBMCs was the topic of Melanie Scherer's master's thesis [155]. She was supervised by Barbara Hochecker. One result of the work was the selection of a suitable CQ concentration for the assay evaluation. The following result of a FACS analysis shows three peaks without CQ and three peaks with 40 µM CQ (**Figure 22**). A shift to the right due to the addition of 40 µM CQ is clearly visible in the fluorescence intensity.

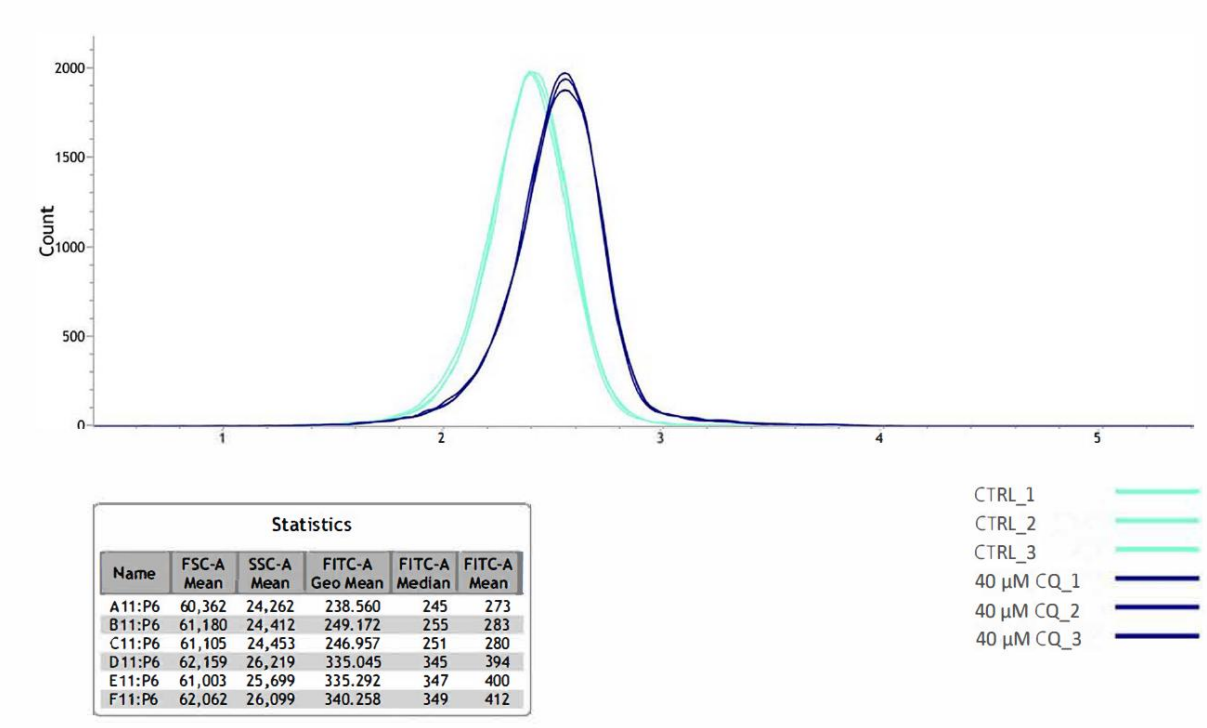

Statistics

Name	FSC-A Mean	SSC-A Mean	FITC-A Geo Mean	FITC-A Median	FITC-A Mean
A11:P6	60,362	24,262	238.560	245	273
B11:P6	61,180	24,412	249.172	255	283
C11:P6	61,105	24,453	246.957	251	280
D11:P6	62,159	26,219	335.045	345	394
E11:P6	61,003	25,699	335.292	347	400
F11:P6	62,062	26,099	340.258	349	412

Figure 22: FACS analysation of PBMCs with 40 µM CQ compared to an untreated control. The curves show three technical replicates of PBMCs without CQ and three technical replicates of PBMCs with 40 µM CQ. A clear shift of the fluorescence intensity to the right is visible due to 40 µM CQ.

To confirm the results of the master thesis [155], a further reproducibility study was carried out, which is shown in **Figure 23**. The study comprises five independent experiments with two conditions – PBMCs with 40 µM CQ and without CQ. Each measurement was performed with three technical replicates. There are no visible differences between the five experiments under both conditions. This is also shown by the statistical analysis using a two-way ANOVA with the Šídák test for multiple comparisons, which shows no significant differences (ns $p>0.5$). The grouped values of the repeated analysis show a significant increase of 37% (****$p < 0.0001$, unpaired t-test) due to the addition of 40 µM CQ to the cells.

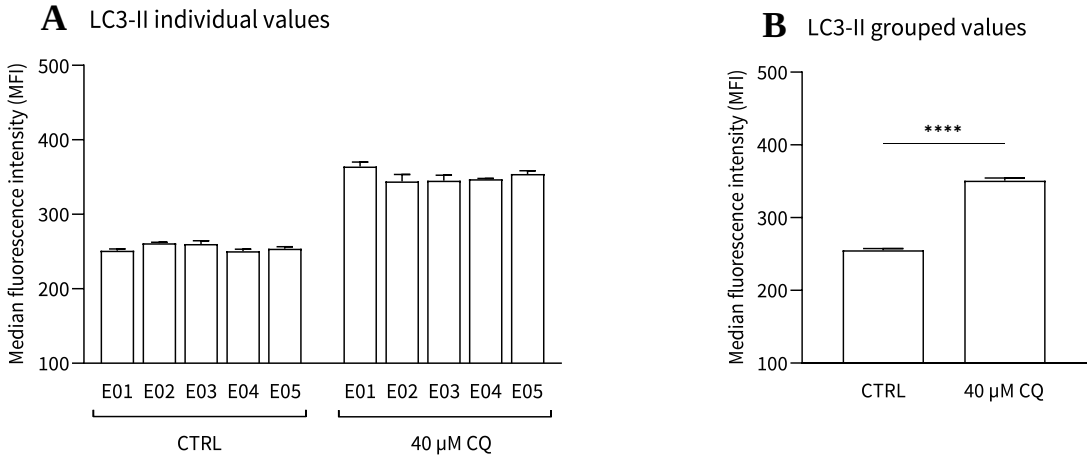

Figure 23: Reproducibility of the Guava® Autophagy LC3 antibody - based Assay Kit. A The individual values of the five repeated experiments of PBMCs with and without 40 µM CQ show no visible and statistical differences (ns $p > 0.5$, two-way ANOVA with the Šídák test for multiple comparisons). **B** The grouped values show a significant increase of 37% (****$p < 0.0001$, unpaired t-test) by 40 µM CQ compared to untreated PBMCs.

The following table shows the numerical values of the mean and SEM of the five repeated experiments (**Table 20**). In the control, the mean value of all five experiments is 255 MFI and with the addition of 40 µM CQ 350 MFI. The largest difference to the mean value of all measurements is 3%.

Table 20: Numerical values of the reproducibility assessment of the Guava® Autophagy Test for human PBMCs

Experiment	Mean [MFI]		SEM [MFI]		Mean (E01 – E05) [MFI]		Mean difference [%]	
	CTRL	40 µM CQ	CTRL	40 µM CQ	CTRL	40 µM CQ	CTRL	40 µM CQ
E01	251	361	3	6			2	3
E02	261	344	2	10			2	2
E03	260	345	4	8	255	350	2	1
E04	250	347	3	1			2	1
E05	253	354	3	5			1	1

3.2 Healthy vs. ME/CFS

3.2.1 Autophagy – PBMCs

To compare the amount of the autophagy marker LC3-II in health and disease, the LC3 levels of eight healthy donors and 23 ME/CFS patients were measured. The following **Figure 24** contains the results of these measurements and shows a significant increase in autophagy in ME/CFS patients compared to healthy donors by 36% (****p < 0.0001, unpaired t-test).

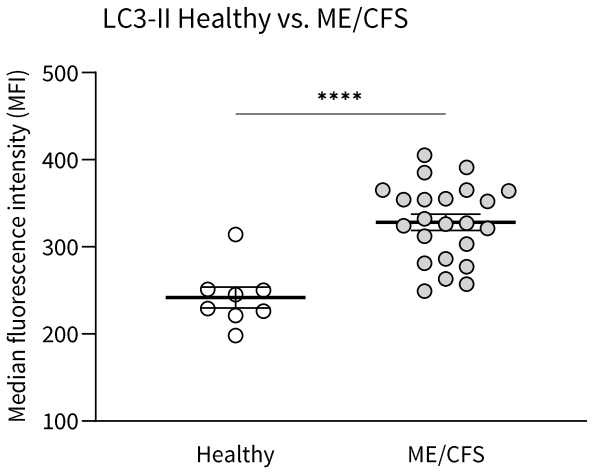

Figure 24: Autophagy in health and disease. LC3-II is significantly increased by 36% (****p < 0.0001, unpaired t-test) in ME/CSF patients compared to healthy donors.

3.2.2 Mitochondrial function – PBMCs

Regarding mitochondrial function, all four parameters basal respiration, ATP production, maximal response and spare respiratory capacity are increased in ME/CFS patients compared to healthy donors. In the case of basal respiration (*p = 0.0414, unpaired t-test) and ATP production (*p = 0.0497, unpaired t-test), this increase is 63.80% and 54.87% respectively and is statistically significant. Maximal response and spare respiratory capacity are increasing by 57.89% (p = 0.1359, unpaired t-test) and 56.02% (p = 0.1783%, unpaired t-test) (**Figure 25**). These data were obtained from six healthy donors and 19 ME/CFS patients.

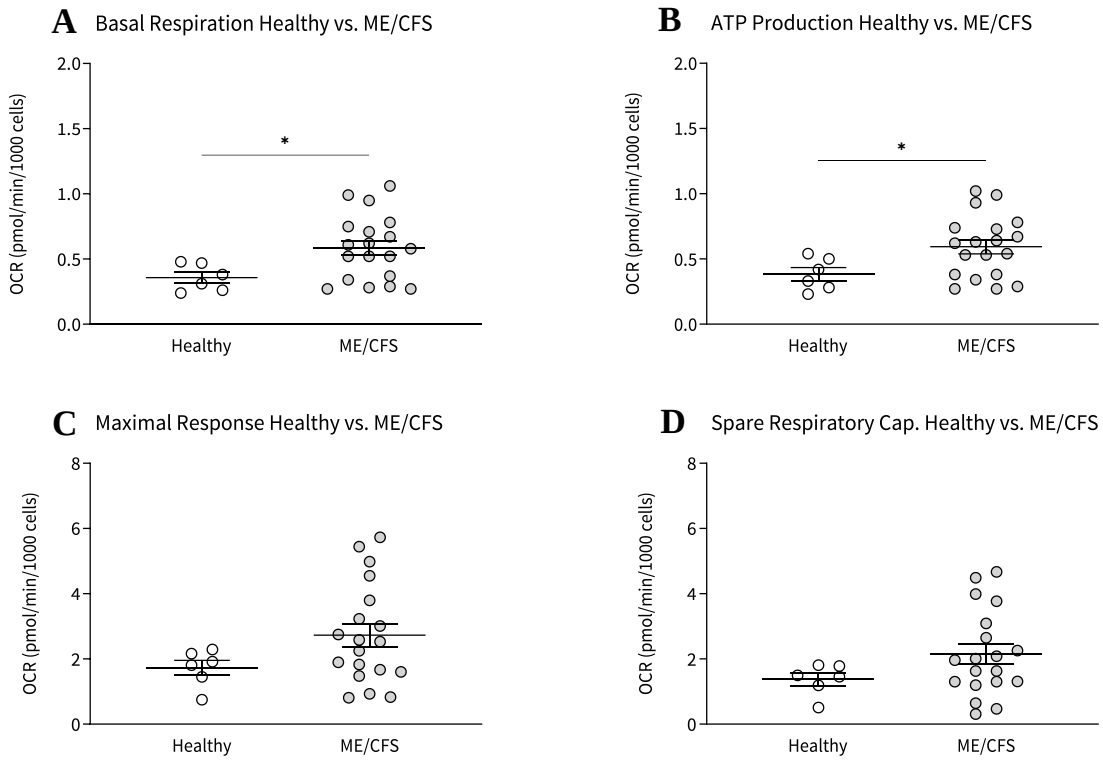

Figure 25: Mitochondrial function in health and disease. A-B Basal respiration and ATP production increase by 63.80% (*p = 0.0414, unpaired t-test) and 54.87% (*p = 0.0497, unpaired t-test) respectively. **C-D** Maximal response and spare respiratory capacity increase by 57.89% (p = 0.1359, unpaired t-test) and 56.02% (p = 0.1783%, unpaired t-test) respectively.

3.3 Ex vivo Hyperthermia

3.3.1 Autophagy – healthy Fibroblasts

Following the successful establishment of an autophagy assay for human fibroblasts, the effect of wIRA irradiation (1 h at 39 °C) on fibroblasts from a healthy eight-year-old male donor was investigated. This experiment was repeated three times and the results are shown in the figure below (**Figure 26**). Data are presented as n-fold autophagosomes per nuclei to focus on the change in the number of autophagosomes rather than the actual number of autophagosomes. The individual experiments show an increase in the number of autophagosomes in all three experiments performed (descriptive without statistical test). This clear effect of wIRA treatment is also reflected in the grouped values of the three experiments conducted, as the n-fold increase in the number of autophagosomes is significantly increased due to the treatment by 142% (**p = 0.0015, unpaired t-test). Results of this study were published in Hochecker *et al.* [161].

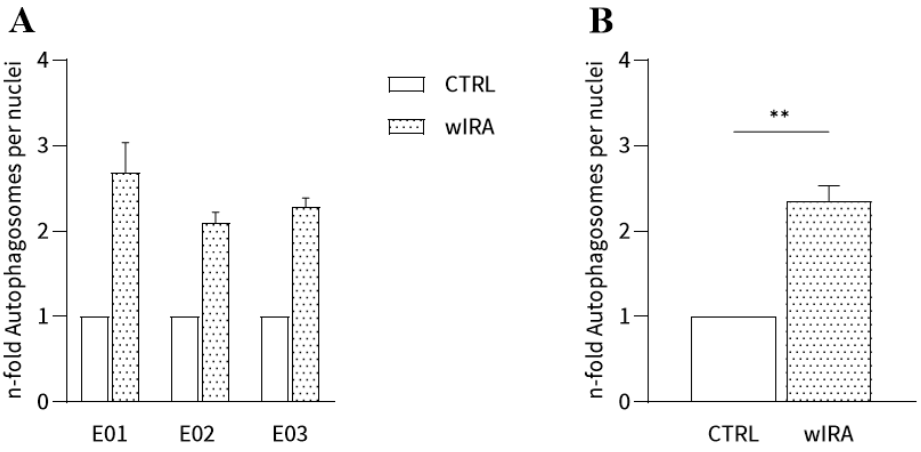

Figure 26: Increased autophagosomes per nuclei by hyperthermia (1 h at 39 °C) in healthy human fibroblasts. A The individual data from three independent experiments all show an increase after one hour of hyperthermia at 39 °C (descriptive without statistical test). **B** The summarised values of the three experiments also show a significant increase by 142%(**p = 0.0015, unpaired t-test) in the number of autophagosomes due to hyperthermia.

The increasing number of autophagosomes per cell nucleus due to hyperthermia cannot only be estimated by the software. The microscopic images of the fibroblasts with the Cytation 1 Imager also provide a visible indication of an increase in autophagosomes. The following images (**Figure 27**) show an image of untreated human fibroblasts and an image of human fibroblasts treated for one hour in the IRAcubator at 39 °C. The images originate from experiment 03 (E03) in the previous figure (**Figure 26**). The comparison of the two images shows that there are more and more intensely stained autophagosomes per nuclei in the treated cells compared to the control group.

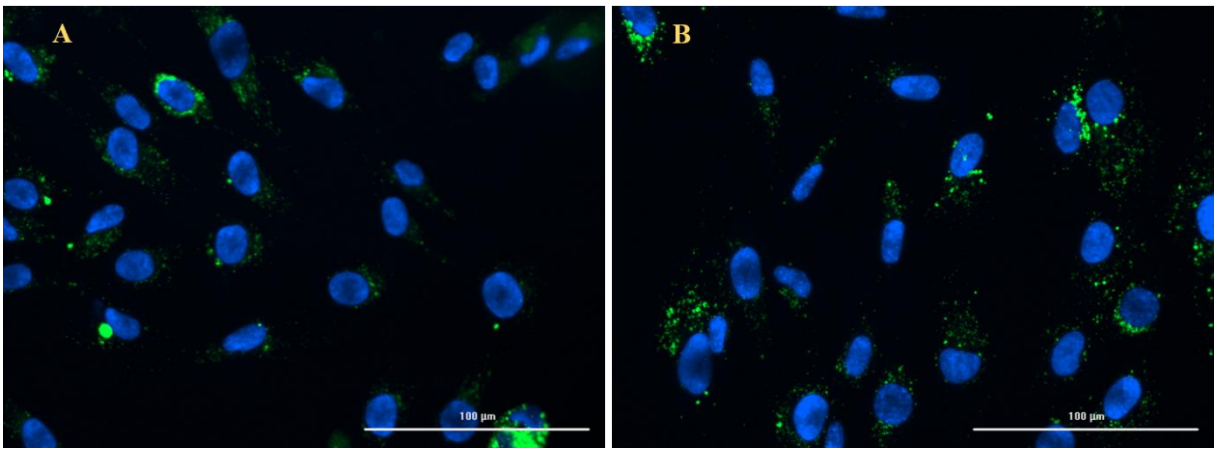

Figure 27: An increased number of autophagosomes due to hyperthermia is visible in microscopic images of human fibroblasts. The treated fibroblasts (B) show more and more intensely stained autophagosomal structures (green dots) per cell nucleus (blue) than the untreated control (A).

3.3.2 Autophagy – PBMCs

a) Healthy Donors

The ex vivo study which contains the wIRA irradiation of isolated PBMCs for one hour at 39 °C, began with the examination of PBMCs from healthy donors. The following figure **Figure 28** shows the results of the measurements of the LC3-II level, a marker of autophagy, of PBMCs from eight healthy donors with and without hyperthermia. Looking at the individual values, each participant shows an increase due to wIRA irradiation compared to the untreated cells (descriptive without statistical test). The individual values represent the mean value of three technical replicates with their SEM. The grouped values of all eight donors are shown as box-whisker diagram with line at the median. Comparison of the two groups using a paired t-test shows a significant increase in the mean LC3-II levels due to wIRA irradiation by 16% (***p = 0.0001).

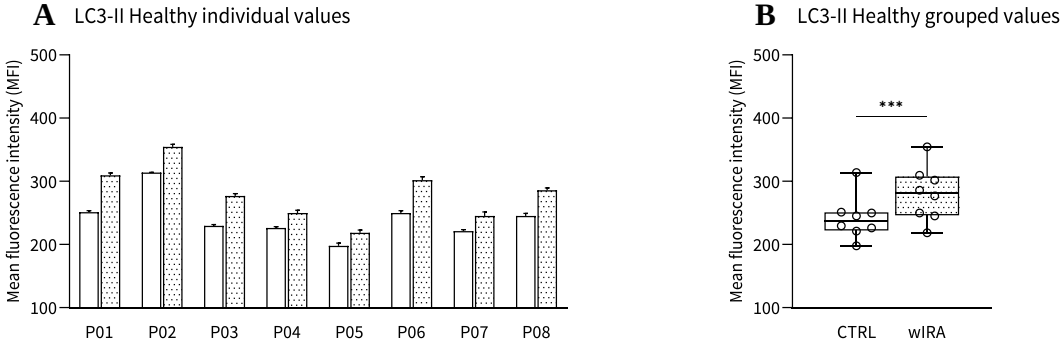

Figure 28: Treatment with ex vivo hyperthermia leads to an increase in the fluorescence intensity of LC3-II in PBMCs from healthy donors. A All eight healthy donors examined show an increase in their LC3 values after one hour at 39°C by wIRA irradiation (descriptive without statistical test). **B** The grouped values of this experiment also show a significant increase by 16% of the mean (***p = 0.0001, paired t-test) due to wIRA treatment.

b) ME/CFS Patients

In addition to the ex vivo examination of PBMCs from healthy donors, PBMCs from ME/CFS patients were also tested for the effect of one hour of wIRA irradiation at 39 °C. **Figure 29** shows the individual data of 23 ME/CFS patients with three technical replicates and the corresponding SEM. An increase in LC3-II values due to hyperthermia can be observed in 18 participants (P01, P02, P03, P04, P05, P06, P07, P09, P12, P14, P17, P18, P19, P20, P21, P22, P23, P24). Participants P08, P10 and P11 show no visible changes due to the treatments, and two participants (P13, P16) show a decrease in LC3-II values due to wIRA irradiation (descriptive without statistical test). The grouped values of all 23 participants are shown in **Figure 29** and indicate a significant increase in the mean LC3-II values due to wIRA irradiation by 7% (****$p < 0.0001$), the statistical analysis was performed with a paired t-test.

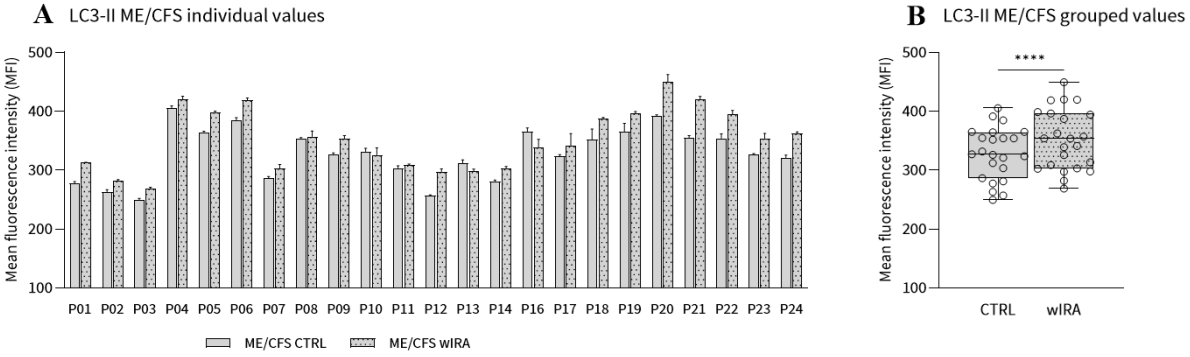

Figure 29: Ex vivo hyperthermia affects LC3-II levels in PBMCs from ME/CFS patients. A Of the total of 23 participants, 18 ME/CFS patients show an increase (P01, P02, P03, P04, P05, P06, P07, P09, P12, P14, P17, P18, P19, P20, P21, P22, P23, P24) in their LC3-II values as a result of the one-hour wIRA treatment at 39 °C. Three participants (P08, P10, P11) show no visible changes in their LC3-II values as a result of hyperthermia and two participants (P13, P16) show a decrease in their LC3-II values (descriptive without statistical test). **B** The grouped values of all participants show a significant increase in their mean LC3-II values by 7% (****$p < 0.0001$, paired t-test) due to the hyperthermia treatment.

c) Healthy vs. ME/CFS

The following box-whisker diagram compares the effect of ex vivo irradiation on LCB-II levels in PBMCs from healthy donors and ME/CFS patients (**Figure 30**). The data show a significant increase in LC3-II for healthy donors by 16% (***p = 0.0001) as well as for ME/CFS patients by 7% (****p < 0.0001). A paired t-test was used for the statistical analysis. These results were published in Hochecker *et al.* [161].

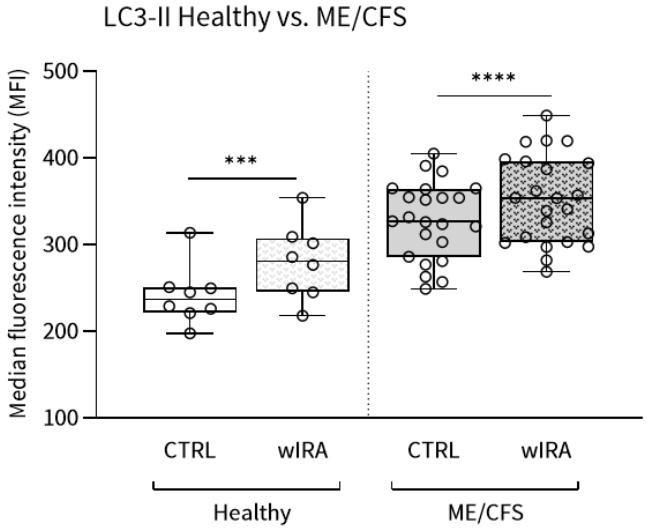

Figure 30: Ex vivo hyperthermia affects LC3-II levels in health and disease. One hour at 39 °C leads to a significant increase in LC3-II levels in PBMCs from healthy donors by 16% (***p = 0.0001, paired t-test) and ME/CFS patients by 7% (****p < 0.0001, paired t-test).

3.3.3 Mitochondrial function – PBMCs

a) Healthy Donors

The results of the effect of wIRA irradiation (1 h, 39 °C) of isolated PBMCs from six healthy donors on their mitochondrial function are shown in **Figure 31**. The individual basal respiration values show an increase due to wIRA treatment in participants P02 and P03. Participant P01 shows no visible changes due to the heat treatment. Three participants (P04, P05, P09) have a slight decrease in basal respiration. The individual parameter of ATP production shows an increase in P01, P02 and P03. The values of participants P04-P09 decrease due to wIRA irradiation. All participants with the exception of P04, which remains at the same level, decrease in the maximal response. The same observation as for the maximum response can also be made for the spare respiratory capacity (descriptive without statistical test). The grouped values of all participants show no visible changes due to the heat treatment in basal respiration (decrease by 2.34%, p = 0.7731, paired t-test) and ATP production (decrease by 2.61%, p = 0.7349, paired t-test), the parameters maximal response

and spare respiratory capacity decrease significantly by 19.75% (*p = 0.0185, paired t-test) and by 24.36% (*p = 0.0148, paired t-test) through hyperthermia.

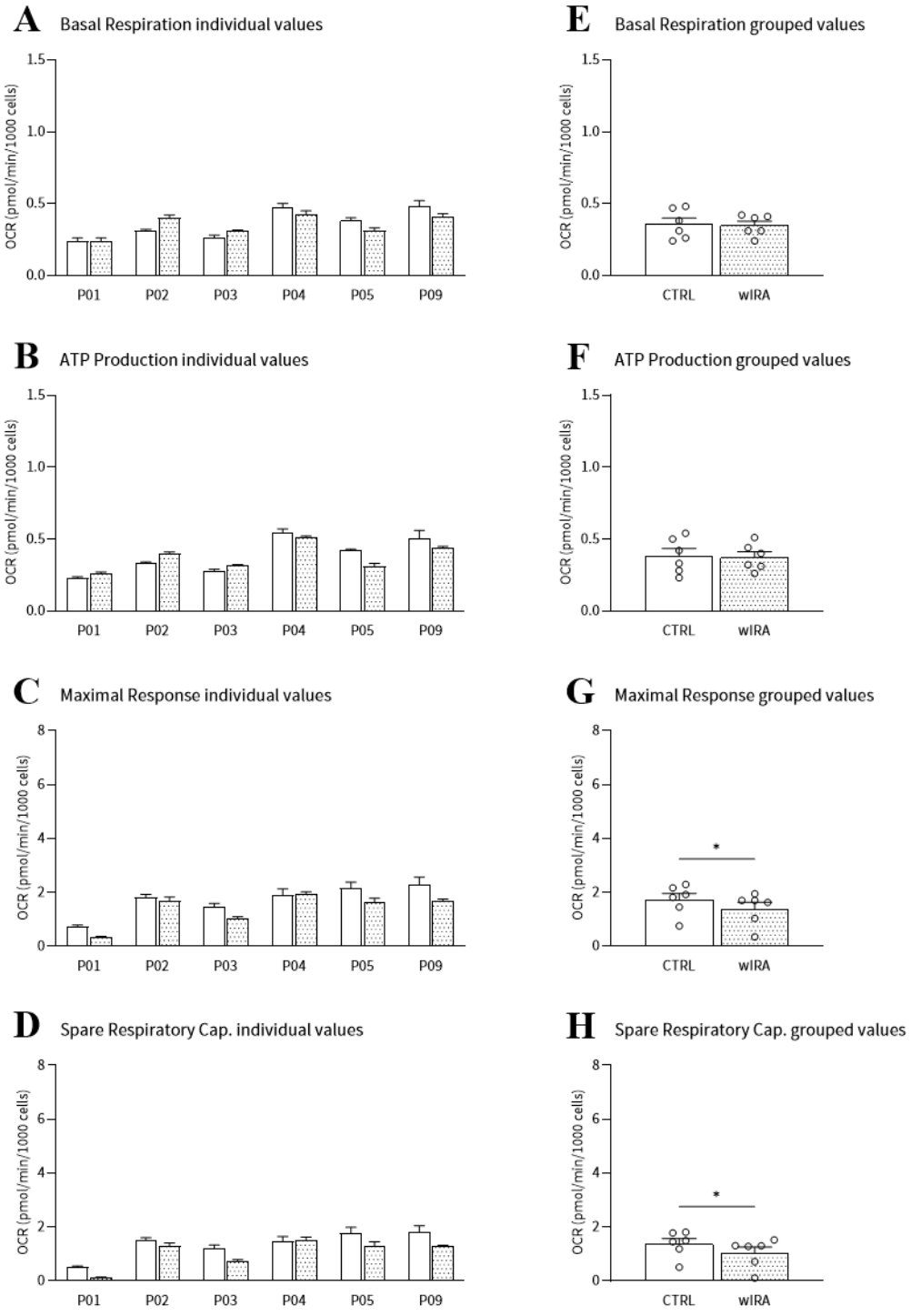

Figure 31: Effect of ex vivo hyperthermia on mitochondrial function in PBMCs from healthy donors (n=6). A In basal respiration, an increase due to wIRA treatment is visible in participants P02 and P03. P01 shows no visible changes due to treatments. P04, P05 and P09 have a slight decrease in basal respiration. **B** An increase in ATP production is observed in P01, P02 and P03. P04-P09 decrease due to wIRA irradiation. **C-D** All participants with the exception of P04, which remains at the same level, decrease in the maximal response and spare respiratory capacity (descriptive without statistical test). **E, F** The grouped values of all participants show no visible changes due to heat treatment in

basal respiration (decrease by 2.34%, p = 0.7731, paired t-test) and ATP production (decrease by 2.61%, p = 0.7349, paired t-test) **G, H** The parameters maximal response (19.75%, *p = 0.0185, paired t-test) and spare respiratory capacity decrease (24.36%, *p = 0.0148, paired t-test) due to heating to 39 °C for one hour.

b) ME/CFS Patients

The effect on hyperthermia was also measured in PBMCs from eleven ME/CFs patients and shown in **Figure 32**. Six participants (P13, P14, P16, P21, P22, P23) show an increase in basal respiration and remain the same in participant P18. A slight decrease is observed in P17 and P19, while participants P20 show a significant decrease. Hyperthermia had a slightly increasing effect on ATP production in seven participants (P13, P14, P16, P18, P21, P22, P23) and a decreasing effect in participants P17, P19, P20 and P24. A decrease was observed in the maximum response of participants P17, P20, P21 and P24. P16 shows no difference due to heat treatment, while the remaining participants P13, P14, P18, P19, P22 and P23 show a slight increase due to wIRA irradiation. The spare respiratory capacity increases slightly in participants P13, P14, P18, P19, P22 and P23 as a result of hyperthermia and decreases in participant P16, P17, P20, P21 and P24 (descriptive without statistical test). The grouped values of all participants show a decrease for all measured mitochondrial parameters as a result of a one-hour hyperthermia treatment at 39 °C. More specific, basal respiration is decreasing by 8.17% (p =0.914, Wilcoxon test), ATP Production by 7.30% (p = 0.8818, Wilcoxon test), maximal response by 24.14% (p = 0.6221, Wilcoxon test) and spare respiratory capacity by 28.21% (p = 0.1161, paired t-test).

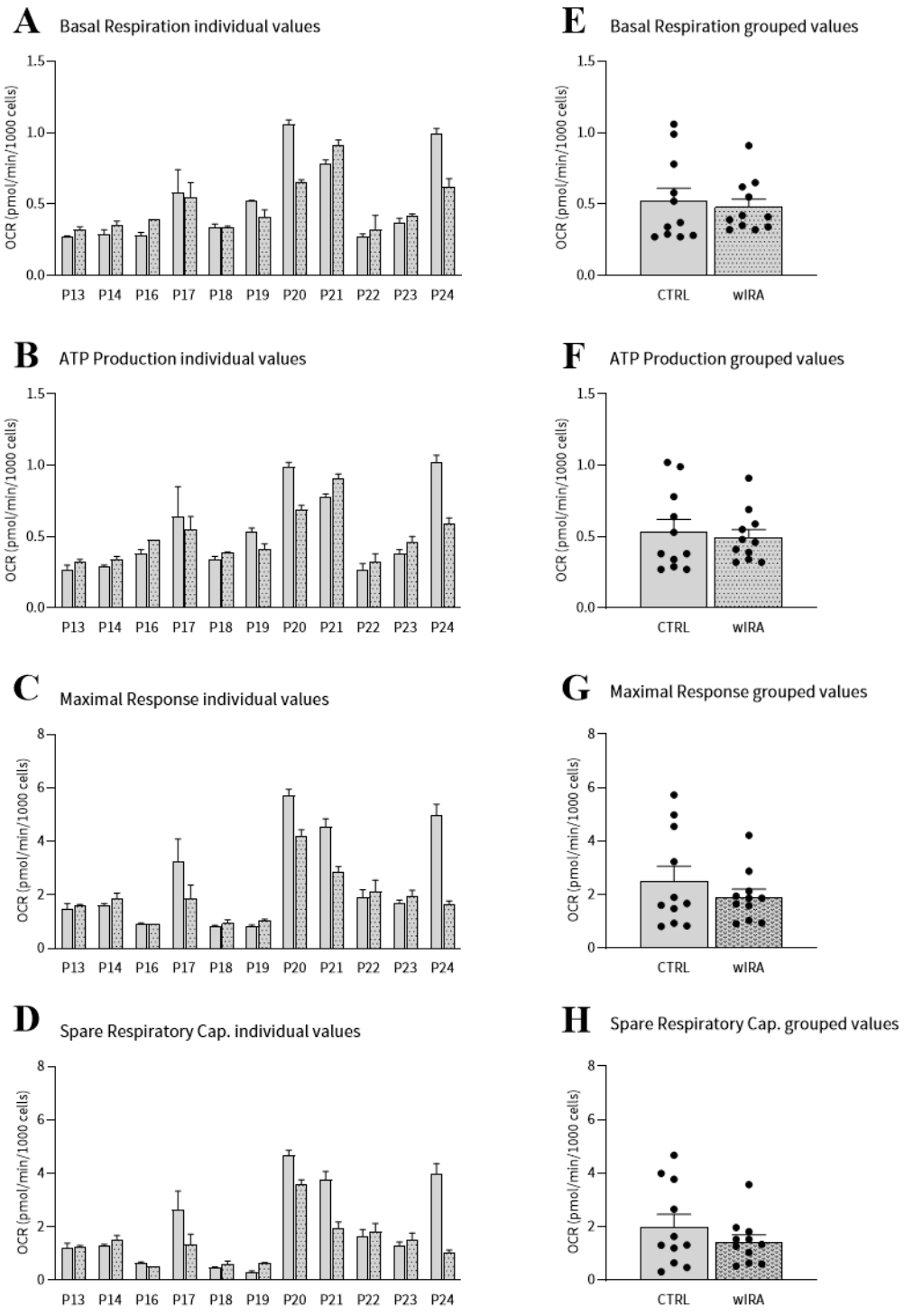

Figure 32: Effect of ex vivo hyperthermia on mitochondrial function in PBMCs of ME/CFS patients (n=11). A Basal respiration does increase six participants (P13, P14, P16, P21, P22, P23) and remains the same in P18 as a result of wIRA irradiation. A decrease is observed in P17, P19, P20 and P24. **B** Hyperthermia has an increasing effect on ATP production in seven participants (P13, P14, P16, P18, P21, P22, P23) and a decreasing effect in participants P17, P19, P20 and P24. **C** There is also a decrease in the maximal response in P17, P20, P21 and P24. P16 shows no difference by heat treatment, while the remaining participants P13, P14, P18, P19, P22 and P23 show an increase by wIRA irradiation. **D** The spare respiratory capacity increases in participants P13, P14, P18, P19, P22 and P23 and decreases in participants P16, P17, P20, P21 and P24 (descriptive without statistical test). **E-H** The grouped values of basal respiration are decreasing by 8.17% ($p = 0.914$, Wilcoxon test), ATP production by 7.30% ($p = 0.8818$, Wilcoxon test), maximal response by 24.14% ($p = 0.6221$, Wilcoxon test) and spare respiratory capacity by 28.21% ($p = 0.1161$, paired t-test).

c) Healthy vs. ME/CFS

The following **Figure 33** shows the comparison of ex vivo hyperthermia on mitochondrial function in health and disease. The comparison of the effects of heat treatment (39 °C for one hour) on the analysed mitochondrial parameters shows a similar picture. The parameters of basal respiration show no visible decrease due to the treatment in healthy donors (2.34%, p = 0.7731, paired t-test) and a slight decrease in ME/CFS patients (8.17%, p =0.914, Wilcoxon test). The same pattern is visible for ATP production with a decrease of 2.61% (p = 0.7349, paired t-test) due to hyperthermia in healthy donors and 7.30% (p = 0.8818, Wilcoxon test) in ME/CFS patients. The effects on maximal response and spare respiratory capacity also appear to be very similar. Maximal response is decreasing by 19.75% (*p = 0.0185, paired t-test) in healthy donors and by 24.14% (p = 0.6221, Wilcoxon test) in ME/CFS patients. Healthy donors decrease by 24.36% (*p = 0.0148, paired t-test) in their spare respiratory capacity due to wIRA irradiation and by 28.21% (p = 0.1161, paired t-test) in ME/CFS patients. These results were published in Hochecker *et al.* [161].

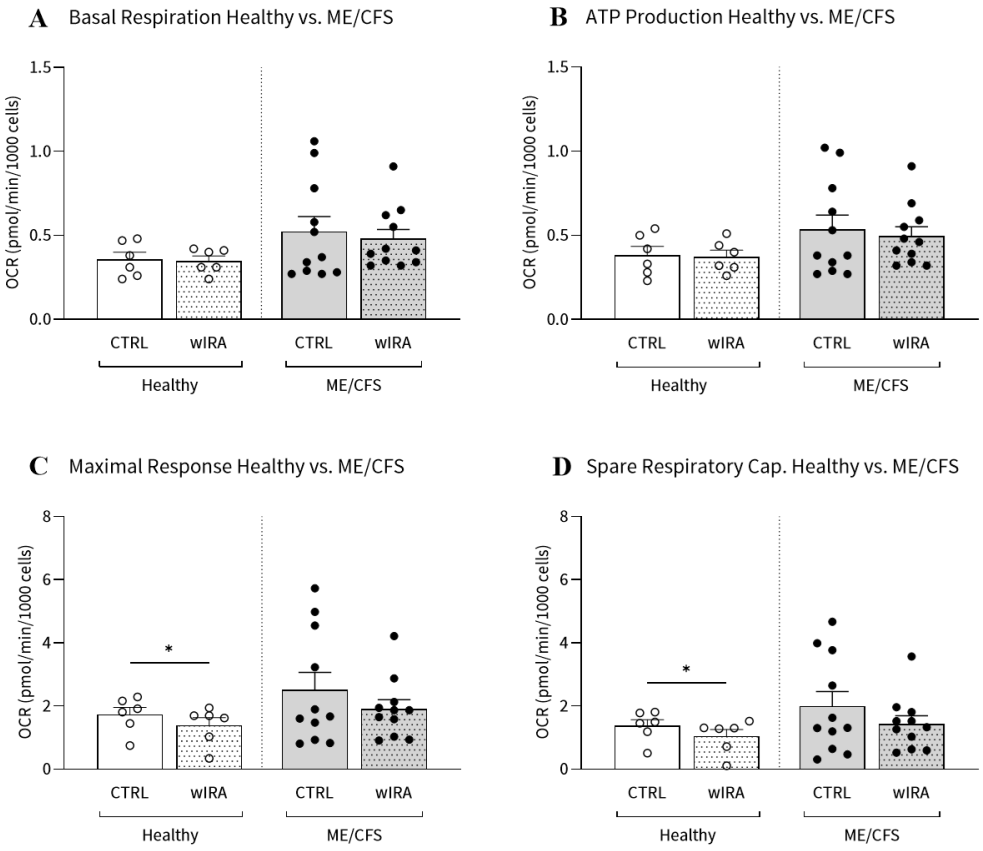

Figure 33: Impact of ex vivo hyperthermia on mitochondrial function in health (n=6) and disease (n=11). A comparison of the effects of heat treatment (39 °C for one hour) on the mitochondrial parameters analysed reveals a similar picture. **A-B** Basal respiration decreases in healthy donors (2.34%, p = 0.7731, paired t-test) and in ME/CFS patients (8.17%, p = 0.914, Wilcoxon test). ATP production decrease by 2.61% (p = 0.7349, paired t-test) in healthy donors and by 7.30% (p = 0.8818, Wilcoxon test) in ME/CFS patients. **C** Maximal response is decreasing by 19.75% (*p = 0.0185, paired t-test) in healthy donors and by 24.14% (p = 0.6221, Wilcoxon test) in ME/CFS patients. **D** Spare respiratory capacity decrease by 24.36% (*p = 0.0148, paired t-test) in healthy donors and by 28.21% (p = 0.1161, paired t-test) in ME/CFS patients.

3.3.4 mRNA expression – PBMCs

a) Healthy Donors

Autophagy - associated genes

The following **Figure 34** shows the n-fold expression of autophagy genes in PBMCs from eight healthy donors with and without one-hour ex vivo heat treatment at 39 °C. Six participants (P01, P02, P04, P06, P07, P08) show a decrease in *ULK1* expression, while no changes are seen in participant P03. A slight increase in *ULK1* gene expression was observed in one participant (P05). Four participants (P01, P02, P04, P06) show an increase in their *BECN1* expression, two participants (P03, P08) remain at the same level and a decrease is observed in P05 and P07. Six (P01, P02, P03, P06, P07, P08) of the eight participants show a decrease in their mRNA expression of *ATG7*, the remaining participants P04 and P05 show no changes in their *ATG7* expression. *MAP1LC3B* expression increases in three participants (P01, P02, P04), remains the same in participants P06 and P08 and decreases in three participants (P03, P05, P07) (descriptive without statistical test). The grouped values indicate a non-significant decrease in *ULK1* by 5.88% ($p = 0.2656$, Wilcoxon test) and significant decrease in *ATG7* by 15.63% (**$p = 0.0060$, paired t-test) in mRNA expression due to hyperthermia treatment. *BECN1* and *MAP1LC3B* show a slight but non-significant increase in mRNA expression by 2.75% ($p = 0.4067$, paired t-test) and by 5.75% ($p = 0.4245$, paired t-test).

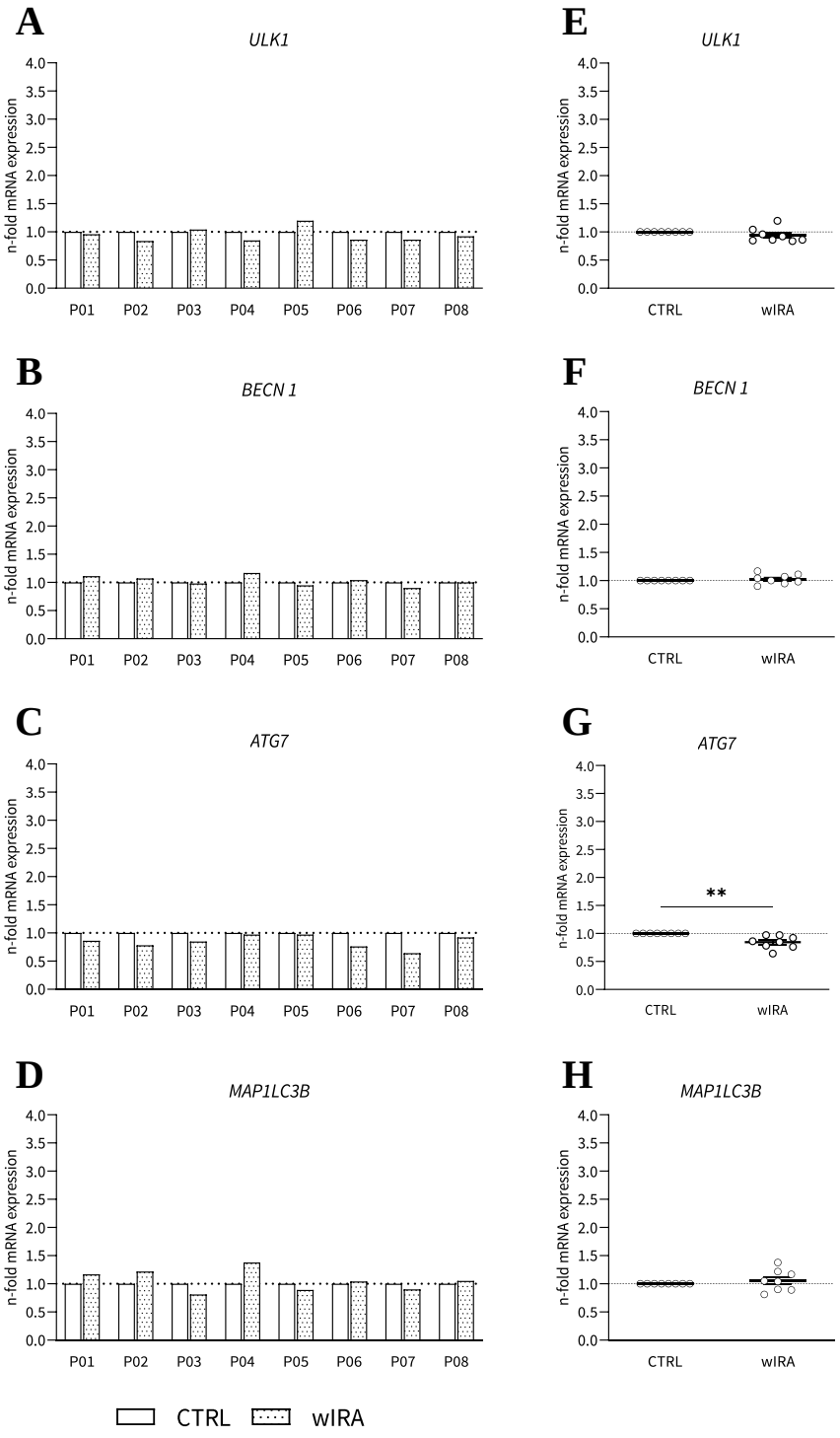

Figure 34: Effect of ex vivo wIRA irradiation on genes encoding proteins involved in the autophagosomal process in PBMCs from healthy donors. A Treatment led to a decrease in *ULK1* in six participants (P01, P02, P04, P06, P07, P08), while no visible change was observed in participant P03. Participant P05 shows a slight increase in the mRNA expression of *ULK1*. **B** In the case of *BECN1*, an increase in expression can be observed in the four participants P01, P02, P04 and P06. The two participants P03 and P08 remain at the same level, while a decrease is observed in P05 and P07. **C** The majority of participants show a decrease in the expression of *ATG7* (P01, P02, P03, P06, P07, P08). P04 and P05 show no changes in their expression. **D** *MAP1LC3B* expression increases in the three participants P01, P02 and P04, remains the same in P06 and P08 and decreases in the three participants P03, P05 and P07 (descriptive without statistical test). **E** *ULK1* decreases by 5.88% ($p = 0.2656$, Wilcoxon test). **F** *BECN1* increases in mRNA expression by 2.75% ($p = 0.4067$, paired t-test) **G** The expression of *ATG7* shows a significant decrease of 15.64% (**$p = 0.0060$, paired t-test) in mRNA. **H** *MAP1LC3B* displays a slight but non-significant increase of 5.75% ($p = 0.4245$, paired t-test) in mRNA expression.

The impact of hyperthermia (1 h, 39 °C) on genes encoding autophagy-regulating proteins in PBMCs from healthy donors is shown in **Figure 35** below. *AMPK1α* expression is increased by heat treatment in three participants (P01, P02 P04), while the two participants P03 and P06 show no changes and the remaining participants P05, P07 and P08 show decreases. The gene expression of *FOXO3* decreases in four participants (P02, P03, P05, P07), remains the same in participant P04 and increases in the three donors P01, P06 and P08. All eight participants show an increase in *SIRT1* expression due to hyperthermia (descriptive without statistical test). This is also reflected in the grouped values by a significant increase in *SIRT1* by 40.38% (**p = 0.0026, paired t-test). The grouped values of *AMPK1α* is increasing by 6.00% (p = 0.4536, paired t-test) and *FOXO3* decreases by 1.50% (p = 0.7908, paired t-test) as an effect of hyperthermia on their expression.

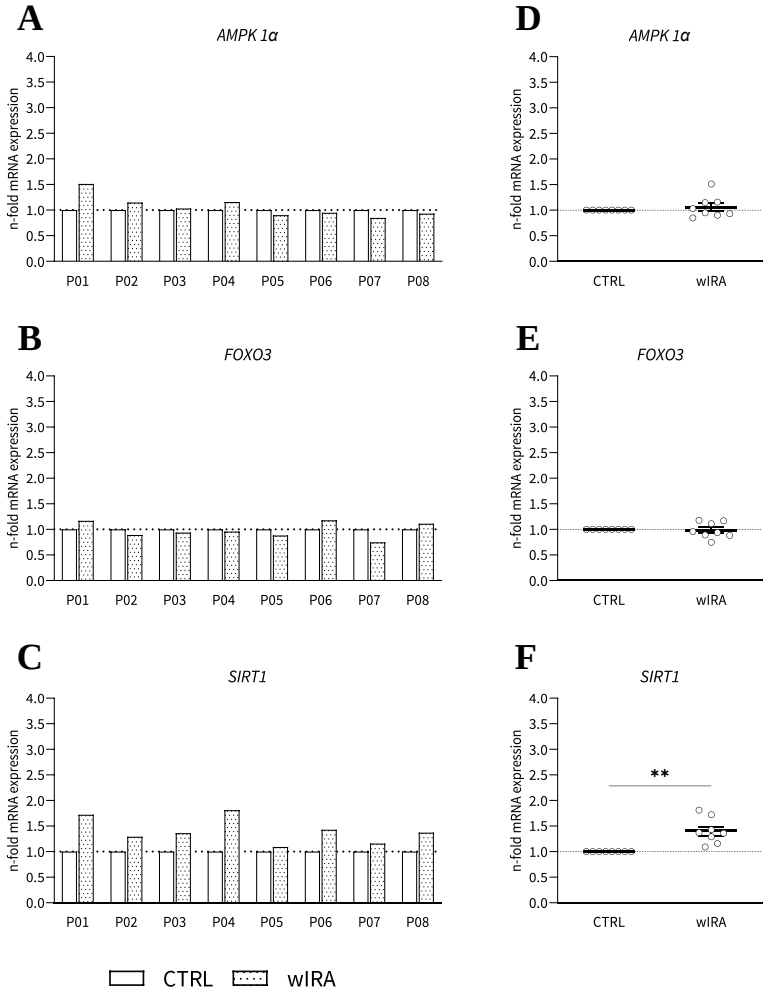

Figure 35: Impact of ex vivo hyperthermia on genes encoding proteins involved in the regulation of autophagy in PBMCs from healthy donors. A The three participants P01, P02 and P04 show an increase in the expression of *AMPK1α*. Participants P03 and P06 remain at the same level, whereas P05, P07 and P08 decrease as a result of the treatment. **B** The gene expression of *FOXO3* decreases in four participants (P02, P03, P05, P07), remains the same in participant P04 and increases in the three donors P01, P06 and P08. **C** An increase in the expression of *SIRT1* can be observed in all participants. (descriptive without statistical test) **D-E** The grouped values of *AMPK1α* is increasing by 6.00% (p = 0.4536, paired t-test) and *FOXO3* decreases by 1.50% (p = 0.7908, paired t-test) **F** There is a significant increase in the mRNA expression of *SIRT1* by 40.38% (**p = 0.0026, paired t-test) as a result of heat treatment.

Mitochondrial function – associated genes

The response of the mitochondrial genes *SIRT3*, *TFAM*, *NDUFS1* and *SOD2* from healthy donors to heat treatment (1 h, 39 °C) was also analysed in PBMCs (**Figure 36**). The expression of *SIRT3* in five participants (P03, P05, P06, P07, P08) showed no changes due to the treatment. Participants P02 and P04 showed reduced expression, while expression increased in participant P01. In the five participants P01, P02, P03, P04 and P05, *TFAM* expression increases, in participants P06 and P08 there are no changes and in participant P07 the expression decreases. *NDUFS1* expression remains at the same level in five participants (P03, P04, P05, P06, P07), decreases in P02 and increases in P01 and P08. Four participants (P01, P02, P03, P06) show an increase in their *SOD2* expression, while the other four participants (P04, P05, P07, P08) remain at the same level (descriptive without statistical test). The grouped values show a decrease by 3.00% for *SIRT3* ($p = 0.2812$, Wilcoxon test). The expression of *TFAM* and *NDUFS1* shows a slight increase by 9.75% ($p = 0.0501$, paired t-test) and by 4.38% ($p = 0.9688$, Wilcoxon test). *SOD2* is significant increasing by 16.00% ($^*p = 0.0424$, paired t-test) in expression due to wIRA irradiation.

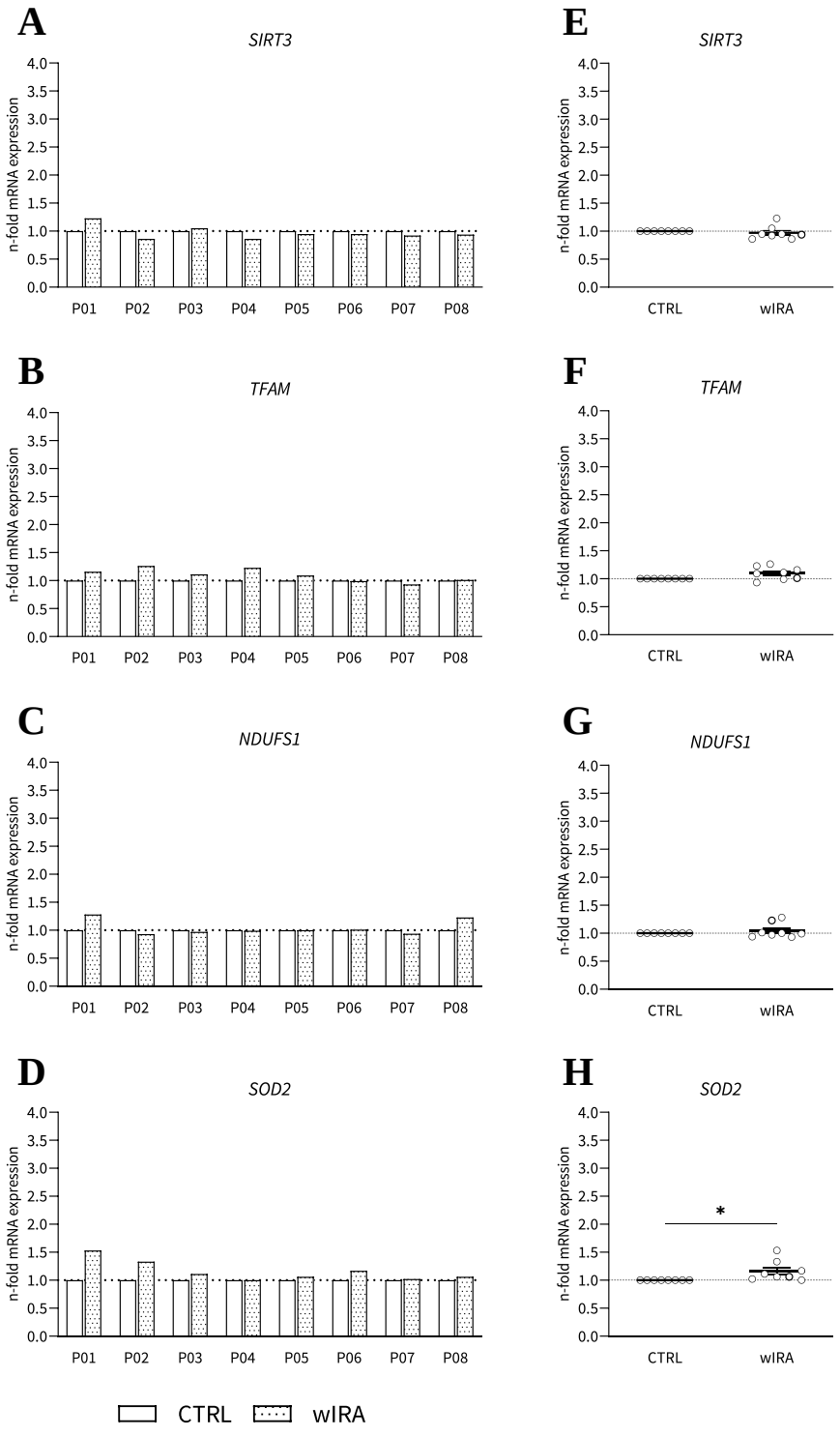

Figure 36: Effect of ex vivo wIRA irradiation on genes encoding proteins involved in mitochondrial function in PBMCs from healthy donors. A The expression of *SIRT3* remains at the same level in five participants (P03, P05, P06, P07, P08) due to heat treatment. P02 and P04 show a decrease in expression and P01 an increase. **B** In the case of *TFAM* expression, the five participants P01, P02, P03, P04 and P05 show an increase. Participant P07 displays a decrease and P06 and P08 remain at the same level due to hyperthermia. **C** *NDUFS1* expression remains at the same level in five participants (P03, P04, P05, P06, P07), decreases in P02 and increases in P01 and P08. **D** For *SOD2* expression, P01, P02, P03 and P06 show an increase, while participants P04, P05, P07 and P08 remain at the same level (descriptive without statistical test). **E** The grouped values show a decreasing by 3.0% ($p = 0.2812$, Wilcoxon test) for *SIRT3*. **F** *TFAM* shows an increase by 9.75% ($p = 0.0501$, paired t-test). **G** *NDUFS1* increases by 4.38% ($p = 0.9688$, Wilcoxon test). **H** *SOD2* shows a significant increase by 16.00% ($^*p = 0.0424$, paired t-test) in expression due to wIRA irradiation.

Additional genes

The additional markers *HSPA5* and *IL-10* show the following results after heat treatment of isolated PBMCs from healthy donors (**Figure 37**). In four participants (P02, P04, P06, P08) the expression of *HSPA5* increases and the other four participants (P01, P03, P05, P07) remain at the same level. In summary, this leads to a significant increase in *HSPA5* expression of 17.38% (*p = 0.0471, paired t-test). For *IL-10* expression, four participants (P02, P06, P07, P08) show a decrease, three participants (P01, P03, P05) remain at the same level and participant P04 increases due to hyperthermia (descriptive without statistical test). The grouped values of *IL-10* show a not significant decrease by 12.25% (p = 0.2506, paired t-test).

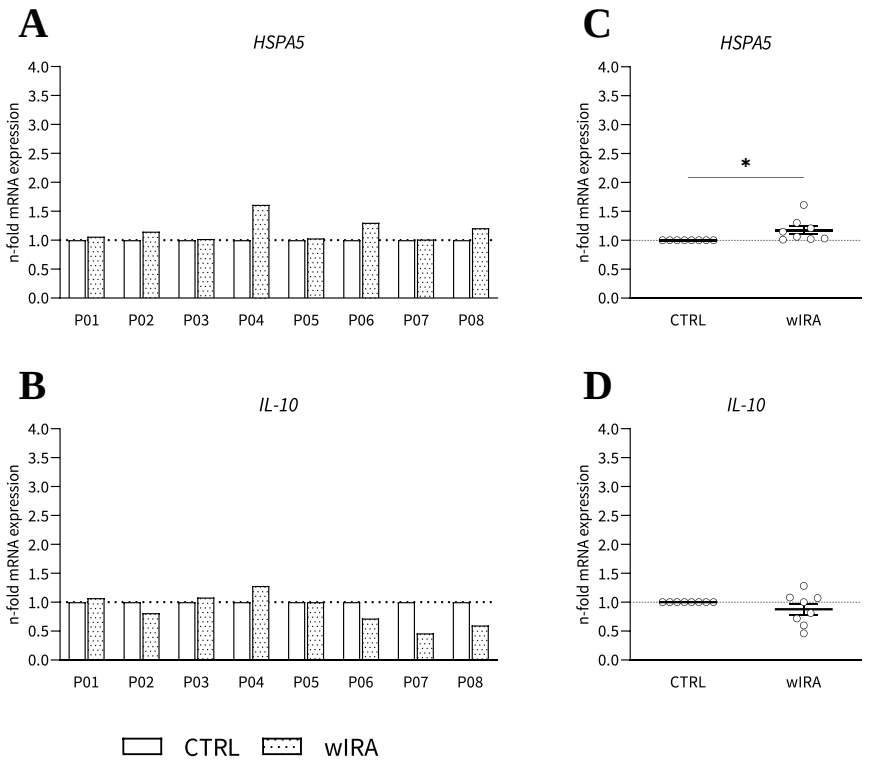

Figure 37: Effects of ex vivo hyperthermia on additional markers in PBMCs from healthy donors. A The expression of *HSPA5* increases in four participants (P02, P04, P06, P08) and remains the same in P01, P03, P05 and P07. **C** The grouped values for *HSPA5* show a significant increase by 17.38% (*p = 0.0471, paired t-test) due to the heat treatment. **B** The four participants P02, P06, P07 and P08 show a decrease in the expression of *IL-10*. P01, P03 and P05 show no changes, whereas P04 shows an increase due to hyperthermia (descriptive without statistical test). **D** The grouped values show a not significant decrease by 12.25% (p = 0.2506, paired t-test) in *IL-10*.

b) ME/CFS Patients

Autophagy – associated genes

The influence of ex vivo heat treatment on gene expression was also investigated in PBMCs from 20 ME/CFS patients. In the case of autophagy genes *ULK1* expression increases in five participants (P05, P10, P16, P20, P21), five remain at the same level (P01, P02, P07, P12, P13) and ten decrease (P03, P04, P06, P08, P11, P17, P18, P19, P22, P23) through the treatment. *BECN1* expression increases in ten participants (P03, P07, P08, P13, P17, P18, P19, P21, P22, P23), remains the same in four (P01, P04, P06, P11) and decreases in six (P02, P05, P10, P12, P16, P20). In 14 participants (P02, P04, P05, P06, P07, P08, P10, P11, P12, P16, P17, P18, P20, and P22) decreased the *ATG7* expression, two participants increased (P19, P21) and four participants (P01, P03, P13 and P23) remained on the same level (descriptive without statistical test). In summery this leads to a significant decrease in *ATG7* expression by 14.95% (**p = 0.0024, paired t-test). *MAP1LC3B* expression increases in 15 participants (P01, P02, P03, P05, P06, P07, P08, P10, P11, P17, P18, P19, P21, P22, P23), is maintained in P04, P12, P13 and P16 and decreases in P20. In summary *MAP1LC3B* expression increases significantly by 19.65% (***p = 0.0001, paired t-test). *ULK1* is increasing by 3.10% (p = 0.2142, Wilcoxon test) and *BECN1* by 5.70% (p = 0.0907, paired t-test) in the grouped values (**Figure 38**).

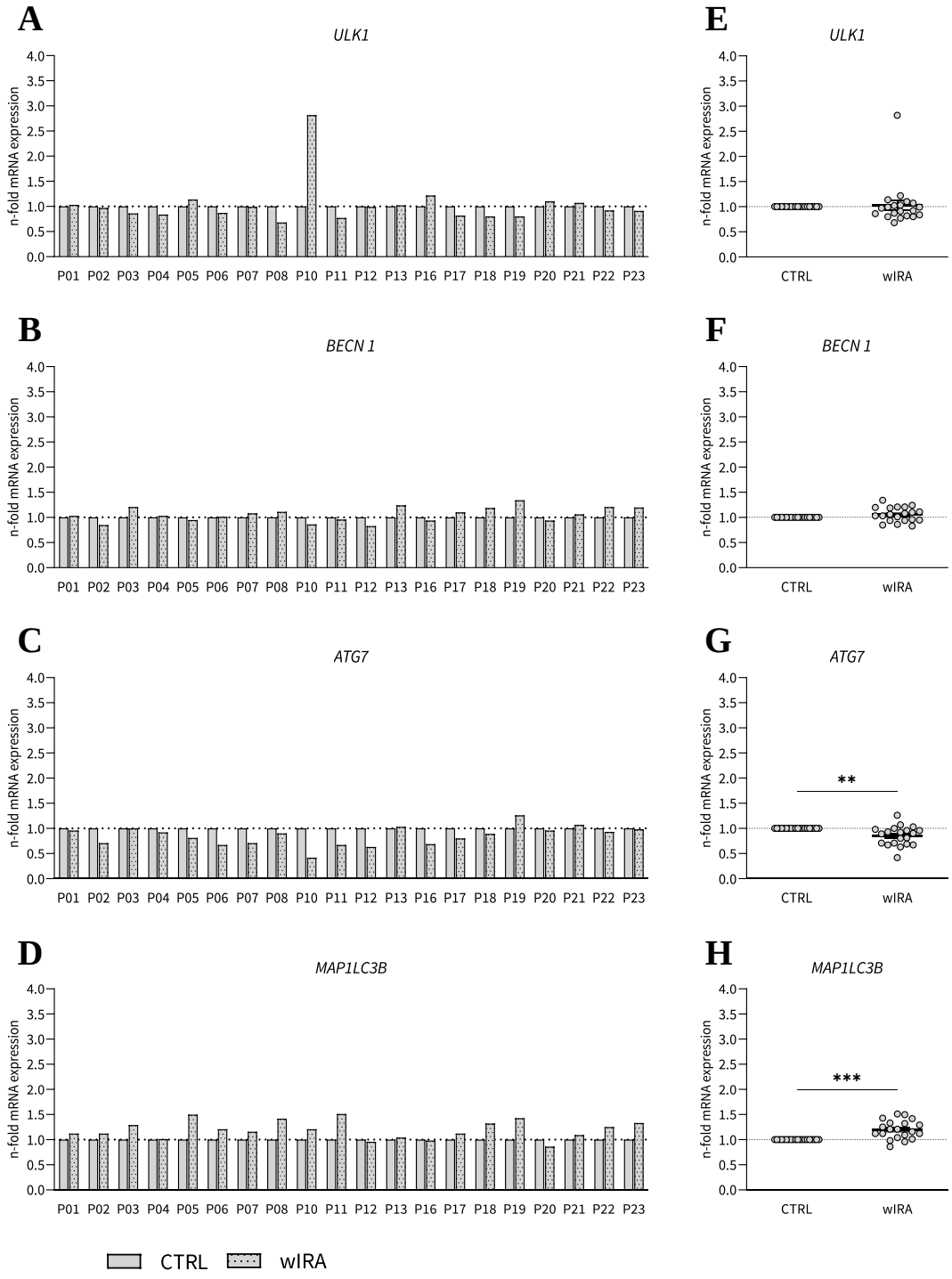

Figure 38: Effect of ex vivo wIRA irradiation on genes encoding proteins involved in the autophagosomal process in PBMCs of ME/CFS patients. A *ULK1* expression increases in five participants (P05, P10, P16, P20, P21), five remain at the same level (P01, P02, P07, P12, P13) and ten decrease (P03, P04, P06, P08, P11, P17, P18, P19, P22, P23). **B** *BECN1* expression increases in ten participants (P03, P07, P08, P13, P17, P18, P19, P21, P22, P23), remains the same in four (P01, P04, P06, P11) and decreases in six (P02, P05, P10, P12, P16, P20). **C** *ATG7* shows an increase in expression for P19 and P21. Expression remains at the same level for P01, P03, P13 and P23 and decreases in 14 participants (P02, P04, P05, P06, P07, P08, P10, P11, P12, P16, P17, P18, P20, P22). **D** *MAP1LC3B* expression increases in 15 participants (P01, P02, P03, P05, P06, P07, P08, P10, P11, P17, P18, P19, P21, P22, P23), is maintained in P04, P12, P13 and P16 and decreases in P20. **E-F** *ULK1* and *BECN1* increase by 3.10% ($p = 0.2142$, Wilcoxon test) and by 5.70% ($p = 0.0907$, paired t-test) in the grouped values. **G-H** The expression of *ATG7* decreases significantly by 14.95% (**$p = 0.0024$, paired t-test) due to heat treatment and that of *MAP1LC3B* increases significantly by 19.65% (***$p = 0.0001$, paired t-test).

In addition to analysing the gene expression of autophagy genes, the expression of genes encoding autophagy-regulating proteins was tested after heat treatment (1 h, 39 °C) of PBMCs from ME/CFS patients (**Figure 39**). The expression of *AMPK1α* increased in eight participants (P03, P05, P06, P07, P08, P13, P17, P19), but remained the same in participants P01, P04 and P18. Reduced expression was observed in the remaining nine participants (P02, P10, P11, P12, P16, P20, P21, P22, P23). *FOXO3* increases in eight participants (P05, P10, P13, P16, P17, P19, P20, P21), remains the same in P04, P07, P11, P23 and decreases in eight participants (P01, P02, P03, P06, P08, P12, P18, P22). The grouped values of gene expression of *AMPK1α* (+2.35%, p = 0.6311, paired t-test) and *FOXO3* (+ 0.75%, p = 0.8251, paired t-test) show no noteworthy changes due to hyperthermia, while *SIRT1* is significantly increased after heat treatment by 33.10% (****p < 0.0001, paired t-test). This is due to the increase in *SIRT1* in 17 participants (P01, P02, P03, P04, P05, P06, P07, P08, P11, P13, P16, P17, P18, P19, P21, P22, P23). Despite the fact that the other three participants (P10, P12, P20) show a decline in their expression.

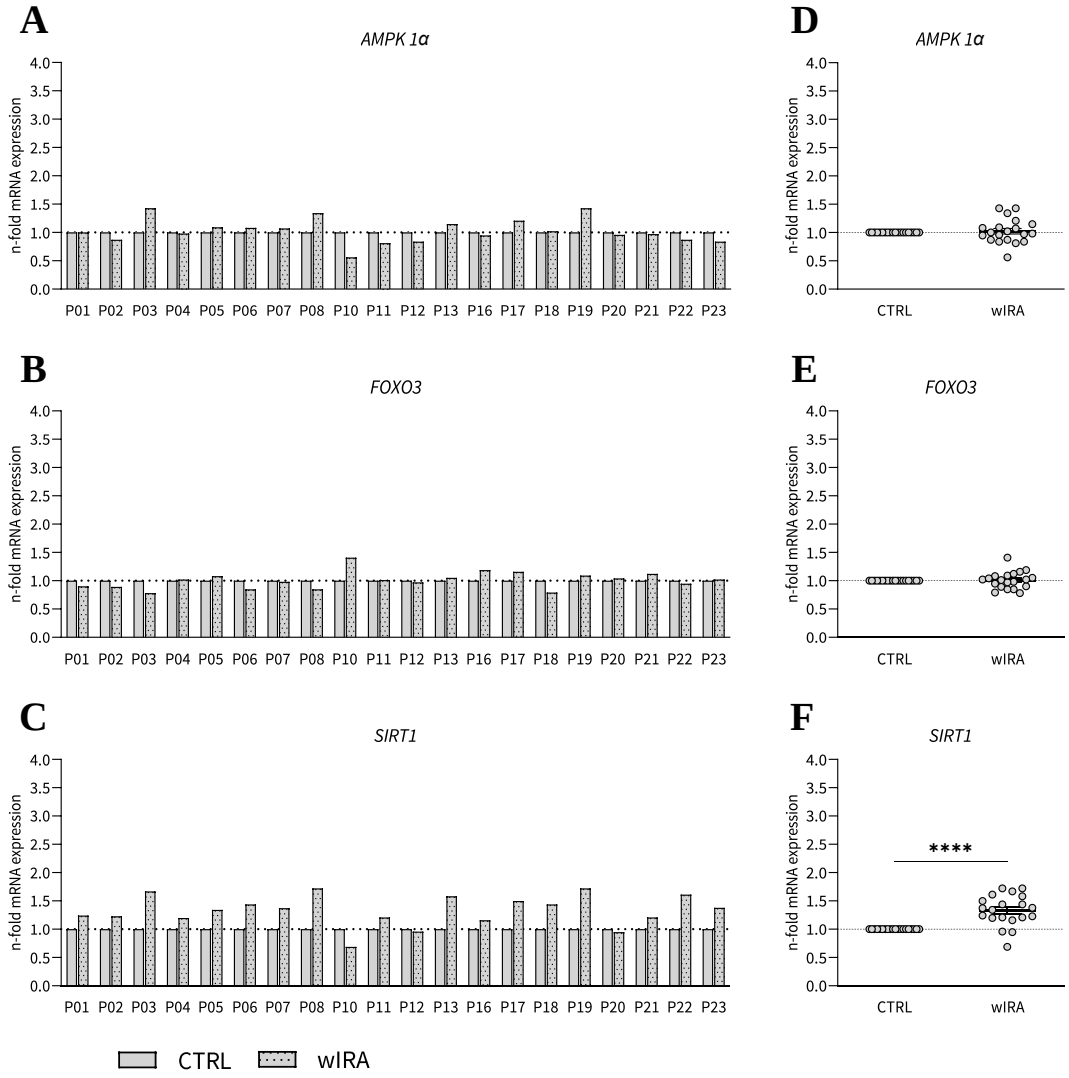

Figure 39: Effects of ex vivo hyperthermia on genes encoding proteins involved in the regulation of autophagy in PBMCs of ME/CFS patients. A *AMPK1α* expression is elevated by hyperthermia in eight participants (P03, P05, P06, P07, P08, P13, P17, P19). Expression remains at the same level in P01, P04 and P18 and decreases in the other nine participants (P02, P10, P11, P12, P16, P20, P21, P22, P23). **B** *FOXO3* increases in eight participants (P05, P10, P13, P16, P17, P19, P20, P21), remains the same in P04, P07, P11, P23 and decreases in eight participants (P01, P02, P03, P06, P08, P12, P18, P22). **C** Only three participants show a decrease in *SIRT1* expression (P10, P12, P20), all other participants show an increase in *SIRT1* expression (P01, P02, P03, P04, P05, P06, P07, P08,P11, P13, P16, P17, P18, P19, P21, P22, P23) (descriptive without statistical test). **D-E** The grouped values show no relevant changes for *AMPK1α* (+2.35%, p = 0.6311, paired t-test) and *FOXO3* (+ 0.75%, p = 0.8251, paired t-test). **F** The expression of *SIRT1* is significantly increased by 33.10% (****p < 0.0001, paired t-test) after heat treatment.

Mitochondrial function – associated genes

The impact of hyperthermia (1 h, 39 °C) on mitochondrial gene expression in PBMCs from ME/CFS patients is shown in **Figure 40**. The results show an increase in *SIRT3* expression in eight participants (P01, P02, P04, P05, P10, P16, P17 and P20), no changes in participants P11, P19 and P22, while the other nine participants (P03, P06, P07, P08, P12, P13, P18, P21, P23) show a decrease in their expression. *TFAM* expression increases in twelve participants (P01, P02, P03, P04, P07, P08, P11, P13, P17, P18, P19, P22), remains the same in two patients (P06, P20) and decreases

in six (P05, P10, P12, P16, P21, P23). Of the total of 20 participants, twelve participants (P01, P04, P06, P07, P10, P11, P12, P16, P20, P21, P22, P23) decrease in their *NDUFS1* expression due to hyperthermia, seven participants (P03, P05, P08, P13, P17, P18, P19) increase, while the one remaining participant P02 shows no changes. The grouped values of the expressions of *SIRT3* shows an increase of 12.40% ($p = 0.8194$, Wilcoxon test), *TFAM* of 6.40% ($p = 0.1678$, paired t-test). *NDUFS1* shows a decrease by 3.90% ($p = 0.3595$, paired t-test) due to hyperthermia. *SOD2* expression increases in 13 participants (P03, P05, P06, P07, P08, P11, P12, P17, P18, P19, P21, P22, P23), decreases in four (P01, P02, P10, P13) and remains the same in three (P04, P16, P20). In summary, this leads to a significant increase in the grouped values of *SOD2* by 18.15% (**$p = 0.0086$, paired t-test).

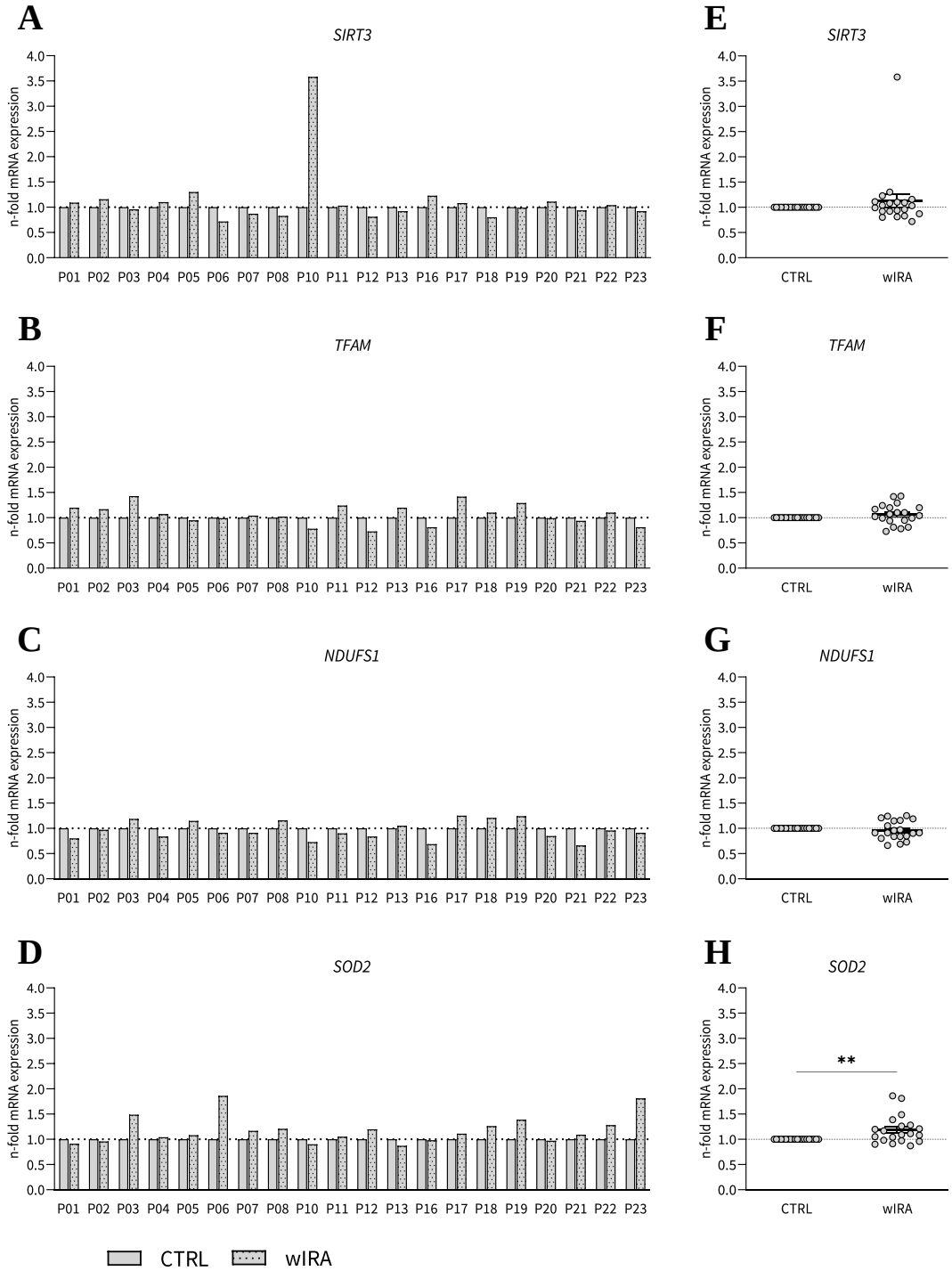

Figure 40: Effect of ex vivo wIRA irradiation on genes encoding proteins involved in mitochondrial function in PBMCs of ME/CFS patients. A *SIRT3* expression is increased by heat treatment in eight participants (P01, P02, P04, P05, P10, P16, P17, P20). The participants P11, P19 and P22 remain at the same level and nine participants show a decrease (P03, P06, P07, P08, P12, P13, P18, P21, P23). **B** The expression of *TFAM* increases in twelve participants (P01, P02, P03, P04, P07, P08, P11, P13, P17, P18, P19, P22), remains the same in two patients (P06, P20) and decreases in six (P05, P10, P12, P16, P21, P23). **C** *NDUFS1* expression decreases in most participants (P01, P04, P06, P07, P10, P11, P12, P16, P20, P21, P22, P23), increases in seven participants (P03, P05, P08, P13, P17, P18, P19) and remains the same in one (P02). **D** *SOD2* expression increases in 13 participants (P03, P05, P06, P07, P08, P11, P12, P17, P18, P19, P21, P22, P23), decreases in four (P01, P02, P10, P13) and remains the same in three (P04, P16, P20) (descriptive without statistical test). **E.** Grouped values of *SIRT3* shows an increase of 12.40% ($p = 0.8194$, Wilcoxon test)**. F** *TFAM* expression is increasing by 6.40% ($p = 0.1678$, paired t-test). **G** *NDUFS1* shows a decrease by 3.90% ($p = 0.3595$, paired t-test). **H** *SOD2* is significantly increased after heat treatment by 18.15% (**$p = 0.0086$, paired t-test).

Additional genes

The additional markers *HSPA5* and *IL-10* show the following results after heat treatment of isolated PBMCs from 20 ME/CFS patients **Figure 41**. In 16 participants (P01, P03, P04, P05, P06, P07, P08, P11, P12, P13, P17, P18, P19, P21, P22, P23) the expression of *HSPA5* increases, P20 is maintained and in the other three (P02, P10, P16) it decreases. In summary, this leads to a significant increase in *HSPA5* expression by 12.55% (***p = 0.0003, paired t-test). *IL-10* expression increases in seven participants (P05, P06, P08, P18, P19, P21, P22), remains in three (P04, P11, P23) and decreases in ten (P01, P02, P03, P07, P10, P12, P13, P16, P17, P20). The grouped values of *IL-10* are decreasing by 3.30% (p = 0.6245, paired t-test).

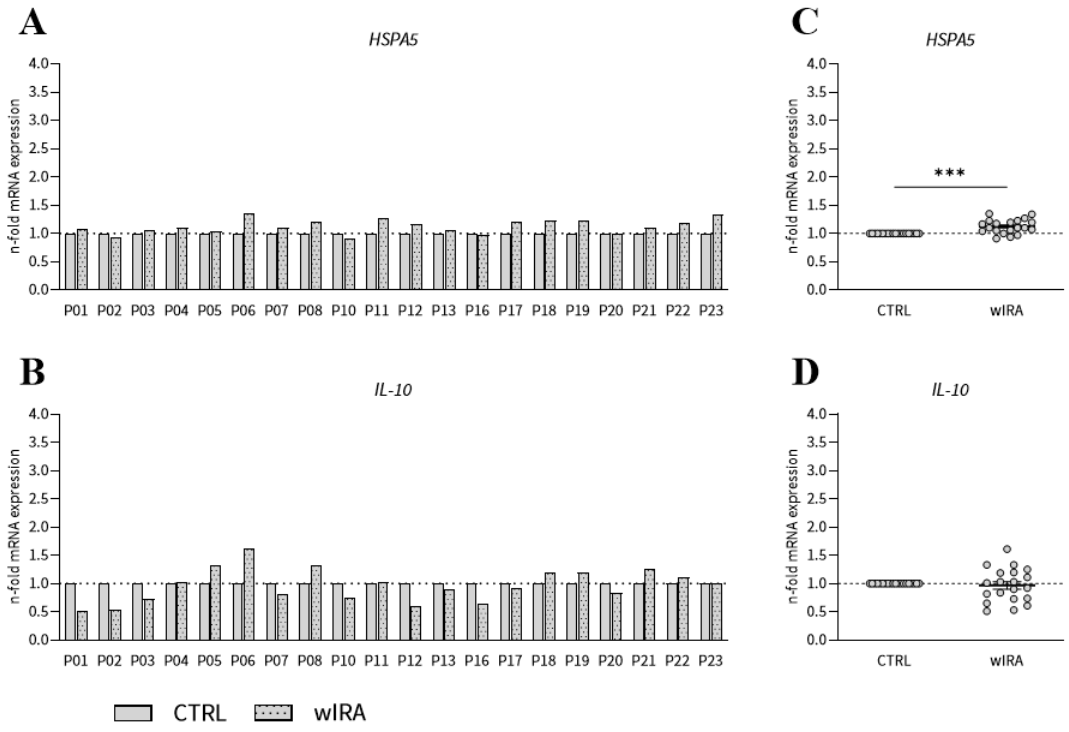

Figure 41: Effects of ex vivo hyperthermia on additional markers in PBMCs of ME/CFS patients. A *HSPA5* expression increases with hyperthermia in 16 participants (P01, P03, P04, P05, P06, P07, P08, P11, P12, P13, P17, P18, P19, P21, P22, P23), remains the same in P20 and decreases in three (P02, P10, P16). **B** *IL-10* expression increases in seven participants (P05, P06, P08, P18, P19, P21, P22), remains in three (P04, P11, P23) and decreases in ten (P01, P02, P03, P07, P10, P12, P13, P16, P17, P20). **C-D** The grouped values show a significant increase by 12.55% (***p = 0.0003, paired t-test) in the expression of *HSPA5* due to wIRA irradiation, while *IL-10* is decreasing by 3.30% (p = 0.6245, paired t-test).

c) Healthy vs. ME/CFS

Autophagy – associated genes

To compare the effect of ex vivo hyperthermia on PBMCs from healthy donors with PBMCs from ME/CFS patients, the data of the measured mRNA expressions of the two groups are presented in a collective figure for each gene considered. The first **Figure 42** shows the expression of the autophagy genes. The four analysed genes *ULK1*, *BECN1*, *ATG7* and *MAP1LC3B* show a similar pattern of expression in health and disease. *ULK1* is decreasing by 5.88% (p = 0.2656, Wilcoxon test) in healthy donors and increasing by 3.10% (p = 0.2142, Wilcoxon test) in ME/CFS patients. In the case of *BECN1* the mRNA expression is increasing by 2.75% (p = 0.4067, paired t-test) in healthy donors and by 5.70% (p = 0.0907, paired t-test) in ME/CFS patients. In addition, the expression of *ATG7* is significantly reduced in health by 15.63% (**p = 0.0060, paired t-test) and disease by 14.95% (**p = 0.0024, paired t-test). *MAP1LC3B* shows a non-significant increase by 5.75% (p = 0.4245, paired t-test) in the healthy group, while the expression of *MAP1LC3B* increases significantly in ME/CFS patients by 19.65% (***p ≤ 0.001, paired t-test). These results were published in Hochecker *et al.* [161].

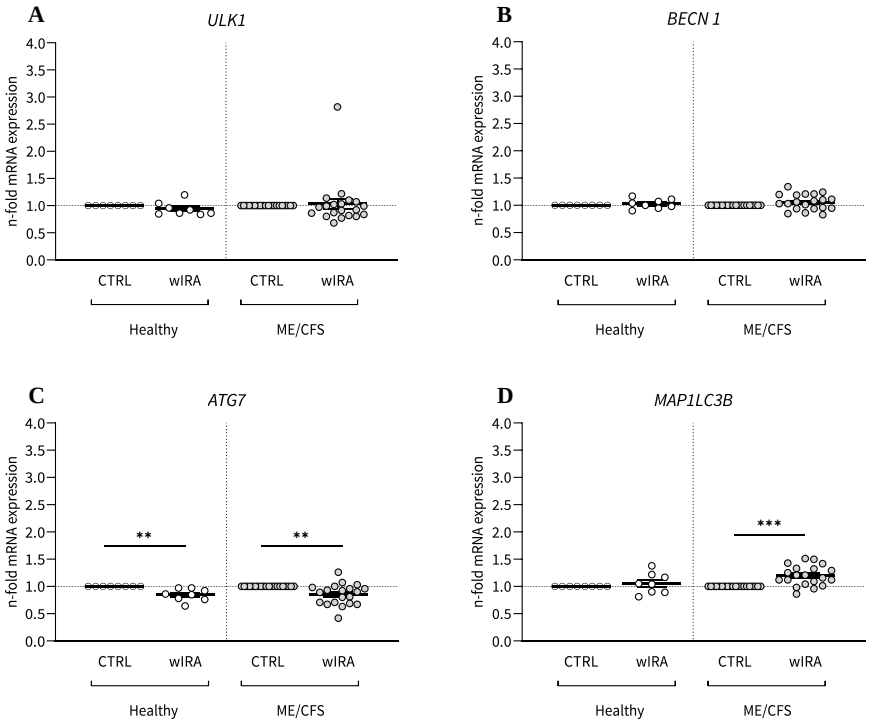

Figure 42: Health vs. disease - effect of ex vivo wIRA irradiation on genes encoding proteins involved in the autophagosomal process in PBMCs. A *ULK1* is decreasing by 5.88% (p = 0.2656, Wilcoxon test) in healthy donors and increasing by 3.10% (p = 0.2142, Wilcoxon test) in ME/CFS patients. **B** *BECN1* is increasing by 2.75% (p = 0.4067, paired t-test) in healthy donors and by 5.70% (p = 0.0907, paired t-test) in ME/CFS patients. **C** *ATG7* shows a significant decrease by hyperthermia in health by 15.63% (**p = 0.0060, paired t-test) and disease by 14.95% (**p = 0.0024, paired t-test). **D** The expression

of *MAP1C3B* increases significantly in ME/CFS patients by 19.65% (***p = 0.0001, paired t-test), paired t-test), while it is not significant in healthy donors 5.75% (p = 0.4245, paired t-test).

The comparison of the mRNA expression of genes coding for proteins regulating autophagy also shows a very similar pattern in their expression in health and disease (**Figure 43**). The expression of *AMPK1α* shows an increase by 6.00% (p = 0.4536, paired t-test) in healthy donors and by 2.35% (p = 0.6311, paired t-test) in ME/CFS patients. *FOXO3* decreases by 1.50% (p = 0.7908, paired t-test) in healthy donors and increases by 0.75% (p = 0.8251, paired t-test) in ME/CFS patients. In the case of *SIRT1*, the healthy donors (+ 40.38%, **p = 0.0026, paired t-test) and the ME/CFS patients (+33.10%, ****p < 0.0001, paired t-test) show a significant increase in their gene expression. These results were published in Hochecker *et al.* [161].

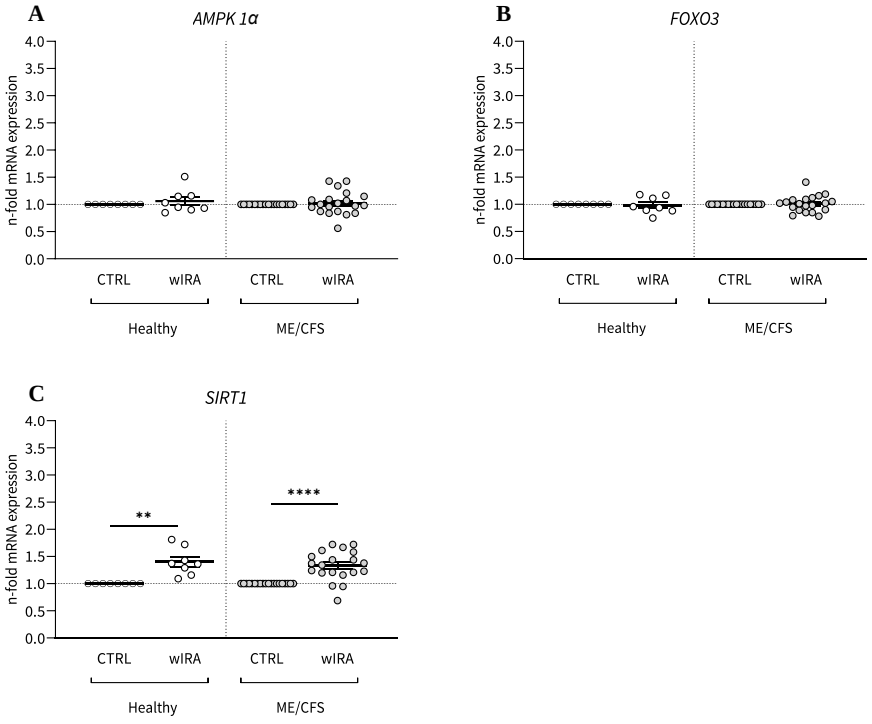

Figure 43: Health vs. disease - impact of ex vivo hyperthermia on genes encoding proteins involved in the regulation of autophagy in PBMCs. A *AMPK1α* increases by 6.00% (p = 0.4536, paired t-test) in healthy donors and by 2.35% (p = 0.6311, paired t-test) in ME/CFS patients. **B** *FOXO3* decreases by 1.50% (p = 0.7908, paired t-test) in healthy donors and increases by 0.75% (p = 0.8251, paired t-test) in ME/CFS patients. **C** *SIRT1* expression shows a significant increase in gene expression in health by 40.38% (**p ≤ 0.01, paired t-test) and disease by 33.10% (****p < 0.0001, paired t-test).

Mitochondrial function – associated genes

The expression of the mitochondrial genes *SIRT3*, *TFAM*, *NDUFS1* and *SOD2* also shows a similar response in PBMCs from healthy donors and PBMCs from ME/CFS patients to heat treatment (1 h, 39 °C) (**Figure 44**). The expression of *SIRT3* decrease by 3.00% for *SIRT3* (p = 0.2812, Wilcoxon test) in healthy donors and increases by 12.40% (p = 0.8194, Wilcoxon test) in ME/CFS patients. The mRNA expression of *TFAM* increases by 9.75% (p = 0.0501, paired t-test) in healthy donors and by 6.40% (p = 0.1678, paired t-test) in ME/CFS patients. *NDUFS1* shows a slight increase by 4.38% (p = 0.9688, Wilcoxon test) in healthy donors, whereas the expression is decreasing by 3.90% (p = 0.3595, paired t-test) in ME/CFS patients. The expression of *SOD2* increases significantly in PBMCs from healthy donors by 16.00% (*p = 0.0424, paired t-test) and PBMCs from ME/CFS patients by 18.15% (**p = 0.0086, paired t-test). These results were published in Hochecker *et al.* [161].

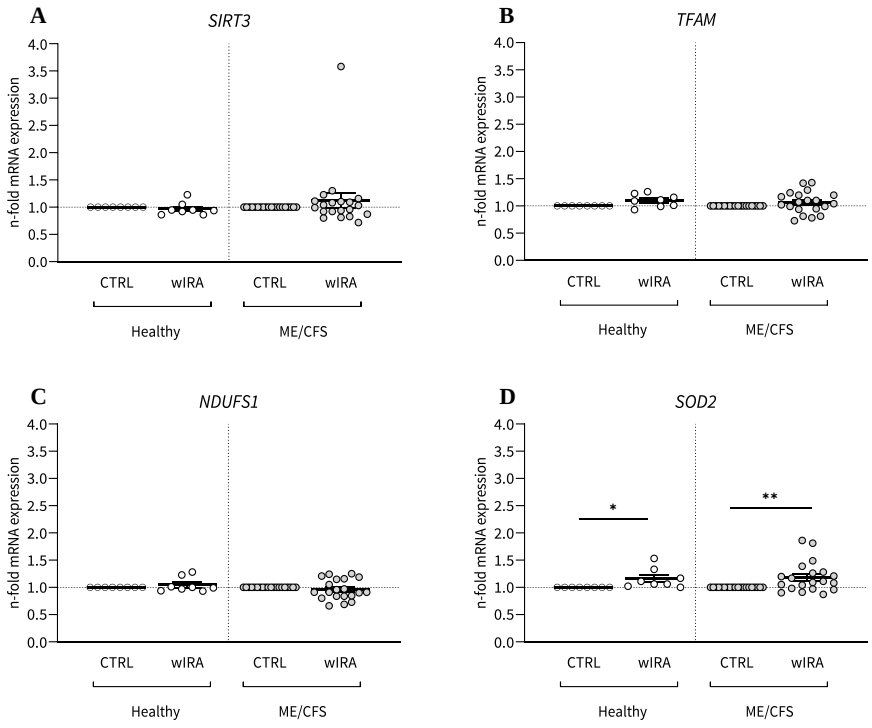

Figure 44: Health vs. disease - effect of ex vivo wIRA irradiation on genes encoding proteins involved in mitochondrial function in PBMCs. A *SIRT3* decrease by 3.00% for *SIRT3* (p = 0.2812, Wilcoxon test) in healthy donors and increases by 12.40% (p = 0.8194, Wilcoxon test) in ME/CFS patients.**-B** *TFAM* increases by 9.75% (p = 0.0501, paired t-test) in healthy donors and by 6.40% (p = 0.1678, paired t-test) in ME/CFS patients. **C** *NDUFS1* shows a slight increase by 4.38% (p = 0.9688, Wilcoxon test) in healthy donors, in ME/CFS patients it is decreasing by 3.90% (p = 0.3595, paired t-test) **D** The expression of *SOD2* increases significantly in healthy donors by 16.00% (*p = 0.0424, paired t-test) and ME/CFS patients by 18.15% (**p = 0.0086, paired t-test).

Additional genes

The additional markers *HSPA5* and *IL-10* were also compared in their expression after hyperthermia in PBMCs from healthy donors and ME/CFS patients (**Figure 45**). The expression of *HSPA5* is significantly increased in both the healthy group by 17.83% (*p = 0.0471, paired t-test) and the ME/CFS group by 12.55% (***p = 0.0003, paired t-test). The expression of *IL-10* is decreasing by 12.25% (p = 0.2506, paired t-test) in the healthy group and by 3.30% (p = 0.6245, paired t-test) in the ME/CFS patients. These results were published in Hochecker *et al.* [161].

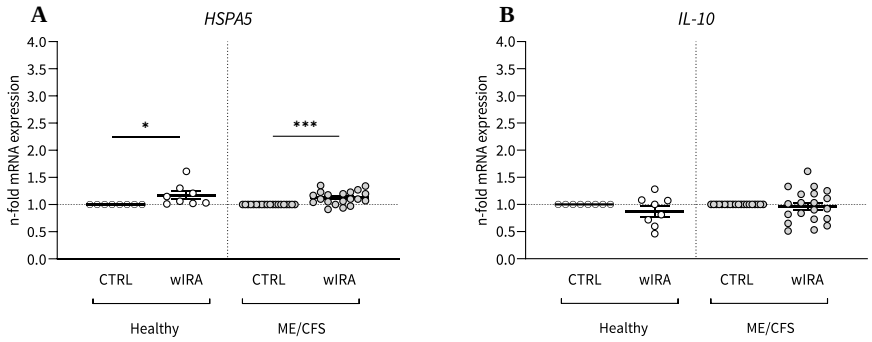

Figure 45: Health vs. disease - effects of ex vivo hyperthermia on additional markers in PBMCs. A The expression of *HSPA5* is significantly increased in healthy donors by 17.83% (*p = 0.0471, paired t-test) and ME/CFS patients by 12.55% (***p = 0.0003, paired t-test), a significant increase in the expression of *HSPA5* is observed after heat treatment. **B** *IL-10* is decreasing by 12.25% (p = 0.2506, paired t-test) in the healthy group and by 3.30% (p = 0.6245, paired t-test) in the ME/CFS patients.

3.4 In vivo Hyperthermia

3.4.1 Autophagy – PBMCs

In contrast to the ex vivo study, not only isolated PBMCs were treated in the in vivo study, but nine ME/CFS patients underwent a session of whole-body hyperthermia (one-hour whole-body hyperthermia (WBH)-therapy with body-core temperature (Tc) max = 39 °C). The results of this study were published in Hochecker *et al.* [162]. When analysing the result of the measurement of LC3-II in PBMCs of ME/CFS patients before and after whole-body hyperthermia, a clear influence of the treatment can be identified (**Figure 46**). More precisely, all nine participants display a reduction in their LC3-II values. These results are confirmed by the grouped values of LC3-II of all nine participants before and after treatment. The grouped values also show a significant reduction in the mean by 18% (**p = 0.0065, paired t-test) of LC3-II by whole-body hyperthermia. Comparing these grouped values from ME/CFS patients with the grouped values of LC3-II from nine healthy donors [160] using an unpaired t-test, an increase in the mean by 20% (p = 0.0538) between healthy donors and ME/CFS patients is visible.

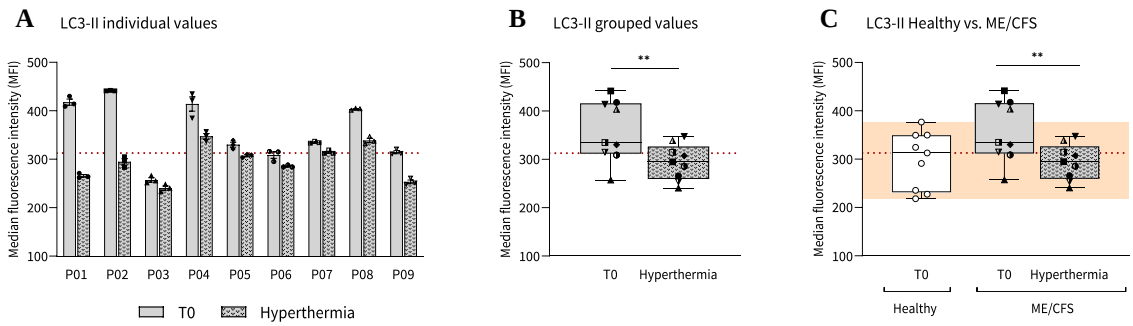

Figure 46: Whole-body hyperthermia treatment (one-hour WBH-therapy with Tc max = 39 °C) causes the higher LC3-II basal levels of ME/CFS patients to return to the range of LC3-II basal levels of healthy donors. A Nine ME/CFS patients show a decrease in LC3-II values with one session of whole-body hyperthermia. **B** The grouped LC3-II values of all nine participants also show a significant decrease in the mean by 18% (**p = 0.0065, paired t-test) as a result of the treatment. **C** A comparison of the data of ME/CFS patients before and after treatment with the basal values of healthy donors (median at the red dotted line) shows an increased mean in the basal value of LC3-II (20%, p = 0.0538, unpaired t-test). The orange area shows the range of values for the healthy comparison group.

3.4.2 Mitochondrial function – PBMCs

All mitochondrial parameters of nine ME/CFS patients, namely basal respiration, ATP production, maximal respiration and spare respiratory capacity, were affected by a session of whole-body hyperthermia (**Figure 47**). More specifically, all nine ME/CFS patients show an increase in all mitochondrial parameters. This is evident in both the individual data and the grouped data. In the grouped data, basal respiration increases by 66.60% (**p = 0.0040, paired t-test), ATP production by 61.41% (**p = 0.0023, paired t-test), maximal response by 97.88% (**p = 0.0071, paired t-test) and spare respiratory capacity by 112.35% (**p = 0.0086, paired t-test). Comparison of grouped data from nine ME/CFS patients at T0 with data from six healthy donors shows that basal respiration and ATP production are increased by 46.43%(p = 0.0869, unpaired t-test) and 35.25% (p = 0.145, unpaired t-test) in ME/CFS patients. T0 values of maximal response are also 3.52% (p = 0.8992, unpaired t-test) higher in ME/CFS patients, whereas spare respiratory capacity is 8.71% (p = 0.7642, unpaired t-test) lower in ME/CFS patients compared to the healthy control group.

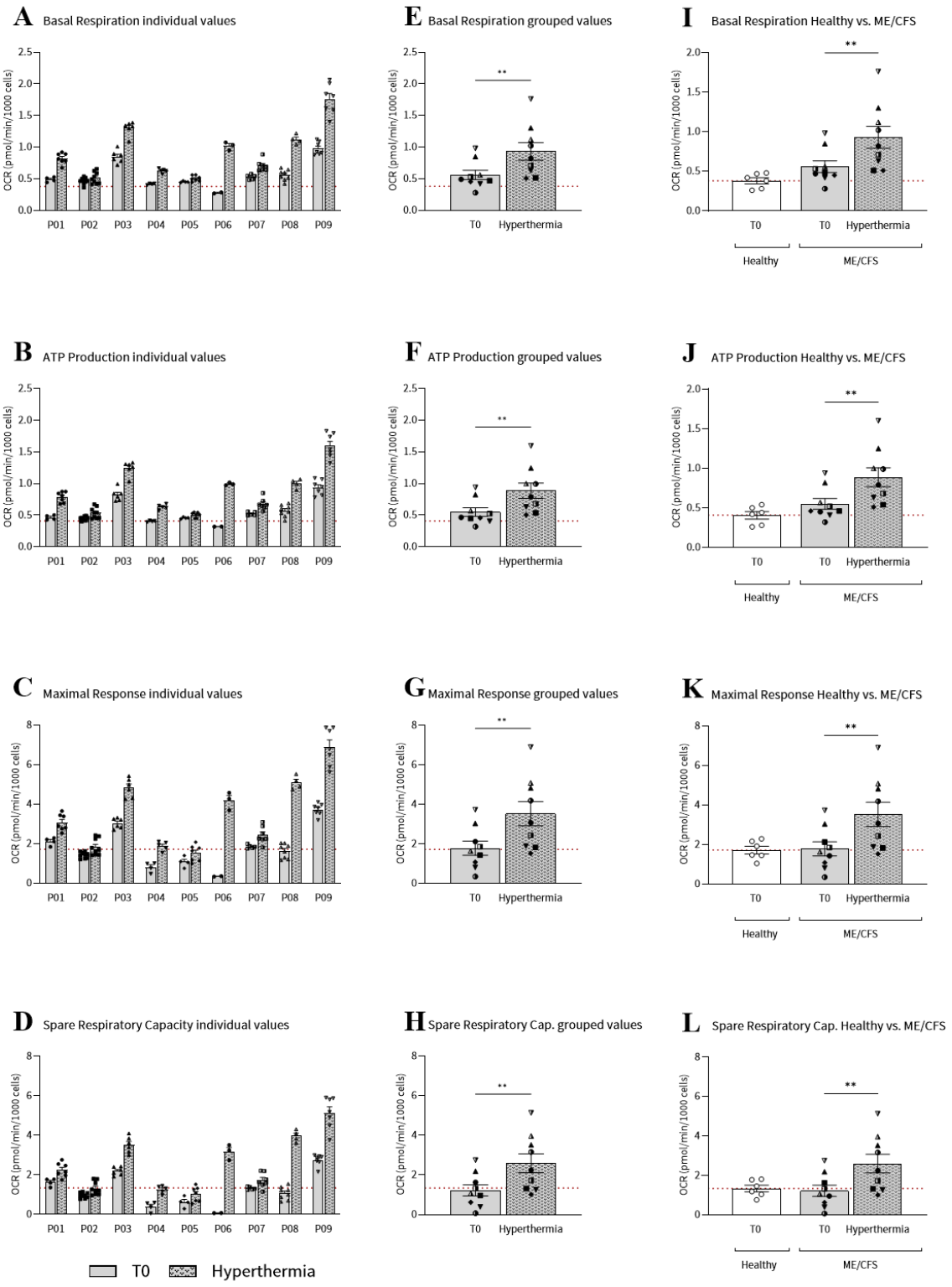

Figure 47: All measured mitochondrial parameters increase in PBMCs of nine ME/CFS patients immediately after WBH. **A-D** All participants show an increase in all measured parameters (descriptive without statistical test). **E-H** Basal respiration of the grouped data of nine ME/CFS patients increases by 66.60% with WBH (**p = 0.0040, paired t-test). ATP production increases by 61.41% (**p = 0.0023, paired t-test), maximal response by 97.88% (**p = 0.0071, paired t-test) and spare respiratory capacity by 112.35% (**p = 0.0086, paired t-test). **I-L** Comparison of the grouped T0 data of ME/CFS patients (n=9) with an untreated healthy control group (n=6) shows an increased basal respiration of 46.43% in ME/CFS patients (p = 0.0869, unpaired t-test). ATP production is 35.25% higher (p = 0.145, unpaired t-test) and the maximal response is 3.52% (p = 0.8992, unpaired t-test) higher in ME/CFS patients. The spare respiratory capacity is 8.71% (p = 0.7642, unpaired t-test) lower in ME/CFS patients (mean of healthy data at the red dotted line).

3.4.3 mRNA expression – PBMCs

Autophagy – associated genes

Besides the cellular parameters of autophagy, the molecular level was also studied by measuring autophagy-related genes **Figure 48**. After one session of WBH, the expression of *ULK1* increased in two participants (P06, P09), remained the same in three participants (P01, P02, P04) and showed a decrease in four participants (P03, P05, P07, P08). The expression of *BECN1* increased in four participants (P01, P04, P05, P06), remained the same in P02 and decreased in four participants (P03, P07, P08, P09). Four participants (P02, P03, P07, P09) show an increased expression of *ATG7*, while the other five show a decrease (P01, P04, P05, P06, P08) (descriptive without statistical test). *MAP1LC3B* increases in five participants (P02, P04, P05, P06, P09), remains the same in P01 and P07 and decreases in P03 and P08. In the grouped values *ULK1* decreases by 3.00% as a result of hyperthermia ($p = 0.7925$, paired t-test). *BECN1* increased by 6.11% ($p = 0.5147$, paired t-test), *ATG7* by 1.00% ($p = 0.9221$, paired t-test) and *MAP1LC3B* by 20.33% ($p = 0.1125$, paired t-test).

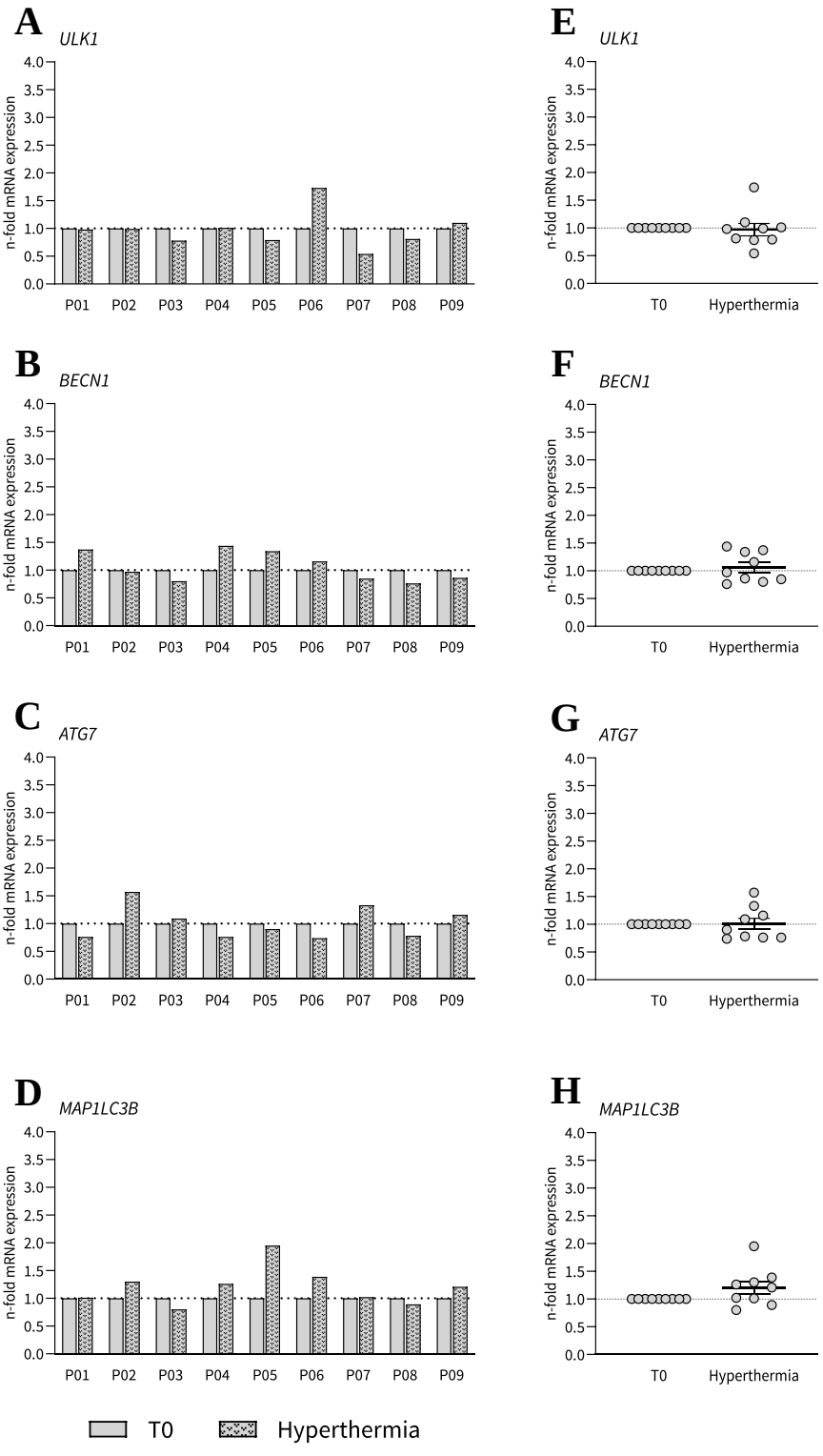

Figure 48: Effect of in vivo wIRA irradiation on genes encoding proteins involved in the autophagosomal process in PBMCs of ME/CFS patients (n=9). **A** WBH leads to an increase in *ULK1* expression in two participants (P06, P09), in three participants (P01, P02, P04) it remains the same and in four participants (P03, P05, P07, P08) it decreases. **B** *BECN1* expression increases in four participants (P01, P04, P05, P06), remains the same in P02 and decreases in four participants (P03, P07, P08, P09). **C** Four participants (P02, P03, P07, P09) show an increase in *ATG7* expression, while the other five show a decrease (P01, P04, P05, P06, P08). **D** *MAP1LC3B* increases in five participants (P02, P04, P05, P06, P09), remains the same in P01 and P07 and decreases in P03 and P08. **E-H** The grouped values show a decrease in *ULK1* by 3.00% as a result of hyperthermia ($p = 0.7925$, paired t-test). *BECN1* increased by 6.11% ($p = 0.5147$, paired t-test), *ATG7* by 1.00% ($p = 0.9221$, paired t-test) and *MAP1LC3B* by 20.33% ($p = 0.1125$, paired t-test).

In connection with autophagy, other genes coding for proteins that are crucial for autophagy regulation were analysed (**Figure 49**). The mean values of all participants show *AMPK1α* and *SIRT1* increased by 13.00% (p = 0.1429, paired t-test) and 30.89% (p = 0.1886, paired t-test), respectively, after one session of WBH. *FOXO3* also increased by 2.78% (p = 0.8110, paired t-test). In the individual values, the expression of *AMPK1α* increases in five participants (P01, P04, P06, P07, P09), remains the same in two (P02, P05) and decreases in participants P03 and P08. Five participants (P01, P02, P04, P05, P06) show increased expression of *SIRT1*, two remain the same (P08, P09), while expression decreases in P03 and P07. *FOXO3* increases in three participants (P01, P02, P07), remains the same in P03, P05 and P06 and decreases in P04, P08 and P09.

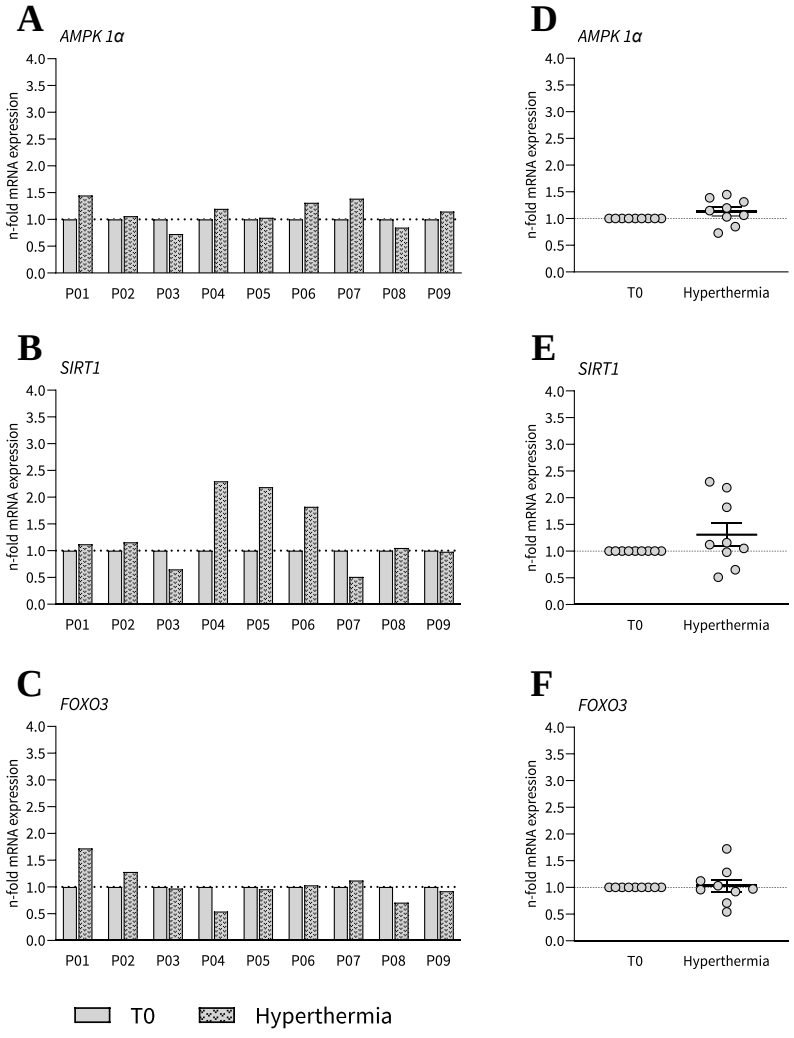

Figure 49: Effect of WBH on genes encoding proteins involved in the regulation of autophagy in PBMCs of nine ME/CFS patients. A The expression of *AMPK1α* increases in five participants (P01, P04, P06, P07, P09) by one session of WBH, remains the same in two (P02, P05) and decreases in P03 and P08. **B** Five participants (P01, P02, P04, P05, P06) show an increased expression of *SIRT1*, two remain at the same level (P08, P09), while P03 and P07 decrease. **C** *FOXO3* increases in three participants (P01, P02, P07), remains the same in P03, P05 and P06 and decreases in P04, P08 and P09. **D-F** The mean values of *AMPK1α* and *SIRT1* increased by 13.00% (p = 0.1429, paired t-test) and 30.89% (p = 0.1886, paired t-test), respectively, after one session of WBH. *FOXO3* increases by 2.78% (p = 0.8110, paired t-test).

Mitochondrial function – associated genes

The genes *SIRT3*, *TFAM*, *NDUFS1* and *SOD2* were selected for the analysis of mitochondrial genes (**Figure 50**). The grouped values show a decrease in *SIRT3* expression by 10.22% ($p = 0.0508$, Wilcoxon test), which occurs in six participants (P03, P04, P05, P06, P07 P08), whose expression decreases. Participant P09 remains at the same level and two participants (P01, P02) increase their *SIRT3* expression. The expression of *TFAM* increases in three participants (P02, P07, P09), remains the same in P05 and decreases in five (P01, P03, P04, P06, P08). To summarise, *TFAM* increases by 0.11% ($p = 0.9905$, paired t-test). *NDUSF1* increases in six participants (P01, P02, P04, P05, P07, P08), remains at the same level in P09 and decreases in participants P03 and P06. The grouped values show a slight increase by 19.67% ($p = 0.1602$, Wilcoxon test) in *NDUFS1* expression. *SOD2* also shows an increase in expression in the summary of all participants by 22.89% ($p = 0.3162$, paired t-test). Looking at the individual values, *SOD2* increases in three participants each (P02, P05, P06), remains the same (P04, P08, P09) and decreases (P01, P03, P07).

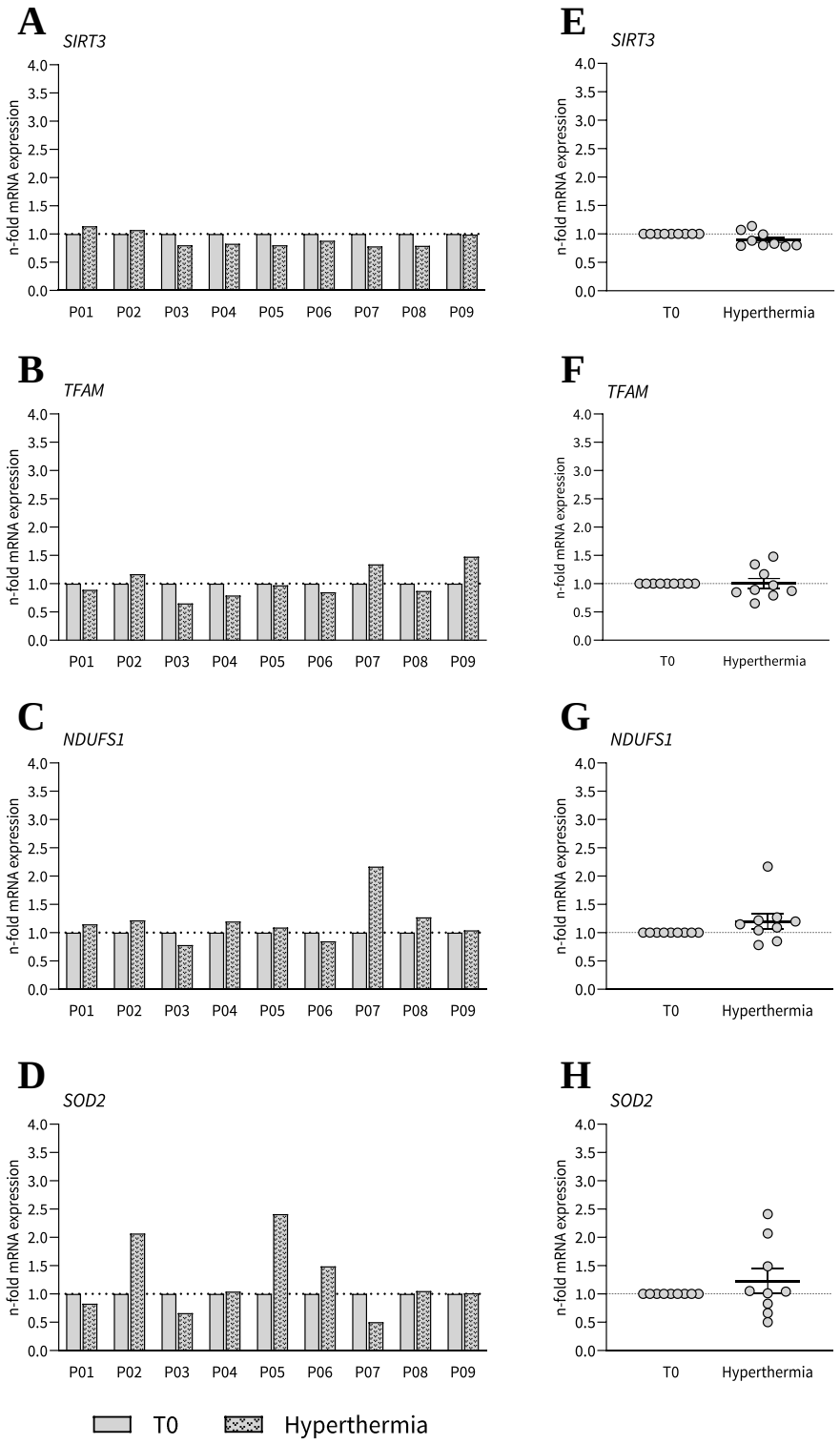

Figure 50: Effect of in vivo wIRA irradiation on genes encoding proteins involved in mitochondrial function in PBMCs from ME/CFS patients (n=9). A One session of WBH leads to an increase in *SIRT3* expression in two participants (P01, P02), in P09 the expression remains at the same level and in six participants (P03, P04, P05, P06, P07, P08) it decreases. **B** The expression of *TFAM* increases in three participants (P02, P07, P09), remains the same in P05 and decreases in five (P01, P03, P04, P06, P08). **C** The expression of *NDUSF1* increases in six participants (P01, P02, P04, P05, P07, P08), remains at the same level in P09 and decreases in participants P03 and P06. **D** The expression of *SOD2* increases (P02, P05, P06), remains (P04, P08, P09) and decreases (P01, P03, P07) in three participants each. **E-H** The grouped values of *SOD2*, *NDUFS1* and *TFAM* increased by 22.89% ($p = 0.3162$, paired t-test), 19.67% ($p = 0.1602$, Wilcoxon test) and 0.11% ($p = 0.9905$, paired t-test), respectively. *SIRT3* mRNA expression decreased by 10.22% ($p = 0.0508$, Wilcoxon test).

Additional genes

The grouped values of the additional markers *HSPA5* and *IL-10* show an increase by 48.33% (p = 0.2188, Wilcoxon test) and 37.33% (p = 0.1367, Wilcoxon test), respectively, as a result of hyperthermia (**Figure 51**). In the individual data the expression of *HSPA5* increased in five participants (P01, P02, P04, P05, P06) and decreased in four (P03, P07, P08, P09) by one session of WBH. *IL-10* increased in seven participants (P01, P02, P04, P05, P06, P08, P09) and decreased in P03 and P07.

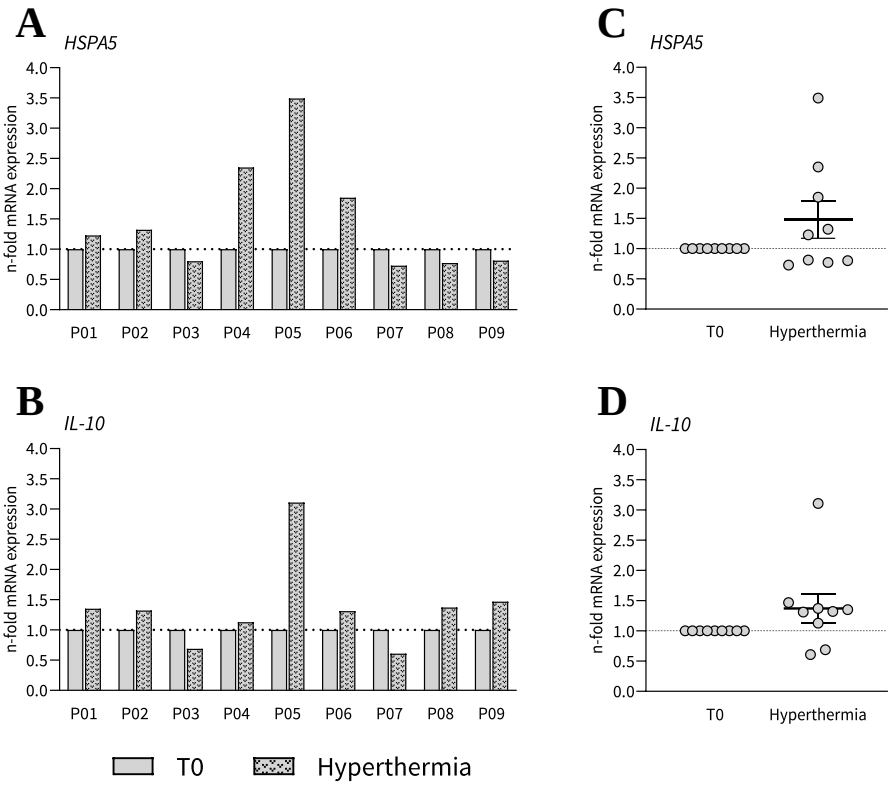

Figure 51: Effects of in vivo hyperthermia on additional markers in PBMCs of nine ME/CFS patients. A The expression of *HSPA5* is increased in five participants (P01, P02, P04, P05, P06) and decreased in four (P03, P07, P08, P09) by one session of WBH. **B** *IL-10* increased in seven participants (P01, P02, P04, P05, P06, P08, P09) and decreased in P03 and P07. **C-D** The mean values of *HSPA5* and *IL-10* show an increase by 48.33% (p = 0.2188, Wilcoxon test) and 37.33% (p = 0.1367, Wilcoxon test), respectively.

3.5 Ex vivo vs. in vivo Hyperthermia

3.5.1 Autophagy – PBMCs

The comparison of the effect of ex vivo and in vivo hyperthermia treatment on the LC3-II value of PBMCs from ME/CFS patients shows an inverse effect (**Figure 52**). While heat treatment of isolated PBMCs leads to a significant increase in LC3-II by 7% (****p < 0.0001, paired t-test), whole-body hyperthermia shows a significantly decreasing effect on LC3-II by 18% (**p = 0.0065, paired t-test).

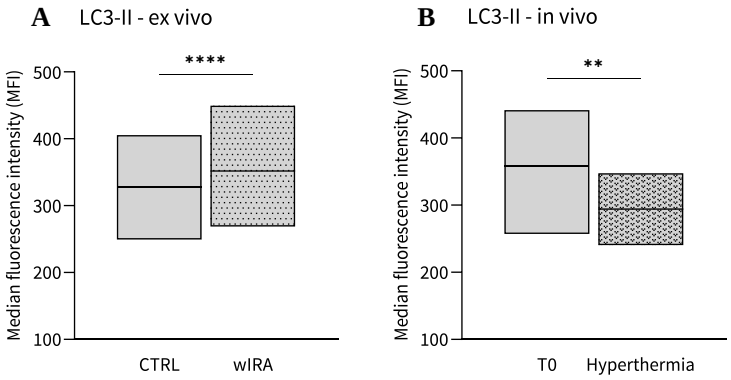

Figure 52: Contrasting effects of ex vivo hyperthermia and WBH on LC3-II levels in PBMCs of ME/CFS patients. A-B While wIRA irradiation of isolated PBMCs causes a significant increase in LC3-II levels by 7% (****p < 0.0001, paired t-test), wIRA therapy of ME/CFS patients shows a significant decrease in LC-II levels in their PBMCs by 18% (**p = 0.0065, paired t-test).

3.5.2 Mitochondrial function – PBMCs

Like the effect on the autophagy marker LC3-II, the effect of ex vivo and in vivo treatments on mitochondrial parameters in ME/CFS patients is contrasting (**Figure 53**). Ex vivo treatment shows a decrease in all investigated parameters by irradiation of PBMCs. More specific, basal respiration is decreasing by 8.17% (p =0.914, Wilcoxon test), ATP production by 7.30% (p = 0.8818, Wilcoxon test), maximal response by 24.14% (p = 0.6221, Wilcoxon test) and spare respiratory capacity by 28.21% (p = 0.1161, paired t-test). While a session of WBH leads to a significant increase in all investigated mitochondrial parameters: basal respiration increases by 66.60% (**p = 0.0040, paired t-test), ATP production by 61.41% (**p = 0.0023, paired t-test), maximal response by 97.88% (**p = 0.0071, paired t-test) and spare respiratory capacity by 112.35% (**p = 0.0086, paired t-test).

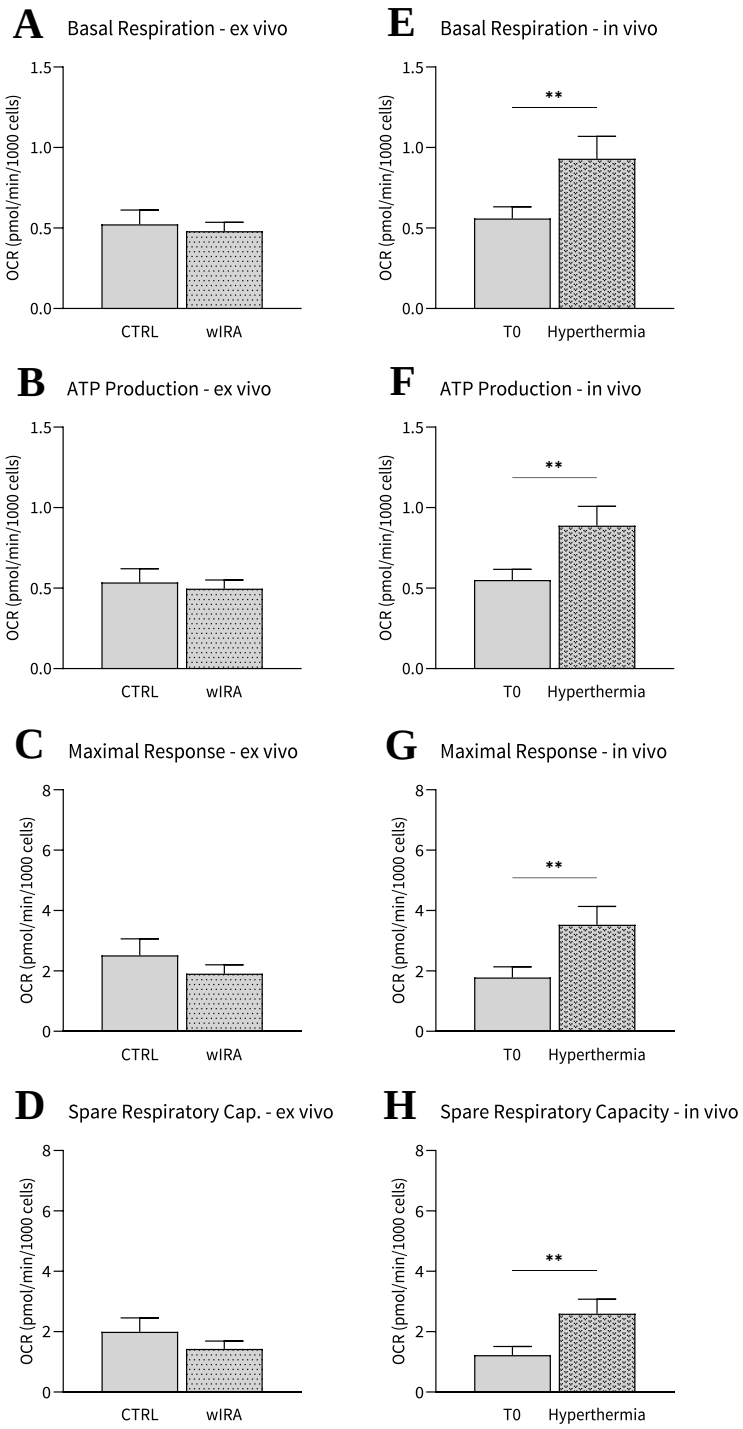

Figure 53: Contrasting effects of ex vivo hyperthermia and WBH on all mitochondrial parameters analysed in PBMCs of ME/CFS patients. A-D Basal respiration are decreasing by 8.17% ($p = 0.914$, Wilcoxon test), ATP Production by 7.30% ($p = 0.8818$, Wilcoxon test), maximal response by 24.14% ($p = 0.6221$, Wilcoxon test) and spare respiratory capacity by 28.21% ($p = 0.1161$, paired t-test).**E-H** Basal respiration increases by 66.60% (**$p = 0.0040$, paired t-test), ATP production by 61.41% (**$p = 0.0023$, paired t-test), maximal response by 97.88% (**$p = 0.0071$, paired t-test) and spare respiratory capacity by 112.35% (**$p = 0.0086$, paired t-test).

3.5.3 mRNA expression – PBMCs

Autophagy – associated genes

The **Figure 54** compares the expression of autophagy genes after ex vivo and in vivo heat treatment. The response of the genes in their expression seems to be very similar in both groups. There are no significant differences in *ULK1* in ex vivo (+3.10%, p = 0.2142, Wilcoxon test) and in vivo (-3.00%, (p = 0.7925, paired t-test) treatment. *BECN1* is increasing non-significantly ex vivo (5.70%, p = 0.0907, paired t-test) and in vivo (6.11%, p = 0.5147, paired t-test). The expression of *MAP1LC3B* increases in both groups, significant in ex vivo treatment by 19.65% (***p = 0.0001, paired t-test) and not significant by 20.33% (p = 0.1125, paired t-test) due to WBH. Only *ATG7* shows a slight difference between both groups, as expression is significantly reduced by ex vivo hyperthermia by 14.95% (**p = 0.0024, paired t-test), while WBH shows an increase by 1.00% (p = 0.9221, paired t-test).

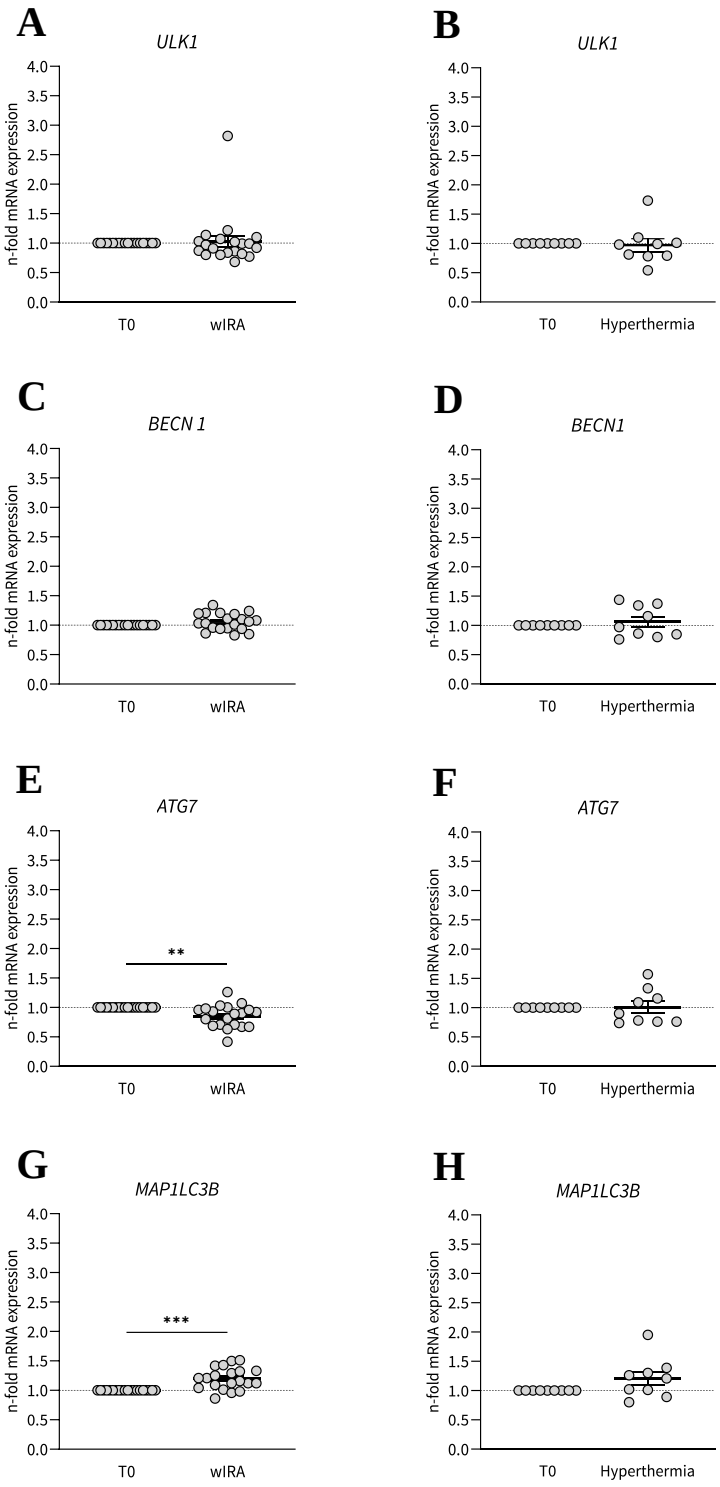

Figure 54: Comparison of the influence of in vivo and ex vivo hyperthermia on the mRNA expression of autophagy genes in PBMCs of ME/CFS patients. A-B *ULK1* increase ex vivo (3.10%, p = 0.2142, Wilcoxon test) and decrease in vivo (3.00%, (p = 0.7925, paired t-test) **C-D** *BECN1* is increasing non-significant ex vivo (5.70%, p = 0.0907, paired t-test) and in vivo (6.11%, p = 0.5147, paired t-test).**E-F** *ATG7* is significantly reduced by hyperthermia treatment of isolated PBMCs by 14.95% (**p = 0.0024, paired t-test), while WBH shows donor variability in *ATG7* expression but increases by 1.00% (p = 0.9221, paired t-test) on average. **G-H** *MAP1LC3B* increases in both groups, significant in ex vivo treatment by 19.65% (***p = 0.0001, paired t-test) and not significant by 20.33% (p = 0.1125, paired t-test) due WBH.

The comparison of the response of genes that regulate autophagy to ex vivo and in vivo treatment also shows a similar pattern for all genes analysed (**Figure 55**). The expression of *AMPK1α* is increasing ex vivo (2.35%, p = 0.6311, paired t-test) and in vivo (13.00%, p = 0.1429, paired t-test). *FOXO3* shows no noteworthy changes with either form of treatment (ex vivo: + 0.75%, p = 0.8251, paired t-test; in vivo: + 2.78%, p = 0.8110, paired t-test). There is an increase in the expression of *SIRT1* in both groups, which is significant in the ex vivo treatment (33.10%, ****p < 0.0001, paired t-test) and not significant after one session of WBH (30.89%, p = 0.1886, paired t-test).

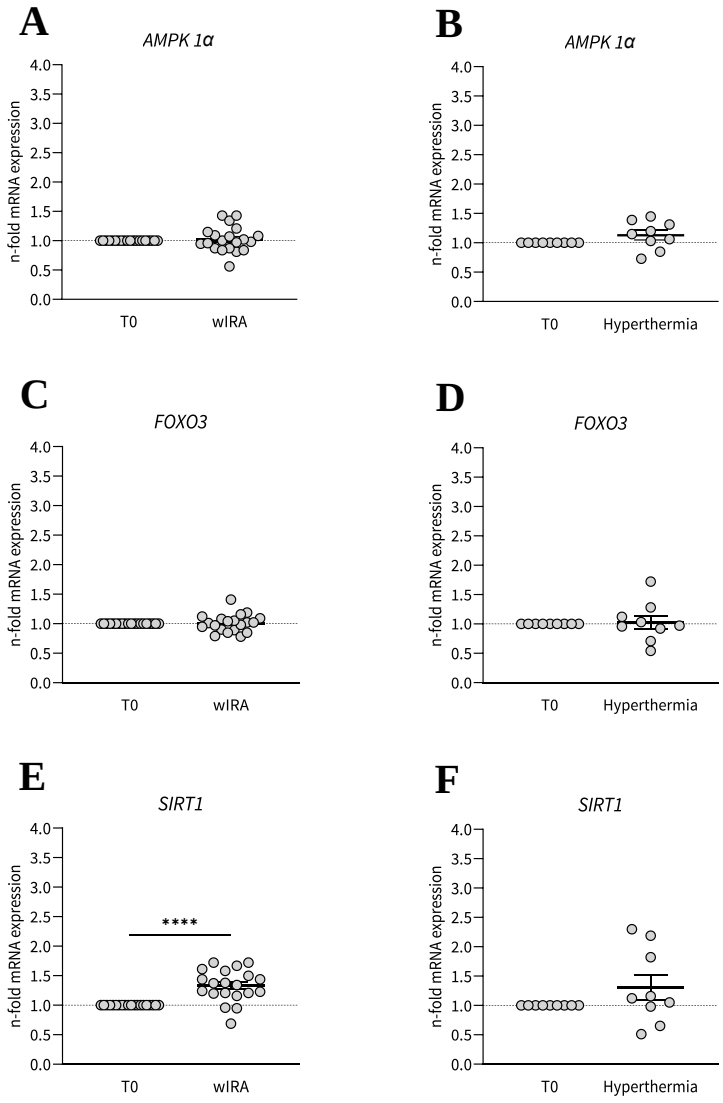

Figure 55: Comparison of the expression of autophagy regulating genes after ex vivo treatment and WBH in human PBMCs from ME/CFS patients. A-B *AMPK1α* is increasing ex vivo (2.35%, p = 0.6311, paired t-test) and in vivo (13.00%, p = 0.1429, paired t-test). **C-D** *FOXO3* showed no noteworthy changes with either form of treatment (ex vivo: + 0.75%, p = 0.8251, paired t-test; in vivo: + 2.78% (p = 0.8110, paired t-test) **E-F** *SIRT1* increases in both groups, which is significant in the ex vivo treatment (33.10%, ****p < 0.0001, paired t-test) and not significant after one session of WBH (30.89%, p = 0.1886, paired t-test).

Mitochondrial function – associated genes

The response of the mitochondrial genes to ex vivo and in vivo treatment also shows great similarity (**Figure 56**). Ex vivo the *TFAM* expression is increasing by 6.40% (p = 0.1678, paired t-test) and in vivo by 0.11% (p = 0.9905, paired t-test). The expression of *SOD2* is significantly increased after ex vivo hyperthermia by 18.15% (**p = 0.0086, paired t-test) and not significantly increased by 22.89% (p = 0.3162, paired t-test) after WBH. The expression of *SIRT3* increases ex vivo by 12.40% (p = 0.8194, Wilcoxon test) in vivo *SIRT3* mRNA expression decreased by 10.22% (p = 0.0508, Wilcoxon test). *NDUFS1* shows a decrease ex vivo by 3.90% (p = 0.3595, paired t-test) and an increase due to WBH by 19.67% (p = 0.1602, Wilcoxon test).

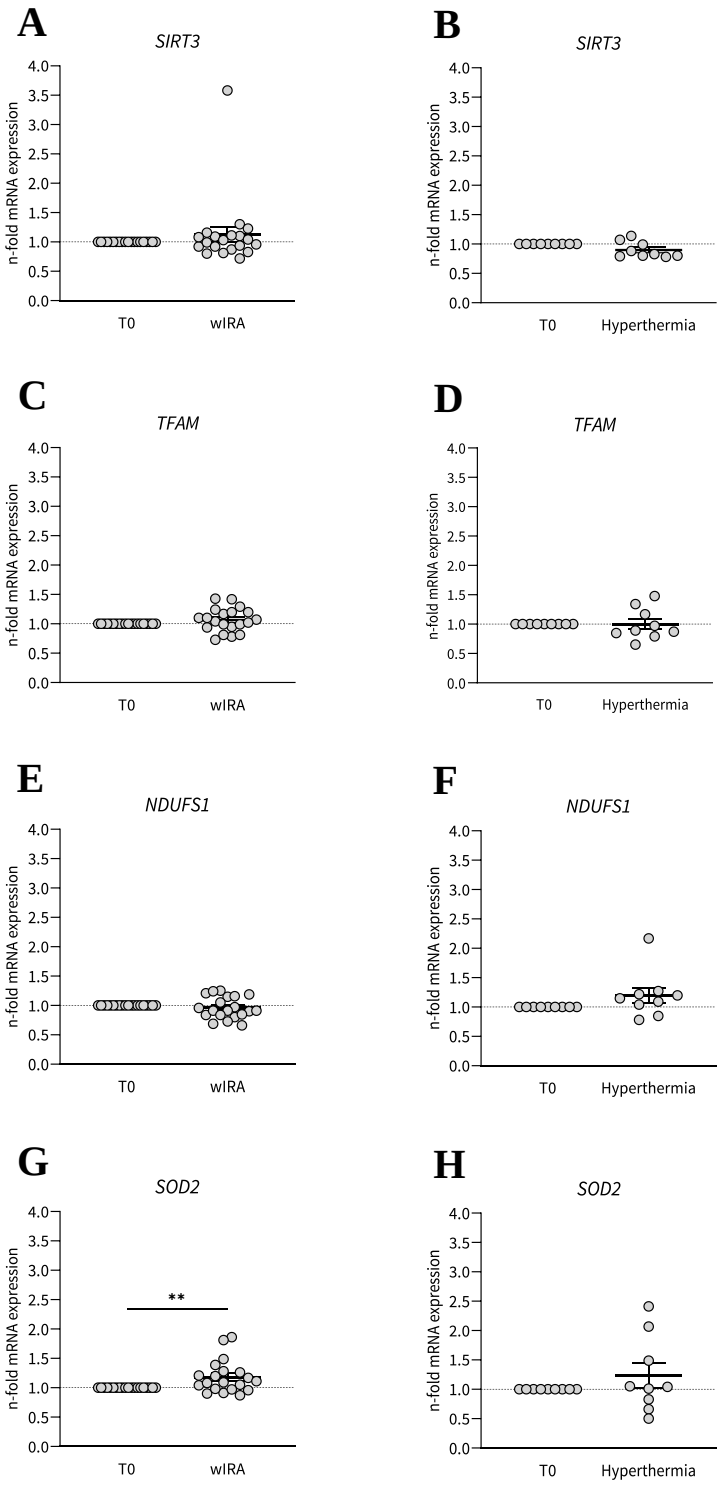

Figure 56: Comparison of the gene expression of mitochondrial genes in PBMCs after ex vivo treatment or WBH. A-B .*SIRT3* increases ex vivo by 12.40% (p = 0.8194, Wilcoxon test) in vivo *SIRT3* mRNA expression decreased by 10.22% (p = 0.0508, Wilcoxon test). **C-D** *TFAM* expression is increasing ex vivo by 6.40% (p = 0.1678, paired t-test) and in vivo by 0.11% (p = 0.9905, paired t-test) **E-F** *NDUFS1* shows a decrease ex vivo by 3.90% (p = 0.3595, paired t-test) and an increase due to WBH by 19.67% (p = 0.1602, Wilcoxon test) **G-H** *SOD2* is significantly increased after ex vivo hyperthermia by 18.15% (**p = 0.0086, paired t-test) and not significantly increased by 22.89% (p = 0.3162, paired t-test) after WBH.

Additional genes

The ex vivo and in vivo comparison of the additional marker for mRNA expression *HSPA5* and *IL-10* shows a slight difference in the response of *IL-10* to hyperthermia (**Figure 57**). *IL-10* expression showed a decreasing by 3.30% (p = 0.6245, paired t-test) due to ex vivo treatment and a non-significant increase by 37.33% (p = 0.1367, Wilcoxon test) in WBH. *HSPA5*, however, shows an increase in both groups, this increase is significant in ex vivo hyperthermia by 12.55% (***p = 0.0003, paired t-test) and not significant by 48.33% (p = 0.2188, Wilcoxon test) due to WBH.

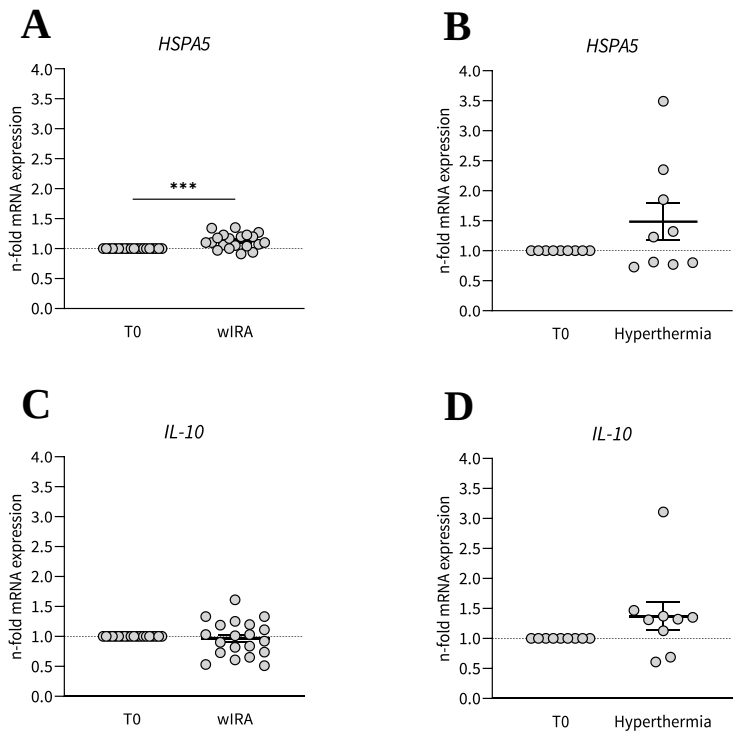

Figure 57: Comparison of additional markers in PBMCs after ex vivo heat treatment and WBH. A-B The mRNA expression of *HSPA5* increases in both groups, significantly in the ex vivo treatment by 12.55% (***p = 0.0003, paired t-test) and not significantly in the WBH by 48.33% (p = 0.2188, Wilcoxon test). **C-D** *IL-10* expression showed a decreasing by 3.30% (p = 0.6245, paired t-test) due to ex vivo treatment and a non-significant increase by 37.33% (p = 0.1367, Wilcoxon test) in WBH.

3.5.4 Autophagy vs. Mitochondrial function

To conclude the chapter on the comparison of the effect of wIRA treatment ex vivo and in vivo, the following **Figure 58** shows the parameters of autophagy and mitochondrial function ex vivo and in vivo. Not all four parameters were selected for the mitochondrial function, only basal respiration and spare respiratory capacity. ATP production shows a similar pattern to basal respiration and maximal respiration shows a similar pattern to spare respiratory capacity. This figure serves to summarise the main effects of wIRA irradiation and to visualise the opposite effect ex vivo and in vivo. The figure shows an increase in the autophagy marker LC3-II by wIRA irradiation of isolated cells and a slight decrease in basal respiration and spare respiratory capacity. In contrast, whole-body hyperthermia irradiation leads to a decrease in the autophagy marker and an increase in basal respiration and spare respiratory capacity. Comparing the data with those of healthy donors, the untreated values of ME/CFS patients are higher than those of healthy donors in autophagy and basal respiration. The ex vivo data for free respiratory capacity show increased levels in ME/CFS patients compared to healthy donors and the in vivo data show similar levels for both groups. In the case of autophagy, ex vivo hyperthermia leads to an even greater increase in LC3-II in ME/CFS patients, resulting in a higher delta compared to healthy donors. However, in vivo treatment leads to an equalisation with the healthy data. Basal respiration shows a minimisation of the delta to healthy donors by ex vivo treatment and a higher delta by increased OCR with in vivo treatment. The spare respiratory capacity decreases with ex vivo treatment, while a session of whole-body hyperthermia leads to an increase.

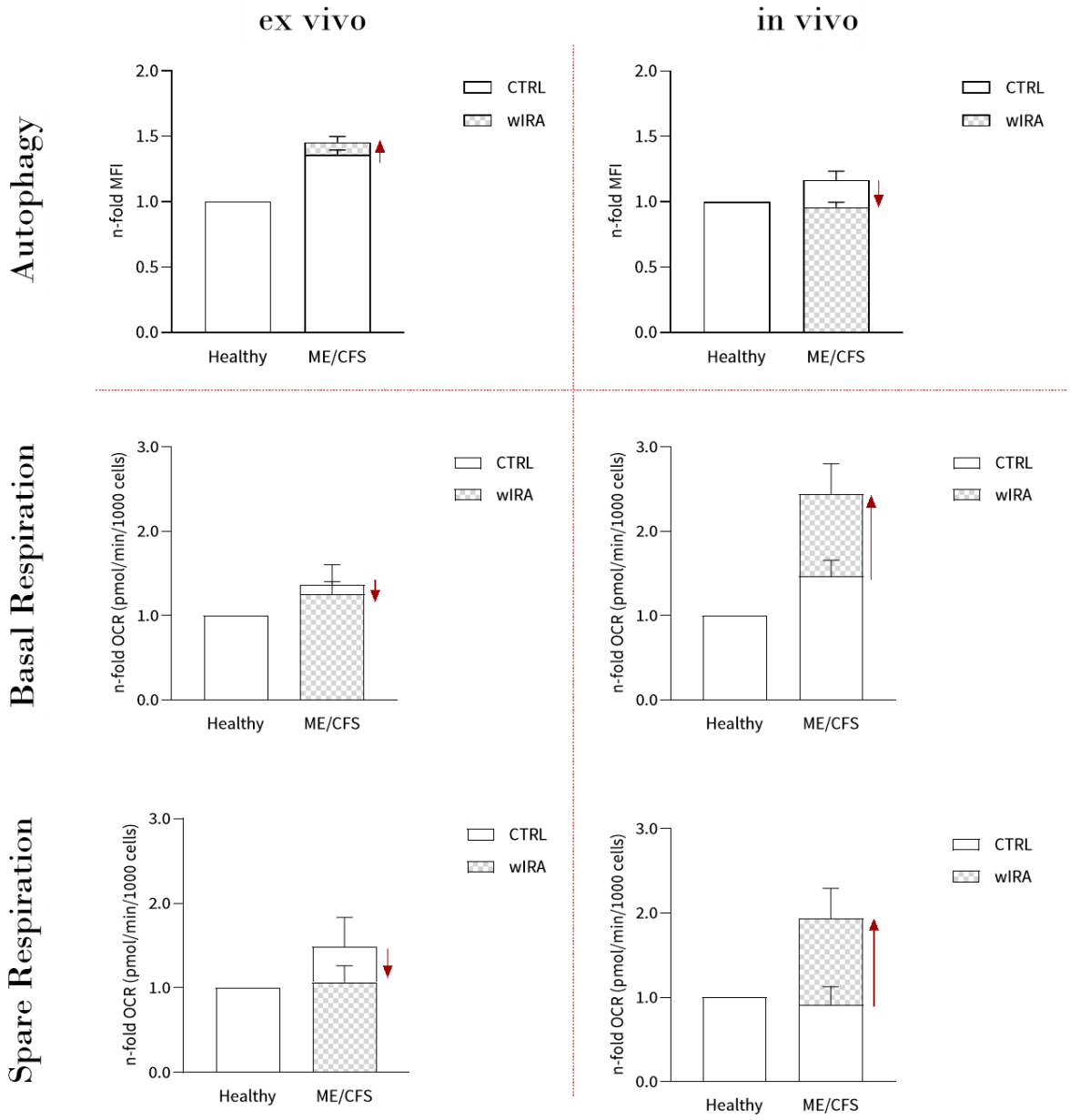

Figure 58: Summary of the comparison of ex vivo and in vivo hyperthermia. The measurements show contrasting effects of the different treatments. While the autophagy marker LC3-II decreases with the ex vivo treatment, it increases with the in vivo treatment. In mitochondrial function it is exactly the contrary. Basal respiration decreases ex vivo and increases by in vivo treatment. Spare respiratory capacity decreases ex vivo and increases due to one session of whole-body hyperthermia.

4 Discussion

To date, little is known about the severe disease ME/CFS, resulting in a shortage of satisfactory treatment options [2]. To address this problem, this thesis focuses on the investigation of the central cellular mechanisms of autophagy and mitochondrial function in PBMCs from ME/CFS patients compared to healthy donors. Impaired autophagy is associated with various diseases and pathophysiological conditions, including autoimmune, cardiovascular, neurodegenerative and metabolic diseases [20]. Therefore, there may also be a link between the multisystemic disease ME/CFS and impaired autophagy. Measuring mitochondrial function is crucial when it comes to fatigue, as the main function of mitochondria is to produce energy in the form of ATP [106]. In addition to the investigation of the basal levels, hyperthermia was tested as a possible treatment option for ME/CFS. This form of treatment was chosen because of its long-standing use in treating various diseases. These include depression [17], psoriatic arthritis [77] and, most notably, cancer [12,13,15]. There are also indications that hyperthermia has a positive clinical effect on patients with ME/CFS [163,164]. To evaluate the investigated parameters, the results are discussed in this chapter. Firstly, the established autophagy assays are analysed for their suitability and significance. Subsequently, the values of autophagy and mitochondrial function of ME/CFS patients are discussed in comparison to healthy donors. After analysing the differences at the basal level without treatment, hyperthermia treatment is examined as a possible therapeutic option.

4.1 Establishment of autophagy assays

An important aim of this work is the investigation of the central cellular process of autophagy. In order to do justice to this topic, it was first necessary to establish a suitable assay system for measuring autophagy. The overall aim was to establish a suitable method for measuring autophagy in human PBMCs. The original plan was to achieve this by first developing an assay for human fibroblasts and then transferring it to human PBMCs. However, this transfer did not work, so a further test system was developed for human PBMCs. The specific process and outcome are discussed below.

In order to be suitable for the questions addressed in this work, the requirements for the test first had to be defined. The test should require the smallest possible sample quantity or cell number, as the sample quantity is limited and further tests have to be carried out with the same sample. For this reason, immunoblotting is not suitable due to the large amount of sample material required [95]. Another aspect is that the assay should not be very time-consuming, as the effect of hyperthermia should be measured as quickly as possible. For this reason methods such as the LC3-HiBiT reporter assay or other reporter systems are also not suitable for measuring the immediate cellular response, as transfection as well as subsequent expression of the reporter proteins are

required [96]. In order to minimise errors in the test procedure, the test should also not be too difficult to handle. It is also very important that the assay provides reliable results, is reproducible and can measure differences between different treatment options.

The CYTO-ID® Autophagy Detection Kit has been used for the quantification of autophagy in human fibroblasts. This test allows the quantification of autophagosomes using a dye specific for autophagosomal structures. Furthermore, the number of autophagosomes per cell can be determined by additional staining of the cell nuclei. The principle of the assay is also described in chapter 1.4. The use of a dye enables the examination of primary cells and is not very time-consuming to prepare and perform. In addition, the assay requires a small sample size, in the case of human fibroblasts 10,000 cells/well. Overall, the assay is simple and quick to perform, as can be seen in chapter 2.2.1 a), where the method is described. The reproducibility of the assay was tested by repeating the assay five times under the same conditions **Figure 19**. The results of this test showed no significant deviations. The highest SEM within the technical replicates was 2.23 autophagosomes per nucleus and the highest deviation of the individual five experiments from the mean value of all experiments (15.83) was 1.65 autophagosomes per nucleus **Table 19**. Furthermore, the result of using a sensitive CQ concentration proves the reproducibility and the ability of the assay to measure differences under different conditions **Figure 20**. The results show a significant increase in the number of autophagosomes per nucleus by treatment with CQ, an inhibitor for the fusion of lysosomes with autophagosomes. In conclusion, this assay fulfils all defined requirements for the quantification of autophagosomes in human fibroblasts and is suitable for measuring the effects of heat treatment on autophagy. As mentioned above, the original plan was to transfer the test to human PBMCs after establishing it for human fibroblasts. However, due to the round cell morphology and small size of PBMCs, this was not possible as the imager had difficulties obtaining clear images, resulting in the software being unable to distinguish individual autophagosomes (**Figure 21**). One limitation of the CYTO-ID test is the lack of knowledge about the specificity of the staining. However, in one study, vesicular structures were stained with the CYTO-ID dye shortly after amino acid deprivation, which largely colocalise with RFP-LC3-positive structures and react to known autophagy modulators. This indicates that autophagosomal structures are dyed. [165]

For human PBMCs, the Guava® assay was chosen for the quantification of autophagosomes. The principle of the assay is the labelling of the autophagy marker LC3-II by a FITC-conjugated anti-LC3B antibody. A more detailed description of the method can be found in the chapter 1.4. Due to the antibody-based LC3-II labelling, the method is quick and easy to perform (chapter 2.2.1 b)). In addition, the assay does not require much sample material (500,000 cells/well). The reproducibility and the ability to measure differences by intervention were tested by repeating the same experiment

five times (**Figure 23**). This experiment was performed with two conditions, a control and the addition of 40 µM of the inhibitor CQ. The results show no significant changes between the same conditions, and the highest derivative of the individual experiments to the mean (350) of all five is 3%, demonstrating the reproducibility of the test. Furthermore, a clear difference is recognisable due to the inhibition of the fusion of the lysosome with the autophagosome by CQ, as the fluorescence increases significantly with the addition of 40 µM CQ. This also suggests that the assay is suitable for measuring the effect of heat treatment on autophagy in human PBMCs. However, it is difficult to capture the dynamic process of autophagy with static measurement methods. The method used measures cellular autophagosomes by labelling the marker LC3B-II, which generally indicates the extent of cellular autophagy activity. A limitation is that the accumulation of autophagosomes is not always indicative of autophagy induction. It can also indicate blockage of autophagosomal maturation and completion of the autophagy pathway by lysosomal degradation [95]. However, since an additional chloroquine control (data not shown), which prevents lysosomal degradation, was carried out in each test and an increased LC3B-II level was achieved as a result, at least a malfunction in the degradation of the lysosomes can be ruled out. It is also recommended to use more than one method to measure autophagy. Therefore, mRNA expression of autophagy-related genes was also measured [154]

4.2 Healthy vs. ME/CFS

Once all the necessary test systems were available, basal levels of mitochondrial parameters indicative of their function and autophagy were measured in healthy donors and ME/CFS patients. The comparison of these basal parameters could help to identify possible disease-related changes in mechanisms and provide possible explanations. The measurement of the autophagy marker LC3-II shows a significant increase in LC3-II levels in ME/CFS patients compared to healthy donors. The measured mitochondrial parameters basal respiration, ATP production, maximal response and spare respiratory capacity, also show an increase in OCR in ME/CFS patients compared to healthy donors (**Table 21**).

Table 21: Summary of the measured differences in ME/CFS patients compared to healthy participants

ME/CFS vs. Healthy	
Autophagy	
LC3-II intensity	35.75%⇧****
Mitochondrial function	
Basal Respiration	63.80%⇧*
ATP Production	54.87%⇧*
Maximal Response	57.89%⇧
Spare Respiratory Capacity	56.02%⇧

These results are surprising, as a decrease in autophagy and mitochondria was expected in ME/CFS patients. This assumption is based on the function of autophagy, which is to maintain cellular homeostasis and to remove damaged and potentially harmful cellular components. In a disease such as ME/CFS, therefore, the assumption would be that autophagy is reduced rather than increased. Unfortunately, little is known about the effects of ME/CFS on autophagy. A 2022 study shows that the autophagy-related protein ATG13, which is a part of the initial ULK1 complex, is highly elevated in the serum of ME/CFS patients, suggesting impaired metabolic processes of autophagy. More specifically, high levels of ATG13 in serum indicate that it has been phosphorylated and that the autophagy process in the cell has been aborted - resulting in ATG13 being translocated from the cell to the serum. [150] In addition, this study and another study [166] show increased protein aggregation in ME/CFS patients. Combining these results, several causes might be present in ME/CFS patients. Either ME/CFS patients form more protein aggregates than usual, leading to increased autophagy, as suggested by our results. Or an impairment of the autophagy mechanism leads to increased aggregation of proteins. The accumulation of proteins due to impaired autophagy can also be observed in other neurodegenerative diseases such as Alzheimer's and Parkinson's, but also in normal ageing [167]. In addition, the inflammatory characteristics of ME/CFS patients would suggest a decrease in autophagy, as autophagy balances and modulates immune activation to avoid excessive inflammation, e.g. by indirectly suppressing inflammasome activation [168]. However, excessive activation of autophagy has been also demonstrated to promote inflammation and apoptosis in chronic obstructive pulmonary disease (COPD) [169]. An increased apoptosis through excessive autophagy could also explain the significantly lower values of T regulatory cells in blood of ME/CFS patients [170]. Another connection between autophagy and diseases is that autophagy can also promote tumour growth. Strongly growing cancer cells require cellular building blocks for their metabolism and energy production. At this stage of cancer development, autophagy acts as an ally, supplying the tumour cells with all the essential cellular intermediates they need to meet their metabolic requirements as they proliferate. [171] However, this aspect plays no role in the pathological pattern of ME/CFS.

Interestingly, our data show not only increased autophagy but also elevated mitochondrial function in ME/CFS patients compared to healthy donors. Reactive oxygen species (ROS) could be a possible link between these two factors. Intracellular ROS are mainly generated by the electron transport chain in the inner membrane of mitochondria [172] and can oxidise organelles, nucleic acids, proteins and lipids, leading to cell damage [173]. The supposedly higher function of the mitochondria could lead to higher ROS production and consequently to a greater amount of damaged proteins. Damaged proteins and organelles in turn lead to the induction of autophagy. The connection between mitochondria and diseases is not new. However, this connection exists between mutations in the mitochondrial DNA that lead to mitochondrial dysfunction. Reduced activity of complex I

can be observed in Parikinson's disease, for example, or mitochondrial ROS formation and inhibition of energy metabolism in Alzheimer's disease. [174] An exception that is similar to the results of this thesis is Cockayne syndrome, which also shows an increase in mitochondrial function. The accelerated ageing disorder Cockayne syndrome is characterised by progressive brain atrophy, leukodystrophy, cachexia and growth retardation and is caused by mutations affecting DNA repair mechanisms. In addition, as mentioned above, a possible mitochondrial involvement in this disease has been suggested. [175] However, considering the nature of the disease and the symptoms, there are no obvious links between Cockayne syndrome and ME/CFS. Looking more precisely at the results of this work on mitochondrial function, it can be seen that the oxygen consumption rate in all four parameters basal respiration, ATP production, maximum response and spare respiratory capacity are increased in ME/CFS patients compared to healthy donors. This effect is more pronounced for the basal respiration (SEM = 0.06) and ATP production (SEM = 0.05) parameters than for the maximal response (SEM = 0.35) and spare respiratory capacity (SEM = 0.30) parameters, as the latter two parameters exhibit greater donor variability and thus a higher SEM (**Figure 25**). As the name suggests, basal respiration ensures oxygen consumption at the basic level. ATP production represents the consumption of oxygen for the regeneration of ATP. From these results, it can be concluded that the mitochondria of ME/CFS patients consume more oxygen at basal level and for ATP production compared to healthy donors. It could therefore be surmised that mitochondrial dysfunction is present, leading to inefficient ATP production with increased oxygen consumption. Studies in this area showed no difference in ATP parameters between healthy donors and ME/CFS patients or an increased ATP level in non-mitochondrial ATP in ME/CFS patients and no difference in mitochondrial ATP [147,176]. These results could support the hypothesis that more oxygen is consumed but not more ATP is produced. Maximal response and spare respiratory capacity are also increased in ME/CFS patients compared to healthy donors. (**Table 21**). Maximal response shows the maximum rate of respiration that the cell can achieve. Spare respiratory capacity indicates the capability of the cell to respond to an energetic demand as well as how closely the cell is to respiring to its theoretical maximum. The cell's ability to respond to demand can be an indicator of cell fitness or flexibility. [177] The elevation of this parameters suggests that ME/CFS patients are more responsive to stress and have a higher ability to respond to energetic demands than mitochondria from healthy donors. Given the link between fatigue and energy production through oxidative phosphorylation, these results are much unexpected. One possible explanation could be a higher proton leak in ME/CFS patients, which would lead to higher oxygen consumption without ATP production. However, this is not clearly confirmed by the measurement data, which show a slight but statistically insignificant increase in proton leak (data not shown). Another explanation could be that the cells are more sensitive to the uncoupler FCCP, resulting in even higher permeability to protons and thus higher oxygen consumption.

Interestingly, other researchers have observed similar results. For example. Lawson *et al.* also compared blood cells from ME/CFS patients with a healthy control group and found that ATP levels are higher in the patients and the enzymatic activities of the complexes in the electron transport chain remain intact [147]. Another study from 2019, which investigated the activity of complexes I, II and IV in skeletal muscle and PBMCs, also confirms these results by finding that there are no significant differences in the activity of the individual mitochondrial complexes [149]. Both studies and the present study initially assumed mitochondrial dysfunction, and in all cases the mitochondrial activity showed a different picture. All studies therefore came to the same conclusion: mitochondrial function does not appear to be the problem. The cause may lie upstream of the mitochondrial respiratory chain. [149]

4.3 Hyperthermia studies

After analysing the basal differences between health and disease in the mechanisms of autophagy and mitochondrial function, the question of a possible treatment option for ME/CFS remains. The treatment investigated in this work is heat therapy, more precisely heating to 39 °C due to wIRA irradiation for one hour. To analyse the effect of heat, the cellular processes of autophagy, mitochondrial function and the mRNA of genes associated with these mechanisms are subsequently measured. This evaluation is divided into two studies, the ex vivo study and the in vivo study. The ex vivo study describes the investigation of the effects of heat treatment of isolated human cells from healthy donors and ME/CFS patients by wIRA irradiation. The in vivo study describes the investigation of the effect of a session of whole-body hyperthermia in ME/CFS patients.

4.3.1 Ex vivo study

As the primary aim is to treat patients, a specific heat source, wIRA radiation, was applied. This heat source is already used in humans as a treatment option in the form of whole-body hyperthermia with the 'IRATHERM®1000' infrared-A system. For this reason, the manufacturers of these devices have developed a miniaturisation of this form of heat treatment with the `IRAcubator` (Von Ardenne Institute of Applied Medical Research GmbH, Dresden, Germany) in order to be able to irradiate the cell culture under comparable conditions. Two types of human cells were analysed in this work. Firstly, human fibroblasts from a young healthy donor and secondly, human PBMCs from healthy donors and from ME/CFS patients. All isolated cells were treated with wIRA irradiation at 39 °C for 60 min and compared with an untreated control group that remained in a normal incubator at 37 °C and 5% CO_2 for 60 min. In human fibroblasts, only the effect on autophagy was measured in a healthy donor. In PBMCs, the parameters of autophagy, mitochondrial function and mRNA expression of relevant genes were determined.

The results of the measurements of the effect of hyperthermia on human fibroblasts from a healthy donor showed that the number of autophagosomes per cell nucleus increased significantly in all three experiments performed. This significant increase can also be seen in the grouped values of the three experiments (**Figure 26**). The activating effect of wIRA irradiation on autophagy in healthy human fibroblasts is a good complementary result, but the focus of this work is on human PBMCs, as they can mirror the processes in the human organism and sample collection is comparatively simple. As with the heat treatment of human fibroblasts, the one-hour hyperthermia of isolated PBMCs from healthy donors also shows an activating effect on autophagy through the significant increase in the median fluorescence intensity of LC3-II. This increase is present in the individual values of all eight healthy participants analysed as well as in the grouped values (**Figure 28**). Treatment of isolated PBMCs from 23 ME/CFS patients showed an increase in LC3-II in 18 participants. The remaining five participants showed either no effect or a slight decrease, demonstrating donor variability in the effect of wIRA irradiation in PBMCs of ME/CFS patients. However, a significant increase in LC3-II can also be observed in the grouped values (**Figure 29**). The effect of heat treatment on mitochondrial function in PBMCs is not as clear as in autophagy. The six healthy participants analysed show donor variability in all measured mitochondrial parameters. The grouped values of basal respiration and ATP production show no recognisable changes due to heat treatment. However, a significant decrease in the grouped values can be observed for maximal response and spare respiratory capacity (**Figure 31**). For all four mitochondrial parameters, a non-significant decrease was also observed in the grouped values of eleven ME/CFS patients. The individual values of these participants also show donor variability (**Figure 32**). A total of thirteen genes were analysed with regard to their reaction to heat treatment. Seven of them are related to the process of autophagy (*ULK1*, *BECN1*, *ATG7*, *MAP1LC3B*, *AMPK1α*, *FOXO3* and *SIRT1*), four of them in connection with mitochondrial function (*SIRT3*, *TFAM*, *NDUFS1* and *SOD2*) and the remaining genes *HSPA5* and *IL-10* as additional markers in connection with the heat response. Most of the analysed genes show the same pattern in their response to hyperthermia in health and disease. Since all individual values of the eight healthy donors and 20 ME/CFS patients show donor variability, only the grouped values are discussed. In the context of autophagy-related genes, *ULK1*, *BECN1*, *AMPK1α* and *FOXO3* show no noteworthy changes by wIRA irradiation. The gene *ATG7* shows a significant decrease in healthy donors and ME/CFS patients, while *MAP1LC3B* does not increase significantly in healthy donors and increases significantly in ME/CFS patients. *SIRT1* is also significantly increased in healthy and diseased individuals (**Figure 42**, **Figure 43**). The mitochondrial genes *SIRT3*, *TFAM* and *NDUFS1* show only slight changes due to hyperthermia in both groups. In contrast, the mRNA expression of *SOD2* increases significantly in both healthy donors and ME/CFS patients (**Figure 44**). The gene of the heat shock protein *HSPA5* is also significantly increased in healthy donors and ME/CFS patients. IL-10 is slightly decreased in healthy donors and

shows slight changes due to hyperthermia in ME/CFS patients (**Figure 45**). The following **Table 22** summarises all the results of the human PBMCs in the ex vivo study.

Table 22: Overview of the results of wIRA treatment of isolated human PBMCs (ex vivo study)

	Healthy	ME/CFS
	Autophagy	
LC3-II intensity	16%⇧***	7%⇧****
	Mitochondrial function	
Basal Respiration	2.34%⇩	8.17%⇩
ATP Production	2.61%⇩	7.30%⇩
Maximal Response	19.75%⇩*	24.14%⇩
Spare Respiratory Cap.	24.36%⇩	28.21%⇩
	mRNA expression	
ULK1	5.88%⇩	3.10%⇧
BECN1	2.75%⇧	5.70%⇧
ATG7	15.63%⇩**	14.95%⇩**
MAP1LC3B	5.75%⇧	19.65%⇧***
AMPK1α	6.00%⇧	2.35%⇧
FOXO3	1.50%⇩	0.75%⇧
SIRT1	40.38%⇧**	33.10%⇧****
SIRT3	3.00%⇧	12.40%⇧
TFAM	9.75%⇧	6.40%⇧
NDUFS1	4.38%⇧	3.90%⇩
SOD2	16.00%⇧*	18.15%⇧**
HSPA5	17.38%⇧*	12.55%⇧***
IL-10	12.25%⇩	3.30%⇩

4.3.2 In vivo study

The in vivo study comprises the examination of human PBMCs from nine ME/CFS patients exposed to one hour of whole-body hyperthermia at Tc max = 39 °C. The data of LC3-II, mitochondrial function and mRNA expression were measured one day before therapy and immediately after therapy. Since no healthy donors underwent whole-body hyperthermia, the data can only be compared with those of healthy donors without therapy. For mitochondrial function, the data from this ex vivo study were used. In the case of autophagy, the data from this study were not comparable as the test was performed one day after blood collection. Therefore, data from another study were used, as indicated in the method section 2.2.4. A session of WBH in ME/CFS patients leads to a decrease in LC3-II in all nine participants compared to their initial value. This decrease is reflected in the grouped values. Compared with the values of untreated healthy donors, the baseline level of ME/CFS patients is significantly higher than that of healthy donors and leads to rebalancing by WBH, as the LC3-II values fall back to the level of healthy donors as a result of hyperthermia. Interestingly, when considering not only the grouped data, but also the individual participants, a

strong reduction can be seen, especially in patients with a greatly increased basal level of LC3-II. Participants P01, P02, P04 and P08 all have an MFI of around 400, which is significantly higher than the value of around 300 seen in healthy participants. Among the ME/CFS patients who had an MFI of approximately 300 prior to therapy, there was no strong decrease as a result of therapy. The only exception is patient P09, who showed a further decrease in LC3-II due to WBH despite an initial value of approximately 300. Nevertheless, this individual observation strongly suggests that WBH leads to rebalancing, particularly in cases of high initial values, and that a strong reduction is not always seen (**Figure 46**). The four mitochondrial parameters basal respiration, ATP production, maximal response and spare respiratory capacity showed an increase in all individual values of all nine participants as well as in the group values. The grouped basal values of the ME/CFS patients were slightly increased in all parameters compared to the healthy donors and even increased further due to a session of WBH. Although the grouped data show an increased basal value in ME/CFS patients compared to healthy patients, some individual patients have a lower initial value. Patients P02, P04, P05 and P06 have lower values for all four measured mitochondrial parameters than the healthy comparison group. It can therefore be assumed that these patients definitely have a deficit in mitochondrial function. For all four patients, a WBH session leads to an increase in all measured mitochondrial values, bringing them into the range of the healthy comparison group. (**Figure 47**) Examination of the mRNA expression of genes related to autophagy and mitochondrial function showed no significant changes as a result of WBH in any of the thirteen genes analysed. A slight but non-significant increase was observed in the expression of the genes *MAP1LC3B*, *SIRT1*, *NDUFS1*, *SOD2*, *HSPA5* and *IL-10* (**Figure 48-51**).

4.3.3 Ex vivo vs. in vivo study

This chapter contains the comparison of the effect of ex vivo and in vivo hyperthermia on PBMCs from ME/CFS patients. In contrast to the comparison of the effect on wIRA irradiation of isolated PBMCs from healthy donors and ME/CFS patients, the data obtained show major differences. These differences are mainly in the response of autophagy and mitochondrial function to heat therapy. **Table 23** below provides an overview of the grouped results of the two studies, which clearly show these differences. While LC3-II intensity increases significantly by heat treatment of isolated PBMCs, a session of WBH leads to the opposite effect - a significant decrease (**Figure 52**). The same opposite effect is observed for mitochondrial function. Ex vivo treatment leads to a decreased OCR, while WBH leads to a significant increase (**Figure 53**). Only the measured mRNA expression shows a similar pattern in both studies. *MAP1LC3B*, *SIRT1*, *SOD2* and *HSPA5* are significantly increased in the ex vivo study and not significantly in the in vivo study. A clear induction can be recognised in the percentage increase of these genes ex vivo and in vivo, but no statistical difference can be determined due to the high scatter and the small sample size of nine participants in vivo.

Differences in expression can be recognised for *ATG7*, *NDUFS1* and *IL-10*. *ATG7* shows a significant decrease in human PBMCs in the ex vivo study and no significant effect in the in vivo study. There is a slight but non-significant increase in mRNA expression of *NDUFS1* in vivo, while ex vivo treatment shows no major change. In the case of *IL-10*, the expression shows no major changes in the ex vivo study, but an increase of 37.33% in vivo. The other genes *ULK1*, *BECN1*, *AMPK1α*, *FOXO3*, *SIRT3* and *TFAM* show no changes in their expression in either study. (**Figure 54-58**). **Table 23** illustrates the opposite effect of wIRA irradiation on autophagy and mitochondrial function in the ex vivo and in vivo study. These results were much unexpected and pose a challenge to explain. However, the next chapter provides a holistic view of all the data obtained and leads to a hypothesis that could possibly explain this contrasting effect.

Table 23: Comparison of ex vivo and in vivo wIRA treatment in ME/CFS patients

	Ex vivo	**In vivo**
	Autophagy	
LC3-II intensity	7%⇧****	18%⇩**
	Mitochondrial function	
Basal Respiration	8.17%⇩	66.60%⇧**
ATP Production	7.30%⇩	61.41%⇧**
Maximal Response	24.14%⇩	97.88%⇧**
Spare Respiratory Cap.	28.21%⇩	112.35%⇧**
	mRNA expression	
ULK1	3.10%⇧	3.00%⇩
BECN1	5.70%⇧	6.11%⇧
ATG7	14.95%⇩**	1.00%⇧
MAP1LC3B	19.65%⇧***	20.33%⇧
AMPK1α	2.35%⇧	13.00%⇧
FOXO3	0.75%⇧	2.78%⇧
SIRT1	33.10%⇧****	30.89%⇧
SIRT3	12.40%⇧	10.22%⇩
TFAM	6.40%⇧	0.11%⇧
NDUFS1	3.90%⇩	19.67%⇧
SOD2	18.15%⇧**	22.89%⇧
HSPA5	12.55%⇧***	48.33%⇧
IL-10	3.30%⇩	37.33%⇧

4.4 Hyperthermia as a possible treatment option for ME/CFS?!

As described in the previous chapter, the results were unpredictable, as a similar response of hyperthermia to the cellular mechanisms in both studies had been expected. However, a similar response was only observed in the response of mRNA expression of the investigated genes. The response of autophagy and mitochondrial function show exactly the opposite effect in the in vivo

study compared to the ex vivo study. In order to find a possible explanation for the differences, the discussion first takes a step back and focuses on the initial cellular situation before the treatment. This makes it possible to assess whether the contrasting results are due to the treatment or whether there could be another cause. In chapter 4.2, the comparison of healthy donors and ME/CFS patients without wIRA treatment was discussed. The results show increased autophagy and mitochondrial function in ME/CFS compared to healthy donors. Since the same participants were examined in the ex vivo study, the same results are present for basal levels before treatment. Looking at basal levels in the in vivo study, the data show a similar pattern - LC3-II is significantly increased in ME/CFS patients compared to healthy donors. In terms of mitochondrial function, basal respiration and ATP production are slightly increased in ME/CFS patients, while maximal response and spare respiratory capacity show no differences between health and disease. Since the increase in maximal response and spare respiratory capacity was also not as clear in chapter 4.2, this lack of difference could be explained by the small number of participants in the in vivo study. Due to this fact, the small differences are considered negligible, which also means that mitochondrial function has the same starting point in both studies.

Since a different starting point of the cell status between the studies has been ruled out, the cause for the contrasting results must lie somewhere else. Both hyperthermia treatments were carried out with exactly the same heat radiation, so this can also be ruled out. The analysed cells are also the same, but a major difference is the environment in which they are located during the treatment. While in the ex vivo study only the isolated PMBCs are treated, in the in vivo study the PBMCs are surrounded by a whole organic system. As mentioned in chapter 4.2, some researchers assume that the function of the mitochondria is not disturbed, but that there is a problem with the upstream sources for the mitochondria. A crucial source required for oxidative phosphorylation is oxygen. Without oxygen, cellular respiration - also known as aerobic respiration - cannot function smoothly. [178] A further assumption is that without sufficient oxygen, the transfer of electrons to oxygen is not possible and electrons accumulate in the mitochondrial transport chain [179]. Oxygen is transported to the cells via our bloodstream through the erythrocytes. Interestingly, the findings on the link between reduced blood flow and ME/CFS are not new. A 2012 study by Newton *et al.* showed impaired dilation of blood vessels in ME/CFS [50]. A correlation between the severity of endothelial dysfunction and the severity of ME/CFS disease was demonstrated by Scherbakov *et al.* [51]. It is hypothesised that impaired blood circulation may reduce tissue oxygenation in ME/CFS. The lack of oxygen in ME/CFS patients could explain the slightly higher baseline level of mitochondrial function compared to healthy ones, as the cells are resupplied with sufficient oxygen during the assay conduction and all accumulated electrons in the mitochondrial transport chain are utilised for ATP production in a short time. Another possible explanation could be that the cells of ME/CFS

patients try to compensate for the lack of oxygen by producing more mitochondria or more complexes in the respiratory chain, which would also lead to higher mitochondrial function compared to healthy donors under oxygen conditions. However, the results of this study did not support this hypothesis, at least for complex I, as the expression of *NDUFS1*, the largest nuclear subunit of complex I, was not increased in ME/CFS patients compared to healthy donors (appendix **Figure A63**). Lawson *et al.* also suggested that the increased ATP production in ME/CFS patients may be related to a pathological mechanism in which more ATP is produced by anaerobic glycolysis [147], which also matches the oxygen deprivation hypothesis. The finding of higher lactate levels, the end product of anaerobic glycolysis, in ME/CFS patients is also consistent with this hypothesis [53].

As already mentioned, whole-body hyperthermia is associated with increased oxygen partial pressure and improved blood circulation [10,164]. This means that whole-body hyperthermia restores the oxygen supply and reactivates mitochondrial function. The higher LC3-II levels in ME/CFS patients compared to healthy donors can also be explained by the hypoxia theory. Autophagy is activated as a survival mechanism under hypoxia by the hypoxia-inducible factor (HIF), as Bellot *et al.* have shown in normal and cancer cell lines [180]. After whole-body hyperthermia, oxygen supply is restored and LC3-II levels decrease to the healthy donor range. When only the PBMCs are treated with wIRA irradiation, the oxygen factor plays no role, leading to an even stronger activation of autophagy due to heat stress, as also shown in the work of McCormick *et al.* [181].

In the context of mRNA expression, the patterns of all studied genes are similar in their response to wIRA treatment of isolated PBMCs from healthy donors and ME/CFS patients (**Table 22**). Looking at the genes *ULK1*, *BECN1*, *ATG7*, *MAP1LC3B*, *AMPK1α*, *FOXO3* and *SIRT1*, which reflect the response of the molecular mechanisms underlying the autophagosomal process, *MAP1LC3B* and *SIRT1* are the only genes that respond as expected. Both genes increase in expression upon heat treatment and therefore mimic the increase in the measured cellular autophagy marker LC3B-II. The strongest response to heat treatment in mRNA expression is observed in *SIRT1* mRNA expression. Both groups, healthy donors (**$p \leq 0.01$) and ME/CFS patients (****$p \leq 0.0001$), show a significant increase in *SIRT1* gene expression by heat treatment. In the work of Lee *et al.* an induction of *SIRT1* mRNA expression was also found in human dental pulp cells after 30 min at 42 °C [182], confirming our results. This is particularly interesting with regard to the autophagy-activating function of *SIRT1* through deacetylation of lysine residues on key autophagy proteins [183]. Amirkavei *et al.* examined the effect of hormetic heat shock (HHS) on mRNA expression in human ARPE-19 cells by a single HHS shock at 42 °C for 30 min in a water bath followed by recovery at 37 °C for 3, 12, and 24 hours. They observed a time-dependent response in

the regulation of central autophagy-associated genes. *MAP1LC3B* was declared as an 'early-response gene' because the highest response occurred 3 hours after HHS, which is also consistent with the data of this work, as the isolation of the mRNA occurred immediately after heat treatment of the isolated PBMCs. The fact that the isolation of the mRNA after the in vivo treatment was delayed by the necessary transport to the laboratories and the lower response of *MAP1LC3B* (**Table 23**) support the early response theory. Examining their results of *BECN1* expression at the three different time points, an increase in mRNA is only observed after 12 hours of recovery and even occurs after 24 hours. The immediate measurement after heat treatment in this work suggests that the wrong time frame was chosen to detect an effect on *BECN1* mRNA expression. Amirkavei *et al.* also observed no changes in *ATG7* expression at any of the time points measured. These results confirm the in vivo results of this work, as no change was visible due to whole-body hyperthermia. However, the ex vivo study shows a significant decrease in *ATG7* mRNA expression in isolated PBMCs from healthy donors (**$p \leq 0.01$) and ME/CFS patients (**$p \leq 0.01$). Since the autophagy marker LC3B also increases, the decreased expression of *ATG7* could be a mechanism to downregulate autophagy to rebalance the amount of autophagy. [184] The mRNA of the genes *SOD2*, *SIRT3*, *TFAM* and *NDUFS1* was measured in connection with mitochondrial function. Due to the increased mitochondrial function caused by whole-body hyperthermia, an increase in mitochondrial genes was expected. In the case of *SOD2* and *NDUFS1*, a slight but non-significant increase was observed, confirming our hypothesis. Since increased mitochondrial function increases ROS, it is not surprising that the mRNA expression of the potent antioxidant *SOD2* also increases. The measured data of the n-fold mRNA expression of *SOD2* also show a high scatter. This indicates a different response of the donors to heat stress. A comparison of these data with a study on mammalian cells (buffalo granulosa cells) at different temperatures showed a slight decrease in *SOD2* mRNA expression at 39.5 °C, while at 40.5 °C there was a strong increase in *SOD2* expression [185]. This shows the fine regulation of this heat response and explains the variability of the donors. *TFAM* shows no change in mRNA expression by whole-body hyperthermia. In addition, the mRNA of *HSPA5*, the gene of the HSP70 protein, and *IL-10* were measured, and both showed a non-significant increase due to body hyperthermia. Amirkavei *et al.* also showed heat-activated expression of HSP70 [184]. The increased *IL-10* expression could be a reflection of the immunomodulatory effect of whole-body hyperthermia and is also visible in other studies [78,186].

To summarise, the results of this thesis leads to the hypothesis shown in **Figure 59**. It implies the idea of a disturbed blood circulation in ME/CFS, which leads to hypoxia in the cells. This hypoxia leads to a stress-induced activation of autophagy. In the case of mitochondrial function, this leads to an accumulation of electrons in the respiratory chain, as the transfer of electrons to oxygen is not possible without sufficient oxygen. These electrons can be released under aerobic conditions during

the experiment. The excess of electrons due to the previous accumulation under hypoxic conditions leads to a higher oxygen consumption than in healthy donors. Whole-body hyperthermia induces blood flow, which leads to termination of hypoxia. The restored supply of oxygen stops the stress response of the cells and autophagy returns to a 'normal/healthy' level. In addition, oxygen consumption increases even further due to the restored oxygen supply via the blood flow as well as the oxygen supply under aerobic experimental conditions.

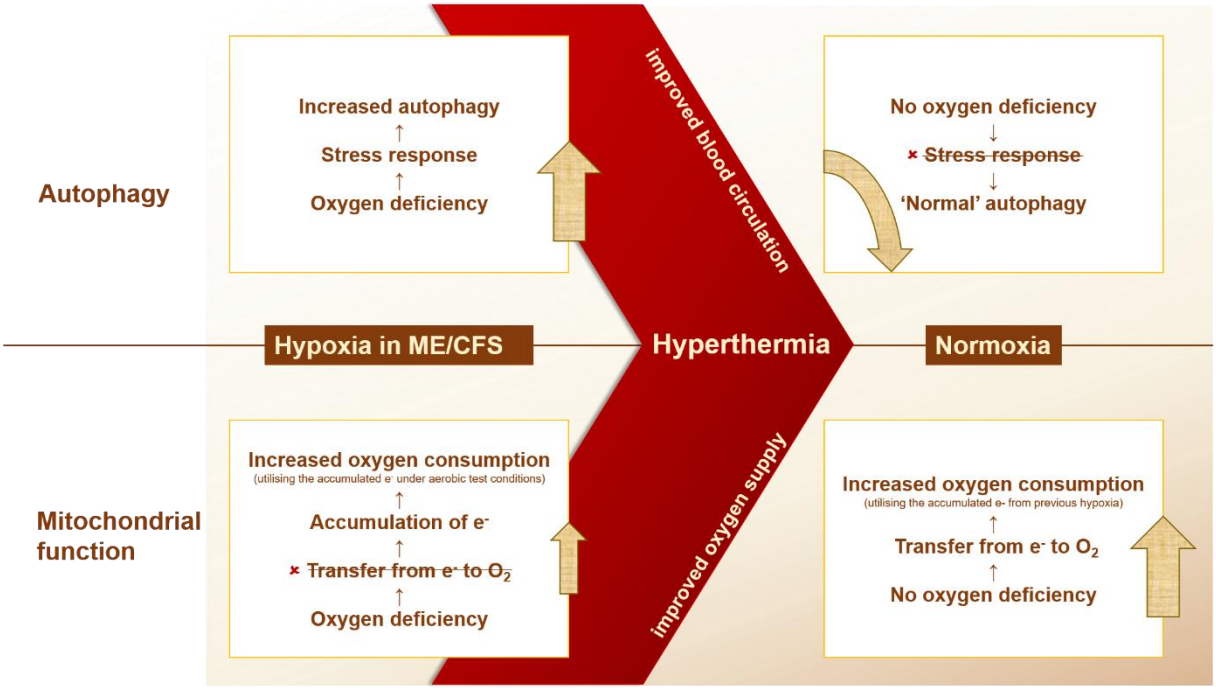

Figure 59: Schematic overview of the hypothesis. The disturbed blood flow in ME/CFS leads to hypoxia and stress-induced activation of autophagy as well as to an accumulation of electrons and thus to higher oxygen consumption under aerobic experimental conditions. Whole-body hyperthermia restores normoxia, leading to a decrease in autophagy due to the termination of the stress response and to an even higher oxygen consumption due to the utilisation of the accumulated electrons under aerobic conditions.

Regardless of whether this hypothesis can be proven or not, the results of this thesis definitely show an effect of whole-body hyperthermia on autophagy (rebalancing) and mitochondrial function (stimulation) of PBMCs from ME/CFS patients. Other studies on whole-body hyperthermia and ME/CFS patients also show that perceived fatigue decreased significantly after therapy. In addition, negative mood, including anxiety, depression and fatigue, and performance status improved significantly after therapy. [163,164] Another study showed an interaction between heat and hypoxia. After repeated exercise sessions under heat stress, people show physiological adaptations, such as improved oxygen saturation at rest and lower heart rate and core temperature at submaximal exercise under hypoxic/altitude conditions. [187].

4.5 Strengths and limitations of the hyperthermia studies

As with most studies, the design of the current study is associated with limitations. One of these limitations is the unequal number of measurements in the three tests autophagy, mitochondrial function and gene expression. This is partly due to the fact that the study design of the ex vivo study was changed during the trial. The initial cell samples from the ME/CFS participants were only tested for autophagy and gene expression with and without wIRA treatment. The investigation of the effect of wIRA treatment on mitochondrial function started with participant 09. The fact that some participants do not have data for all parameters tested is due to insufficient sample size and thus not enough cells for all measurements. A further limitation is that all participating ME/CFS patients are undergoing medical treatment, so the influence of this individual treatment cannot be determined. However, it would be ethically unacceptable to deny patients their treatment for this study. A further limitation is that the in vivo study is a small study with only nine participants, which reduces the statistical significance. However an effect was observed in all nine participants, which is exceptional and speaks very strongly in favour of the treatment and represents a strength of this study. The low number of test subjects is due to the fact that the samples had to be analysed as quickly as possible (within a few hours), as the tests carried out are cellular tests and it cannot be ruled out that the cells are affected by the hours of transport. This rapid measurement without long hours in a non-physical environment is also a strength of this study. This study also only investigated the immediate cellular response to hyperthermia. Further studies that also observe the long-term effects, disease progression and examination of multiple WBH sessions are needed. In addition, the underlying mechanisms of the induced changes in autophagy and mitochondrial function are still unclear, so that further experiments are required to investigate these. In this context, further experiments measuring parameters such as the quantification of ROS and ATP as well as analysing the mRNA expression of HIF would be of interest.

5 Conclusion

There are still many gaps in knowledge when it comes to the serious disease ME/CFS. Questions regarding the aetiology and pathophysiology remain unanswered. A clear diagnosis is also difficult because there is no biomarker for ME/CFS. This lack of understanding of the disease means that curative treatment is currently not possible. In particular, little is known about the underlying cellular and molecular mechanisms of the disease. For this reason, this study determined and compared the cellular mechanisms of autophagy and mitochondrial function in ME/CFS patients and healthy participants. The development of suitable assays for the determination of autophagy was an initial part of this work. Furthermore, these mechanisms were also measured in relation to a possible treatment option - hyperthermia.
The overarching objective of this doctoral thesis, which is to identify a treatment option for ME/CFS, has been divided into three primary questions, which will be addressed in this conclusion.

1. Do key cellular mechanisms differ in ME/CFS patients compared to healthy donors and if so, how?
To answer these questions, PBMCs from healthy donors and ME/CFS patients were analysed for autophagy and mitochondrial function and compared.

The results of this work show a difference in the cellular mechanism in PBMCs from ME/CFS patients compared to healthy donors. In the area of autophagy, the marker LC3-II is significantly increased in ME/CFS patients. The same pattern can be observed for mitochondrial function, as all four parameters shown are elevated in ME/CFS. This increase is statistically significant for basal respiration and ATP production and not significant for maximal response and spare respiratory capacity. This result indicates an imbalance in cellular function due to an overreaction. This study hypothesises that the imbalance could be due to impaired blood circulation and a lack of oxygen in the cells in ME/CFS. This lack of oxygen could lead to a stress response in the cells, followed by induced autophagy. Mitochondrial function could be inhibited by the lack of oxygen. When oxygen supply is restored during the assay performance, increased mitochondrial activity could be the consequence.

2. Does heat treatment have an effect on the central cellular mechanisms of <u>isolated</u> human cells?
The effect of wIRA irradiation (39 °C, 1 hour) on autophagy, mitochondrial function and mRNA expression of related genes was investigated in isolated PBMCs from healthy donors and ME/CFS patients as well as in human fibroblasts from a healthy donor.

Hyperthermia of isolated PBMCs from ME/CFS patients and healthy donors leads to a further increase in the LC3-II marker. As the isolated cells are no longer in the organism during the treatment, the oxygen supply is guaranteed and the hypothesis of oxygen deficiency is

irrelevant. The further activation of autophagy could therefore be explained by the heat stress reaction. This stress reaction can be observed in healthy donors as well as in ME/CFS patients. The wIRA irradiation shows no effect on the mitochondrial parameters basal respiration and ATP production, while maximal respiration and spare respiratory capacity decrease. This pattern can be observed in healthy donors as well as in ME/CFS patients. Oxygen supply is also present here, as the isolated cells are no longer in the organism during treatment and the test procedure. Without this inhibition of mitochondrial function due to the lack of oxygen, the cells of ME/CFS patients react similarly to the cells of healthy donors. The mRNA expression of the autophagy-related gene *ATG7* decreases significantly upon heat treatment, while the expression of *MAP1LC3B* and *SIRT1* increases. The mitochondrial gene *SOD2* and the gene *HSPA5* also increase as a result of heat therapy. In summary, wIRA irradiation of isolated PBMCs has a significant impact on central cellular mechanisms.

3. Does <u>whole-body hyperthermia in ME/CFS patients</u> have an effect on central cellular parameters?

The effect of a one-hour whole-body hyperthermia session with a maximum core body temperature (T_c) of 39 °C in ME/CFS patients on autophagy, mitochondrial function and mRNA expression of corresponding genes was investigated.

A session of whole-body hyperthermia also has a significant effect on PBMCs of ME/CFS patients. The autophagy marker LC3-II decreases significantly with a session of WBH. As previously shown, autophagy is increased in ME/CFS patients compared to healthy donors. The reduction by whole-body hyperthermia leads to a rebalancing of autophagy markers back to healthy levels. In the case of mitochondrial function, the four parameters basal respiration, ATP production, maximal response and spare respiratory capacity increase due to whole-body hyperthermia. Based on the hypothesis of a disturbed oxygen supply in ME/CFS, whole-body hyperthermia could lead to a restoration of this oxygen supply by stimulating blood circulation. This restoration could stop the stress response in the cells, reducing autophagy back to normal levels. Mitochondrial function is in turn increased, as they are restored to full functionality through the supply of oxygen. Examination of the effect of WBH on the mRNA expression of related genes shows no statistically significant changes, but the genes *MAP1LC3B*, *SIRT1*, *NDUFS1*, *SOD2*, *HSPA5* and *IL-10* show a slight increase.

In summary the results of this thesis show an effect of whole-body hyperthermia on autophagy and the mitochondrial function in PBMCs from nine participating ME/CFS patients. Altogether, it seems that heat treatment could be an effective way to treat not just one but multiple symptoms, allowing ME/CFS patients to have a better quality of life.

6 Concluding remarks

Besides all the interesting scientific findings, it is the human being that really counts. So this work will end with the testimony of a ME/CFS patient who experienced a positive effect from a session of whole-body hyperthermia. This underlines the positive effect that was measured in this work.

'The hyperthermia really did me good. In my memory, the flu symptoms were much better. They were no longer constantly very severe and the recovery phases were no longer weeks long. They were still long, but much shorter. I also had swollen lymph nodes less often. Since then, I have only had occasional sore throats and earaches. I had the feeling that it was receding again after a while. I still have aching limbs. I spoke to my mum. Her external perspective is that I'm much more active and resilient again since the hyperthermia. At times I was worse again, but never as bad as before. She says that since then I can take part in conversations better again, even over longer periods of time.'

~ 31-year-old female patient with severe CFS/ME

References

[1] Estévez-López F, Mudie K, Wang-Steverding X, et al. Systematic Review of the Epidemiological Burden of Myalgic Encephalomyelitis/Chronic Fatigue Syndrome Across Europe: Current Evidence and EUROMENE Research Recommendations for Epidemiology. J Clin Med. 2020;9. DOI: 10.3390/jcm9051557.

[2] Bested AC, Marshall LM. Review of Myalgic Encephalomyelitis/Chronic Fatigue Syndrome: an evidence-based approach to diagnosis and management by clinicians. Rev Environ Health. 2015;30:223–249.

[3] Clayton EW. Beyond myalgic encephalomyelitis/chronic fatigue syndrome: an IOM report on redefining an illness. JAMA. 2015;313:1101–1102.

[4] Institute of Medicine. Beyond Myalgic Encephalomyelitis/Chronic Fatigue Syndrome: Redefining an Illness. Mil Med. 2015;180:721–723.

[5] Lim E-J, Son C-G. Review of case definitions for myalgic encephalomyelitis/chronic fatigue syndrome (ME/CFS). J Transl Med. 2020;18:289.

[6] Castro-Marrero J, Sáez-Francàs N, Santillo D, et al. Treatment and management of chronic fatigue syndrome/myalgic encephalomyelitis: all roads lead to Rome. Br J Pharmacol. 2017;174:345–369.

[7] Reinhold HS, Endrich B. Tumour microcirculation as a target for hyperthermia. Int J Hyperthermia. 1986;2:111–137.

[8] Szasz AM, Minnaar CA, Szentmártoni G, et al. Review of the Clinical Evidences of Modulated Electro-Hyperthermia (mEHT) Method: An Update for the Practicing Oncologist. Front Oncol. 2019;9:1012.

[9] Hellige G. Wärmetherapie mit Wassergefilterter Infrarot-A-Strahlung. Grundlagen und Anwendungsmöglichkeiten. in Wärmetherapie Mit Wassergefilterter Infrarot-A-Strahlung. Grundlagen und Anwendungsmöglichkeiten, eds P. Vaupel and W. Krüger. 1995.

[10] Hoffmann G. Principles and working mechanisms of water-filtered infrared-A (wIRA) in relation to wound healing. GMS Krankenhaushygiene Interdisziplinar [Internet]. 2007;2:Doc54. Available from: https://www.ncbi.nlm.nih.gov/pmc/articles/PMC2831244/.

[11] Piotr G. Essential Facts on the History of Hyperthermia and their Connections with Electromedicine. arXiv: Medical Physics. 2017.

[12] Colombo R, Salonia A, Leib Z, et al. Long-term outcomes of a randomized controlled trial comparing thermochemotherapy with mitomycin-C alone as adjuvant treatment for non-muscle-invasive bladder cancer (NMIBC). BJU Int. 2011;107:912–918.

[13] Huilgol NG, Gupta S, Sridhar CR. Hyperthermia with radiation in the treatment of locally advanced head and neck cancer: a report of randomized trial. J Cancer Res Ther. 2010;6:492–496.

[14] Harima Y, Nagata K, Harima K, et al. A randomized clinical trial of radiation therapy versus thermoradiotherapy in stage IIIB cervical carcinoma. 2001. Int J Hyperthermia. 2009;25:338–343.

[15] Overgaard J, Gonzalez Gonzalez D, Hulshof MC, et al. Randomised trial of hyperthermia as adjuvant to radiotherapy for recurrent or metastatic malignant melanoma. European Society for Hyperthermic Oncology. Lancet. 1995;345:540–543.

[16] Meffert B, Hochmuth O, Steiner M, et al. Effects of a multiple mild infra-red-A induced hyperthermia on central and peripheral pulse waves in hypertensive patients. Medical & biological engineering & computing [Internet]. 1991;29:NS45-8. Available from: https://pubmed.ncbi.nlm.nih.gov/1813746/.

[17] Janssen CW, Lowry CA, Mehl MR, et al. Whole-Body Hyperthermia for the Treatment of Major Depressive Disorder: A Randomized Clinical Trial. JAMA psychiatry [Internet]. 2016;73:789–795. Available from: https://pubmed.ncbi.nlm.nih.gov/27172277/.

[18] Rabinowitz JD, White E. Autophagy and metabolism. Science. 2010;330:1344–1348.

[19] Zaffagnini G, Martens S. Mechanisms of Selective Autophagy. J Mol Biol. 2016;428:1714–1724.

[20] Galluzzi L, Baehrecke EH, Ballabio A, et al. Molecular definitions of autophagy and related processes. EMBO J. 2017;36:1811–1836.

[21] Lim S, Smith KR, Lim S-TS, et al. Regulation of mitochondrial functions by protein phosphorylation and dephosphorylation. Cell Biosci. 2016;6:25.

[22] Chen Q, Vazquez EJ, Moghaddas S, et al. Production of reactive oxygen species by mitochondria: central role of complex III. Journal of Biological Chemistry [Internet]. 2003;278:36027–36031. Available from: https://www.sciencedirect.com/science/article/pii/S002192582083405X.

[23] Muirhead N, Muirhead J, Lavery G, et al. Medical School Education on Myalgic Encephalomyelitis. Medicina (Kaunas). 2021;57. DOI: 10.3390/medicina57060542.

[24] Fukuda K, Straus SE, Hickie I, et al. The chronic fatigue syndrome: a comprehensive approach to its definition and study. International Chronic Fatigue Syndrome Study Group. Annals of internal medicine [Internet]. 1994;121:953–959. Available from: https://pubmed.ncbi.nlm.nih.gov/7978722/.

[25] Carruthers BM, Jain AK, Meirleir KL de, et al. Myalgic Encephalomyelitis/Chronic Fatigue Syndrome. Journal of Chronic Fatigue Syndrome [Internet]. 2003 [cited 2024 Sep 2];11:7–115. Available from: https://www.meresearch.org.uk/wp-content/uploads/2012/11/2003-Carruthers-Canadian-Definition-JCFS.pdf.

[26] Jason. The Development of a Revised Canadian Myalgic Encephalomyelitis Chronic Fatigue Syndrome Case Definition. American Journal of Biochemistry and Biotechnology. 2010;6:120–135.

[27] David S. Bell. The Doctor`s Guide to Chronic Fatigue Syndrome: Understanding, Treating, and Living with CFIDS. [place unknown]: DA CAPO PRESS - A Member of the Perseus Books Group; 1995.

[28] van Houdenhove B, Kempke S, Luyten P. Psychiatric aspects of chronic fatigue syndrome and fibromyalgia. Curr Psychiatry Rep. 2010;12:208–214.

[29] Wojcik W, Armstrong D, Kanaan R. Is chronic fatigue syndrome a neurological condition? A survey of UK neurologists. Journal of Psychosomatic Research [Internet]. 2011;70:573–574. Available from: https://www.sciencedirect.com/science/article/pii/S0022399911000572.

[30] Underhill R, Baillod R. Myalgic Encephalomyelitis/Chronic Fatigue Syndrome: Organic Disease or Psychosomatic Illness? A Re-Examination of the Royal Free Epidemic of 1955. Medicina (Kaunas). 2020;57. DOI: 10.3390/medicina57010012.

[31] Lacerda EM, Geraghty K, Kingdon CC, et al. A logistic regression analysis of risk factors in ME/CFS pathogenesis. BMC Neurol. 2019;19:275.

[32] Tschopp R, König RS, Rejmer P, et al. Myalgic encephalomyelitis/chronic fatigue syndrome (ME/CFS): A preliminary survey among patients in Switzerland. Heliyon. 2023;9:e15595.

[33] Chu L, Valencia IJ, Garvert DW, et al. Onset Patterns and Course of Myalgic Encephalomyelitis/Chronic Fatigue Syndrome. Front Pediatr. 2019;7:12.

[34] Arron HE, Marsh BD, Kell DB, et al. Myalgic Encephalomyelitis/Chronic Fatigue Syndrome: the biology of a neglected disease. Front Immunol. 2024;15:1386607.

[35] Underhill RA, O'gorman R. Prevalence of Chronic Fatigue Syndrome and Chronic Fatigue Within Families of CFS Patients. Journal of Chronic Fatigue Syndrome. 2006;13:3–13.

[36] Albright F, Light K, Light A, et al. Evidence for a heritable predisposition to Chronic Fatigue Syndrome. BMC Neurol. 2011;11:62.

[37] Dibble JJ, McGrath SJ, Ponting CP. Genetic risk factors of ME/CFS: a critical review. Hum Mol Genet. 2020;29:R117-R124.

[38] Lande A, Fluge Ø, Strand EB, et al. Human Leukocyte Antigen alleles associated with Myalgic Encephalomyelitis/Chronic Fatigue Syndrome (ME/CFS). Sci Rep. 2020;10:5267.

[39] Matzaraki V, Kumar V, Wijmenga C, et al. The MHC locus and genetic susceptibility to autoimmune and infectious diseases. Genome Biol. 2017;18:76.

[40] Faro M, Sàez-Francás N, Castro-Marrero J, et al. Gender Differences in Chronic Fatigue Syndrome. Reumatología Clínica (English Edition). 2016;12:72–77.

[41] Loebel M, Grabowski P, Heidecke H, et al. Antibodies to β adrenergic and muscarinic cholinergic receptors in patients with Chronic Fatigue Syndrome. Brain Behav Immun [Internet]. 2016;52:32–39. Available from: https://www.sciencedirect.com/science/article/pii/S0889159115300209.

[42] Tanaka S, Kuratsune H, Hidaka Y, et al. Autoantibodies against muscarinic cholinergic receptor in chronic fatigue syndrome. Int J Mol Med. 2003;12:225–230.

[43] Maksoud R, Du Preez S, Eaton-Fitch N, et al. A systematic review of neurological impairments in myalgic encephalomyelitis/ chronic fatigue syndrome using neuroimaging techniques. PLoS One. 2020;15:e0232475.

[44] Sukocheva OA, Maksoud R, Beeraka NM, et al. Analysis of post COVID-19 condition and its overlap with myalgic encephalomyelitis/chronic fatigue syndrome. Journal of Advanced Research [Internet]. 2022;40:179–196. Available from: https://www.sciencedirect.com/science/article/pii/S2090123221002320.

[45] Lee J-S, Sato W, Son C-G. Brain-regional characteristics and neuroinflammation in ME/CFS patients from neuroimaging: A systematic review and meta-analysis. Autoimmun Rev. 2023;23:103484.

[46] Wirth K, Scheibenbogen C. A Unifying Hypothesis of the Pathophysiology of Myalgic Encephalomyelitis/Chronic Fatigue Syndrome (ME/CFS): Recognitions from the finding of autoantibodies against ß2-adrenergic receptors. Autoimmun Rev [Internet]. 2020;19:102527. Available from: https://www.sciencedirect.com/science/article/pii/S1568997220300823.

[47] Wirth KJ, Scheibenbogen C, Paul F. An attempt to explain the neurological symptoms of Myalgic Encephalomyelitis/Chronic Fatigue Syndrome. J Transl Med. 2021;19:471.

[48] Costa DC, Tannock C, Brostoff J. Brainstem perfusion is impaired in chronic fatigue syndrome. QJM. 1995;88:767–773.

[49] van Campen CLMC, Verheugt FWA, Rowe PC, et al. Cerebral blood flow is reduced in ME/CFS during head-up tilt testing even in the absence of hypotension or tachycardia: A quantitative, controlled study using Doppler echography. Clinical Neurophysiology Practice [Internet]. 2020;5:50–58. Available from: https://www.sciencedirect.com/science/article/pii/S2467981X20300044.

[50] Newton DJ, Kennedy G, Chan KKF, et al. Large and small artery endothelial dysfunction in chronic fatigue syndrome. Int J Cardiol. 2012;154:335–336.

[51] Scherbakov N, Szklarski M, Hartwig J, et al. Peripheral endothelial dysfunction in myalgic encephalomyelitis/chronic fatigue syndrome. ESC Heart Fail. 2020;7:1064–1071.

[52] Mathew SJ, Mao X, Keegan KA, et al. Ventricular cerebrospinal fluid lactate is increased in chronic fatigue syndrome compared with generalized anxiety disorder: an in vivo 3.0 T (1)H MRS imaging study. NMR Biomed. 2009;22:251–258.

[53] Ghali A, Lacout C, Ghali M, et al. Elevated blood lactate in resting conditions correlate with post-exertional malaise severity in patients with Myalgic encephalomyelitis/Chronic fatigue syndrome. Sci Rep. 2019;9:18817.

[54] Nicolson GL. Mitochondrial Dysfunction and Chronic Disease: Treatment With Natural Supplements. Integr Med (Encinitas). 2014;13:35–43.

[55] Theoharides TC, Asadi S, Weng Z, et al. Serotonin-selective reuptake inhibitors and nonsteroidal anti-inflammatory drugs--important considerations of adverse interactions especially for the treatment of myalgic encephalomyelitis/chronic fatigue syndrome. J Clin Psychopharmacol. 2011;31:403–405.

[56] Calandre EP, Rico-Villademoros F, Slim M. An update on pharmacotherapy for the treatment of fibromyalgia. Expert Opin Pharmacother. 2015;16:1347–1368.

[57] Navaneetharaja N, Griffiths V, Wileman T, et al. A Role for the Intestinal Microbiota and Virome in Myalgic Encephalomyelitis/Chronic Fatigue Syndrome (ME/CFS)? J Clin Med. 2016;5. DOI: 10.3390/jcm5060055.

[58] Aroniadis OC, Brandt LJ. Fecal microbiota transplantation: past, present and future. Curr Opin Gastroenterol. 2013;29:79–84.

[59] Jones JF, Maloney EM, Boneva RS, et al. Complementary and alternative medical therapy utilization by people with chronic fatiguing illnesses in the United States. BMC Complement Altern Med. 2007;7:12.

[60] Chambers D, Bagnall A-M, Hempel S, et al. Interventions for the treatment, management and rehabilitation of patients with chronic fatigue syndrome/myalgic encephalomyelitis: an updated systematic review. J R Soc Med. 2006;99:506–520.

[61] Alraek T, Lee MS, Choi T-Y, et al. Complementary and alternative medicine for patients with chronic fatigue syndrome: a systematic review. BMC Complement Altern Med. 2011;11:87.

[62] Nijs J, Meeus M, Meirleir K de. Chronic musculoskeletal pain in chronic fatigue syndrome: recent developments and therapeutic implications. Man Ther. 2006;11:187–191.

[63] Vernon CC, Hand JW, Field SB, et al. Radiotherapy with or without hyperthermia in the treatment of superficial localized breast cancer: results from five randomized controlled trials. International Collaborative Hyperthermia Group. International journal of radiation oncology, biology, physics [Internet]. 1996;35:731–744. Available from: https://pubmed.ncbi.nlm.nih.gov/8690639/.

[64] Mallory M, Gogineni E, Jones GC, et al. Therapeutic hyperthermia: The old, the new, and the upcoming. Critical Reviews in Oncology/Hematology [Internet]. 2016;97:56–64. Available from: https://www.sciencedirect.com/science/article/pii/S1040842815300184.

[65] Busch C. Niederrheinische Gesellschaft für Natur- und Heilkunde in Bonn. Aus der Sitzung der medicinischen Section vom 14. März 1866. Berliner klinische Wochenschrift. 1866:245–246.

[66] Bickels J, Kollender Y, Merinsky O, et al. Coley's toxin: historical perspective. Isr Med Assoc J. 2002;4:471–472.

[67] Rowe-Horwege RW. Hyperthermia, Systemic. In: Webster JG, editor Encyclopedia of medical devices and instrumentation; 2006.

[68] Webster JG, editor. Encyclopedia of medical devices and instrumentation. Hoboken, New Jersey: Wiley-Interscience; 2006.

[69] Vaupel PW, Kelleher DK. Metabolic Status and Reaction to Heat of Normal and Tumor Tissue. In: Thermoradiotherapy and Thermochemotherapy; 1995; p. 157–176.

[70] Horsman MR. Tissue physiology and the response to heat. Int J Hyperthermia. 2006;22:197–203.

[71] Koska J, Rovensky J, Zimanova T, et al. Growth hormone and prolactin responses during partial and whole body warm-water immersions. Acta Physiol Scand. 2003;178:19–23.

[72] Lange U, Müller-Ladner U, Dischereit G. Wirkung iterativer Ganzkörperhyperthermie mit wassergefilterter Infrarot-A-Strahlung bei ankylosierender Spondylitis – eine kontrollierte, randomisierte, prospektive Studie. Akt Rheumatol [Internet]. 2017 [cited 2025 Jul 3];42:122–128. Available from: https://d-nb.info/1175450847/34.

[73] Wang J, Shen B, Roppolo JR, et al. Influence of frequency and temperature on the mechanisms of nerve conduction block induced by high-frequency biphasic electrical current. J Comput Neurosci. 2008;24:195–206.

[74] Mischke M. Wirkungen einer einmaligen bzw. seriellen Infrarot-A-Hyperthermie bei Patienten mit arterieller Hypertonie der WHO-Stadien I und II. [Diss.]. Humboldt-Universität Berlin; 18.07.1991.

[75] Ettrich U, Konrad B, Prate K, et al. Milde Ganzkörperhyperthermie in Kombination mit stationärer multimodal orientierter Schmerztherapie: Evaluation bei Patienten mit chronischem unspezifischem lumbalem Rückenschmerz [Mild whole body hyperthermia in combination with inpatient multimodal oriented pain therapy: evaluation in patients with chronic unspecific lumbar back pain]. Orthopade. 2014;43:165–174.

[76] Langhorst J, Koch AK, Kehm C, et al. Mild Water-Filtered Infrared-A Whole-Body Hyperthermia Reduces Pain in Patients with Fibromyalgia Syndrome-A Randomized Sham-Controlled Trial. J Clin Med. 2023;12. DOI: 10.3390/jcm12082945.

[77] Takahashi KA, Tonomura H, Arai Y, et al. Hyperthermia for the treatment of articular cartilage with osteoarthritis. Int J Hyperthermia. 2009;25:661–667.

[78] Zauner D, Quehenberger F, Hermann J, et al. Whole body hyperthermia treatment increases interleukin 10 and toll-like receptor 4 expression in patients with ankylosing spondylitis: a pilot study. Int J Hyperthermia [Internet]. 2014;30:393–401. Available from: https://pubmed.ncbi.nlm.nih.gov/25256892/.

[79] Foerster J, Fleischanderl S, Wittstock S, et al. Infrared-mediated hyperthermia is effective in the treatment of scleroderma-associated Raynaud's phenomenon. The Journal of investigative dermatology [Internet]. 2005;125:1313–1316. Available from: https://pubmed.ncbi.nlm.nih.gov/16354204/.

[80] Atmaca A, Al-Batran S-E, Neumann A, et al. Whole-body hyperthermia (WBH) in combination with carboplatin in patients with recurrent ovarian cancer - a phase II study. Gynecol Oncol. 2009;112:384–388.

[81] Cobarg CC. Physikalische Grundlagen der wassergefilterten Infrarot-A-Strahlung. in Wärmetherapie Mit Wassergefilterter Infrarot-A-Strahlung. Grundlagen und Anwendungsmöglichkeiten, eds P. Vaupel and W. Krüger. 1995:19–28.

[82] Von Ardenne Institue of Applied Medical Research GmbH. IRATHERM 1000M: Water-Filtered Infrared-A Radiation for Whole-Body Hyperthermia [Internet]. Available from: www.iratherm.com.

[83] Walz J, Hinzmann J, Haase I, et al. Ganzkörperhyperthermie in der Schmerztherapie. Eine kontrollierte Studie an Patienten mit Fibromyalgiesyndrom [Whole body hyperthermia in pain therapy. A controlled trial on patients with fibromyalgia]. Schmerz. 2013;27:38–45.

[84] Streffer C. Aspects of metabolic change after hyperthermia. Recent Results Cancer Res. 1988;107:7–16.

[85] Yagawa Y, Tanigawa K, Kobayashi Y, et al. Cancer immunity and therapy using hyperthermia with immunotherapy, radiotherapy, chemotherapy, and surgery. JCMT. 2017;3:218.

[86] Li W, Li J, Bao J. Microautophagy: lesser-known self-eating. Cell Mol Life Sci. 2012;69:1125–1136.

[87] Cuervo AM, Wong E. Chaperone-mediated autophagy: roles in disease and aging. Cell Res. 2014;24:92–104.

[88] Csizmadia T, Juhász G. Crinophagy mechanisms and its potential role in human health and disease. Prog Mol Biol Transl Sci. 2020;172:239–255.

[89] Xu W, Ocak U, Gao L, et al. Selective autophagy as a therapeutic target for neurological diseases. Cell Mol Life Sci. 2021;78:1369–1392.

[90] Fleming A, Bourdenx M, Fujimaki M, et al. The different autophagy degradation pathways and neurodegeneration. Neuron [Internet]. 2022;110:935–966. Available from: https://www.sciencedirect.com/science/article/pii/S0896627322000563.

[91] Wang L, Ye X, Zhao T. The physiological roles of autophagy in the mammalian life cycle. Biol Rev Camb Philos Soc. 2019;94:503–516.

[92] Lu G, Wang Y, Shi Y, et al. Autophagy in health and disease: From molecular mechanisms to therapeutic target. MedComm (2020). 2022;3:e150.

[93] Li X, He S, Ma B. Autophagy and autophagy-related proteins in cancer. Mol Cancer. 2020;19:12.

[94] Ohsumi Y. Historical landmarks of autophagy research. Cell Res. 2014;24:9–23.

[95] Yoshii SR, Mizushima N. Monitoring and Measuring Autophagy. Int J Mol Sci. 2017;18. DOI: 10.3390/ijms18091865.

[96] Promega Corporation. Autophagy LC3 HiBiT Reporter Assay System. 4/25 [cited 2025 Jun 8]. [place unknown]: [publisher unknown].

[97] Kisiel MA, Klar AS. Isolation and Culture of Human Dermal Fibroblasts. Methods Mol Biol. 2019;1993:71–78.

[98] Murphy MP, Hartley RC. Mitochondria as a therapeutic target for common pathologies. Nat Rev Drug Discov. 2018;17:865–886.

[99] Harmuth T, Prell-Schicker C, Weber JJ, et al. Mitochondrial Morphology, Function and Homeostasis Are Impaired by Expression of an N-terminal Calpain Cleavage Fragment of Ataxin-3. Front Mol Neurosci. 2018;11:368.

[100] Kummer E, Ban N. Mechanisms and regulation of protein synthesis in mitochondria. Nat Rev Mol Cell Biol. 2021;22:307–325.

[101] Giacomello M, Pyakurel A, Glytsou C, et al. The cell biology of mitochondrial membrane dynamics. Nat Rev Mol Cell Biol. 2020;21:204–224.

[102] McCarron JG, Wilson C, Sandison ME, et al. From structure to function: mitochondrial morphology, motion and shaping in vascular smooth muscle. J Vasc Res. 2013;50:357–371.

[103] Jakobs S, Stephan T, Ilgen P, et al. Light Microscopy of Mitochondria at the Nanoscale. Annu Rev Biophys. 2020;49:289–308.

[104] Westermann B. Mitochondrial fusion and fission in cell life and death. Nat Rev Mol Cell Biol [Internet]. 2010;11:872–884. Available from: https://www.nature.com/articles/nrm3013.

[105] Gruschus JM, Morris DL, Tjandra N. Evidence of natural selection in the mitochondrial-derived peptides humanin and SHLP6. Sci Rep [Internet]. 2023;13:14110. Available from: https://www.nature.com/articles/s41598-023-41053-0.

[106] Alberts B, Johnson A, Lewis J, et al. Molekularbiologie der Zelle. 5th edn. [place unknown]: WILEY-VCH Verlag GmbH & Co. KGaA; 2011.

[107] Cooper GM, editor. The Cell: A Molecular Approach. 2nd edition. [place unknown]: Sinauer Associates; 2000.

[108] Deshpande OA, Mohiuddin SS, editors. StatPearls [Internet]. [place unknown]: StatPearls Publishing; 2023.

[109] Wu Z, Ho WS, Lu R. Targeting Mitochondrial Oxidative Phosphorylation in Glioblastoma Therapy. Neuromol Med [Internet]. 2022;24:18–22. Available from: https://link.springer.com/article/10.1007/s12017-021-08678-8.

[110] Agilent Technologies, Inc. Seahorse XF Cell Mito Stress Test Kit User Guide.

[111] Meßmer A. Ex vivo analysis of caloric restriction in humans with a focus on mitochonrial function [Dissertation]. Konstanz: Universität Konstanz; 2025.

[112] Kaur S, Sharma N, Kumar V, et al. The Role of Mitophagy in Various Neurological Diseases as a Therapeutic Approach. Cell Mol Neurobiol. 2023;43:1849–1865.

[113] Rambold AS, Lippincott-Schwartz J. Mechanisms of mitochondria and autophagy crosstalk. Cell Cycle [Internet]. 2011 [cited 2024 Aug 21];10:4032–4038. Available from: https://www.ncbi.nlm.nih.gov/pmc/articles/PMC3272286/pdf/cc1023_4032.pdf.

[114] Uoselis L, Nguyen TN, Lazarou M. Mitochondrial degradation: Mitophagy and beyond. Mol Cell. 2023;83:3404–3420.

[115] Hailey DW, Rambold AS, Satpute-Krishnan P, et al. Mitochondria supply membranes for autophagosome biogenesis during starvation. Cell. 2010;141:656–667.

[116] Zhang C-S, Lin S-C. AMPK Promotes Autophagy by Facilitating Mitochondrial Fission. Cell Metab. 2016;23:399–401.

[117] Maruyama T, Noda NN. Autophagy-regulating protease Atg4: structure, function, regulation and inhibition. J Antibiot (Tokyo). 2017;71:72–78.

[118] Scherz-Shouval R, Shvets E, Fass E, et al. Reactive oxygen species are essential for autophagy and specifically regulate the activity of Atg4. EMBO J. 2007;26:1749–1760.

[119] Redza-Dutordoir M, Averill-Bates DA. Interactions between reactive oxygen species and autophagy: Special issue: Death mechanisms in cellular homeostasis. Biochim Biophys Acta Mol Cell Res. 2021;1868:119041.

[120] Ding X, Zhu C, Wang W, et al. SIRT1 is a regulator of autophagy: Implications for the progression and treatment of myocardial ischemia-reperfusion. Pharmacological Research [Internet]. 2024;199:106957. Available from: https://www.sciencedirect.com/science/article/pii/S1043661823003134.

[121] Nogueiras R, Habegger KM, Chaudhary N, et al. Sirtuin 1 and sirtuin 3: physiological modulators of metabolism. Physiol Rev. 2012;92:1479–1514.

[122] Bánréti A, Sass M, Graba Y. The emerging role of acetylation in the regulation of autophagy. Autophagy. 2013;9:819–829.

[123] Motta MC, Divecha N, Lemieux M, et al. Mammalian SIRT1 represses forkhead transcription factors. Cell. 2004;116:551–563.

[124] Eijkelenboom A, Burgering BMT. FOXOs: signalling integrators for homeostasis maintenance. Nat Rev Mol Cell Biol. 2013;14:83–97.

[125] Lu P, Kamboj A, Gibson SB, et al. Poly(ADP-ribose) polymerase-1 causes mitochondrial damage and neuron death mediated by Bnip3. J Neurosci. 2014;34:15975–15987.

[126] Azad MB. The Role of BNIP3 in Proliferation and Hypoxia-Induces Autophagy: Implications for Cancer Therapy. [place unknown]: University of Manitoba, Winnipeg, Manitoba, Canada; 2010.

[127] Wang S, Li H, Yuan M, et al. Role of AMPK in autophagy. Front Physiol. 2022;13:1015500.

[128] Sanchez AMJ, Csibi A, Raibon A, et al. AMPK promotes skeletal muscle autophagy through activation of forkhead FoxO3a and interaction with Ulk1. J Cell Biochem. 2012;113:695–710.

[129] Zhang J, Xiang H, Liu J, et al. Mitochondrial Sirtuin 3: New emerging biological function and therapeutic target. Theranostics. 2020;10:8315–8342.

[130] Xi S, Chen W, Ke Y. Advances in SIRT3 involvement in regulating autophagy-related mechanisms. Cell Div. 2024;19:20.

[131] Zhang Q, Siyuan Z, Xing C, et al. SIRT3 regulates mitochondrial function: A promising star target for cardiovascular disease therapy. Biomed Pharmacother [Internet]. 2024;170:116004. Available from: https://www.sciencedirect.com/science/article/pii/S0753332223018024.

[132] Palma FR, He C, Danes JM, et al. Mitochondrial Superoxide Dismutase: What the Established, the Intriguing, and the Novel Reveal About a Key Cellular Redox Switch. Antioxid Redox Signal. 2020;32:701–714.

[133] Chidambaram SB, Anand N, Varma SR, et al. Superoxide dismutase and neurological disorders. IBRO Neuroscience Reports [Internet]. 2024;16:373–394. Available from: https://www.sciencedirect.com/science/article/pii/S2667242123022856.

[134] Kang I, Chu CT, Kaufman BA. The mitochondrial transcription factor TFAM in neurodegeneration: emerging evidence and mechanisms. FEBS Lett. 2018;592:793–811.

[135] Picca A, Lezza AMS. Regulation of mitochondrial biogenesis through TFAM-mitochondrial DNA interactions: Useful insights from aging and calorie restriction studies. Mitochondrion [Internet]. 2015;25:67–75. Available from: https://www.sciencedirect.com/science/article/pii/S1567724915300258.

[136] Qi B, Song L, Hu L, et al. Cardiac-specific overexpression of Ndufs1 ameliorates cardiac dysfunction after myocardial infarction by alleviating mitochondrial dysfunction and apoptosis. Exp Mol Med. 2022;54:946–960.

[137] Lopez-Fabuel I, Le Douce J, Logan A, et al. Complex I assembly into supercomplexes determines differential mitochondrial ROS production in neurons and astrocytes. Proc Natl Acad Sci U S A. 2016;113:13063–13068.

[138] Ni Y, Hagras MA, Konstantopoulou V, et al. Mutations in NDUFS1 Cause Metabolic Reprogramming and Disruption of the Electron Transfer. Cells. 2019;8. DOI: 10.3390/cells8101149.

[139] Hu C, Yang J, Qi Z, et al. Heat shock proteins: Biological functions, pathological roles, and therapeutic opportunities. MedComm (2020). 2022;3:e161.

[140] Li T, Fu J, Cheng J, et al. New progresses on cell surface protein HSPA5/BiP/GRP78 in cancers and COVID-19. Front Immunol. 2023;14:1166680.

[141] Loonen AJM. Putative role of immune reactions in the mechanism of tardive dyskinesia. Brain, Behavior, & Immunity - Health [Internet]. 2023;33:100687. Available from: https://www.sciencedirect.com/science/article/pii/S2666354623001011.

[142] Mollazadeh H, Cicero AFG, Blesso CN, et al. Immune modulation by curcumin: The role of interleukin-10. Crit Rev Food Sci Nutr. 2019;59:89–101.

[143] Huang K, Lidbury BA, Thomas N, et al. Machine learning and multi-omics in precision medicine for ME/CFS. J Transl Med [Internet]. 2025;23:68. Available from: https://translational-medicine.biomedcentral.com/articles/10.1186/s12967-024-05915-z.

[144] Kleiveland CR, editor. The Impact of Food Bioactives on Health: in vitro and ex vivo models [Internet]. [place unknown]: Springer; 2015.

[145] Sun Y, Zhang Z, Qiao Q, et al. Immunometabolic changes and potential biomarkers in CFS peripheral immune cells revealed by single-cell RNA sequencing. J Transl Med [Internet]. 2024;22:925. Available from: https://translational-medicine.biomedcentral.com/articles/10.1186/s12967-024-05710-w.

[146] Fernandez-Guerra P, Gonzalez-Ebsen AC, Boonen SE, et al. Bioenergetic and Proteomic Profiling of Immune Cells in Myalgic Encephalomyelitis/Chronic Fatigue Syndrome Patients: An Exploratory Study. Biomolecules [Internet]. 2021;11:961. Available from: https://www.researchgate.net/publication/352839952_Bioenergetic_and_Proteomic_Profiling_of_Immune_Cells_in_Myalgic_EncephalomyelitisChronic_Fatigue_Syndrome_Patients_An_Exploratory_Study.

[147] Lawson N, Hsieh C-H, March D, et al. Elevated Energy Production in Chronic Fatigue Syndrome Patients. J Nat Sci. 2016;2.

[148] Castro-Marrero J, Cordero MD, Sáez-Francas N, et al. Could mitochondrial dysfunction be a differentiating marker between chronic fatigue syndrome and fibromyalgia? Antioxid Redox Signal. 2013;19:1855–1860.

[149] Tomas C, Brown AE, Newton JL, et al. Mitochondrial complex activity in permeabilised cells of chronic fatigue syndrome patients using two cell types. PeerJ. 2019;7:e6500.

[150] Gottschalk G, Peterson D, Knox K, et al. Elevated ATG13 in serum of patients with ME/CFS stimulates oxidative stress response in microglial cells via activation of receptor for advanced glycation end products (RAGE). Mol Cell Neurosci [Internet]. 2022;120:103731. Available from: https://www.sciencedirect.com/science/article/pii/S1044743122000379.

[151] François A, Julian A, Ragot S, et al. Inflammatory Stress on Autophagy in Peripheral Blood Mononuclear Cells from Patients with Alzheimer's Disease during 24 Months of Follow-Up. PLoS One. 2015;10:e0138326.

[152] Barbati C, Celia AI, Colasanti T, et al. Autophagy Hijacking in PBMC From COVID-19 Patients Results in Lymphopenia. Front Immunol. 2022;13:903498.

[153] Granata S, Bruschi M, Verlato A, et al. Autophagy Activation in Peripheral Blood Mononuclear Cells of Peritoneal Dialysis Patients. Kidney International Reports [Internet]. 2023;8:1852–1863. Available from: https://www.sciencedirect.com/science/article/pii/S2468024923013633.

[154] Beckmann S, Rana N, Luty W. Methods in mammalian autophagy research. Cell [Internet]. 2010 [cited 2024 May 9];140:313–326. Available from: https://www.agilent.com/cs/library/applications/autophagy-analysis-using-object-spot-counting-5994-3378EN-agilent.pdf.

[155] Scherer M. Influence of caloric restriction (CR) on autophagy in human primary cells. [place unknown]; 2022.

[156] Schöller-Mann A, Matt K, Hochecker B, et al. Ex vivo Assessment of Mitochondrial Function in Human Peripheral Blood Mononuclear Cells Using XF Analyzer. Bio Protoc. 2021;11:e3980.

[157] Livak KJ, Schmittgen TD. Analysis of relative gene expression data using real-time quantitative PCR and the 2(-Delta Delta C(T)) Method. Methods. 2001;25:402–408.

[158] Hochecker B, Matt KC, Meßmer AL, et al. Quantification of Autophagosomes in Human Fibroblasts Using Cyto-ID® Staining and Cytation Imaging. Bio Protoc. 2024;14:e5025.

[159] Bell DS. The Doctor's Guide to Chronic Fatigue Syndrome: Understanding, Treating, and Living with CFIDS. [place unknown]: Da Capo Press; 1995.

[160] Hochecker B, Scherer M. LC3-II fluorescence intensity in PBMCs from healthy donors and ME/CFS patients (CTRL + whole-body hyperthermia). [place unknown]; 2024.

[161] Hochecker B, Molinski N, Matt K, et al. Heat treatment in health and disease: How water-filtered infrared-A (wIRA) irradiation affects key cellular mechanisms in myalgic encephalomyelitis/chronic fatigue syndrome (ME/CFS) patients compared to healthy donors. Journal of thermal biology [Internet]. 2024;120:103813. Available from: https://www.sciencedirect.com/science/article/pii/S0306456524000317.

[162] Hochecker B, Matt K, Scherer M, et al. Heat vs. Fatigue: Hyperthermia as a Possible Treatment Option for Myalgic Encephalomyelitis/Chronic Fatigue Syndrome (ME/CFS). Int J Mol Sci. 2025;26:5339.

[163] Soejima Y, Munemoto T, Masuda A, et al. Effects of Waon therapy on chronic fatigue syndrome: a pilot study. Intern Med. 2015;54:333–338.

[164] Munemoto T, Soejima Y, Masuda A, et al. Increase in the Regional Cerebral Blood Flow following Waon Therapy in Patients with Chronic Fatigue Syndrome: A Pilot Study. Intern Med. 2017;56:1817–1824.

[165] Oeste CL, Seco E, Patton WF, et al. Interactions between autophagic and endo-lysosomal markers in endothelial cells. Histochem Cell Biol [Internet]. 2013;139:659–670. Available from: https://link.springer.com/article/10.1007/s00418-012-1057-6.

[166] Nunes JM, Kruger A, Proal A, et al. The Occurrence of Hyperactivated Platelets and Fibrinaloid Microclots in Myalgic Encephalomyelitis/Chronic Fatigue Syndrome (ME/CFS). Pharmaceuticals (Basel). 2022;15. DOI: 10.3390/ph15080931.

[167] Leidal AM, Levine B, Debnath J. Autophagy and the cell biology of age-related disease. Nat Cell Biol. 2018;20:1338–1348.

[168] Deretic V, Levine B. Autophagy balances inflammation in innate immunity. Autophagy. 2018;14:243–251.

[169] Ryter SW, Lam HC, Chen Z-H, et al. Deadly triplex: smoke, autophagy and apoptosis. Autophagy. 2011;7:436–437.

[170] Rivas JL, Palencia T, Fernández G, et al. Association of T and NK Cell Phenotype With the Diagnosis of Myalgic Encephalomyelitis/Chronic Fatigue Syndrome (ME/CFS). Front Immunol. 2018;9:1028.

[171] Saha S, Panigrahi DP, Patil S, et al. Autophagy in health and disease: A comprehensive review. Biomed Pharmacother [Internet]. 2018;104:485–495. Available from: https://www.sciencedirect.com/science/article/pii/S0753332218309053.

[172] Shadel GS, Horvath TL. Mitochondrial ROS signaling in organismal homeostasis. Cell [Internet]. 2015;163:560–569. Available from: https://www.ncbi.nlm.nih.gov/pmc/articles/PMC4634671/.

[173] Pizzino G, Irrera N, Cucinotta M, et al. Oxidative Stress: Harms and Benefits for Human Health. Oxid Med Cell Longev. 2017;2017:8416763.

[174] Lin MT, Beal MF. Mitochondrial dysfunction and oxidative stress in neurodegenerative diseases. Nature [Internet]. 2006;443:787–795. Available from: https://www.nature.com/articles/nature05292.

[175] Scheibye-Knudsen M, Croteau DL, Bohr VA. Mitochondrial deficiency in Cockayne syndrome. Mech Ageing Dev. 2013;134:275–283.

[176] Tomas C, Lodge TA, Potter M, et al. Assessing cellular energy dysfunction in CFS/ME using a commercially available laboratory test. Sci Rep [Internet]. 2019;9:11464. Available from: https://www.nature.com/articles/s41598-019-47966-z.

[177] Technologies A, Inc. Seahorse XF Cell Mito Stress Test Kit User Guide.

[178] Green DE, Tzagoloff A. The mitochondrial electron transfer chain. Arch Biochem Biophys. 1966;116:293–304.

[179] Guarente L. Mitochondria--a nexus for aging, calorie restriction, and sirtuins? Cell. 2008;132:171–176.

[180] Bellot G, Garcia-Medina R, Gounon P, et al. Hypoxia-induced autophagy is mediated through hypoxia-inducible factor induction of BNIP3 and BNIP3L via their BH3 domains. Mol Cell Biol. 2009;29:2570–2581.

[181] McCormick JJ, King KE, Côté MD, et al. Regulation of autophagy following ex vivo heating in peripheral blood mononuclear cells from young adults. Journal of thermal biology [Internet]. 2020;91:102643. Available from: https://pubmed.ncbi.nlm.nih.gov/32716884/.

[182] Lee S, Min K, Bae W, et al. Role of SIRT1 in heat stress- and lipopolysaccharide-induced immune and defense gene expression in human dental pulp cells. J Endod. 2011;37:1525–1530.

[183] Sacitharan PK, Bou-Gharios G, Edwards JR. SIRT1 directly activates autophagy in human chondrocytes. Cell Death Discov. 2020;6:41.

[184] Amirkavei M, Plastino F, Kvanta A, et al. Hormetic Heat Shock Enhances Autophagy through HSF1 in Retinal Pigment Epithelium Cells. Cells. 2022;11. DOI: 10.3390/cells11111778.

[185] Faheem MS, Ghanem N, Gad A, et al. Adaptive and Biological Responses of Buffalo Granulosa Cells Exposed to Heat Stress under In Vitro Condition. Animals (Basel). 2021;11. DOI: 10.3390/ani11030794.

[186] Kozłowski HM, Sobocińska J, Jędrzejewski T, et al. Fever-range whole body hyperthermia leads to changes in immune-related genes and miRNA machinery in Wistar rats. Int J Hyperthermia. 2023;40:2216899.

[187] Willmott AGB, Diment AG, Chung HC, et al. Cross-adaptation from heat stress to hypoxia: A systematic review and exploratory meta-analysis. Journal of thermal biology. 2024;120:103793.

7 Appendix

7.1 Attachment to results

The following results serve on the one hand to complete the results and on the other hand to explain certain areas of the study design. For mitochondrial function, the remaining parameter measured, namely non-mitochondrial function, is presented. The delta Ct values are included for the gene expression analyses.

7.1.1 Establishment of time management for the performance of the Guava® Autophagy LC3 antibody-based assay

Since the isolation of PBMCs from whole blood places a strain on the cells, it was investigated whether the results of the LC3-II measurement differ if the cells are measured immediately after isolation or after a 24-hour resting phase. For this measurement, three independent tests were carried out under both conditions. The first graph shows the individual data and the second graph shows the grouped values (**Figure A60**). The grouped values show an increased measurement of LC3-II of 16 % with a statistical significance (*p = 0.0242, unpaired t-test). Based on these results, in the first study (ex vivo), the treatment with subsequent LC3-II determination was not carried out until one day after PBMC isolation. This was no longer possible for the in vivo measurement, as the direct influence of the WBH was to be determined, so the measurement was carried out directly after PBMC isolation.

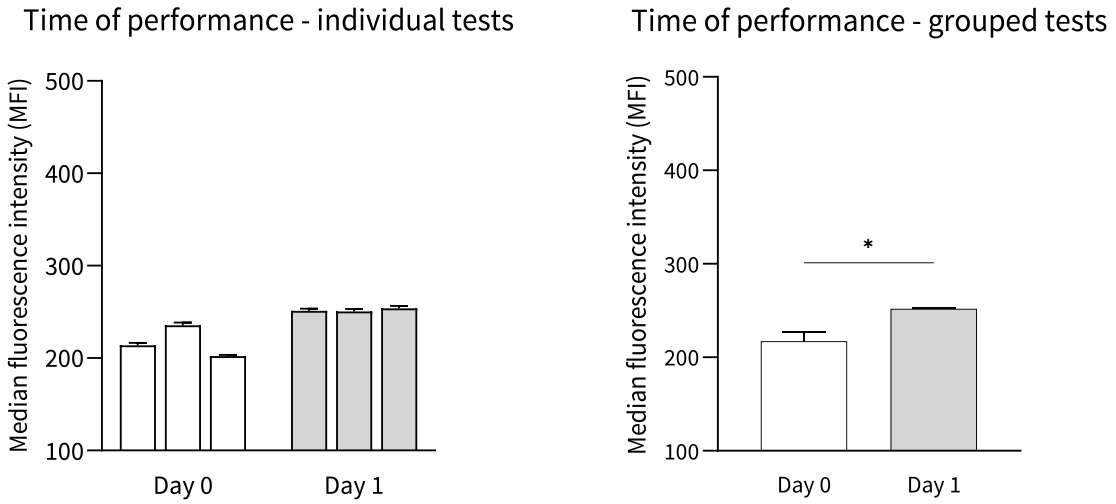

Figure A60: Determination of the optimum time for performing the autophagy assay. Investigation of whether the results of the LC3-II measurement differ when the cells are measured immediately after isolation or after a 24-hour resting phase. The grouped values show an increased value of LC3-II of 16 % with a statistical significance (*p = 0.0242, unpaired t-test) when measured after a 24 h resting phase compared to an immediately measurement after PBMC isolation.

7.1.2 Healthy vs. ME/CFS

Comparing the non-mitochondrial respiration of healthy donors with that of ME/CFS patients (**Figure A61**), it was found that the PBMCs of ME/CFS patients had a 6.34% higher OCR (p = 0.7112, unpaired t-test).

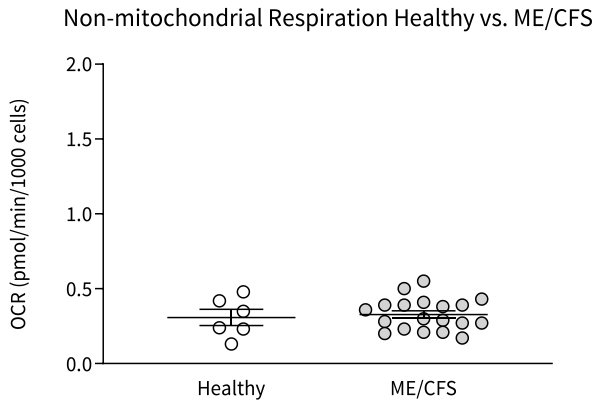

Figure A61: Healthy vs. ME/CFS non-mitochondrial Respiration. PBMCs from ME/CFS patients have a 6.34% higher OCR (p = 0.7112, unpaired t-test) compared to healthy donors.

The following **Figure A62** shows the comparison of delta Ct values of autophagy-related genes in PBMCs from ME/CFS patients and healthy donors. The following genes show a lower value in ME/CFS patients compared to healthy donors: *ULK1* (11%, p = 0.3688, Mann-Whitney test), *BECN1* (40.7%, p = 0.4353, Mann-Whitney test), *ATG7* (24.11%, p = 0.765, Mann-Whitney test), *AMPK1α* (68.34%, p = 0.2145, Mann-Whitney test), *SIRT1* (28.67%, p = 0.5207, unpaired t-test), *FOXO3* (14.8%, p = 0.9712, Mann-Whitney test). The remaining gene *MAP1LC3B i*ncreased by 4.51% (p = 0.2145, Mann-Whitney test) in ME/CFS patients compared to healthy donors.

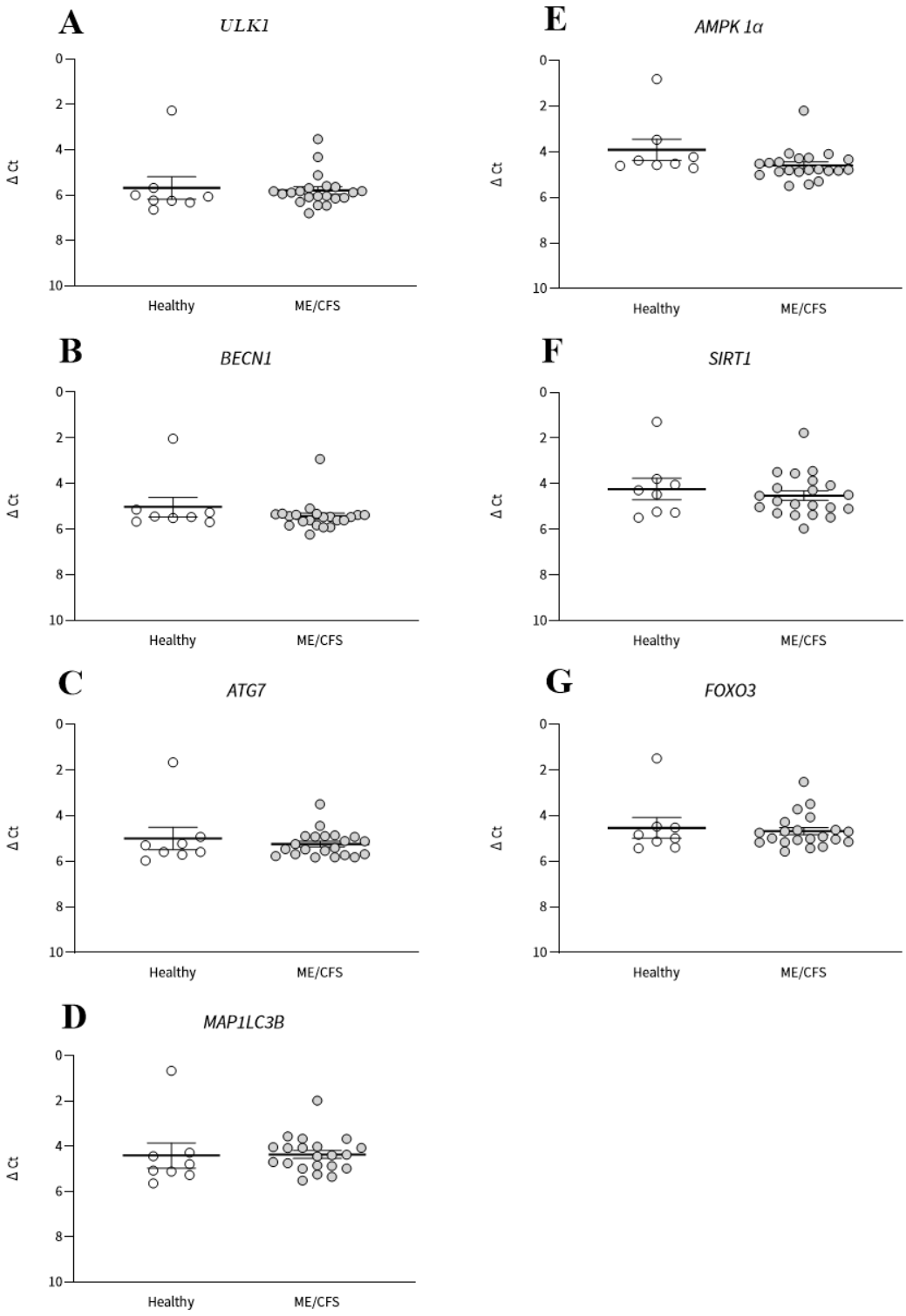

Figure A62: Healthy vs. ME/CFS ΔCt of autophagy related genes. A-C; E-G *ULK1* (11%, p = 0.3688, Mann-Whitney test), *BECN1* (40.7%, p = 0.4353, Mann-Whitney test), *ATG7* (24.11%, p = 0.765, Mann-Whitney test), *AMPK1α* (68.34%, p = 0.2145, Mann-Whitney test), *SIRT1* (28.67%, p = 0.5207, unpaired t-test) and *FOXO3* (14.8%, p = 0.9712, Mann-Whitney test) show a lower value in ME/CFS patients compared to healthy donors. D *MAP1LC3B* increased by 4.51% (p = 0.2145, Mann-Whitney test) in ME/CFS patients compared to healthy donors.

The following genes show a lower value in ME/CFS patients compared to healthy donors: *SIRT3* (36.25%, *p = 0.0284, unpaired t-test), *TFAM* (34.83%, p = 0.0509, unpaired t-test), *NDUFS1* (3.45%, p = 0.8616, unpaired t-test) and *HSPA5* (14.72%, p = 0.5254, Mann-Whitney test). *SOD2* and *IL-10* are increased by 24.52% (p = 0.395, Mann-Whitney test) and 37.64% (p = 0.3604, unpaired t-test) in ME/CFS patients compared to healthy donors (**Figure A63**).

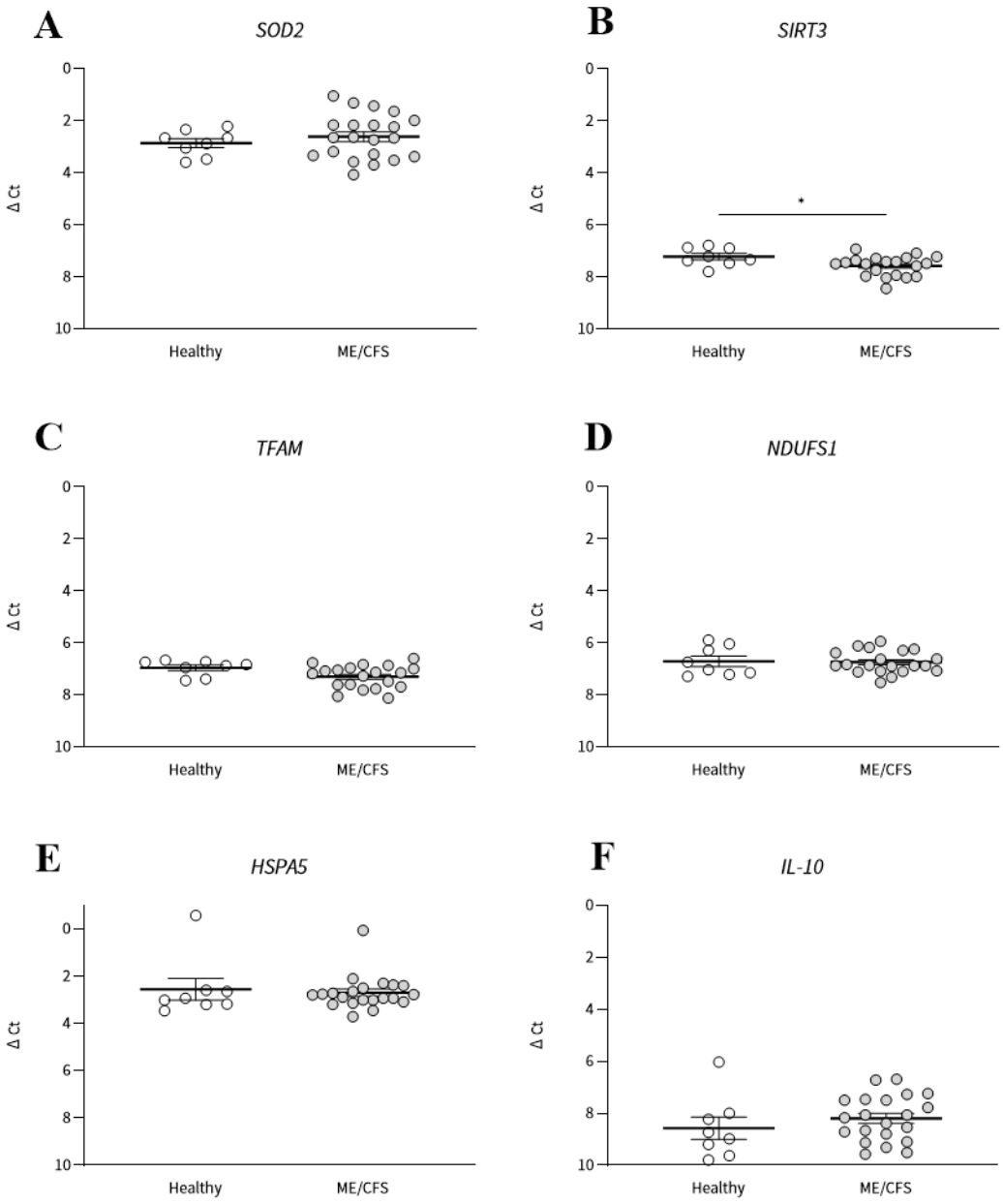

Figure A63: Healthy vs. ME/CFS ΔCt of mitochondrial related and additional genes. A *SOD2* is increased by 24.52% (p = 0.395, Mann-Whitney test) in ME/CFS patients. **B – E** *SIRT3* (36.25%, *p = 0.0284, unpaired t-test), *TFAM* (34.83%, p = 0.0509, unpaired t-test), *NDUFS1* (3.45%, p = 0.8616, unpaired t-test) and *HSPA5* (14.72%, p = 0.5254, Mann-Whitney test) show a lower value in ME/CFS patients compared to healthy donors. **E** *IL-10* is increased by 37.64% (p = 0.3604, unpaired t-test) in ME/CFS patients.

7.1.3 Ex vivo study

The following graphs (**Figure A64**) show the effect of hyperthermia on wIRA-irradiated isolated PBMCs from healthy donors and ME/CFS patients. Taking a closer look at the healthy cells, two out of six donors (P01, P04) show an increase, one remains at the same level (P02) and three decrease (P03, P05, P09) due to the treatment. The grouped data show a decrease of 3.78% ($p = 0.5635$, paired t-test). The treatment of cells from ME/CFS patients leads to a decrease in six donors (P13, P17, P18, P19, P20, P24), one remains the same (P16) and in four donors it increases (P14, P21, P22, P23) due to hyperthermia. The grouped data show a decrease of 4.59% ($p = 0.6007$, paired t-test). The comparison of the effects of the treatment between the two groups shows a similar picture, as both groups decrease in their non-mitochondrial function as a result of the hyperthermia.

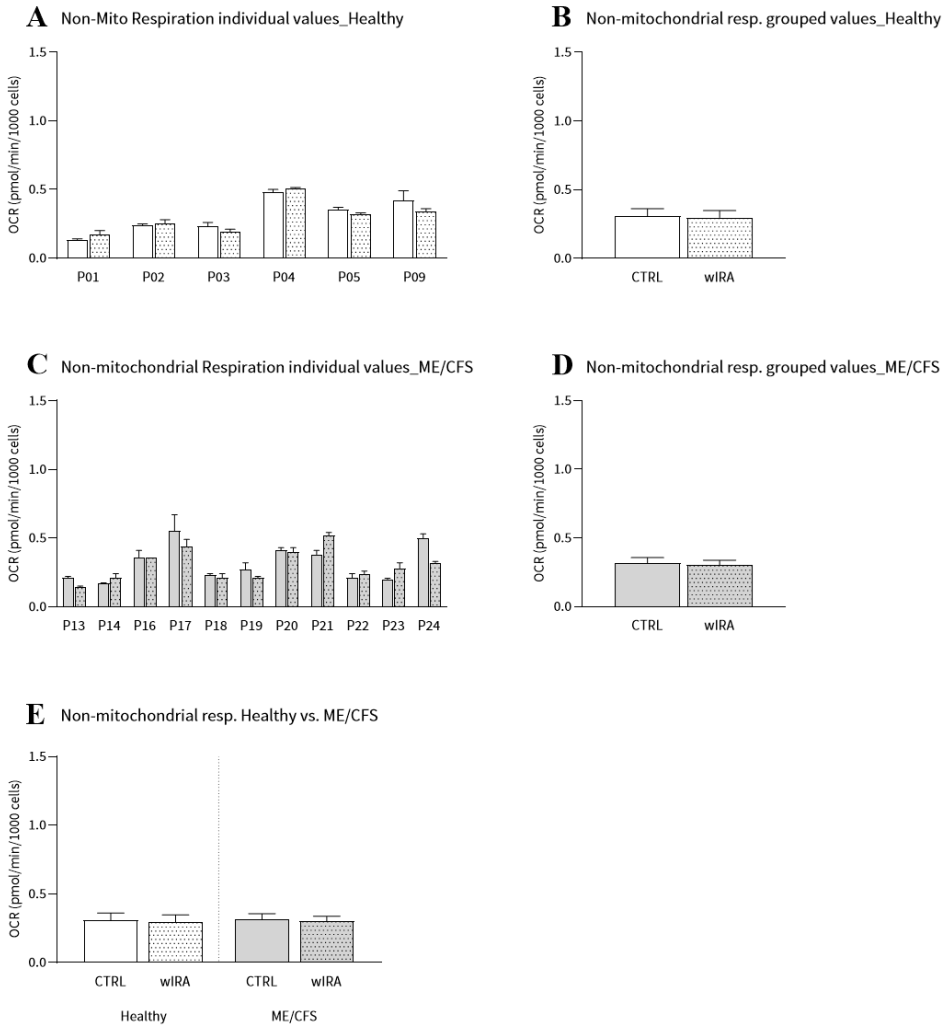

Figure A64: Effect of ex vivo wIRA treatment on non-mitochondrial respiration in Health and Disease. A Two healthy donors show an increase (P04, P04), one remains at the same level (P02) and three decrease (P03, P05, P09) due to wIRA. **B** The grouped data of healthy donors show a decrease of 3.78% ($p = 0.5635$, paired t-test). **C** The treatment of cells from ME/CFS patients leads to a decrease in six donors (P13, P17, P18, P19, P20, P24), in P16 it remains the same and in four donors it increases (P14, P21, P22, P23) due to hyperthermia. **D** The grouped data show a decrease of 4.59% ($p = 0.6007$, paired t-test). **E** There is a similar response to the treatment in health and disease.

Hyperthermia treatment of isolated PBMCs from healthy volunteers resulted in decreased delta Ct for three autophagy-related genes: *ULK1* (12%, p = 0.1172, Wilcoxon test), *ATG7* (28.38%, **p = 0.0078, Wilcoxon test) and *FOXO3* (6.13%, p = 0.8438, Wilcoxon test). For the remaining two genes *MAP1LC3B* (9%, p = 0.3672, Wilcoxon test) *BECN1* (1.5%, p = 0.7266, Wilcoxon test), *AMPK1α* (4.13%, p = 0.9375, Wilcoxon test) and *SIRT1* (44.38%, **p = 0.0040, paired t-test), the treatment led to an increased delta Ct value. The isolated cells from ME/CFS patients show a similar pattern. One small difference is that the Ct value only decreases for two genes, namely *ULK1* (6%, p = 0.2194, Wilcoxon test) and *ATG7* (24.65%, **p = 0.0038, Wilcoxon test). The other five genes *BECN1* (8.85%, p = 0.0586, Wilcoxon test), *MAP1LC3B* (26.45%, ****p < 0.0001, Wilcoxon test), *SIRT1* (40.25%, **** p < 0.0001, Wilcoxon test), *AMPK1α* (2.45%, p < 0.708, Wilcoxon test) and *FOXO3* (8.85%, p = 0.4921, Wilcoxon test) are increasing due to hyperthermia (**Figure A65**).

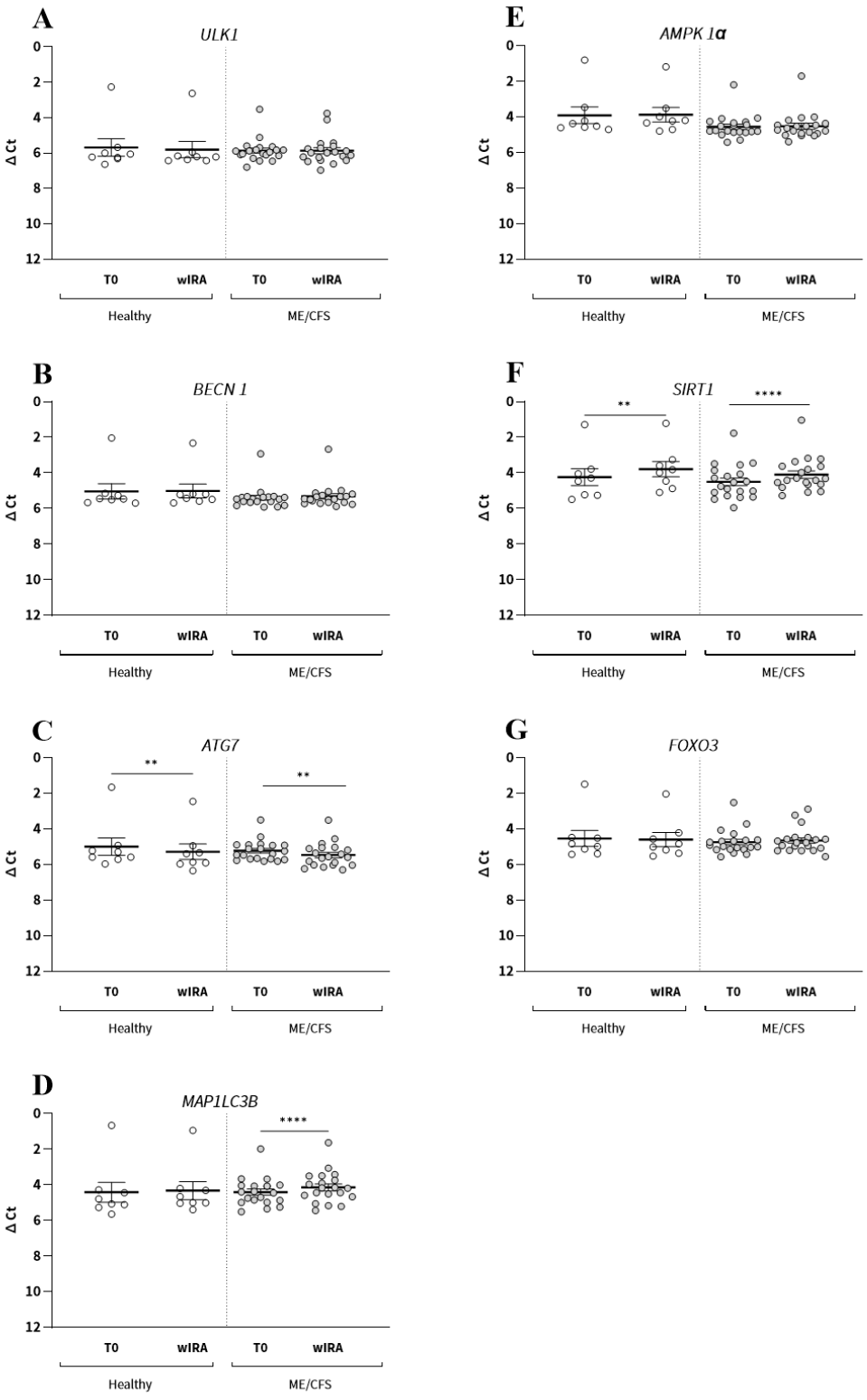

Figure A65: Ex vivo ΔCt of Autophagy related genes. A *ULK1* decreases in healthy donors (12%, p = 0.1172, Wilcoxon test) and ME/CFS (6%, p = 0.2194, Wilcoxon test) due to wIRA. **B** *BECN1* increases in healthy donors (1.5%, p = 0.7266, Wilcoxon test) and in ME/CFS (8.85%, p = 0.0586, Wilcoxon test). **C** *ATG7* decreases in health (28.38%, **p = 0.0078, Wilcoxon test) and disease (24.65%, **p = 0.0038, Wilcoxon test). **D** In healthy donors *MAP1LC3B* (9%, p = 0.3672, Wilcoxon test) is increasing as well as in ME/CFS patients (26.45%, ****p < 0.0001, Wilcoxon test). **E** *AMPK1α* is increasing in health (4.13%, p = 0.9375, Wilcoxon test) and in ME/CFS (2.45%, p < 0.708, Wilcoxon test). **F** *SIRT1* is increasing in health (44.38%, **p = 0.0040, paired t-test) and disease (40.25%, **** p < 0.0001, Wilcoxon test). **G** *FOXO3* decreases in health (6.13%, p = 0.8438, Wilcoxon test) and increases in ME/CFS (8.85%, p = 0.4921, Wilcoxon test).

Hyperthermia treatment of isolated PBMCs from healthy donors resulted in decreased delta Ct for the genes *SIRT3* (8.5%, p = 0.2247, paired t-test) and *IL-10* (33.5%, p = 0.104, paired t-test). The remaining four genes *SOD2* (16.6%, p = 0.054, paired t-test), *TFAM* (9.6%, p = 0.0892, paired t-test), *NDUFS1* (1.75%, p = 0.7873, paired t-test) and *HSPA5* (18.9%, p = 0.1406, Wilcoxon test) are increasing due to hyperthermia. The PBMCs from ME/CFS patients show a decreased delta Ct for the genes *NDUFS1* (8.55%, p = 0.1367, paired t-test) and *IL-10* (9.5%, p = 0.3742, paired t-test). The genes *SOD2* (20.8%, **p = 0.0086, paired t-test) and *HSPA5* (18.5%, ****p < 0.0001, Wilcoxon test) show a significant increase due to wIRA irradiation and the genes *SIRT3* (6.45%, p = 0.9061, Wilcoxon test) and *TFAM* (6%, p = 0.3061, paired t-test) a non-significant increase (**Figure A66**).

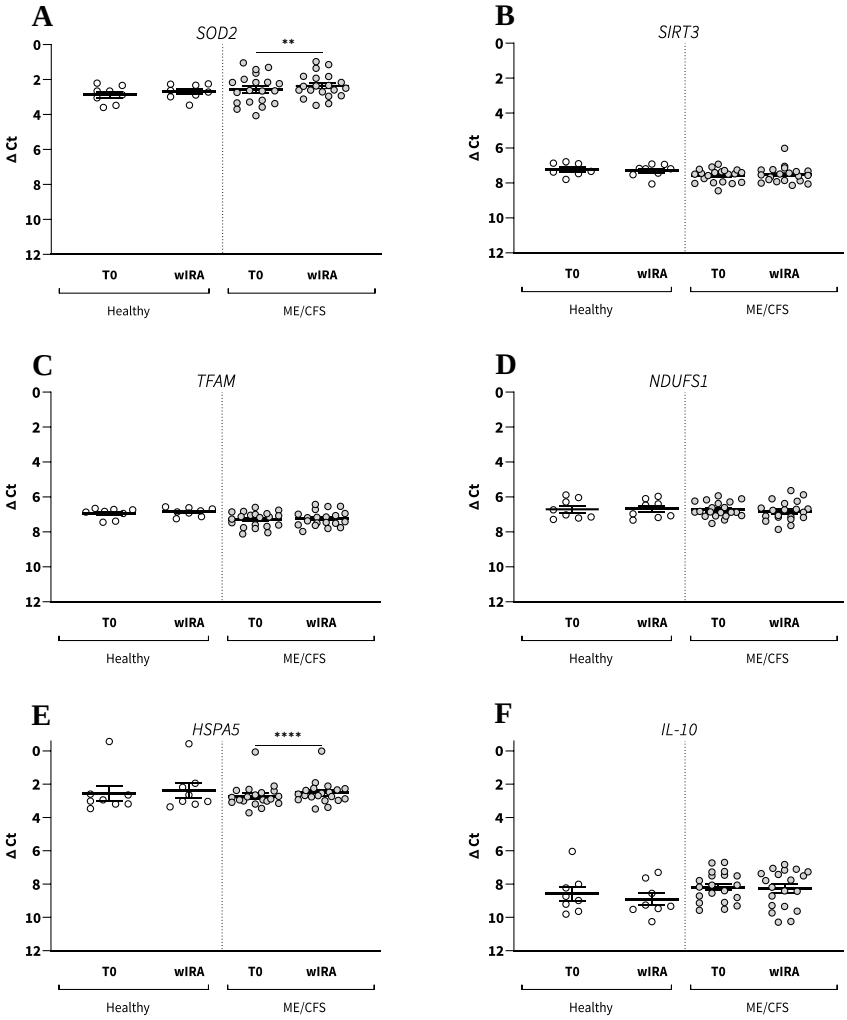

Figure A66: Ex vivo ΔCt of mitochondrial related and additional genes. A *SOD2* is increasing in healthy donors (16.6%, p = 0.054, paired t-test) as well as in ME/CFS patients (20.8%, **p = 0.0086, paired t-test). **B** *SIRT3* decreased in healthy donors (8.5%, p = 0.2247, paired t-test) and increase in ME/CFS patients (6.45%, p = 0.9061, Wilcoxon test). **C** *TFAM* is increasing in health (9.6%, p = 0.0892, paired t-test) and disease (6%, p = 0.3061, paired t-test). **D** *NDUFS1* decreased in healthy donors (8.55%, p = 0.1367, paired t-test) and ME/CFS patients (8.55%, p = 0.1367, paired t-test). **E** *HSPA5* increased in health (18.9%, p = 0.1406, Wilcoxon test) and ME/CFS (18.5%, ****p < 0.0001, Wilcoxon test). **F** *IL-10* decreased in healthy donors (33.5%, p = 0.104, paired t-test) and in ME/CFS patients (9.5%, p = 0.3742, paired t-test).

7.1.4 In vivo study

A session of whole-body hyperthermia leads to an increase in non-mitochondrial respiration in seven ME/CFS patients (P01, P02, P03, P04, P06, P08 and P09), as shown in **Figure A67**. The two participants P05 and P07 show no treatment-related changes. The grouped values show a statistically significant increase of 40.89% (*p = 0.0126, paired t-test) due to WBH. A comparison of the basal values of ME/CFS patients with healthy donors shows a lower non-mitochondrial function in ME/CFS patients by 16.20% (p = 0.4064, unpaired t-test).

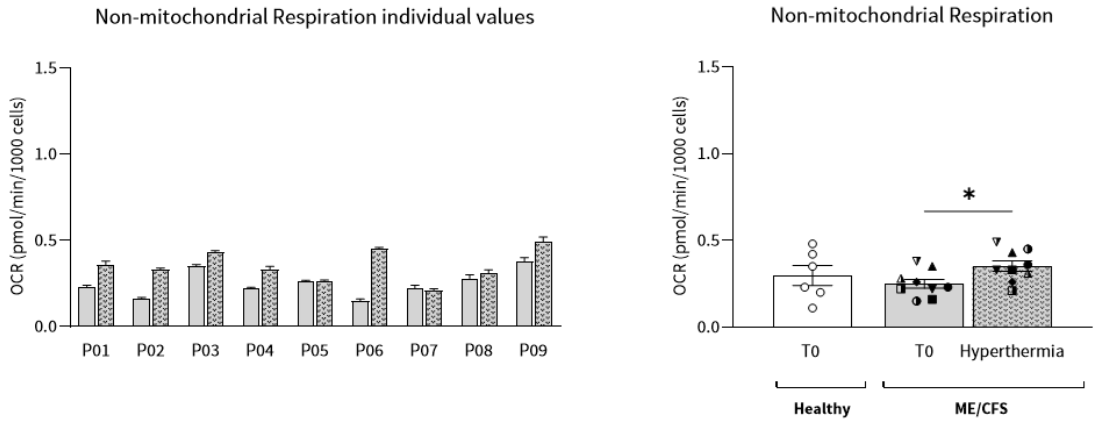

Figure A67: Effect of in vivo hyperthermia treatment on the Non-mitochondrial respiration in ME/CFS. Seven ME/CFS patients (P01, P02, P03, P04, P06, P08 and P09) show an increase by wIRA irradiation. The two participants P05 and P07 show no changes. The grouped values show a statistically significant increase of 40.89% (*p = 0.0126, paired t-test) due to WBH. A comparison of the basal values of ME/CFS patients with healthy donors shows a lower non-mitochondrial function in ME/CFS patients by 16.20% (p = 0.4064, unpaired t-test).

When comparing the basal delta Ct values of ME/CFS patients with data from healthy donors (**Figure A68**), the three autophagy-related genes *ULK* (96.2%, ****p < 0.0001, unpaired t-test), *MAP1LC3B* (6.7%, p = 0.748, unpaired t-test) and *FOXO3* (21.1%, p = 0.2896, unpaired t-test) are elevated in ME/CFS. Whole-body hyperthermia treatment leads to a decrease in the delta Ct values of *ULK1* (11.2%, p = 0.4836, paired t-test) and *FOXO3* (2.9%, p = 0.8587, paired t-test) and to a further increase in *MAP1LC3B* (22.1%, p = 0.1229, paired t-test). The remaining genes *BECN1* (66.1%, **p = 0.0010, unpaired t-test), *ATG7* (107.3%, ****p < 0.0001, unpaired t-test), *AMPK1α* (40.7%, p = 0.2003, Mann-Whitney test) and *SIRT1* (3.7%, p = 0.9107, unpaired t-test) are decreased at their baseline levels in ME/CFS compared to healthy donors. A session of wIRA irradiation leads to an increase in *BECN1* (4.4%, p = 0.7239, paired t-test), *AMPK1α* (14.4%, p = 0.2109, Wilcoxon test) and *SIRT1* (22.4%, p = 0.3905, paired t-test). Only the *ATG7* (3.8%, p = 0.7846, paired t-test) gene shows a further decrease as a result of the therapy.

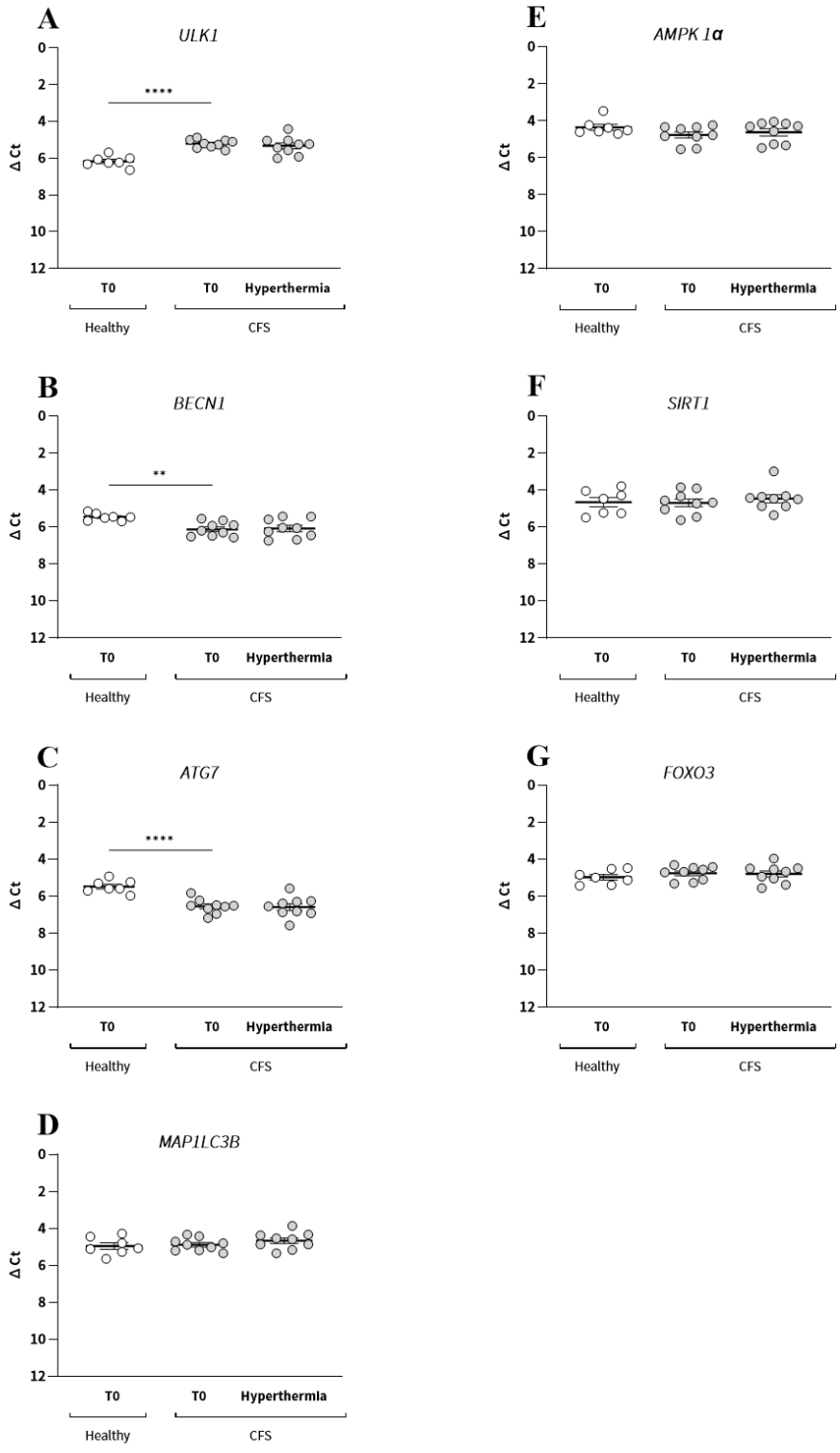

Figure A68: In vivo ΔCt of autophagy related genes. **A** *ULK* (96.2%, ****p < 0.0001, unpaired t-test) is elevated in ME/CFS compared to healthy donors and decrease due to wIRA (11.2%, p = 0.4836, paired t-test). **B** *BECN1*is lower compared to the control (66.1%, **p = 0.0010, unpaired t-test) and increases due to hyperthermia (4.4%, p = 0.7239, paired t-test). **C** *ATG7* is decreased in ME/CFS on the basal level (107.3%, ****p < 0.0001, unpaired t-test) and decreases further by wIRA (3.8%, p = 0.7846, paired t-test). **D** *MAP1LC3B* is elevated in ME/CFS (6.7%, p = 0.748, unpaired t-test) and increase further by hyperthermia (22.1%, p = 0.1229, paired t-test). **E** *AMPK1α* is lower in ME/CFS (40.7%, p = 0.2003, Mann-Whitney test) and increase due to treatment (14.4%, p = 0.2109, Wilcoxon test). **F** *SIRT1* is lower in ME/CFS (3.7%, p = 0.9107, unpaired t-test) and increase by wIRA (22.4%, p = 0.3905, paired t-test). **G** *FOXO3* is elevated in ME/CFS (21.1%, p = 0.2896, unpaired t-test) and increase further by treatment (2.9%, p = 0.8587, paired t-test).

The basal delta Ct values are reduced for five genes in ME/CFS patients compared to healthy donors (**Figure A69**). These genes are *SOD2* (17.4%, p = 0.5795, unpaired t-test), *SIRT3* (5.3%, p = 0.7355, unpaired t-test), *TFAM* (25.9%, p = 0.1091, unpaired t-test), *NDUFS1* (9.7%, p = 0.6817, unpaired t-test) and *IL-10* (60%, p = 0.0565, unpaired t-test). WBH treatment leads to a further decrease in *SIRT3* (16.6%, p = 0.0547, Wilcoxon test) and *TFAM* (4.3%, p = 0.7244, Wilcoxon test). The other genes *SOD2* (12.9%, p = 0.6146, paired t-test), *NDUFS1* (20.1%, p = 0.1881, paired t-test) and *IL-10* (31.1%, p = 0.2052, paired t-test) show an increase due to hyperthermia. The basal level of *HSPA5* (31.1%, p = 0.0583, Mann-Whitney test) is elevated in ME/CFS patients compared to healthy donors, and treatment leads to a further increase in *HSPA5* (34.8%, p = 0.4258, Wilcoxon test).

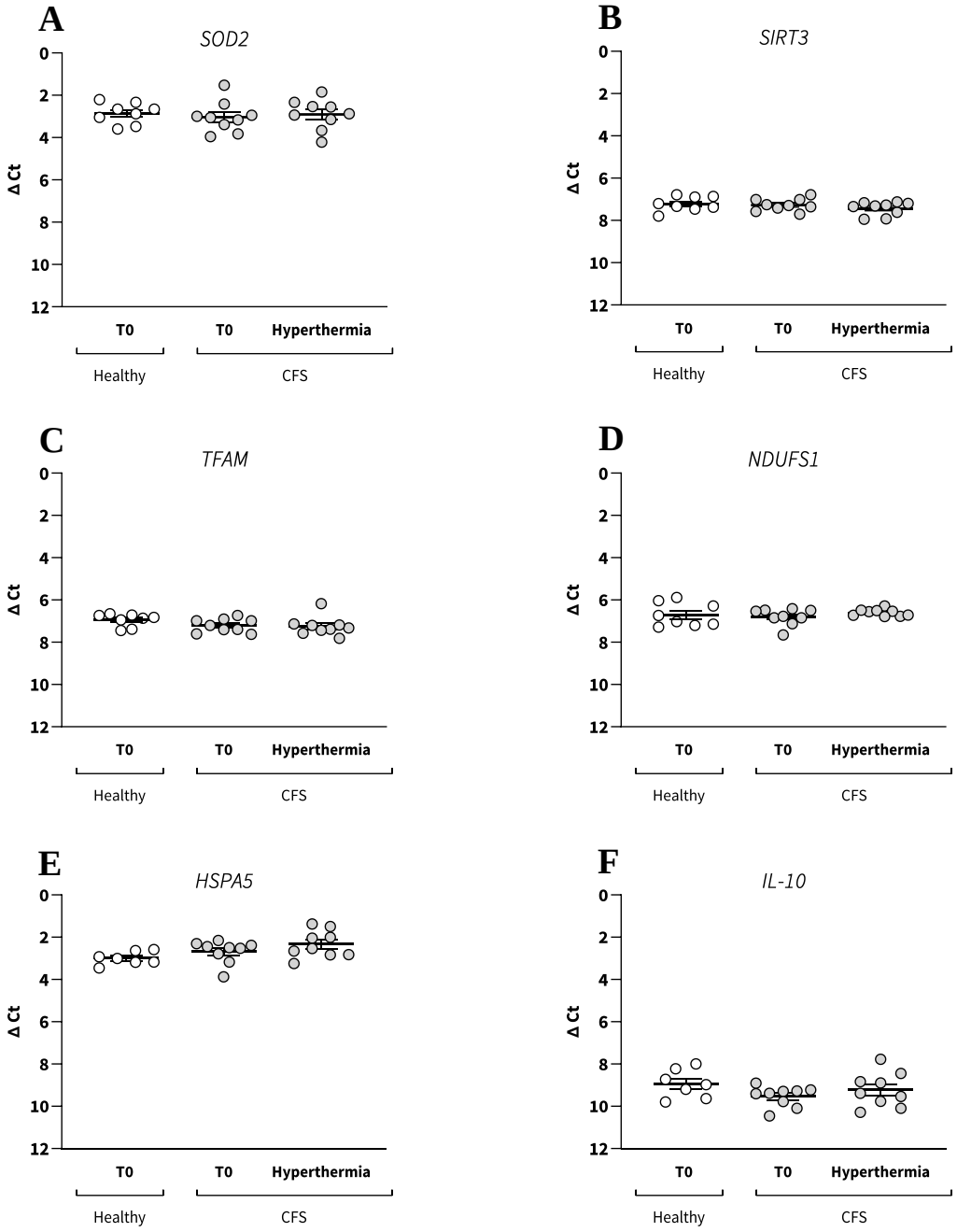

Figure A69: In vivo ΔCt of mitochondrial related and additional genes. A *SOD2* is reduced in healthy donors on the basal level (17.4%, p = 0.5795, unpaired t-test) and increase (12.9%, p = 0.6146, paired t-test) due to hyperthermia. **B** *SIRT3* is lower in health (5.3%, p = 0.7355, unpaired t-test) and decrease further (16.6%, p = 0.0547, Wilcoxon test) by therapy. **C** A lower *TFAM* value is visible in ME/CFS patients (25.9%, p = 0.1091, unpaired t-test), a WBH session leads to a further decrease (4.3%, p = 0.7244, Wilcoxon test). **D** *NDUFS1* is also lower in ME/CFS (9.7%, p = 0.6817, unpaired t-test) the treatment leads to an increasing (20.1%, p = 0.1881, paired t-test). **E** The basal level of *HSPA5* (31.1%, p = 0.0583, Mann-Whitney test) is elevated in ME/CFS and hyperthermia leads to a further increase (34.8%, p = 0.4258, Wilcoxon test). **F** *IL-10* is decreased in ME/CFS (60%, p = 0.0565, unpaired t-test), WBH leads to an increase (31.1%, p = 0.2052, paired t-test).

7.2 Acknowledgements

This work would not have been possible without the help of others, so I would like to express my heartfelt thanks for their support and encouragement throughout this journey.

First of all, I would like to thank my supervisor, **Prof. Dr. Jörg Bergemann**, for the opportunity to conduct my work as an associated doctoral candidate as part of the InViTe doctoral programme. This cooperative doctoral programme (Kooperatives Promotionskolleg (KPK) InViTe Sigmaringen/Konstanz) was funded by the Baden-Württemberg Ministry of Science, Research and the Arts, to whom I would also like to express my thanks. **Jörg**, thank you for every scientific discussion, your enthusiasm for the topic and your valuable input. But also for your trust and belief in me! You always stand behind your team members and stand up for them. I am very grateful to you for that!

I would also like to thank my supervisor **Prof. Dr. Alexander Bürkle** from the University of Konstanz. I would like to thank you for your scientific contribution, your interest in my work and your advice during thesis committee meetings. Your enthusiasm is inspiring and it was always a pleasure to discuss the results with you.

I am also very grateful to my cooperation partners **Dr. Alexander von Ardenne** and **Noah Molinski** from the Von Ardenne Institute for Applied Medical Research GmbH. Especially for the construction of the IRAcubator, without which the ex vivo studies would not have been possible. But also for every meeting with scientific discussions, good ideas, advice and much more. This work was funded by the Professor Manfred von Ardenne Forschungsförderungsgesellschaft e.V., to whom I would also like to express my thanks. This support would not have been possible without **Alexander von Ardenne**. Thank you very much for your trust in us and our work. It was a pleasure to work with you! I would also like to thank **Dr. Achim Schneider** and **Dr. Stefan Pieper** and their teams for carrying out and monitoring the whole-body hyperthermia treatment and for taking the blood samples. Thank you very much for your interest and support of our research! We are aware of the increased effort that this cooperation entails for you and thank you all the more for your support.

My special thanks go to the members and former members of the Bergemann lab in Sigmaringen. Many thanks to **Katja, Alica, Melanie, Sonja** and **Daniel** for every listen, laugh, advice and for your uncountable support in many ways. I would especially like to thank **Katja** for every discussion, her valuable scientific input and the numerous proofreading actions; I can always count on you - Thank you very much!

Without the support of my **family and friends**, this dissertation would not have been possible. So thank you very much for your understanding, even if you didn't understand everything, your patience, your motivating speeches, your listening, your faith in me and for every prayer.

The greatest thanks goes to the source of all that I am and have - **God**! Thank you for all the great people and opportunities you have given me. Thank you for your love, your kindness, your humility, your faithfulness, your patience and so much more. It was your trust in me and the strength you gave me that stopped me from giving up during the difficult times. May your light shine and heal the hearts, bodies and souls of all people – Amen!

7.3 Publications

Scherer M, **Hochecker B**, Matt K, Meßmer A, Bergemann J. Detection of Autophagy in Human Peripheral Blood Mononuclear Cells using Guava® Autophagy and Flow Cytometry. Bio-protocol. *io-protocol* 15(18): e5457. DOI: 10.21769/BioProtoc.5457

Hochecker B, Matt K, Scherer M, Meßmer A, von Ardenne A, Bergemann J. Heat vs. Fatigue - Hyperthermia as a possible treatment option for myalgic encephalomyelitis/chronic fatigue syndrome (ME/CFS). *International Journal of Molecular Sciences*. 2025; 26(11):5339. https://doi.org/10.3390/ijms26115339

Hochecker B, Matt K, Meßmer A, Scherer, M, Bergemann J. Quantification of Autophagosomes in Human Fibroblasts Using Cyto-ID® Staining and Cytation Imaging. Bio-protocol. 2024: 14(13): e5025. doi: 10.21769/BioProtoc.5025

Hochecker B, Molinski N, Matt K, et al. Heat treatment in health and disease: How water-filtered infrared-A (wIRA) irradiation affects key cellular mechanisms in myalgic encephalomyelitis/chronic fatigue syndrome (ME/CFS) patients compared to healthy donors. J Therm Biol. 2024;120:103813.

Schöller-Mann A, Matt K, **Hochecker B**, Bergemann J. Ex vivo assessment of mitochondrial function in human peripheral blood mononuclear cells using XF Analyzer. Accepted for publication in Bio-protocol in February 2021

Matt K, **Hochecker B**, Schöller-Mann A, Bergemann J. mRNA expression of ageing-associated genes in calorie reduction is subject to donor variability and can be induced by calorie restriction mimetics. Nutr Health. 2020;26(3):253-262. doi:10.1177/0260106020932732

Schöller-Mann A, Matt K, Schniertshauer D, **Hochecker B**, Bergemann J. 12 days of in vivo caloric reduction can improve important parameters of aging in humans. Mech Ageing Dev. 2020;188:111238. doi:10.1016/j.mad.2020.111238

7.4 Poster presentations

Schöller-Mann A, **Hochecker B**, Matt K, Bergemann J. Innovative diagnostics for therapy support. Diagnostics-4-Future Conference, November 27-28, 2019 in Konstanz

Schöller-Mann A, **Hochecker B**, Matt K, Müller S, Schniertshauer D, Bergemann J. Various Parameters of Aging, including Mitochondrial Function, are improved by Caloric Reduction. 10th Anniversary - Targeting Mitochondria, October 28-29, 2019 in Berlin

No congresses until 2022 due to COVID

Schniertshauer D, **Hochecker B**, Enzmann F, Bergemann J. Influence of ubiquinol on energy metabolism and DNA repair enzyme hOGG1 in mitochondria of human skin fibroblasts. Targeting Mitochondria, October 27-28, 2022 in Berlin

Hochecker B, von Ardenne A, Molinski N, Schniertshauer D, Bergemann J. Influence of water-filtered infrared-A (wIRA) hyperthermia on autophagy in human skin fibroblasts. Skin Ageing & Challenges 2022; November 17-18 2022 in Lisbon, Portugal

Hochecker B, Matt K, Scherer M, Schniertshauer D, Bergemann J. Influence of water-filtered infrared-A (wIRA) hyperthermia and spermidine on autophagy in human skin fibroblasts. Skin Ageing & Challenges 2023; November 9-10 2023 in Lisbon, Portugal

Hochecker B, von Ardenne A, Molinski N, Bergemann J. Heat treatment in healthy and disease: How water-filtered infrared-A irradiation affects key cellular mechanisms in ME/CFS patients compared to healthy donors. Poster Session, Department of Biology Uni Konstanz, Juli 2023 in Konstanz

Hochecker B. Hyperthermie. Tag der Forschung, Hochschule Albstadt-Sigmaringen, October 2023 in Albstadt

Bergemann J, Matt K, **Hochecker B**, Scherer M. Wir wollen Menschen helfen – gesund zu werden und gesund zu bleiben. Tag der Forschung, Hochschule Albstadt-Sigmaringen, Juni 2024 in Sigmaringen

Hochecker B, Matt K, Bergemann J. Heat vs. Fatigue. Tag der Forschung, Hochschule Albstadt-Sigmaringen, Juli 2025 in Albstadt

7.5 Poster Award

Hochecker B, Matt K, Scherer M, Schniertshauer D, Bergemann J. Influence of water-filtered infrared-A (wIRA) hyperthermia and spermidine on autophagy in human skin fibroblasts. Skin Ageing & Challenges 2023; November 9-10 2023 in Lisbon, Portugal